Synthesis of a Phthalocyanine Scaffold as a Core of Highly Glycosylated Dendritic Structures and a Novel Fluorenyl Spiro-Annelated Phthalocyanine

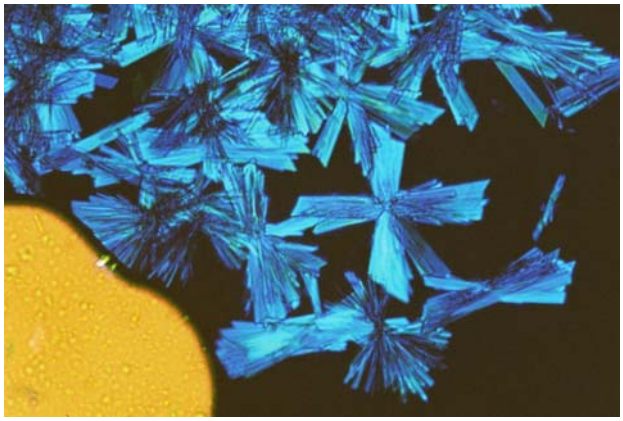

Doctoral dissertation for the granting of the degree

'doctor rerum naturalium'

at the

Department of Chemistry

Faculty of Mathematics, Informatics and Natural Sciences

University of Hamburg

submitted by

Dipl.-Ing. Herwig BERTHOLD

from Graz/Austria

– Hamburg 2008 –

Day of dissertation defense, 22nd August 2008.

1. Reviewer: Prof. Dr. Joachim Thiem
2. Reviewer: Prof. Dr. Chris Meier

This doctoral thesis was elaborated from March 2003 until March 2008 under the supervision of Prof. Dr. J. Thiem and the guidance of Dr. Theo Schotten, Center for Applied Nanotechnology (CAN) GmbH Hamburg and the Department of Chemistry, University of Hamburg, financially supported by Lilly Forschung GmbH Hamburg (2003-2006) and a research fellowship of the S.O.H.N.-R&D Foundation (2006-2008).

I am deeply grateful to Prof. Thiem for the admittance in his work group, his constant interest and his confidence in my work.

Diese Arbeit widme ich in größter Hochachtung meinen lieben Eltern Jenny Berthold & Rudolf Willinger.

If it’s to be,

it’s up to me!

Geht nicht,

gibt’s nicht!

TOPIC

Since their discovery early in the last century, phthalocyanines (Pcs) have been of great interest to chemists, physicists and industrial scientists and have become one of the most studied of all organic functional materials. In addition to their use as blue and green colorants, they are a versatile class of functional dyes. Phthalocyanines have been widely studied for their applications in various disciplines and are of increasing interest for applications in nonlinear optics (including optical limitation), xerography (as photoconductors), optical data storage (as the laser absorption layer within recordable compact discs)[1, 2] molecular electronics, solar energy conversion, catalysis and as the active component of gas sensors.[3, 4]

For all of the above mentioned industrial applications uniform thin films are needed in order to further explore and exploit the fascinating optical and electronic properties of the phthalocyanine (Pc) ring system. Spin coating has been demonstrated to be a simple, quick and reproducible method of fabricating uniform films. However, solubility in volatile organic solvents is a prerequisite for this technique. Previous studies have shown that substituents on the Pc ring system with various functional groups is the method of choice to this end and will crucially affect the nanoscale structure of the resulting film.

Apart from the use in materials science, phthalocyanines are also highly promising for their applications as diagnostics and therapy in medicine, namely for magnetic resonance imaging (MRI)[5] and photodynamic therapy (PDT).[6, 7] Substituents with hydrophilic character can not only enhance the solubility of the macrocycles in biological media but also prevent their aggregation, which is a precondition for photosensitization[8, 9] in PDT. For target selectivity (*e.g.* for imaging or combating tumor cells) in a living organism, the goal must be to decorate the periphery of the Pc-core with surface receptor specific substituents.

INTRODUCTION

HISTORY OF DISCOVERY AND ELUCIDATION OF PHTHALOCYANINES[3]

The compound that is now known as phthalocyanine (Pc) was first observed as a highly colored by-product in chemical conversion of some *ortho*-disubstituted benzene derivatives. Braun and Tcherniac observed a dark, insoluble material during the preparation of *ortho*-cyanobenzamide from phthalimide and acetic acid (1907). Similarly, Henri de Diesbach (1880 – 1970) and van der Weid of Fribourg University (Swizerland), obtained a 23% yield of an exceptionally stable, blue material during the Rosenmund-von Braun reaction of *ortho*-dibromobenzene with copper(I)cyanide in refluxing pyridine (1927). Hindsight allows us to identify these by-products as being metal-free and copper(II) Pcs, respectively.

Serendipitously, conditional upon a further coincidence the formation of a blue–green material occurred during the industrial preparation of phthalimide from phthalic anhydride, at the Grangemouth plant of Scottish Dyes Ltd. in the year 1928.

Owing to the business interests of Scottish Dyes, the material was examined by two employees, Dandridge and Dunsworth, whose preliminary studies revealed that the iron-containing by-product had potential as an exceptionally stable and insoluble pigment. A patent covering the preparation and properties of the substance was granted in 1929,[10] when Imperial Chemical Industries (ICI) had already acquired Scottish Dyes in 1928. ICI were eager to understand the structure of this novel colored substance and a sample was sent to Professor Jocelyn F. Thorpe at Imperial College, London. He, in turn, gave it for investigation to a newly appointed lecturer, the remarkable Reginald P. Linstead (1902-66), 'as it appeared that the substance might prove to be of academic interest'.[11] Thus, a collaboration between Linstead and ICI was initiated that culminated in the publication of a series of six papers in the *Journal of the Chemical Society* describing the structure of Pc and the synthesis of some of its metal derivatives.[12, 13, 14, 15]

THE STRUCTURE OF PHTHALOCYANINES[3]

Phthalocyanine is a symmetrical macrocycle composed of four iminoisoindoline units with a central cavity of sufficient size to accommodate various metal ions (*e.g.* Cu^{+II}, Fe^{+II}, Ni^{+II}, Co^{+II}, Zn^{+II}, Mn^{+II}, Al^{+III}, Fe^{+III}, Si^{+IV}, Ti^{+IV}). This structure was confirmed later by X-ray diffraction techniques. It was noted that Pc is closely related to the naturally occurring porphyrin ring system, the differences being the four benzo-subunits and the nitrogen atoms at each of the four *meso* positions. Indeed, occasionally Pc is referred to as tetrabenzotetraazaporphyrin. Like the porphyrin macrocycle, Pc was assumed to exhibit aromatic behaviour owing to its planar conjugated array of 18 π-electrons, as predicted by Hückel's theory of aromaticity, published only a few years earlier.[16]

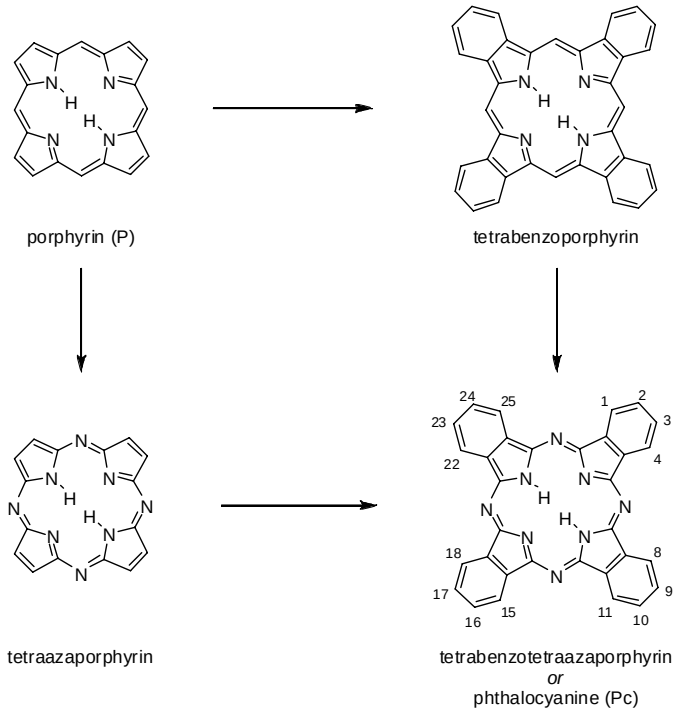

Figure 1 **Structural similarity of porphyrin (P) and phthalocyanine (Pc).**

PHTHALOCYANINE SYNTHESIS[3]

In addition to the structural description, Linstead's initial series of papers contained the experimental details for the preparation of Pcs from phthalodinitrile (*ortho*-dicyanobenzene), which is still considered the best precursor for Pc synthesis on a laboratory scale. Linstead conceived the name phthalocyanine as a combination of the prefix *phthal*, originally from the Greek *naphtha* (rock oil), to emphasise the association with its various phthalic acid-derived precursors, and the Greek *cyanine* (blue).

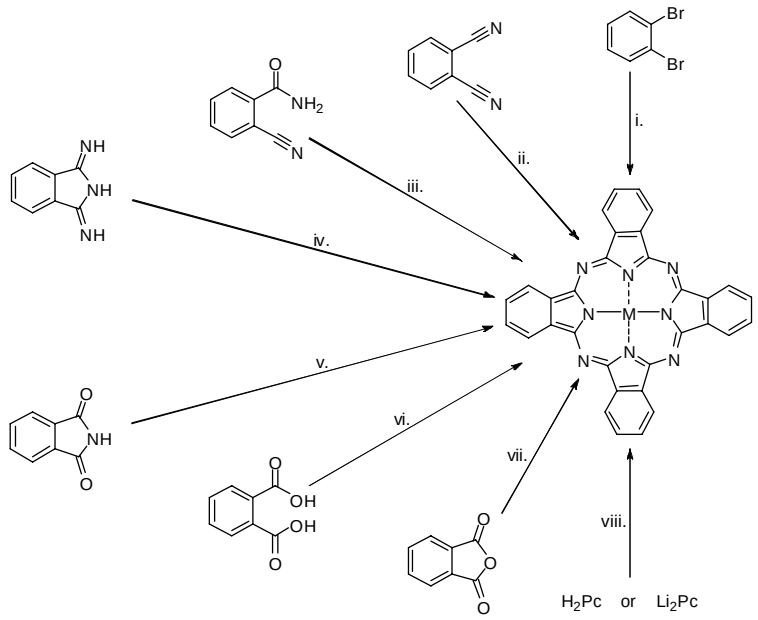

Scheme 1 **Synthetic routes to MPc. Reagent and conditions: i.) Large excess of $Cu^{(+I)}CN$ in conc. solution of refluxed DMF;[17] ii.) Solution of refluxed DMF with metal salt;[18] iii.) High-boiling-point solvent (*e.g.* quinoline) with metal salt at 205 °C;[19] iv.) In 2-ethoxyethanol with metal salt at 50 °C;[20] v.) Solvent free, in fused urea with metal salt at 160 °C;[21] vi.) High-boiling-solvent (*e.g.* nitrobenzene) with urea, metal salt NH_4Cl and AM at 180 °C;[22] vii.) In nitrobenzene with urea, metal salt and AM at 190 °C;[23] or in HMDS and DMF with metal salt and *p*-TsOH at 130 °C;[24] viii.) In refluxed quinoline with metal salt.[25]**

SUBSTITUTED PHTHALOCYANINES: AXIAL VS. PERIPHERAL

A Brief Note on Nomenclature for Substituted Pcs

A system of abbreviations is necessary to avoid the long-winded nature of Pc nomenclature demanded by the IUPAC system. Figure 1 shows the accepted numbering system of the Pc ring. There are sixteen possible sites for macrocycle substitution associated with the four benzo-subunits. The 2, 3, 9, 10, 16, 17, 23, 24 carbon atoms are termed the peripheral (*p*) sites and the 1, 4, 8, 11, 15, 18, 22, 25 carbon atoms are denoted the non-peripheral (*np*) sites. The abbreviation *t* signifies a peripherally tetra-substituted Pc, which is usually composed of four isomers.

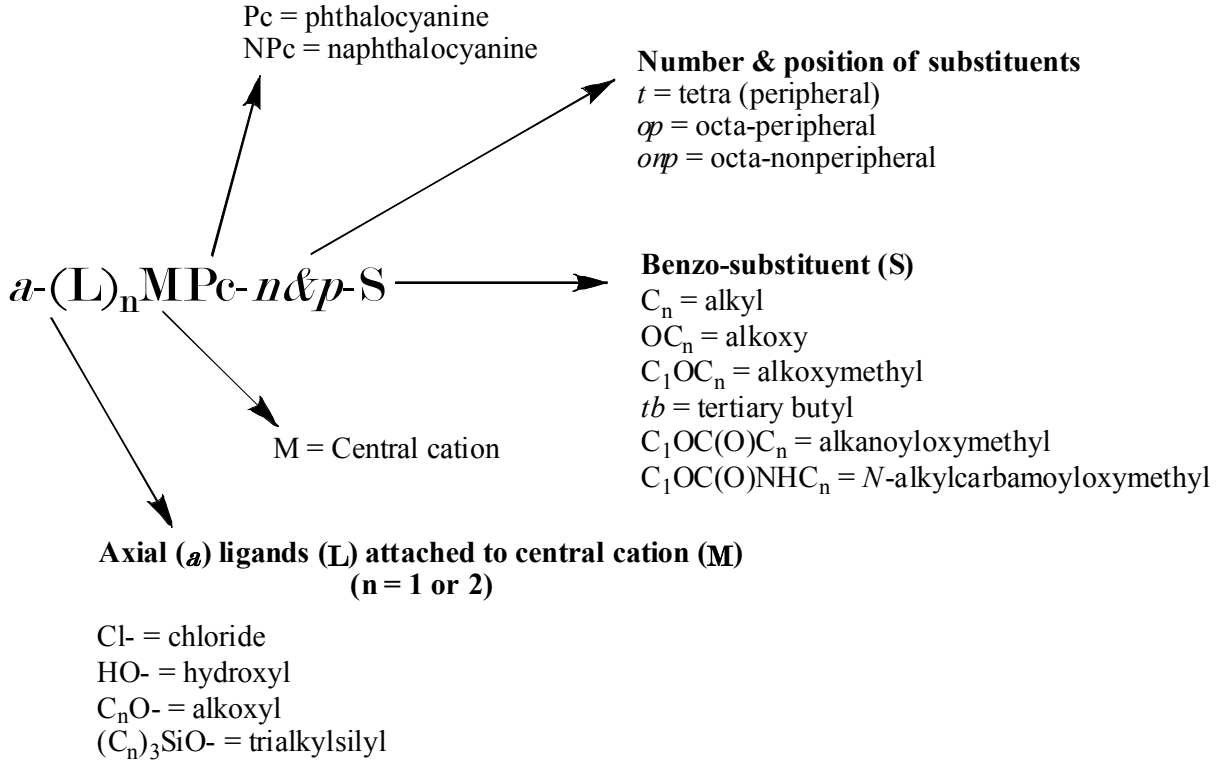

Figure 2 **Summary of phthalocyanine nomenclature.**

Solubility, a Challenging Issue in Pc Applications

As a matter of fact the insolubility of Pcs in most solvents is caused by the strong interaction of the π-electrons of their extended aromatic system and so called π-stacking. Averting these strong interaction increases solubility and can be facilitated by substituents in three ways:

1. axial substituents, by modulating the valence of the central metal.
2. peripheral substituents that are sufficiently space demanding.
3. non-peripheral substituents.

Generally, covalently bound axial ligands require the central metal ion to be at least in a +3 or +4 oxidation state. Examples with axial ligands are known from Al-, Si-, Ge- and Sn-Pcs among others and can only be attached after cyclotetramerisation, whereas the metal ion was utilized as a template. In addition, suitable ligands (*e.g.* pyridines) form coordination bonds with many central metal ions. This accounts for the enhanced solubility of MPcs in pyridine and quinoline.[26]

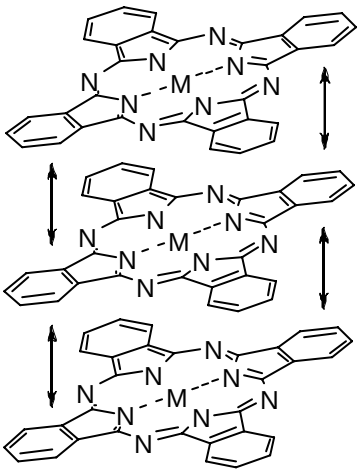

Figure 3 π-stacking of Pcs.

As already mentioned, the substitution pattern at the benzene moiety has a significant influence on solubility. Non-peripheral substituents are most effective in order to diminish π-stacking. Due to mutual sterical hindrance, the Pc is distorted out of plane, but to the expense of increased strain and partial loss of aromaticity in the molecule. In contrast, peripheral substituents have to be much more space demanding in order to prevent π-stacking. Advantageously, here out-of-plane distortion is minimal and resonance stabilization is maintained. Additionally, peripheral substitution offers ample chemical space for derivatization and optimization of properties. Therefore, in terms of medical application, biochemical interactions, isomerical uniformity and thus structure elucidation, a highly substituted *op*-Pc of C4 rotational-symmetry is mostly desirable.

Pcs, a Gift to Molecular Physics and their Applications

The remarkable stability of Pcs has resulted in their use in many landmark experiments in molecular physics. For many new experimental techniques, they have bridged the gap between crystalline inorganic materials (*e.g.* metals and ionic crystals) originally used to develop the specific methodology and its application to molecular materials. Hence, H_2Pc became the 'first organic structure to yield to an absolutely direct X-ray analysis'.[27]
Fields of research are wide spread of this extraordinary class of organic compound and are based upon the remarkable and significant physicochemical properties in:

- Optics
  (UV-vis, fluorescence[28], nonlinear optics – NLO[29])
- Electronic conductivity
  (sensors[30], charge-transfer complexes[31])
- Optoelectronics
  (photoconductivity[32, 33], light harvesting/photovoltaic[34], OLEDs[35], electrochromism[36])
- Catalysis[37]
- Adsorption[38]
- Magnetics[39]

PCs AS PHOTOSENSITIZER FOR PHOTODYNAMIC THERAPY[6, 7]

Definition of PDT

Photodynamic therapy is based upon the photodynamic effect, which may be defined as the destruction or damage of living structures by the combined action of a photosensitizer, visible or near visible light, and oxygen species.
An important part of this is that the radiation employed is not of high energy and that by itself (unlike X-radiation) it is virtually harmless to living matter. The expression of the photodynamic effect is sometimes referred to as "photodynamic action", and this is the term most often used historically, being a translation of the German “photodynamische Wirkung”.

Principles of Quantum Physics as Fundament for the Photodynamic Effect

The destruction of living tissue is ascribed to reactive oxygen species. Two main photooxidation pathways are possible, **Type I** (radical intermediates) and the well documented **Type II** (singlet oxygen) processes.

Mechanism of Type I *(radical intermediates)*

$$Sens \xrightarrow{h\nu} Sens^{*} \qquad \textbf{(eq. 1)}$$

Upon irradition with light of suitable wavelength (hν), excitation of the photosensitizer ($Sens$) leads to ($Sens^{*}$) which forms the neutral acceptor radical ($HA^{\bullet}$) by two possible mechanisms. Either *via* e-transfer to a negative charged acceptor-radical ($A^{\cdot -}$) and subsequent H^{+} acceptance, or directly *via* H-atom transfer.

$$Sens^{*} + A \xrightarrow{e\ \ transfer} Sens^{\cdot +} + A^{\cdot -} \qquad \textbf{(eq. 2)}$$

$$Sens^{*} + AH_2 \xrightarrow{H-atom\ \ transfer} Sens\,H^{\bullet} + HA^{\bullet} \qquad \textbf{(eq. 3)}$$

H^{+}

Reaction of neutral acceptor radicals ($HA^{\bullet}$) with ground state triplet oxygen ($^3O_2$), forms cytotoxic peroxide radicals which induce apoptosis in living cells and lead to tissue necrosis.

$$HA^{\bullet} + {}^3O_2 \longrightarrow HA-OO^{\bullet} \longrightarrow \textit{oxidized products} \qquad \textbf{(eq. 4)}$$

Mechanism of Type II *(singlet oxygen)*

In the chemical literature of photooxygenation processes, employing the widespread porphyrin photosensitizers, *e.g.* zinc(II) tetraphenylporphyrin, the Type II (singlet oxygen) reaction is well documented. Herein, the principle of photodamage in PDT is explained by the following processes [where P = photosensitizer; S_0, S_1 …ground, first excited, singlet states; T_0, T_1 …ground, first excited, triplet states; *isc* = intersystem crossing; $^3O_2$ = ground state triplet dioxygen; $^1O_2$ = first excited singlet state of dioxygen ($^1\Delta_g$)].

$$Sens(S_0) + A \xrightarrow{h\nu} Sens(S_1) \xrightarrow{isc} Sens(T_1) \qquad \textbf{(eq. 5)}$$

The photosensitizer becomes excited to S_1 by absorption of light. *Via* intersystem crossing, the photosensitizer reaches the rarely occurring first excited singlet state (T_1). The probability to reach T_1 increases with the lifetime of S_1.

$$Sens(T_1) + {}^3O_2 \longrightarrow Sens(S_0) + {}^1O_2 \qquad \textbf{(eq. 6)}$$

Due to the very unlikely direct "vertical" conversion from T_1 to S_0, its lifetime is quite long. This augments the chance to hit a molecule whose ground state is a triplet state too. Thus, energy exchange can occur from $Sens(T_1)$ to $^3O_2$ according to equation 6.

$$Biomolecule + {}^1O_2 \longrightarrow oxidized\ product \qquad \textbf{(eq. 7)}$$

Advantageously, with respect to its conversion in the ground state, lifetime of the excited oxygen – ${}^1O_2$ – is extraordinarily prolongated. Because of its high reactivity, ${}^1O_2$ exhibits high cytotoxicity, which can be used to destroy tumor cells.
During this cycle of excitation and relaxation Sens(S_0) → Sens(S_1) → Sens(T_1) → Sens(S_0), the photosensitizer works as catalyst and continuously generates singlet oxygen during irradiation.

The Basic Process in Tumor PDT

The photosensitizer is administered, usually by intravenous injection, although oral o topical administration has also been used. After an interval of approx. 3 – 96 h (the drug – light interval), meanwhile bio-distribution of the substance takes place, the tumor is irradiated with a measured dose of red light, in a wavelength matching the absorption band of the photosensitizer.

The selectivity of damage depends on two main factors:

- the selectivity of the sensitizer for localization in the tumor and consequently low concentrations with respect to localization in normal tissues; and
- the topological, *i.e.* anatomical direction of the light beam (usually a laser)

Visible light in the red region is preferred because biological tissue absorbs and scatters much less than at shorter wavelengths, so that the desired tissue penetration is enhanced.[40]

Introduction to Physical Effects of Fluorescence

A typical Jablonski diagram (Figure 4) illustrates a singlet ground electronic state (the parallel black bars labeled $\mathbf{S_0}$), as well as singlet first excited state ($\mathbf{S_1}$; upper set of parallel green bars) and the triplet first excited state ($\mathbf{T_1}$; upper set of parallel blue bars). At each energy level, fluorophores can exist in a number of vibrational energy levels, which are represented by the multiple lines in each electronic state. Transitions between states are depicted by an arrowhead (representing an electron) followed by a vertical line that traverses the region between the ground and excited state. The electronic transitions are almost instantaneous in nature, often occurring in timeframes ranging from nano to sub-pico seconds.

When a fluorophore absorbs light energy, it is usually excited to a higher vibrational energy level in the first excited state ($\mathbf{S_1}$) before rapidly relaxing to the lowest energy level (A→F). This event, from the upper to lower bars in ($\mathbf{S_1}$), is termed vibrational relaxation or internal conversion and occurs in about a picosecond or less. Fluorescence lifetimes are typically four orders of magnitude slower than vibrational relaxation, giving the molecules sufficient time to achieve a thermally equilibrated lowest-energy excited state prior to fluorescence emission.

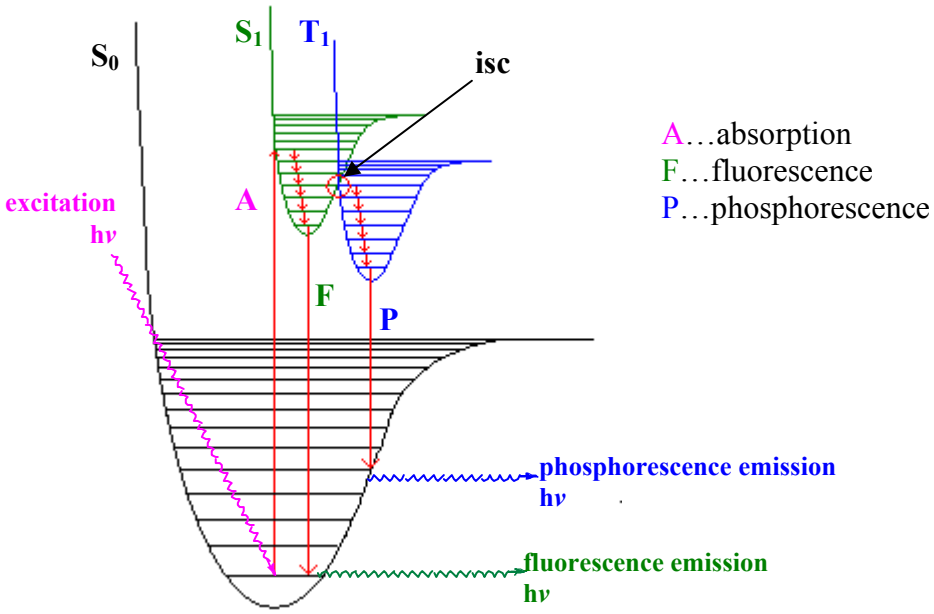

Figure 4 **Jablonski diagram, principle of excitation and emission.**

Phosphorescence decay is similar to fluorescence, except the electron undergoes a spin conversion into a "forbidden" triplet state ($\mathbf{T_1}$) instead of the lowest singlet excited state, a process known as intersystem crossing (**isc**). Emission from the triplet state occurs with lower energy relative to fluorescence; hence emitted photons have longer wavelengths.

Phthalocyanines for Photodynamic Therapy

Serveral substances are known as chromophores and photosensitizer respectively, which absorb light in the visible region, as exemplified in Figure 5.[6] Phthalocyanines are attractive compounds for PDT applications with regard to photophysical properties, as they display strong absorption bands with a high decadic molar absorption coefficient ($\varepsilon > 10^5$ L/mol·cm) in a range of 655 to 752 nm, which refers to red light.[23, 3] As afore mentioned (p. 17), this spectral band is predestined for PDT.

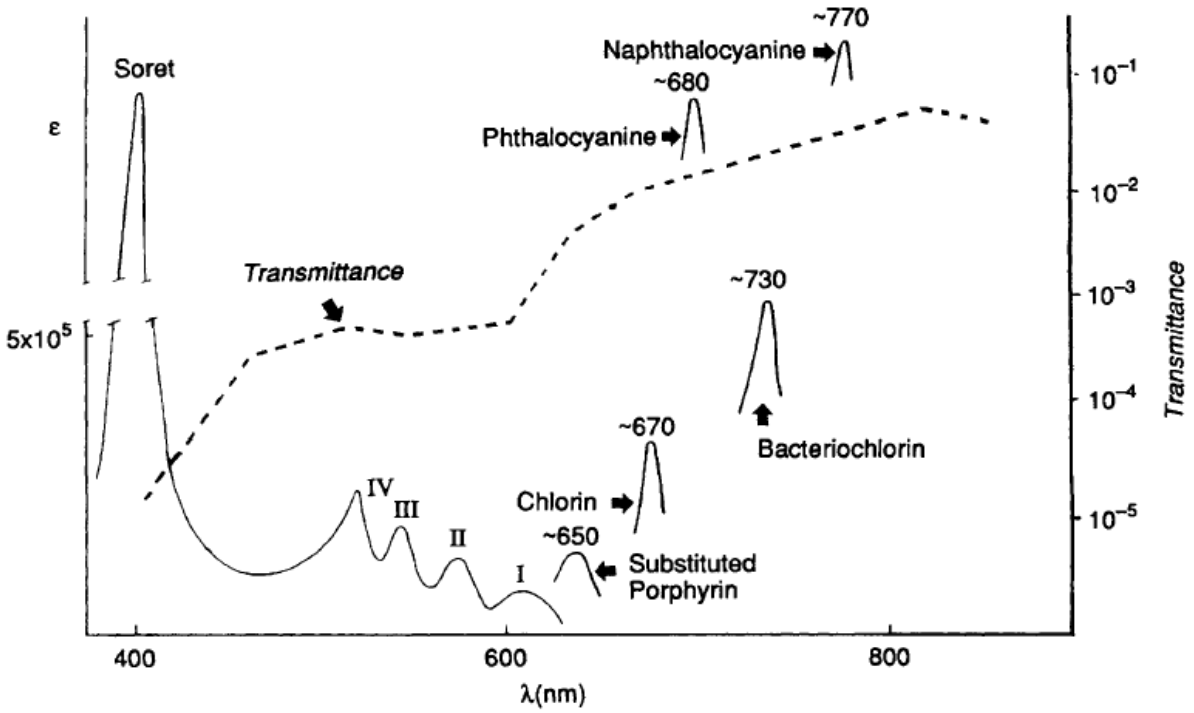

Figure 5 **Photosensitizer absorbance in relation to tissue transmittance. The absorption spectra are schematic: only Band I is shown, except for the porphyrin absorption spectrum on the left. The transmittance curve (– – – –) refers to a sample of human scrotal sac, 7 mm thick.[40] The broad feature at 500 – 600 nm is attributed to absorption by haemoglobin.[6, 7]**

However, solubility properties are poor: for example, phthalocyanine (H_2Pc) and copper(II) phthalocyanine (CuPc) are almost insoluble in common solvents (except concentrated sulphuric acid). Solubility in organic solvents can be improved by alkyl substitution – thus, zinc(II) octapentylphthalocyanine (ZnPc-*op*-C_5H_{11}) is more soluble in organic solvents, and more effective as a PDT agent, than is zinc(II) phthalocyanine (ZnPc) itself.[41] Nevertheless, it still has to be administered *in vivo* as a suspension or as an oil-based emulsion.

Solubility in aqueous media can be conferred *e.g.* by sulfonation. Expectedly, sulfonation of chloroaluminium(III) phthalocyanine (*a*-(Cl)AlPc) gives a complex mixture of mono to tetra sulphonic acids which can be separated by HPLC.[42] A mixture – mainly consisting of the di- and tri-sulphonic acids – has been clinically used in Russia, under the trade name "Photosens" for the PDT of cancer for some years.[43]

Although many of the Pc syntheses (and especially those starting with diacids or anhydrides and metal salts in the presence of urea as an ammonia source) require rather forcing conditions, it has been shown that metal free phthalocyanines can be obtained in acceptable yields – albeit slowly – from phthalonitriles using lithium metal in l-octanol at room temperature.[44, 45]

Phthalocyanines which can be synthesised by currently available methods have been sufficiently numerous to demonstrate the potential of these systems as PDT agents, not only in oncological applications[43] but also as photovirucides in the sterilisation of blood products.[46] Nevertheless it would be useful, both here and in electroactive materials applications, to have more flexible stepwise syntheses at hand, such as already achieved in the related porphyrin chemistry.[47] Although some attention has been paid to this strategy[48, 49, 50, 51] a flexible step-by-step synthesis of broad scope is still needed.

A BRIEF HISTORICAL REVIEW OF PHOTODYNAMIC THERAPY

1st Generation Photosensitizers

It was found that the activity of Haematoporphyrin (HpD) as multicomponent relies more on poorly characterized oligomers than on well-defined monomers of porphyrins. The commercially produced photosensitizers – Photofrin, Photosan, Photogem, and Photocarcinorin – were partially purfied by HPLC or gel permeation chromatography in order to remove biologically inactive monomeric fractions.

Although HpD and its commercial variants have been used extensively in experimental clinical work, these 1st generation photosensitizers have three important disadvantages:

1. They are not very selective, and cause skin sensitization for some weeks.

2. The absorption band in the red, refered to Band I at *ca.* 630 nm (Figure 5), is weak, *i.e.* the material is not a good absorber of the stipulated red light.

3. They are complex and variable mixtures from which it has not proved possible to isolate a single highly active constituent, and which probably does not contain one. The complexity of the mixture arises from both positional isomerism and stereoisomerism (up to 60 peaks in capillary electrophoresis).

Nevertheless, Photofrin®, plays doubtlessly an important role in PDT.
The first clear-cut observations of activity were made with this material, and the first regulatory authorizations for clinical use were obtained on its behalf (Canada, 1993 by QLT PhotoTherapeutics Inc., Vancouver).[52]

2nd Generation Photosensitizers

To meet the shortcomings of 1st generation photosensitizers design criteria for 2nd generation photosensitizers were postulated:

a) Single Substance

The candidate should comprise of a single isomer, as an undeniable prerequisite for the interpretation of dose-response relationships in an extraordinary complex setting in relation to the light treatment (drug-light interval, wavelength, total energy, fluence rate, continuous or intermittent) and finally for clinical approval.

b) **A**dsorption, **D**istribution, **M**etabolization, and **E**xcretion - **T**oxicity (ADME-T)

Any drug, orally administered to a living organism, is subjected to adsorption, distribution, metabolization, and excretion during exhibition of its pharmacokinetic action. Furthermore, low toxicity is of utmost importance. Therefore, the so-called ADME-T properties of a drug are determinant for the pharmacokinetic behaviour of a drug in an organism. In addition to suitable ADME-T properties, particularly selectivity with regard to effective tumor photonecrosis and dark toxicity dictates the therapeutic window. Any generalized photosensitivity remaining after the treatment should be minimal.

c) Solubility

As with conventional drugs, pharmacokinetic and localization properties depend largely on the solution physical chemistry of the substance, and amphiphilic character appears to be important here. Since the heterocyclic nuclei under consideration are generally hydrophobic, it is often hydrophilic substitution that is looked for.

d) Photophysical Parameters

For use in the diagnostic mode, the fluorescence quantum yield (Φ_S) is critical. For therapeutic applications – following the hypothesis that singlet oxygen is the active principle (p. 16) – the energy of the first excited triplet (E_{T_1}) of the sensitizer needs to be greater than 94 kJ/mol (the energy of the singlet state of dioxygen $^1\Delta_g$). Additionally, the overall quantum yield of singlet oxygen (Φ_Δ) should be higher than 0.3. This is achieved,

when the quantum yield on generating the triplet state (Φ_T) of the sensitizer as well as its lifetime is sufficient.

e) Red Absorption

As mentioned earlier (p. 17), strong absorption in the red region is advantageous, because mammalian tissue absorbs and scatters much less in the red than at shorter wavelengths (Figure 5).

Because criterion (e) has been of considerable significance in guiding recent synthetic work, specific attention will be payed on longest wavelength absorption (Band I) for the various systems.

Table 1 **Photosensitizer under development (*a.d.* 1995).**

Company	Head Office	Photosensitizer	Structure
Ciba Geigy/QLT	Basel/Vancouver	$Zn^{(+II)}$ phthalocyanine	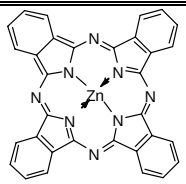 $Zn^{(+II)}$ phthalocyanine
Cytopharm/partner	Manlo Park, California	Porphycenes	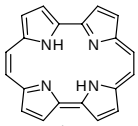 porphycene
DUSA (Deprenyl, USA)	Toronto	6-ALA	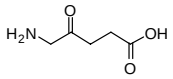 δ-aminolaevulinic acid
Nippon Petrochemical	Tokyo	Monoaspartyl chlorine 'MACE'	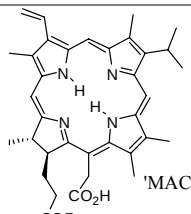 'MACE' R = (*L*)-NHCH(CO_2H)CH_2CO_2H
PDT Inc.	Santa Barbara, California	Purpurins (*e.g.* Sn etiopurpurin)	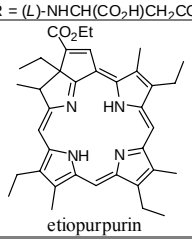 etiopurpurin
Pharmacyclics	Palo Alto, California	Texaphyrins	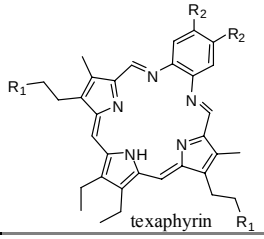 texaphyrin
Quadra Logic Technologies	Vancouver	Benzoporphyrin Derivative	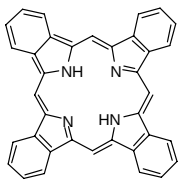 benzoporphyrin
Scotia Pharmaceuticals	Guildford, England	*m*-THPC	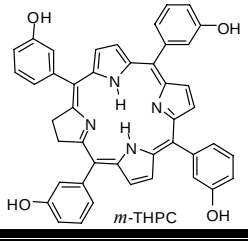 *m*-THPC

PHARMACOKINETIC DEMANDS ON DRUG-LIKE COMPOUNDS

According to the well esteemed and established Lipinski's 'Rule Of 5',[53] an orally active "drug-like" compound has to exhibit certain properties with regard to absorption and permeation.
Experimental and computional approaches predict that absorption or permeation is more likely when there are:

1. *not more than **5** hydrogen bond donors (OH and NH groups).*
2. *not more than 2×**5** hydrogen bond acceptors (notably N and O).*
3. *a molecular weight under **5**00 g/mol.*
4. *a partition coefficient log P less than **5**.*

Endocytosis – the Way Through Cell Membranes for Large Molecules[54]

For molecules not obeying these rules, it is almost impossible to penetrate through cell membranes by passive transport. Consequently, in order to achieve intracellular concentrations of these substances, a phenomenon called active transport (or synonymously active uptake) has to be triggered. Here, unlike passive transport, the crossing of the cell membrane requires the expenditure of cellular energy, often in the form of ATP, to move molecules "uphill" against a concentration gradient or electric potential.
One of the most important and specific active transport mechanisms is a process called endocytosis. The transport of macromolecular and colloidal carriers from the cell surface to lysosomes starts with endocytosis. Generally, endocytosis occurs by multiple mechanisms that fall into two broad categories, 'phagocytosis' (the uptake of large particles) and 'pinocytosis' (the uptake of fluid and solutes).
Phagocytosis is typically restricted to specialized mammalian cells like macrophages, whereas pinocytosis occurs in all cells.

All in common is that cells absorb material (molecules such as proteins) from the outside by engulfing it with their cell membrane. It is used by all cells of the body because most substances important to them are large polar molecules, and thus cannot pass through the hydrophobic plasma membrane. For the purpose to initiate active transport (energy consuming) *via* endocytosis, receptors on the cell membrane have to be stimulated by recognition. Besides other pathways into a cell, the receptor-mediated endocytosis is probably the most efficient one for the specific uptake of macromolecules. Receptor-mediated endocytosis enables an increase of the intracellular concentration of macromolecules up to 1000-fold.

Stimulation by biomolecules

Four major classes of endogenous, modulating molecules – proteinogenic as peptides and proteins, lipidic as lipids and steroids, nucleic acids, and carbohydrates – have been found to be involved in receptor mediated events. The carbohydrate based mechanisms are still the most enigmatic and consequently the pace of development of carbohydrate-based therapeutics has been relatively slow.[55]

Carbohydrates

Carbohydrates play a crucial role in various utmost important biological mechanisms. In general, energy metabolism as *e.g.* glycolysis, Krebs cycle, or gluconeogenesis is well understood. In contrast, the knowledge about carbohydrates as constitutive elements in structural support matrices of plants, *e.g.* in celluloses, lignans, glycans *etc.* and even more as part of glyco-proteins, glyco-lipids, and other conjugates is still very incomplete. The latter are key elements in signaling, cell–cell communication, and molecular and cellular targeting[55, 56, 57, 58], in processes, such as *e.g.* in bacterial and viral infection, cancer metastasis, and inflammatory reactions. As a result, most of the detailed studies of bacterial and viral interactions to date involve lectin–sugar interactions, and not protein–protein ones.[59]

Lectins – sugar-binding proteins

Lectins displayed on the surface of a cell,

- allow oligosaccharides to respond to a variety of external stimuli such as the local concentration of nutrients (chemotaxis).
- allow them to bind and localize cells, displaying appropriate saccharides, a process typified by an early step of inflammatory response: E- and P-selectins, mammalian lectins displayed on the endothelial cell surface following cytokine stimulation, bind sialyl Lewis^x (sLe^x; NeuAcα2,3Galβ1,4(Fucα1,3)GlcNAc) and related oligo-saccharides displayed on circulating leukocytes, leading to the attachment and eventual migration of the leukocyte into the surrounding tissue.
- allow cells to select and take up glycosylated molecules or microorganisms.[55]

Tumor metastasis is proposed to occur in some cases by the same targeting pathway that leukocytes use: binding to endothelial cells through the sLe^a- or sLe^x-selectin interactions, ultimately followed by extravasation.[60]

Unfortunately, saccharides often do not make good therapeutic agents for a variety of reasons. Many natural saccharides are rapidly degraded by digestive, plasma, and cellular glycosidases, and frequently bind to their targets with low affinities, though polyvalency can be used to improve the low-affinity carbohydrate–receptor interactions on cell surfaces.[55, 59]

POLYVALENT INTERACTIONS[59]

Functional Advantages of Polyvalent Interactions

Polyfunctional interactions are characterized by the simultaneous binding of multiple ligands on one biological entity (a molecule, a surface) to multiple receptors on another. These interactions occur throughout biology, and have a number of characteristics that monovalent interactions do not. In many cases, biological systems seem to use polyvalent interactions rather than an equivalent number of monovalent ones, or one very strong monovalent one, because of certain functional advantages.

In principle, the strength of polyvalent interactions can be collectively much stronger than can be reached by a single interaction (monovalent) between a ligand of low molecular weight and a protein, regardless of cooperativity. They can provide the basis for mechanisms of both agonizing and antagonizing biological interactions that are fundamentally different from those available in monovalent systems.[55]

- The tightest known association for a single interaction (monovalent) between a receptor and a small organic ligand is that between biotin and streptavidin ($K^{mono} \approx 10^{15}{}_{M^{-1}}$).[61, 62]
- The polyvalent binding of the most potent, trivalent, naturally occurring oligosaccharides presenting three GalNAc groups to the C-lectin asialoglycoprotein receptor (ASGP-R) on the surface of hepatocytes occurs with $K_{avg}^{poly} = 10^{8}{}_{M^{-1}}$, even though for simple galactose $K^{mono} \approx 10^{3}{}_{M^{-1}}$.[68]

Binding of Polyvalent Molecules to Cells: Bacteria, Antibodies, and Macrophages

Studying the potency of polyvalent molecules, the interaction of antibodies is exemplary and essential to understand the effectiveness.

All classes of antibodies – one of the key groups of proteins making up the immune system – have multiple equivalent receptor sites:

- two (IgD, IgE, IgG, IgA),
- four (IgA),
- six (IgA), or
- ten (IgM).

Polyvalent binding to the structures that these antibodies recognize – antigens or other ligands present on the surfaces of bacteria, viruses, parasites, drugs, "nonself" cells, or other structures including noncovalent complexes not usually present in the blood circulation – seems to be an ubiquitous characteristic of immune recognition.

These interactions may both,

- inhibit processes important to infection (*e.g.*, attachment of a foreign organism to target cells) and
- promote clearance (removal of the foreign particles either by degradation by macrophages and other components of the immune system, or by filtration by the kidney).[63]

Polyvalency is used here for high-affinity binding to surfaces that have repeated epitopes, a defining characteristic of the surfaces of almost all invading pathogens.

Graduated Response

The strength of a signal in a polyvalent system can vary greatly, depending on the number of ligand–receptor pairs that participate. To a first approximation, strength might correlate with number of surface receptors. This capability to generate a broad range of signal strengths (much broader than the binary "on" and "off" of a single ligand occupying a single receptor site) might, in principle, provide a capability to generate a graded (or graduated) response to a biological signal. One example of this type of graded response might be the clearance of pathogens by antibody-mediated attachment to macrophages (Figure 6). Where a single antibody is unable to cause a macrophage to ingest a pathogen (macrophages do not effectively bind to a single antibody), two antibodies can lead to ingestion. More antibodies should further strengthen the degree of polyvalency between pathogen and macrophage, and subsequently increase the likelihood that the pathogen will be recognized and cleared.

Polyvalency provides a mechanism for recognition:

Most pathogens have surfaces that present multiple copies of an epitope. Thus nonspecific adhesion of one receptor on the antibody to a non-polyvalent target on a native (self) surface would not lead to tight, polyvalent adhesion to that surface. Furthermore, macrophages fail to recognize pieces of pathogen if they bind to only a single antibody, but do recognize whole pathogen when it binds to multiple antibodies.

The interaction of a *single* Fc region with its receptor seems to be too weak to induce a response by the macrophage; that is, free (uncomplexed) antibody in solution does not activate macrophages, nor does a single antibody bound to a degraded piece of foreign pathogen.
However, *multiple* antibodies bound to the surface of an infecting particle do interact strongly with multiple receptors on the surface of the macrophage, and give a three-layered structure stabilized at both interfaces through polyvalent interactions (Figure 6).[64, 65, 66]

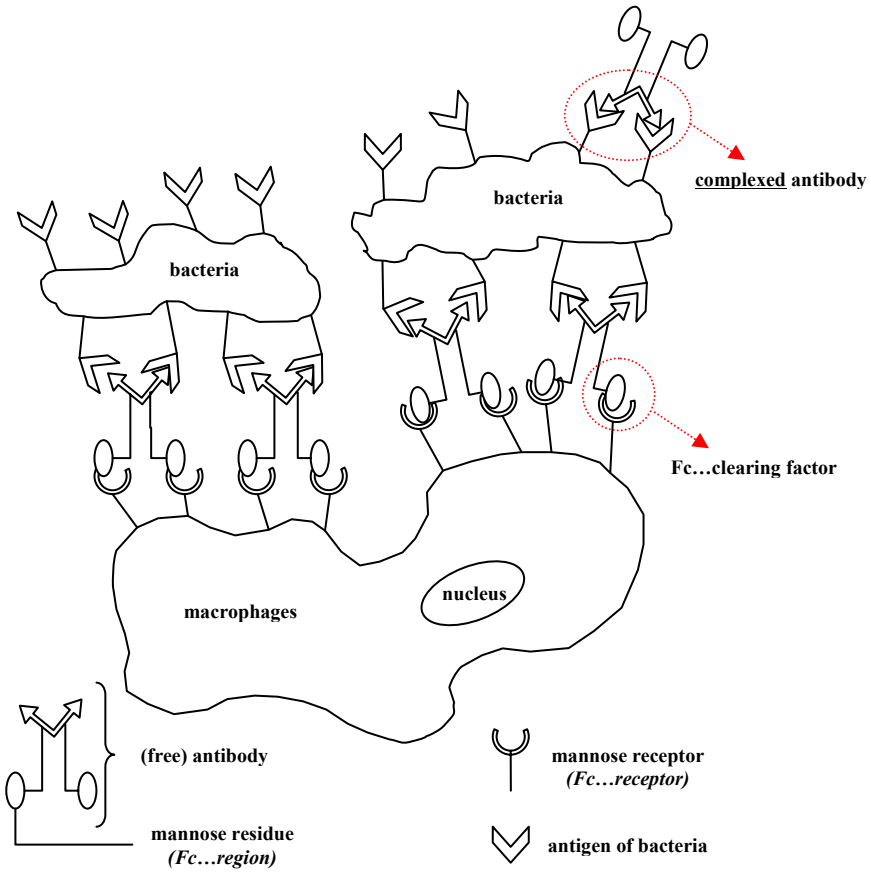

Figure 6 **Clearance of pathogens by antibody-mediated attachment to macrophages: An bacterium coated with IgG *antibodies* is eliminated from the circulation ("cleared") through phagocytosis by a macrophage or neutrophil: The surface of the macrophage has *Fc receptors* that recognize the *Fc region* of IgG molecules. The multivalent binding of the antibody-coated bacterium (or virus) to multiple *Fc receptors* of a macrophage activates the phagocytotic process. Unbound IgG does not bind effectively to the *Fc receptors* on the macrophage. The representations are not drawn to scale.[59]**

Furthermore, not only does polyvalency in this system permit stability and specificity in the recognition of a bacterium by a macrophage, but subsequent action by the macrophage is also critically dependent on polyvalent interactions. Multiple interactions between the macrophage and the antibody-coated bacterium lead to a cross-linking of the surface receptors on the macrophage, triggering an internal signal in the macrophage to ingest (phagocytose) the bacterium, which then leads to its degradation.[67]

ENERGETICALLY CONSIDERATIONS REGARDING POLYVALENCY

Cooperativity

Definition

$\alpha = \frac{\lg(K_N^{poly})}{\lg(K^{mono})^N}$ = the degree of cooperativity.

Classes of polyvalent interactions are

- positively cooperative ($\alpha > 1$, synergistic),
- noncooperative (additive), or
- negatively cooperative ($\alpha < 1$, interfering), respectively.

The best studied positively cooperative systems ($\alpha > 1$, synergistic) in biology, the binding of four O_2 molecules to tetrameric haemoglobin, does not involve polyvalency.
There are presently no convincingly characterized examples of positive cooperativity for polyvalent systems in the literature. As a class, polyvalent interactions have not been quantified sufficiently frequently or carefully for positive cooperativity to be inferred unambiguously in even one system.

Positively cooperative (synergistic, $\alpha > 1$)

As a putative example of a positively cooperative polyvalent interaction, the association of pentameric cholera toxin with GM1, an oligosaccharide portion of the GM1 ganglioside has been studied.
It was found that

- the entropy of the first binding event of a monomeric GM1 derivative to pentameric cholera toxin is equal to the entropy of each subsequent binding event and
- the binding constant of the first ligand was lower than the binding constant of the second by a factor of four.

Calculated purely statistically, the binding constant of the first ligand would be expected to be greater by a factor of 5/2 than the second binding constant. It was concluded that the binding was enhanced enthalpically.

Negatively cooperative (interfering, α < 1)

A probably negatively cooperative example was found when Lee *et al.*[68] studied the binding of di- and trivalent galactose-containing ligands that bind C-type lectins[69] on the surface of hepatocytes[68]; the density of these receptors is unknown.

Table 2 **Binding of mono-, bi-, and trivalent Gal-terminated oligosaccharides to C-type mammalian hepatic lectins.[59, 69]**

Oligosaccharide	*K* for complex of lectin/Gal-oligosaccharide (M^{-1})
Gal(β1)OMe	$K^{mono} = 7 \times 10^4$
Gal(β1,4)GlcNAc(β1,2) Gal(β1,4)GlcNAc(β1,4) Man	$K_2^{bi} = 3 \times 10^7$
Gal(β1,4)GlcNAc(β1,2)Man(α1,6) Gal(β1,4)GlcNAc(β1,2)Man(α1,3) Man Gal(β1,4)GlcNAc(β1,4)	$K_3^{tri} = 2 \times 10^8$

$K^{mono} = 7\ x\ 10^4{}_{M^{-1}}$

$K_2^{bi} = 3\ x\ 10^7{}_{M^{-1}} = 420\ K^{mono}$

$K_3^{tri} = 2\ x\ 10^8{}_{M^{-1}} = 2800\ K^{mono}$

Since $K_2^{bi} < (K^{mono})^2$ and $K_2^{tri} < (K^{mono})^3$ these di- and trivalent ligands also bind with negative cooperativity. These illustrate an important characteristic of polyvalent interactions: Even though bivalent binding in these cases was negatively cooperative, the measured affinity for a bivalent molecule was much higher than for the monovalent molecule. Tight binding does not require positive cooperativity in the sense that this phrase is traditionally used.

Entropy of interaction

Incomplete understanding of entropy in the design of polyvalent inhibitors has resulted in many synthetic polyvalent molecules that are less effective or only marginally more effective than their monovalent counterparts are. The many bivalent systems joined by flexible linkers (*e.g.* oligo(ethylene glycol) or polymethylene) provide examples of systems that can almost be guaranteed to fail for entropic reasons.[70, 71]

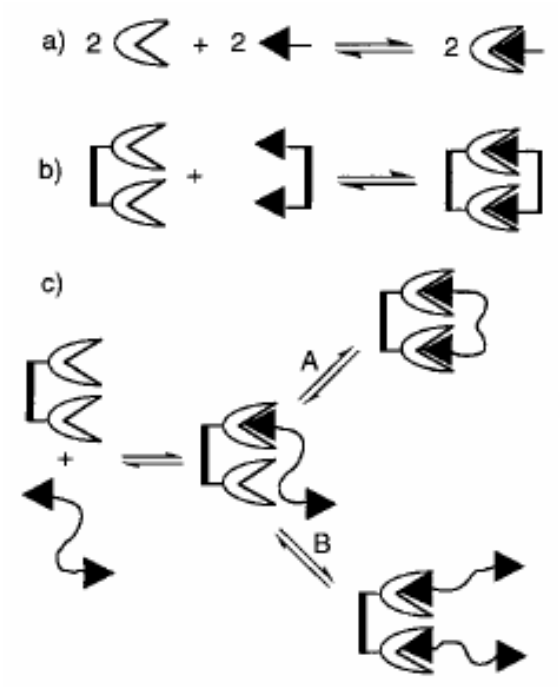

entropy

$$2\Delta S_{trans}^{mono} + 2\Delta S_{rot}^{mono}$$

$$\approx \Delta S_{trans}^{mono} + \Delta S_{rot}^{mono}$$
(maximaly entropically enhanced)

only path A: entropically enhanced

$$\approx \Delta S_{trans}^{mono} + \Delta S_{rot}^{mono} < \Delta S_{conf}^{mono}$$

$$\sum_{path\ A} \approx \Delta S_{trans}^{mono} + \Delta S_{rot}^{mono} + \Delta S_{conf}^{mono}$$

path A & B equal: entropically neutral

$$\approx \Delta S_{trans}^{mono} + \Delta S_{rot}^{mono} = \Delta S_{conf}^{mono}$$

only path B: entropically diminished

$$\approx \Delta S_{trans}^{mono} + \Delta S_{rot}^{mono} > \Delta S_{conf}^{mono}$$

Scheme 2 **Relationships among translational, rotational, and conformational entropies for a divalent system with rigid or flexible linking groups.[59]**

Characteristics of Polyvalent Interactions in Biology

Clearance mechanism of hepatocytes to desialylated blood cells (erythrocyte)

A number of other cell-cell interactions may occur polyvalently. One example may be the clearance of nonsialylated cells from the blood by the liver (Figure 7). Lee *et al.*[72] have examined extensively the role of polyvalency in the association of synthetic di- and trivalent galactose-containing ligands to C-type lectins on the surface of hepatocytes.[72]

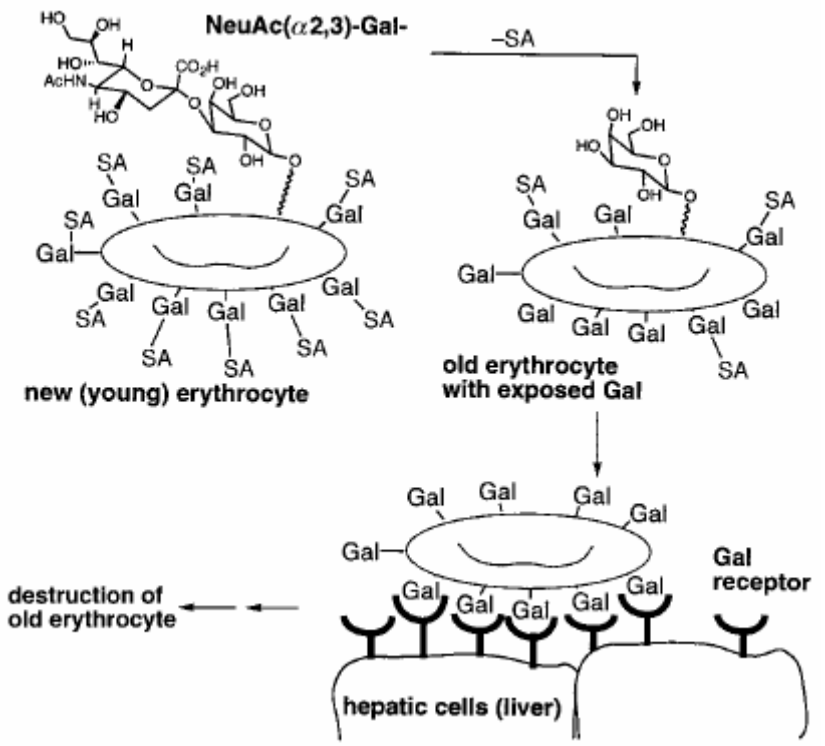

Figure 7 **Clearance of non-sialylated erythrocytes from the blood by liver.[59]**

An example of a cell that becomes progressively desialylated, as a reflection of age, is the red blood cell (erythrocyte). Desialylation exposes a galactosyl group, and occurs as a consequence of the hydrolytic action of different neuraminidases, both free in the blood and bound to endothelial cells that line the interior of the blood vessels. The probability of hepatic clearance may be correlated with the interaction energy between the surfaces of the hepatic cell and the erythrocyte. As the density of galactosyl ligands on the surface of the erythrocyte increase, the interaction energy also increases. Thus as red blood cells age, the density of the

'clearance signal' on their surface increases until the interaction energy between its surface and that of the hepatocyte is sufficiently high for promoting adhesion and clearance. The resulting lifetime of a typical red blood cell in human blood circulation is 120 days. It is suggested that polyvalency may, in this instance, be used as part of a timer that enables the body to judge the age of erythrocytes and select those that are old enough to be removed from circulation and be destroyed.[59] Afore mentioned high affinity of the ASGP-receptor to galactose bearing entities makes this specific receptor as a convenient fundament to test the activity of galactosylated drug like compounds.

ASGP-RECEPTOR[73]

The asialoglycoprotein receptor (ASGP-R) is the first mammalian lectin discovered in humans.[74] Originally described as a hepatic lectin (HL), ASGP-R is a heterodimeric membrane protein that binds and internalizes glycoproteins with terminal galactosyl residues hence mediates clearance of serum glycoproteins containing from the circulation (Pricer *et al.* 1974).[75] However, besides this primary function, ASGP-R has been also linked to other activities like binding and uptake of various pathogenic viruses, such serving as a putative cellular receptor for the hepatitis B[76] and Marburg virus[77] as well as mediating erythroagglutination[78] and others, which all use this membrane protein to enter and infect host cells.[73]

Further studies have confirmed its expression primarily to the sinusoidal face of liver plasma membranes. Its physiological functions have been further proposed to be involved not only in the binding and subsequent internalization of desialylated serum glycoproteins but also in the disposal of cellular fibronectin as well as in the metabolism of hepatic lipoproteins, and in the clearance of serum IgA.

While ASGP-R is primarily expressed on liver cells, there have been reports on ASGP-R expression in extra-hepatic cells, including human bone intestine, testis and kidney (Seow *et al.*)[79]. Nowadays, the ASGP-R system is also considered as a novel approach for targeted gene or drug delivery into liver cells.[80, 81]

HEPG2

The human hepatoma cell line HepG2, that is known to express ASGP-R to a high level,[82] has a high affinity towards galactosyl moieties (as well as to GalNAc). This has been recognized and exploited by several researchers.[9, 83, 84, 85, 86, 87]

It was already demonstrated by Plank *et al.*[88] in 1992 that gene transfer into hepatocytes (*e.g.* HepG2) using ASGP-R mediated endocytosis of DNA complex with an artificial tetra-antennary galactose ligand was possible.

According to several publications, this cell line can be used for fundamental tests on the specific uptake of galactosylated dendritic structures. Furthermore, the use of HepG2 cells as a standardized model would allow me to compare my glycosylated molecules, described in this work, with these of Ng *et al.*[8, 9, 28, 83, 89, 90, 91]by *in Avitro* tests *via* spectroscopic methods.

OBJECTIVE

Phthalocyanine (Pc) and its derivatives constitute one of the most studied classes of organic functional materials. In addition to their widespread use as blue and green colorants, substituted phthalocyanines (Pcs) have found broad use in technical applications already[3] and are of increasing interest for applications in nonlinear optics (including optical limitation),[29] xerography (as photoconductors),[92] liquid-crystalline electronic charge carriers[93, 94] and exciton-transport materials,[95] optical data storage (as the laser absorption layer within recordable discs),[1] photodynamic cancer therapy,[96] solar energy conversion,[97, 98] catalysis[99] and as the active component of gas sensors.[100]
In addition, phthalocyanines are of growing interest in medicine as diagnostics and therapy, namely for magnetic resonance imaging[101] and photodynamic therapy (PDT) respectively.[6, 7, 8, 9, 83, 91]
A serious obstacle on the way to a successful application is satisfactory solubility in either aqueous or organic solvents. This can be achieved by substituents attached axial to the coordinated central metal atom or on the four vacant positions of the four benzene rings of the Pc-core (Figure 1).
Due to the drastic conditions applied during the cyclotetramerization reaction – generally not below 100 °C –[102] to form the extra ordinary stable, extended aromatic system of Pcs from four monomers, only a limited number of substituents on the monomer are reasonable.

Generally, assumed "bioactive" substituents of the monomer like carbohydrates, proteins and nucleosides or even unsaturated hydrocarbons may be considered critically in their stability and may lead to significant side reactions, *e.g.* degradation.

Subsequent modifications on the Pc-core are characterized by severe drawbacks, due to limited solubility of the parent Pc-core.

Therefore, a synthetic route allowing diverse coupling reactions on a modified Pc-scaffold, would be advantageous.

With respect to the listed demands for an ideal 2nd generation photosensitizer[6, 7] (p. 22) for PDT and the requirements for polyvalent interactions in biological systems (pp. 28),[59] a synthetic route would be desirable, based on a Pc-scaffold of following features:

- good solubility under physiologic conditions.
- $^{1}H/^{13}C$ spectroscopically pure, single compound.
- peripheral substitution pattern.
- antennary/dendritic structure.
- C4 symmetry.
- regio- and stereoselective coupling reaction with biomolecule.
- feasability for diversification on Pc-scaffold.
- multigram scale.
- efficent synthetic route to Pc-scaffold.
- cheap starting material.

RESULTS

GENESIS OF THE IDEA

Phosphazene, a Bifocal-Tetradendronal Branching Element[103]

Inspired by the paper of J. Thiem *et al.*[104] about a carbohydrate-functionalized porphyrin and the reviews of R. Bonnett,[6, 7] a strategy was sought for a highly symmetrical, dendritic, soluble Pc-scaffold that can be diversely functionalized with a broad range of biomolecules, in particular carbohydrates.

Numerous dendronal branching elements have been created by chemists since the pioneering works of the Tomalia[105] and the Newkome group[106] in the early 90's.
In 2000, Kim D. Janda *et al.*[107] published a paper, titled *"Stealth Star Polymers: A New High-Loading Scaffold for Liquid-Phase Organic Synthesis"*, in which he introduced 1,1,3,3,5,5-hexachlorocyclotriphosphazene (**1**) as dendrimer core. Janda coined the name, because the phosphazene – only comprised of P and N – is "invisible" for the utmost employed ^{1}H- and ^{13}C-NMR techniques, but can be easily detected by ^{31}P-NMR. This interesting substance is scarcely known in organic chemistry or medicinal chemistry, but evoked an ongoing interest of several work groups in the field of inorganic chemistry, namely H. R. Allcock starting his research in 1960s and C. W. Allen starting in 1970s.

By introducing a *pseudo*-spiro-linkage, at the periphery of a Pc *via* annelated 2,2-dialkylbenzo-1,3-dioxolane rings, McKeown *et al.*[108] attempted to discourage cofacial aggregation by π-stacking. This approach was partially successful and led to improved solubility. Indeed, the steric bulk introduced perpendicular to the Pc plane, seemed to suppress aggregation. In the concept outlined here, an even more pronounced effect should be achieved by replacing the disubstituted dioxolane rings by tetra substituted *o*-phenylenedioxyspirocyclotriphosphazene rings, which are known already in the literature.[23, 109]

However, according to Allcock the 5-membered homo-spiro-phosphazene ring system is unstable towards excess of nitrogen bases such as TEA or pyridine[110] and starts to polymerize at higher temperature.

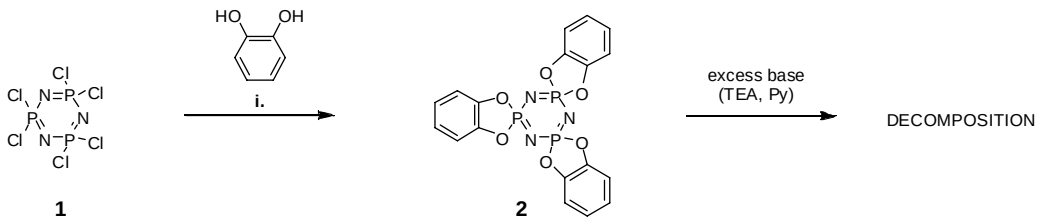

Scheme 3 **First published synthesis of trispiro[4.4.4]phosphazene 2 by Allcock[109]: i.) THF, TEA, catechol, r.t.**

In contrast to the trispiro[4.4.4]phosphazene **2**,[109] it was found that a trispiro[6.6.6]phosphazene ring system is extraordinarily stable.[111, 112] Consequently, the easily prepared dispiro[6.6]phosphazene precursor **3** (Scheme 4) according to Carriedo *et al.*[113] was chosen as a model system for further modifications and stability tests. A three-dimensional picture was optained by X-ray analysis (see Figure 82 and Image 14).

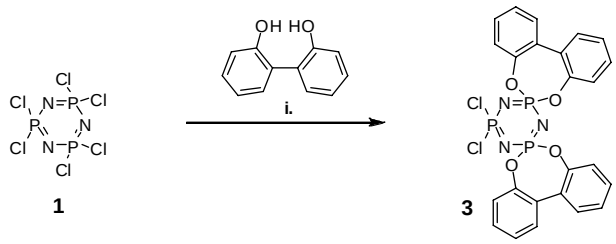

Scheme 4 **Preparation of dispiro[6.6]phosphazene precursor 3: i.) 1.0 equiv. biphenol, acetone, K_2CO_3, r.t., 30 h, 88%.**

This encouraged me to explore the properties of a hitherto unknown trispiro[4.6.6]phosphazene ring system.

Ring closure of a catechol derivative with **3** under Williamson conditions afforded two examples **4** and **5** of the trispiro[4.6.6]phosphazene ring system in excellent yields.

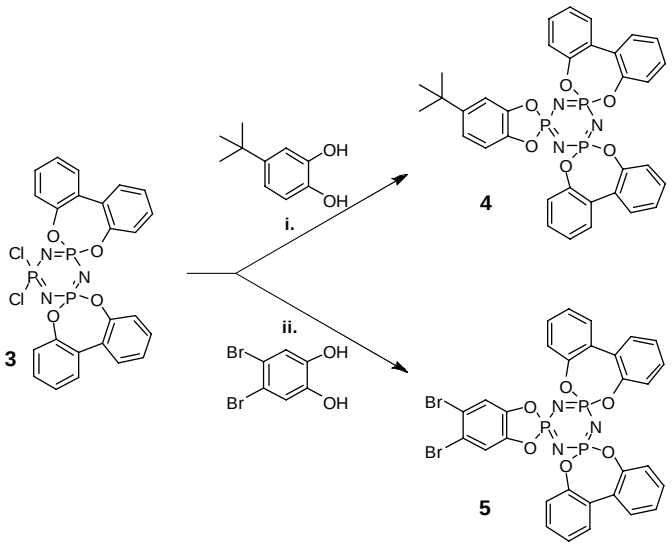

Scheme 5 **Derivatization of dispiro[6.6]phosphazene precursor 3 to a trispiro[4.6.6]phosphazene with catechol derivatives: i.) 1.2 equiv. 4-(*tert*-butyl)catechol, acetone, K_2CO_3, reflux, 24 h, 91%; ii.) 1.3 equiv. 4,5-dibromocatechol, 2-butanone, K_2CO_3, 62 °C, 3 h, 84%.**

However, attempting an aromatic nitrile-halogene exchange, known as Rosenmund-von Braun reaction, with **5** in order to introduce the nitrile functionalities required for Pc synthesis resulted in excessive degradation.

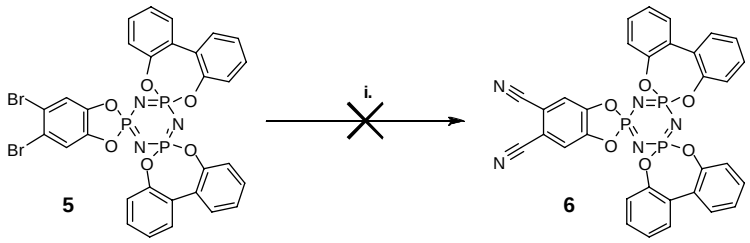

Scheme 6 **Attempted synthesis of a trispiro[4.6.6]phospazene phthalodinitrile 6: i.) DMF, $Cu^{+I}CN$, 150 °C, 16 h.**

It was speculated that the benzo[*d*][1,3,2]-dioxaphosphole unit was still too reactive at higher temperature.

Consequently, in order to further improve stability for subsequent functionalization the dispiro[6.6]phosphazene precursor **3** was reacted with 4,5-dibromo benzene-1,2-dimethanol (**7**). Also this novel trispiro[6.6.6]phosphazene **8** was successfully isolated in almost quantitative yield.

The expected high thermal stability was proven by heating the neat trispiro[6.6.6]phosphazene **8** in an NMR-tube at 250 °C for 15 minutes prior to dissolution in DMSO-d_6. Subsequent NMR (^{1}H, ^{31}P) in DMSO-d_6 showed no signs of decomposition. Disappointingly, a solution of **8** in DMF-d_7 excessively decomposed within 10 minutes on heating to 130 °C and 150 °C according ^{1}H- and ^{31}P-NMR.

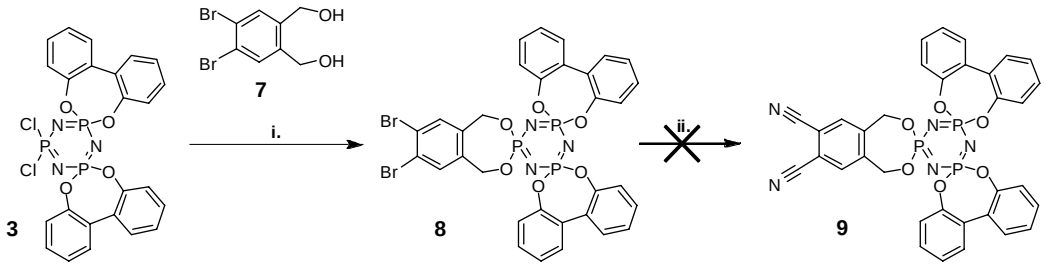

Scheme 7 **Preparation of functionalized trispiro[6.6.6]phosphazene 8: i.) NaH/THF → (1.1 equiv. 7 and 3 in THF), r.t., 20 h, 95%; ii.) DMF, $Cu^{+I}CN$, 150 °C, 16 h.**

Accordingly, an attempted Rosenmund-von Braun reaction of **8** failed. Taking into account that Allcock *et al.*[114] succeeded in synthesizing phosphazenes linearly linked to Pcs in refluxing DMF, it may concluded that the ring strain is still too high.

Obviously, neither a further derivatisation of the trispiro[6.6.6]phosphazene **8**, nor the subsequent cyclotetramerisation of a phosphazene spiro-annelated phthalodinitrile seemed to open a viable route to the desired fourfold spiro-annelated Pc structure **9**. As an ultimate option eventually synthesizing the target structure, the spiro-annelation was envisioned as the final step by reacting an octahydroxymethyl substituted Pc with a large excess of 1,1,3,3,5,5-hexachlorocyclotriphosphazene ($N_3P_3Cl_6$) (**1**) or, preferably 1,1,3,3,5,5-hexafluoro-cyclotriphosphazene ($N_3P_3F_6$). The latter, due to its volatility can be advantageously removed by sublimation.

Nevertheless, solubility issues of the reactants had to be carefully considered. Whereas the octahydroxymethyl Pc precursor was correctly assumed to be only soluble in highly polar solvents, the halogenophosphazenes showed high solubility in unpolar solvents like chlorinated hydrocarbons, cyclic ethers and ketones. Evidently, the reaction conditions had to be anhydrous. Inspired by a paper of Ruf *et al.*[115] this dilemma seemed solvable by employing *O*-silyl protecting groups, thus assuring high solubility in unpolar solvents as well as liability towards fluoride ions. It was speculated that in the reaction of a persilylated octahydroxymethyl Pc with $N_3P_3F_6$ catalytic amounts of fluoride would generate an oxyanion which immediately reacts with the fluorophosphazene,[116] thus maintaining solublity in this autocatalytic process until completion.[117, 118] Ideally, the product would be a sixteen-fold fluoro substituted tetra-spiro-annelated Pc **10**. The remaining fluoro atoms are still highly reactive and may be finally substituted by *O*-nucleophiles thus providing eventually the target structure **11** (Scheme 8).

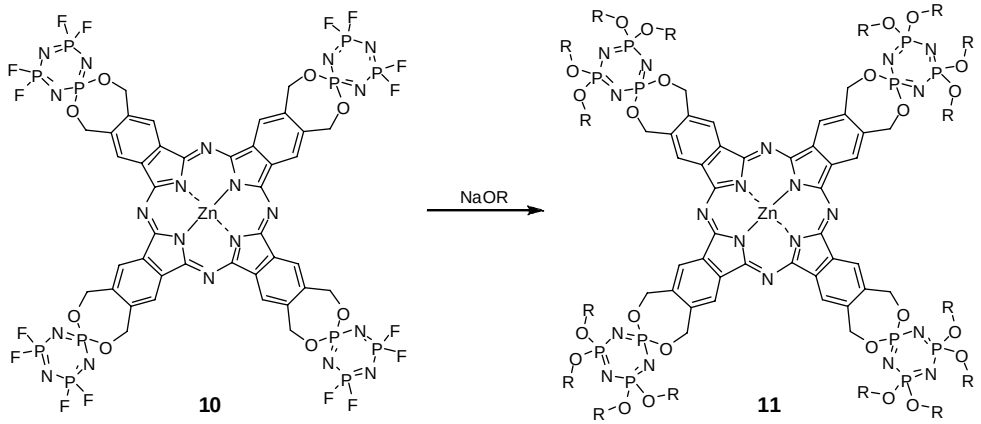

Scheme 8 **Structure and derivatisation of sixteen-fold fluoro substituted tetra-spiro-annelated Pc.**

In pursuit of this synthetic sequence, a feasible access to a fully silyl protected octahydroxmethyl Pc was elaborated.

ROUTES TO AN ISOMERICALLY PURE HIGHLY SOLUBLE OCTA-SUBSTITUTED PC

The Bromination Route

In a first synthetic approach 4,5-dibromo xylene (**12**) was chosen as a starting material for the subsequent transformation to **19** as outlined below:

A first synthetic route was elaborated with respect to current literature and preliminary tests. The framework for a Pc-precursor was listed as follows based on *o*-phthalodinitrile:

1. equal substitution on position 4 and 5 of the aromatic ring, due to symmetry issues.
2. both positions with a methylene unit as spacer, with respect to a spiro-annelation *via* a seven-membered ring.
3. linkage *via* oxygen, due to the oxophilicity of phosphor at a phosphazene derivative.
4. *in situ* coupling in accordance to Vij *et al.*,[116] Paquette *et al.*[117] and Kuwajima *et al.*[118]

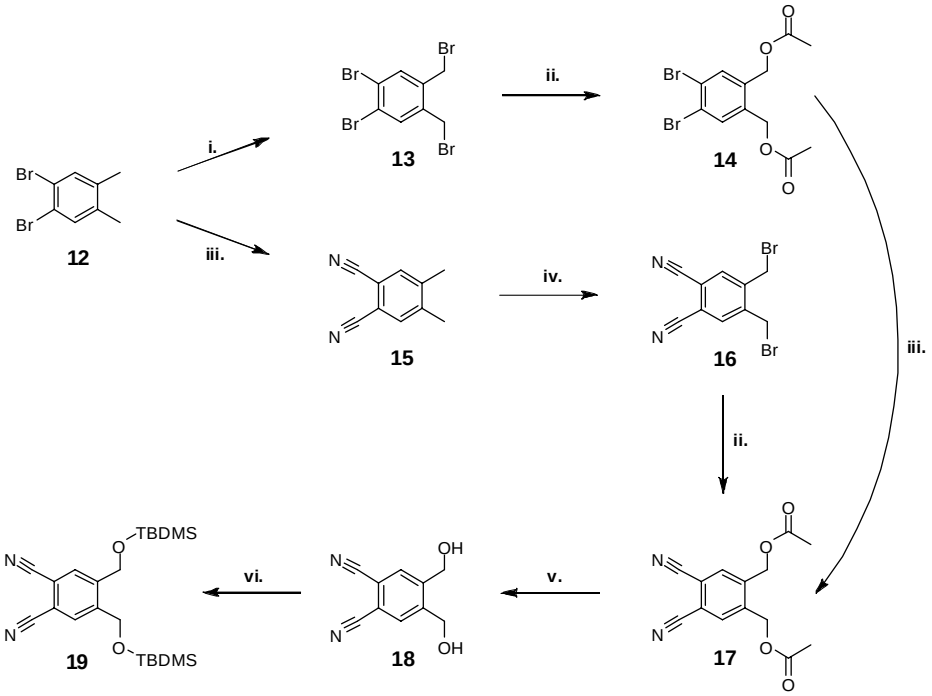

Scheme 9 **First synthetic route to Pc-precursor: i.) 1.0 equiv. NBS, cat. BPO, CCl_4, reflux, 1h, 42%;[119, 120] ii.) NaOAc/HOAc, 116 °C, 17 h, 90%;[121] iii.) 1.5 equiv. CuCN, DMF, 15 h, reflux, 66%;[17] iv.) 1.5 equiv. NBS, BPO, h*v* , CCl_4, 10 h, reflux, 32%;[122] v.) *Pseudomonas cepacia* lipase, acetone/phosphate buffer pH 8, 40 °C, 45 h, 95%;[123] vi.) DMF, imidazole, TBDMSCl, r.t., 24 h, 95%.[124]**

According to the protocol of Pawlowski *et al.*,[17] 4,5-dimethyl-*o*-phthalodinitrile (**15**) was optained in good yields. The side chain bromination of 4,5-dibromo-*o*-xylene (**12**) and 4,5-dimethyl-*o*-phthalodinitrile (**15**) is scarcely described in the literature. However, even under carefully controlled reaction conditions the reported yields could not be reproduced. NMR monitoring of aliquots revealed that dibromination to *α,α'*-dibromo derivatives **12** and **15** was kinetically favored, thus severely reducing the yields and requiring cumbersome purification of the reaction mixtures. Since the direct hydrolysis of the benzyl bromide failed, the hydroxy functionality was introduced *via* acetylation in a boiling mixture of NaOAc/HOAc and subsequent deacetylation. The sensitivity of the nitrile group to hydrolysis required the use of *Pseudomonas cepacia* lipase to cleave the acetyl group gently at pH 8, thus releasing the desired benzylic hydroxy group. Finally, bulky TBDMS protecting groups were attached as described by Corey *et al.*[124] in DMF. Albeit successful, the synthetic route was hampered by the costly starting material 4,5-dibromo-*o*-xylene (**12**), and moderate yields as well as laborious purification of the intermediates (**13**, **16**). Therefore an alternative access to **19** was developed.

The PMDA Route

The second route (Scheme 10) to a 4,5-disubstituted phthalodinitrile **19** is based on the results of Savage *et al.*[125] After Fischer esterification of pyromellitic dianhydride (PMDA) (**20**), ester (**21**) was reduced with $LiAlH_4$ to obtain **22**. Regioselectivity and kinetic control of the reduction was surprisingly high and was easily monitored *via* LC-MS. Isolation of the target compound **22** from starting material **21** and the fully reduced tetra alcohol was performed for characterization, but for bulk preparation the crude reaction mixture was directly subjected to ketalization and reduction, affording **24**. Herein the *tert*-butyldiphenylsilyl (TBDPS) protecting group was chosen, because of its higher stability towards oxidative conditions like Swern oxidation.[126] Furthermore, it is commonly known that this group facilitates crystallization. Several mild and neutral oxidation protocols were unsuccessful. DMSO activated by acetic anhydride[127] gave unidentified by-products, whereas Mn^{+VI} as barium manganate[128, 129] left the methylene hydroxy moieties unchanged. However, a two-step

process employing Swern oxidation to the substituted phthaldialdehyde **27**, and subsequent perborate oxidation afforded the desired phthalic acid **28** as a chalky solid in an excellent overall yield (81%). Additionally, the phthaldialdehyde **27** represents a valuable building block of high synthetic potential and was obtained as highly viscous oil.

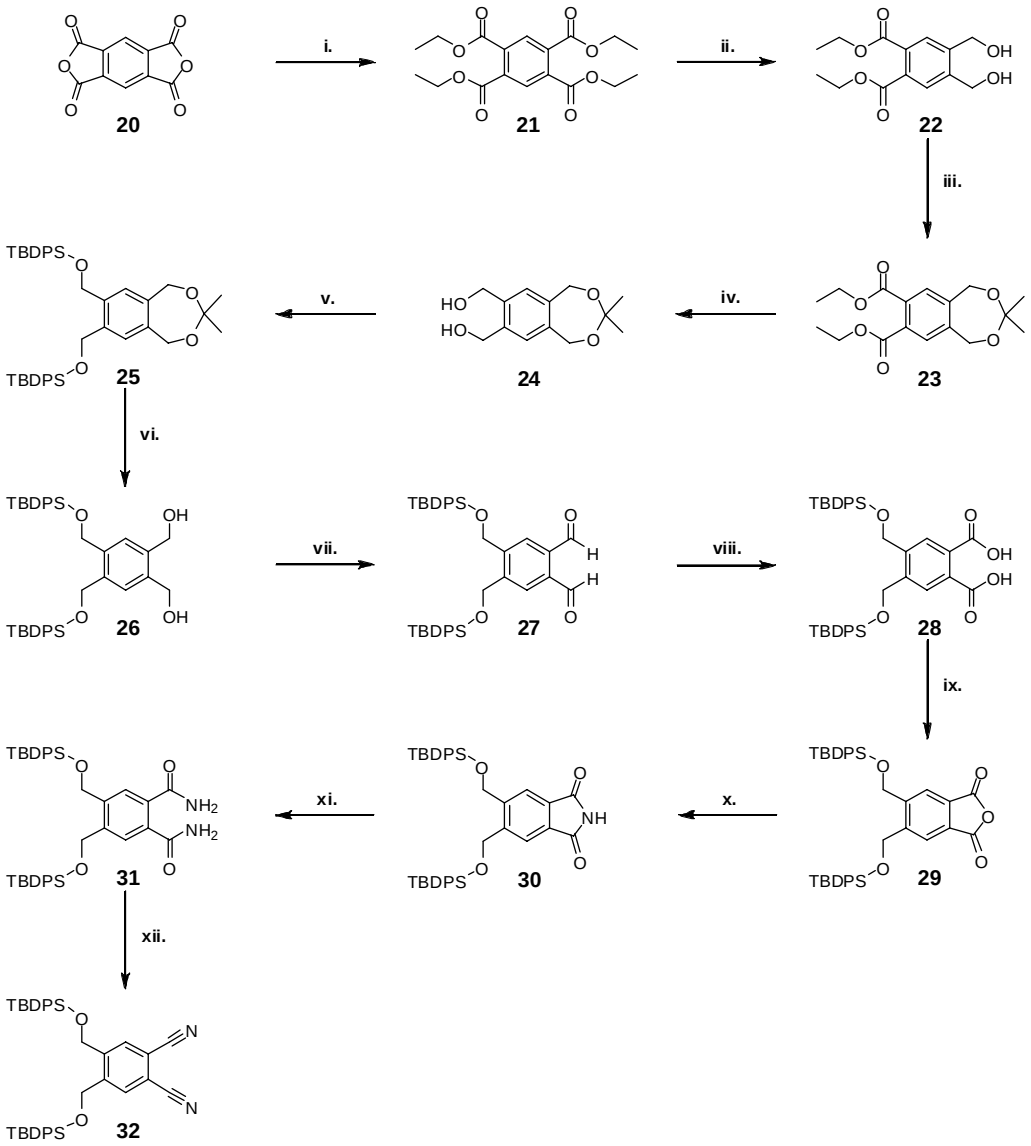

Scheme 10 **Synthesis of Pc-precursors starting from PMDA (20):[1] i.) EtOH, conc. H_2SO_4, MS, reflux, 18 h, 96%; ii.) Et_2O, $LiAlH_4$, reflux, 16 h, 40%; iii.) acetone, 2,2-dimethoxypropane, cat. *p*-TsOH, r.t., 24 h, 96%; iv.) Et_2O, $LiAlH_4$, reflux, 3 h, 86%;[125] v.) DMF, imidazole, 1.1 equiv. TBDPS-Cl, r.t., 24 h, 97%;[124] vi.) acetone/water, cat. *p*-TsOH, r.t., 24 h, 98%; vii.) Swern oxidation, 97%;[130] viii.) HOAc, $NaBO_3 \cdot 4H_2O$, 50 °C, 16 h, 95%;[131] ix.) Ac_2O, 150 °C, 3 h, 95%;[132] x.) formamide, reflux, 3 h, (98%);[133] xi.) NH_3/H_2O, r.t., 48 h, (72%);[133] xii.) $SOCl_2$/DMF, 0-5 °C, r.t., 24 h, (75%).[133]**

[1] Yields in parentheses are taken from literature and are not experimentally ascertained!

The further sequence envisioned activation of the phthalic acid **28** to the corresponding anhydride and subsequent multistep transformation to the dinitrile **32** as outlined in Scheme 10. Advantageously, Uchida *et al.*[24] have published a very efficient route to Pcs directly from anhydrides, thus omitting the lengthy transformation from the phthalic anhydride to the phthalodinitrile (**32**). The reaction was conducted under mild conditions at nearly neutral pH, applying HMDS as concomitant oxygen scavenger and nitrogen source.
The highly crystalline phthalic anhydride **29** was successfully subjected to X-ray analysis (see Figure 8 and Image 1).

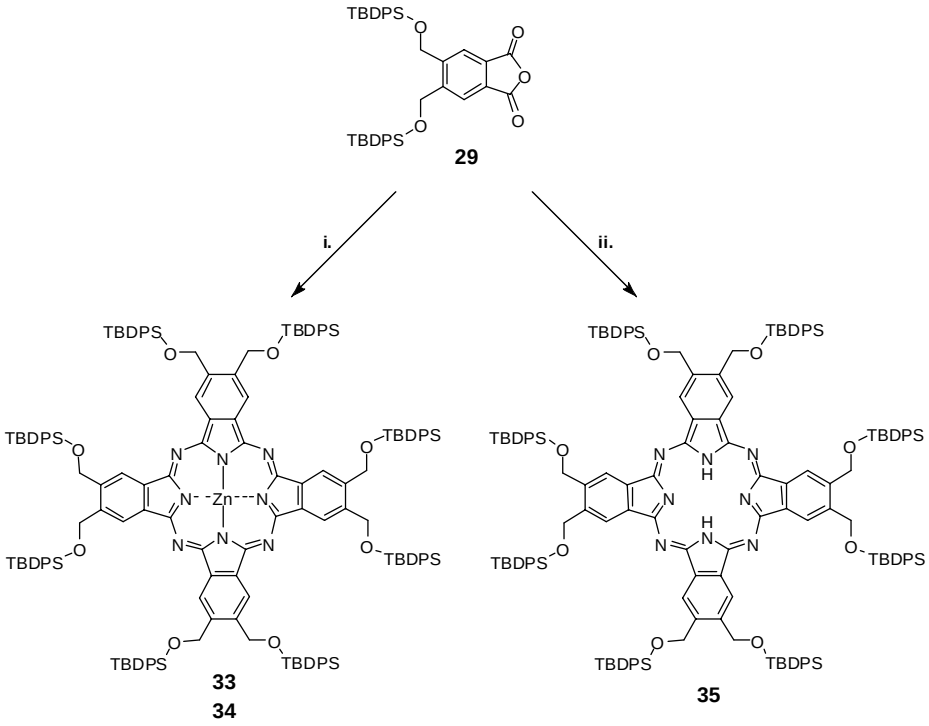

Scheme 11 **Synthesis of ZnPcs 33 and 34 and H_2Pc 35: i.) 6 equiv. HMDS, 1 equiv. DMF, 0.25 equiv. $Zn(OAc)_2$, 0.1 equiv *p*-TsOH, 100→130 °C then 130 °C, 63 h, 72%; ii.) 6 equiv. HMDS, 1 equiv. DMF, 0.1 equiv *p*-TsOH, 100→130 °C then 130 °C, 10 h, 66%.[24]**

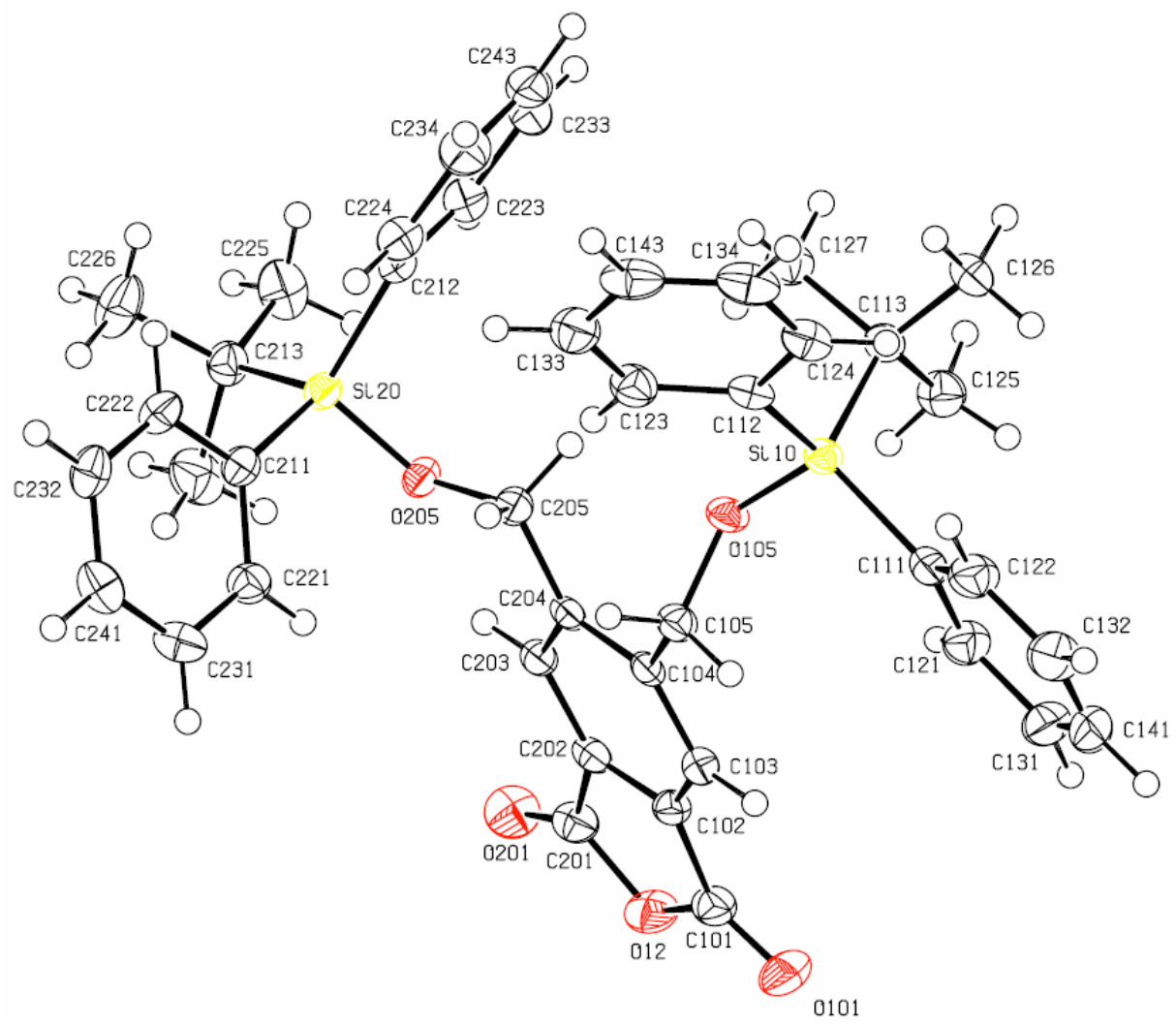

Figure 8 **X-ray structure of 4,5-bis((*tert*-butyldiphenysilyl)oxymethyl)phthalic anhydride (29). Numbered atoms: carbon C = black, oxygen O = red, silicon Si = yellow.**

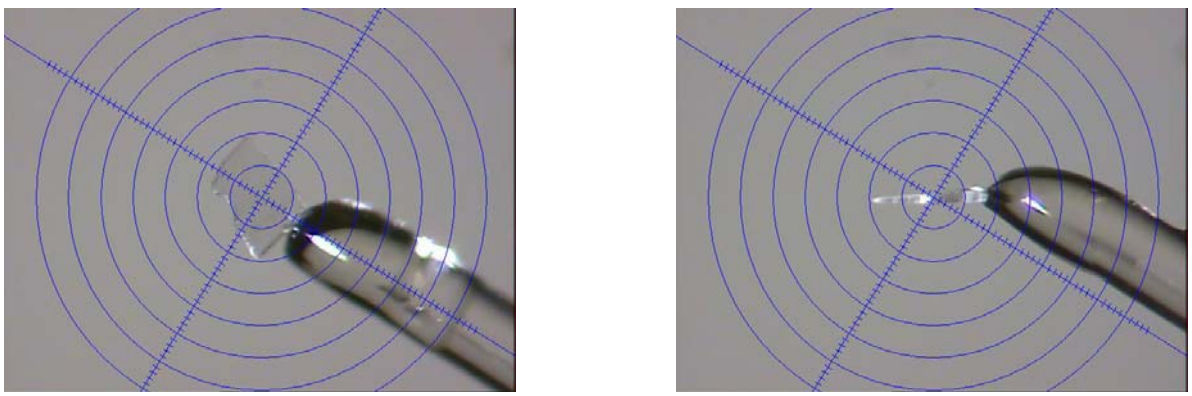

Image 1 **Single crystal of phthalic anhydride 29 during X-ray analysis (viewing angle 0° and 90°).**

Employing these conditions, the novel ZnPc **33**, ZnPc **34** and H_2Pc **35** were successfully synthesized. Flash chromatography and recrystallization from DCM/PE and acetone respectively afforded crystals from **33** and **34** suitable for X-ray analysis. According to X-ray analysis the two product lots, 428 and 488, gave two different results, with respect to the fifth ligand at the coordinated central atom.[134]

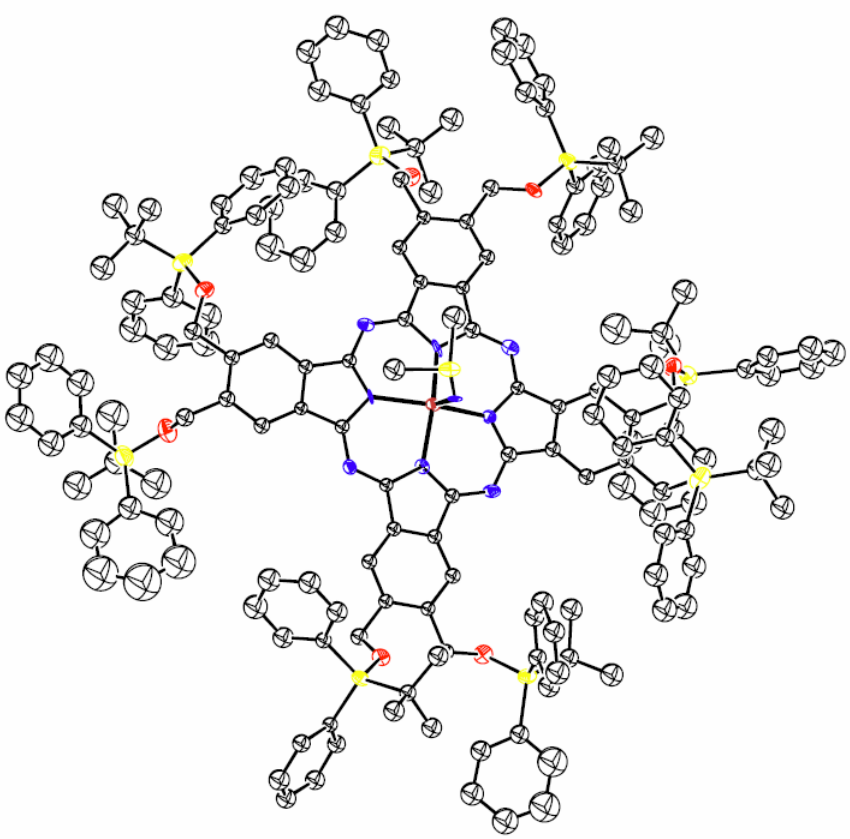

Figure 9 **X-ray structure of *a*-((CH_3)$_2$Si=NH)ZnPc-*op*-CH_2OTBDPS (33) (lot 428, recrystallized from DCM/PE); dimethylsilanimine [(CH_3)$_2$Si=NH] as fifth ligand.[134] Shown atoms: carbon = black, oxygen = red, silicon = yellow, zinc = dark red, nitrogen = blue.**

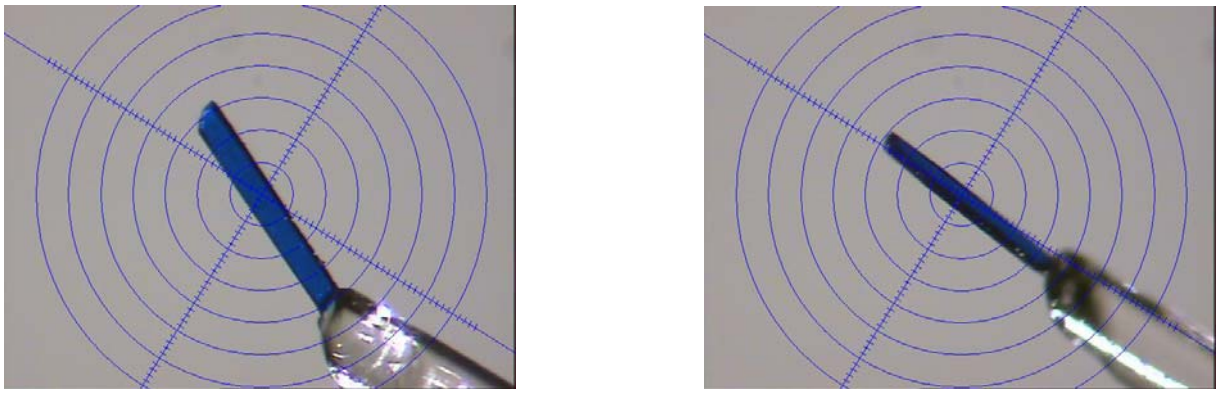

Image 2 **Single crystal of ZnPc 33 from lot 428 while processing X-ray analysis (viewing angle 0° and 90°).**

The fifth ligand in both lots – 428 and 488 – originates from the DMF induced scission of HMDS, liberating ammonia [NH_3] and other fragments such as dimethylsilanimine [$(CH_3)_2Si{=}NH$].[134]

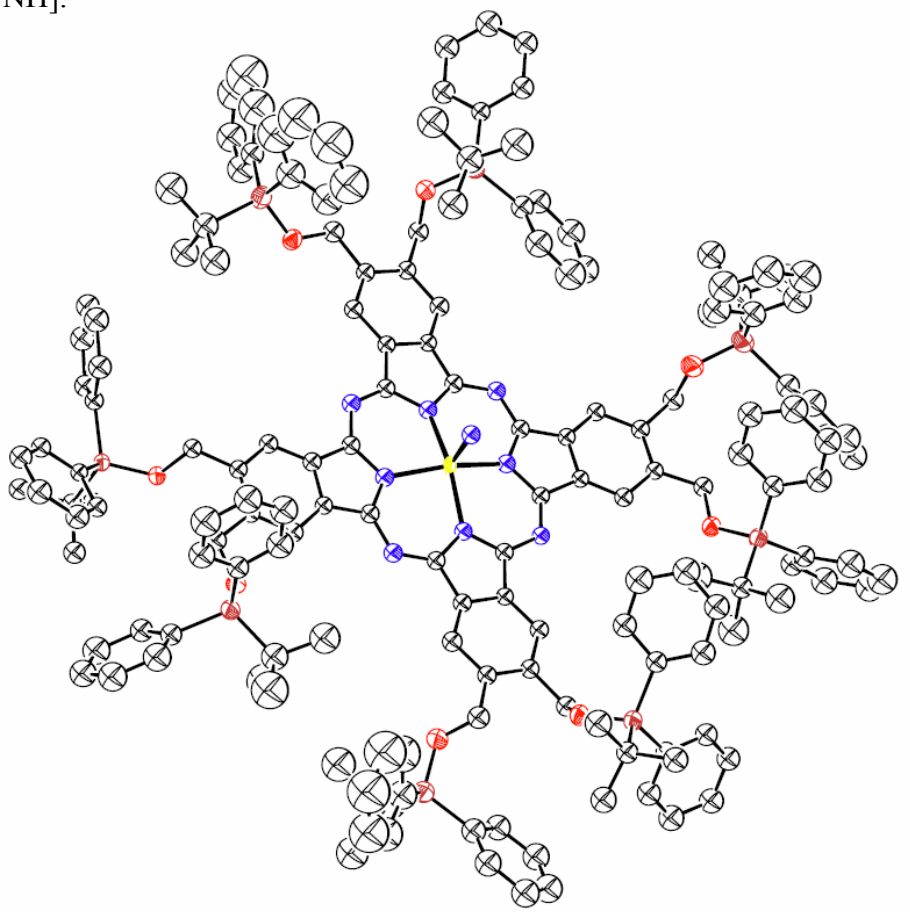

Figure 10 **X-ray structure of *a*-(NH_3)ZnPc-*op*-CH_2OTBDPS (34) (lot 488, recrystallized from acetone); ammonia [NH_3] as fifth ligand.[134] Shown atoms: carbon = black, oxygen = red, silicon = dark red, zinc = yellow, nitrogen = blue. For the purpose of clarity, hydrogen atoms were deleted.**

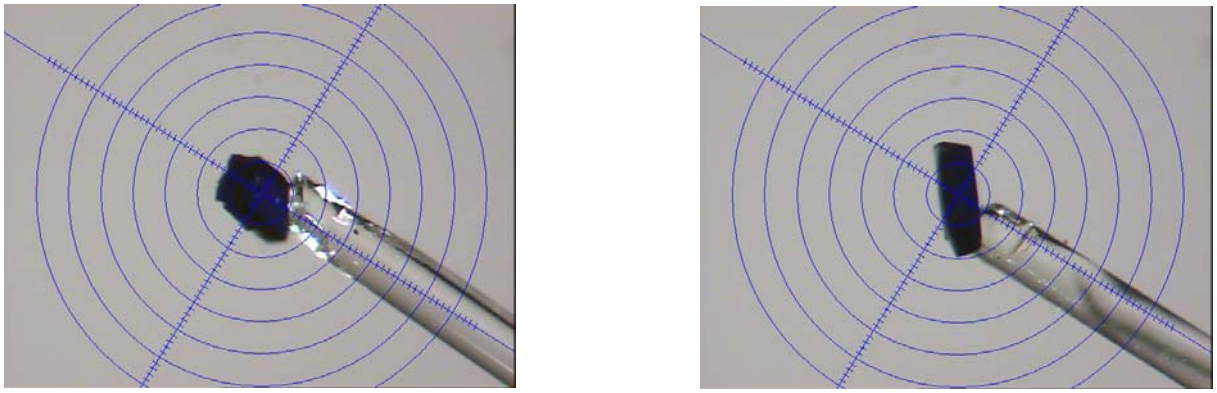

Image 3 **Single crystal of ZnPc 34 from lot 488 while processing X-ray analysis (viewing angle 0° and 90°).**

Preliminary tests for an *in situ* deprotection-substitution reaction for a successful spiro-linkage with the dispiro substituted phosphazene derivative **3** were performed with TBDPS-protected 1,2 benzenedimethanol **36** as shown in Scheme 12:

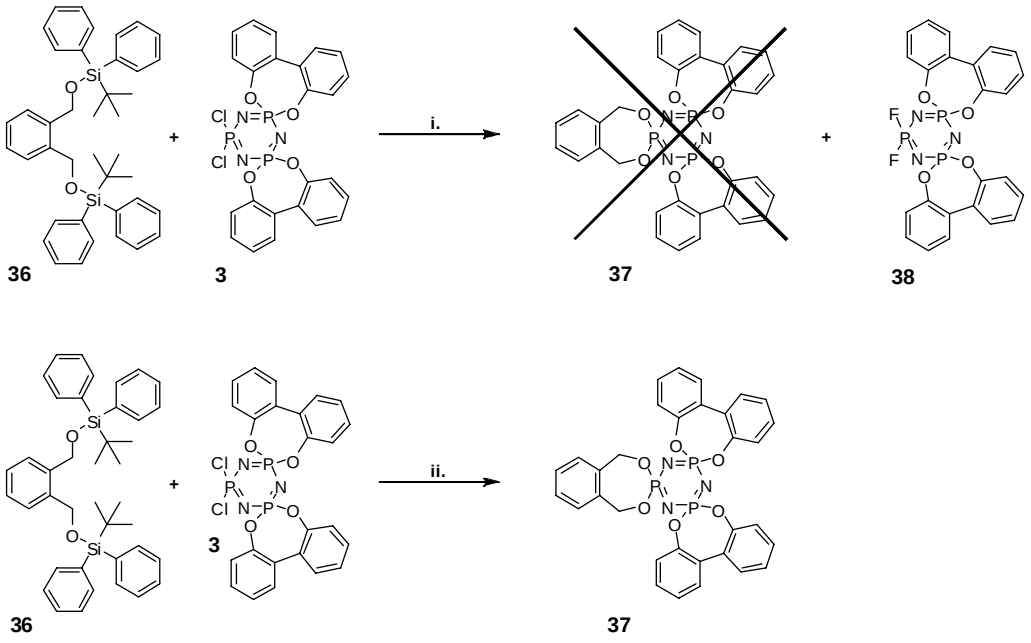

Scheme 12 ***In situ*** **deprotection-substitution: i.) THF, TBAF on silica, r.t., 19 h, 73%;[117, 135] ii.) THF, MS 4Å, BTAF, silyl-deriv. 36, r.t., 40 h then dispiro-$N_3P_3Cl_2$ 3, r.t., 20 h, 62%.[117, 118]**

In order to facilitate work-up, a solid phase supported reagent like TBAF on silica was the first choice as a fluoride source. Surprisingly, due to halogen metathesis the fluorinated dispiro-phosphazene derivative **38** was isolated and the silyl-groups remained unchanged.
In contrast, using BTAF and applying the protocol of Kuwajima *et al.*[118] *in situ* deprotection-substitution was accomplished.

A NEW PC-SCAFFOLD FOR DIVERSE MODIFICATIONS

Disappointingly, this carefully elaborated methodology of *in situ* desilylation and substitution could not be transfered to the ZnPc-*op*-CH_2OTBDPS (**33**).
Rather, after very laborious aqueous work-up deprotected ZnPc-*op*-CH_2OH (**39**) was isolated in quantitative yields and successfully analyzed by NMR and MALDI-TOF. At this point, all efforts to phosphazene modified Pcs were abandoned and the synthetic potential of Pc **39** came into focus. Ultimately, the synthesis of a spiro-annelated Pc derivative was achieved by a different concept (see p. 67)

For upscaling to multi-gram amounts, an optimized deprotection protocol was developed. The advantageous phase catalytic properties of BTAF in a solvent mixture of THF, water, DMSO and TFA at first, turned into a drawback, since removal of the ammonium salt was quite cumbersome.
An alternative deprotecting reagent was TEA•3HF in the same solvent mixture. In contrast, it conveniently could be removed almost quantitatively after neutralization by evaporation.

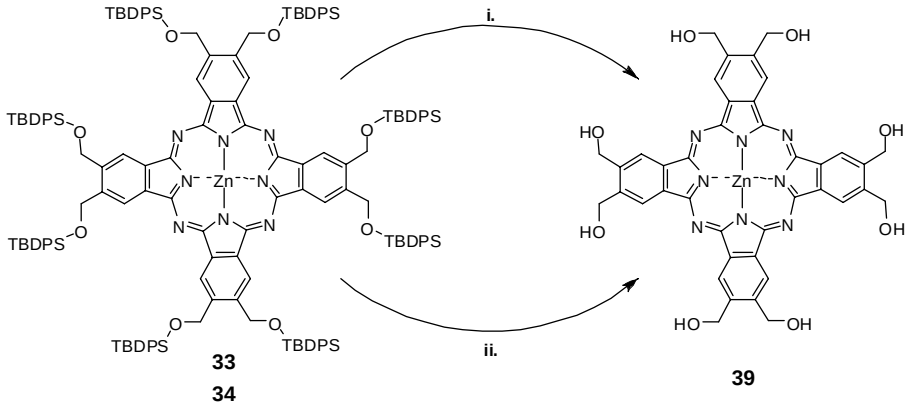

Scheme 13 **Deprotection of ZnPc-*op*-CH_2OTBDPS (33, 34): i.) BTAF, THF, water, TFA, DMSO, r.t., 7 d, light shielded, 95%; ii.) TEA•3HF, THF, water, DMSO, r.t., 4 d, light shielded, 95%.**

As depicted in Figure 11, extractive work-up with an organic biphasic system of DMSO/PE removed the cleaved protecting groups **40** and **41** from ZnPc-*op*-CH_2OH (**39**).

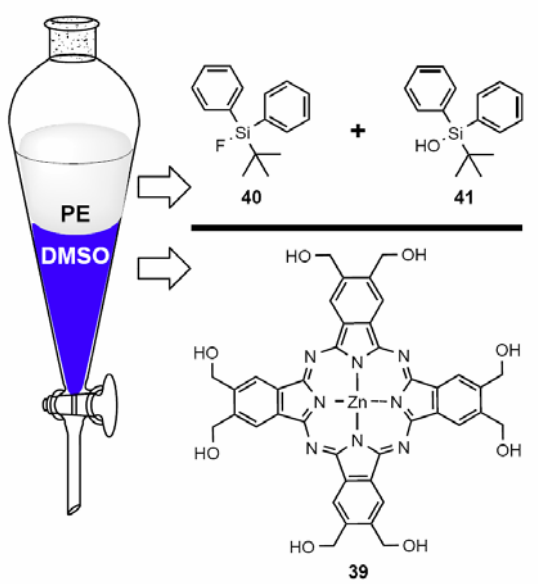

Figure 11 **Liquid-liquid work-up with a PE/DMSO system, extracting the cleaved silyl-protecting moieties 40 and 41.**

In order to save valuable resources of the ZnPc-*op*-CH_2OH (**39**), further derivatisation reactions (oxidation, addition, substitution, *etc.*) were checked on a "fragment", namely 4,5-dimethylbenzene-1,2-dimethanol (**42**) as a model compound according to Scheme 14:

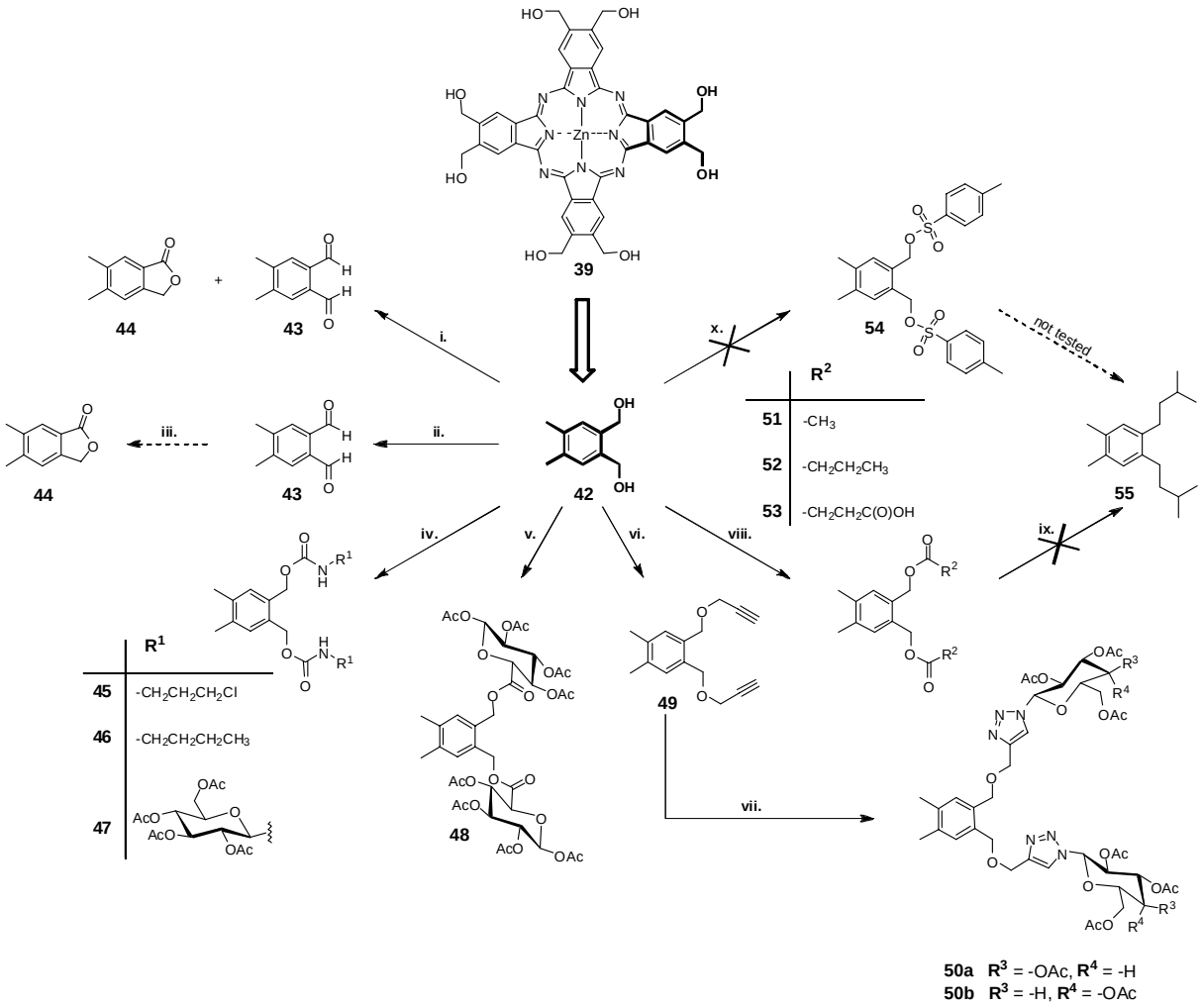

Scheme 14 **Attempts to modify *ortho*-benzylic hydroxy groups on the test-compound 4,5-dimethylbenzene-1,2-dimethanol (42): i.) PDC, DMSO, r.t., 3 d, 47% (44:43 = 71:29);[136, 137, 138] ii.) DMP, DMSO, r.t., 2 h, 80%;[139] iii.) DMP, DMSO, r.t 24 h, mixture of oxidation products;[140, 141, 142] iv.) a) Py, 3-chloropropyl isocyanate, r.t., 6 d, 78%;[143] b) Py, *n*-butyl isocyanate, 50 °C, 48 h, 85%;[144] c) 1,2,3,4-tetra-*O*-acetyl-*β*-D-glucopyranosyl isocyanate, Py, 50 °C, 48 h, 99%;[144] v.) 1,2,3,4-tetra-*O*-acetyl-*β*-D-glucopyranuronoyl chloride, Py, 0 °C → r.t., 48 h, 99%; vi.) DMSO, prop-2-yn bromide 80% in *o*-xylene, aq. 50% NaOH, r.t., 2 d, 85%;[145] vii.) THF/EtOH = 2:1, 0.16 equiv. $CuSO_4 \cdot H_2O$, 0.5 equiv. (+) sodium L-ascorbate, 3 equiv. glycosyl azide 60/71, r.t., 24-42 h, 69-83%;[146] viii.) corresponding anhydride, Py, r.t., 24 h, 70-90%; ix.) Li_2CuCl_4 (0.1 M in THF), *iso*-butylMgBr (2 M in THF), -78 °C – r.t., 12 h;[147, 148, 149] x.) Py, TsCl, r.t. 14 h.[150]**

Successful results of these tests were assigned to ZnPc **39** with further modification if necessary. The positive results are shown in Scheme 19.

Esterification

The notable solubility of the new Pc-scaffold **39** in pyridine suggested acylation, as commonly used in carbohydrate chemistry. Peracetylation with several anhydrides were tested on **42** and successfully transfered to **39**. As it could be expected the solubility increased from acetate to butyrate and gave **66** and **67** respectively. By the use of succinic anhydride the hydrophilicity could be enhanced dramatically and **68** was simply isolated by precipitation in EA. This compound forms liquid crystalline phases as observed with an optical polarising microscope and documented by Image 10 and Image 11.[151]

Peracetylated glucuronic acid chloride **59** (Scheme 15) reacted quantitatively with the test-compound **48** in pyridine at r.t. within 48 hours. Analogously, a reaction between ZnPc **39** and acid chloride **59** took place, indicated by the increased solubility of the reaction product. However, the desired product could not be isolated and identified by NMR. This may again hypothetically be explained by a side-reaction of the ZnPc **39** with the discharged chloride ion. Reactions with methacrylic acid chloride or butyryl chloride failed too.

Synthesis of Glucuronoyl Chloride

The procedure of Tosin *et al.*[152] was slightly modified in the last step. Instead of equivalents or excess of DMF only a catalytic amount of 10 mol% DMF was used. In comparison, the NMR of the white, chalky acid chloride **58** was distinct in the latter case but significant peaks of unidentified impurities were found in the NMR of a purple, chalky solid when executed with equivalents of DMF.

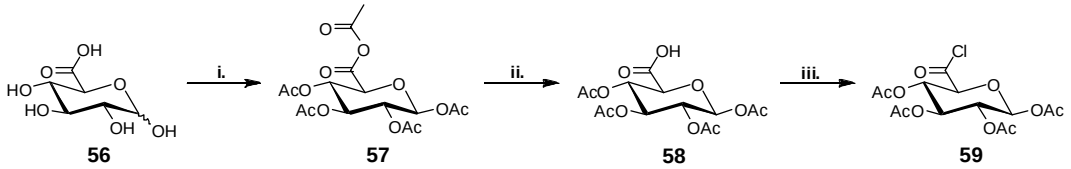

Scheme 15 **Synthesis of 1,2,3,4-tetra-*O*-acetyl-*β*-D-glucopyranuronoyl chloride (59):[152] i.) Ac_2O, I_2, 0 °C / 2 h → r.t. / 3 h, 80%; ii.) THF/water (2:1), r.t., 18 h, 98%;[153] iii.) DCM, $(COCl)_2$, DMF (10 mol%), 0 °C / 30 min → r.t. / 2 h, 95%.[154]**

Attempted Copper Catalyzed C-C-coupling

The cuprate catalyzed coupling of Grignard reagents to benzylic acetates or primary tosylates described by Schlosser *et al*.[148, 149] appeared very compelling for broad homologation of the Pc-scaffold **39**. At least, Grignard reactions with Pcs have been described by Hanack *et al*.[155] Unfortunately, applying the conditions of Schlosser, no coupling reaction took place except that the acetate moiety conventionally reacted to the corresponding tertiary alcohol. The higher reactivity of tosylates offered a second option to enforce the reaction. However, several attempts to obtain the tosylate **54** -even of the test-compound **42**- in DMSO or pyridine failed.

Oxidation

Swern oxidation, usually performed at low temperature (-78 °C) in DCM as co-solvent, was not possible due to the low solubility of the ZnPc **39.** Evidently, neat DMSO could not be used as well, since it solidifies at 18 °C. The neighbour group effect of the vicinal *ortho* hydroxymethylene groups was observed when oxidation of *o*-phthalyl alcohol **42** was attempted with PDC in DMSO under neutral or slightly acidic conditions at ambient temperature. A 1:3 mixture of the desired phthalic aldehyde **43** together with lactone **44** was obtained. The use of DMP in DMSO was described in the literature and successfully testet. Interestingly, extending the reaction time from 2 h to 24 h led to lactonisation. On transfering, the reaction conditions to the ZnPc **39** the color of the reaction mixture changed from blue to green. This bathochromic effect can be interpreted as the extension of the conjugated system due to the generation of carbonyl double bonds. Lately, monitoring *via* TLC as well as isolating the assumed product was very difficult and NMR analysis was not conclusive.

Carbamoylation

In preliminary attempts, three different isocyanates, namely *n*-butyl isocyanate, 1,2,3,4-tetra-*O*-acetyl-*β*-D-glucopyranosyl isocyanate, and 3-chloropropyl isocyanate were reacted readily with the *o*-phthalyl alcohol **42** within 6 days at r.t. or within 48 h at 50 °C in pyridine to form the corresponding carbamates **45**, **46** and **47**.[143, 144, 156] Under the same conditions, reaction of *n*-butyl isocyanate with ZnPc **39** yielded the desired carbamoyl-ZnPc **69**. Even the sterically demanding 1,2,3,4-tetra-*O*-acetyl-*β*-D-glucopyranosyl isocyanate (**62**) reacted smoothly to the isomerically pure, octasubstituted ZnPc **64**. Curiously, reaction of ZnPc **39** with 3-chloropropyl isocyanate resulted in a water-soluble product, unamenable to isolation and characterization. It was hypothesized that the coordinated central atom of ZnPc **39** promoted the quarternization of pyridine with the 3-chloropropyl moiety, thus generating pyridinium salts.

Synthesis of Glucosyl Isocyanate

According to the literature, some pyranosyl isocyanates have been used as building blocks in disaccharides[157]or anti-tumor prodrugs[158]. Encouraged by the promising results with commercial available isocyanates on the ZnPc-*op*-CH_2OH (**39**) (Scheme 14 and Scheme 19), the rarely described synthesis of glucopyranosyl isocyanate **62**[157, 159, 160] was approached.

The glucosyl azide **60**, derived from the synthesis depicted in Scheme 21, was hydrogenated to glucosyl amine **61**. The stereochemical integrity was determined from coupling constants of ^{1}H-NMR and confirmed by X-ray analysis (Figure 12 and Image 4).

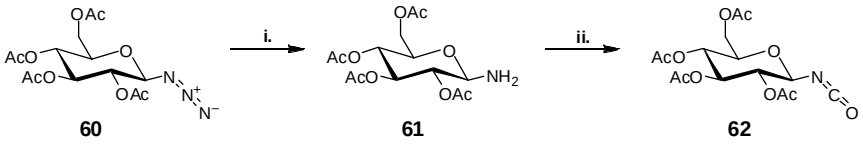

60 **61** **62**

Scheme 16 **Synthesis of 2,3,4,6-tetra-*O*-acetyl-*β*-D-glucopyranosyl isocyanate (62): i.) H_2, Pd/C, EA, r.t., 24 h, 85%;[161] ii.) DCM / sat. aq. $NaHCO_3$, triphosgene, -5 °C to 0 °C, 30 min., 81%.[157, 159, 160]**

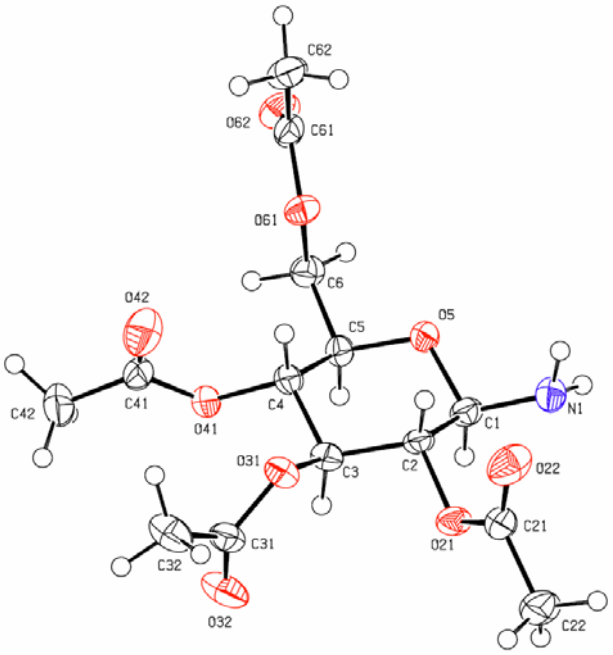

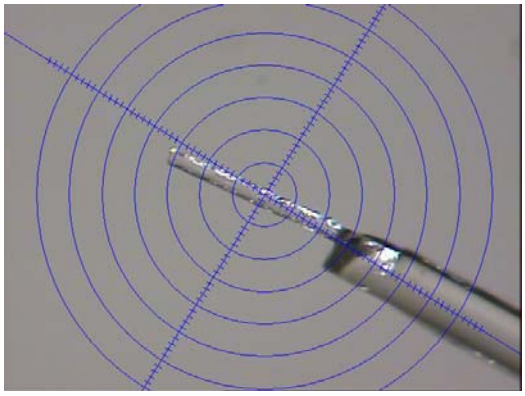

Image 4 **Single crystal for X-ray analysis of 2,3,4,6-tetra-*O*-acetyl-*β*-D-gluco-pyranosyl amine (61) from EA.**

Figure 12 **X-ray structure of 2,3,4,6-tetra-*O*-acetyl-*β*-D-glucopyranosyl amine (61). Numbered atoms: carbon C = black, oxygen O = red, nitrogen N = blue, hydrogen H = white.**

Expectedly, isocyanate **62**, is very susceptible to hydrolysis. Nevertheless, the published procedure is done in a biphasic mixture of DCM and sat. aq. $NaHCO_3$. Therefore, reliably reproducible, high yields can only be achieved by complying with some synthetic "tricks". Essentially, attention must be paid to phase separation during the reaction and during work-up. Thus, during the reaction the biphasic mixture was stirred with 500 rpm, while diluting the organic phase prior to phase separation was found to be advantageous (detailed description in the experimental chapter p. 97). Analytical data of crystals obtained from toluene/n-hexane were in accordance to the literature.[157, 159, 160]

The addition reaction using the test-compound under the conditions, developed for commercial available isocyanates, was satisfying. Analogously, the reaction of 2,3,4,6-tetra-*O*-acetyl-*β*-D-glucopyranosyl isocyanate (**62**) with ZnPc **39** was performed.

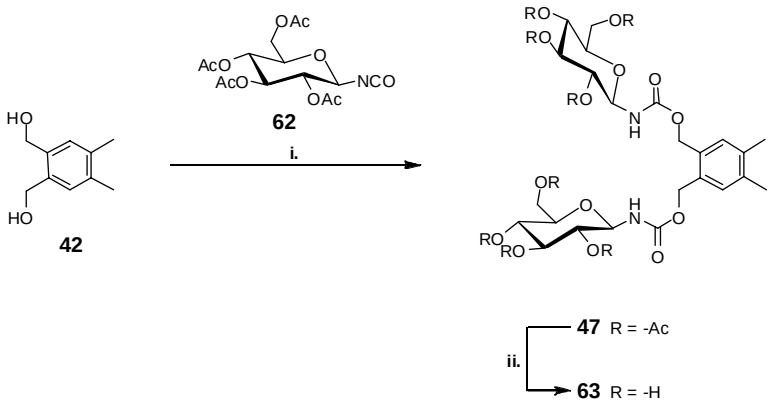

Scheme 17 **Addition of isocyanate 62 to test–compound 42 and deprotection: i.) 3 equiv. 62, Py, 50 °C, 48 h, 99%; ii.) NaOMe/MeOH (~ pH 9), r.t., 96 h, 93%.**

Deprotection *via* transesterification was first checked by using the model substance **47** (Scheme 17). The progress of transesterification could be monitored by TLC on silica gel (*n*-butanol/HOAc/H_2O = 60:20:20). During the course of deprotection three transient spots were observed and interpreted as partially cleaved species. At the endpoint acetyl groups were cleaved quantitatively, whereas the carbamate linkage remained intact, as proven by NMR.

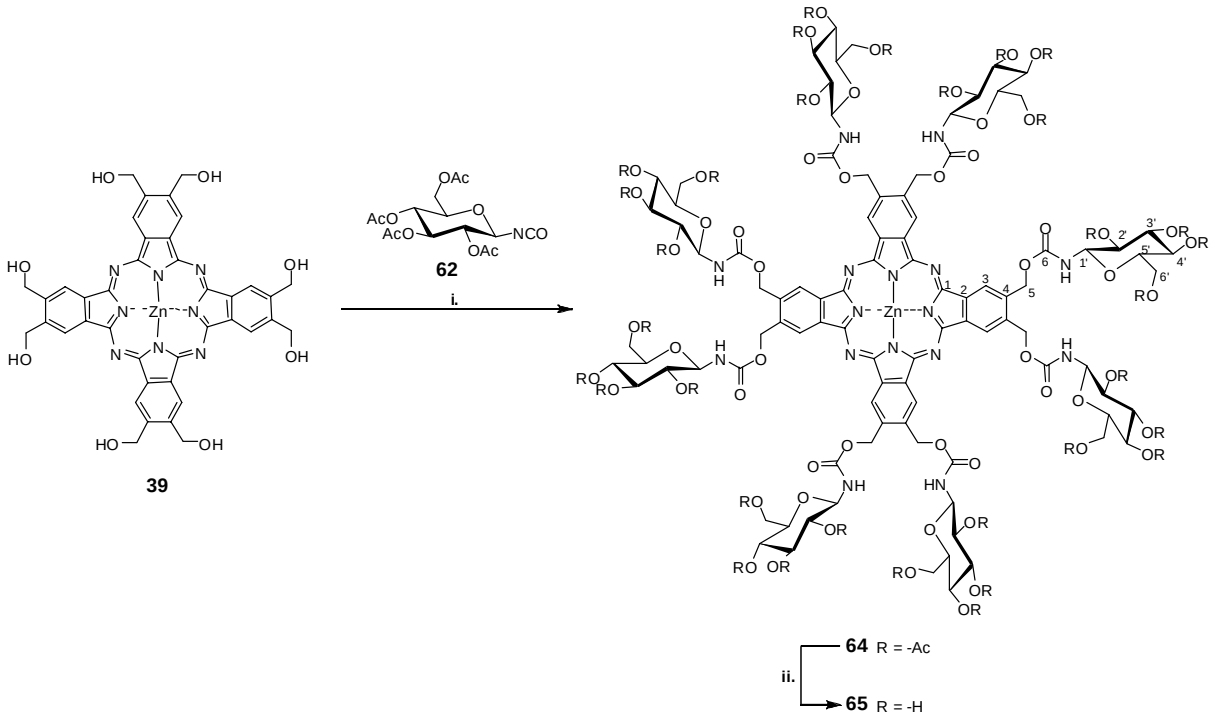

Scheme 18 **Addition of isocyanate 62 to ZnPc 39 and deprotection: i.) 2 equiv. 62, Py, 50 °C, 64 h, 82%; ii.) NaOMe/MeOH (~ pH 9), DMF, r.t., 72 h, 99%.**

This deprotection protocol was applied successfully on glucosylated ZnPc **64**. The low solubility of the fully deprotected derivative in MeOH required the addition of DMF in order to keep partially deprotected intermediates solubilized. Due to its insolubility in most organic solvents, the final product **65** could be isolated simply by centrifugation without supplemental use of ion exchange resin.

O-Alkylation

Despite of the poor solubility of ZnPc **39** in DMF, first attempts for *O*-alkylation were conducted in this solvent employing excess NaH as the base. Expectedly, the reaction run sluggish and no uniform product could be isolated. A breakthrough was achieved by using 50% aqueous NaOH in DMSO as described by Wang *et al.*[145] A clean peralkylation with propargyl bromide afforded ZnPc **69** in good yields.

*ZnPc-op-CH_2OH (**39**)*

As demonstrated above, this novel ZnPc-*op*-CH_2OH (**39**) is a versatile scaffold for a broad variety of new Pc-based molecules, even if the relatively small selection of appropriate solvents – so far DMSO and pyridine – limits the scope of applicable reactions to some extend. Obviously, the eight hydroxy groups, thus generating a solubility profile in organic solvents similar to an unprotected monosaccaride, rule the solubility properties.

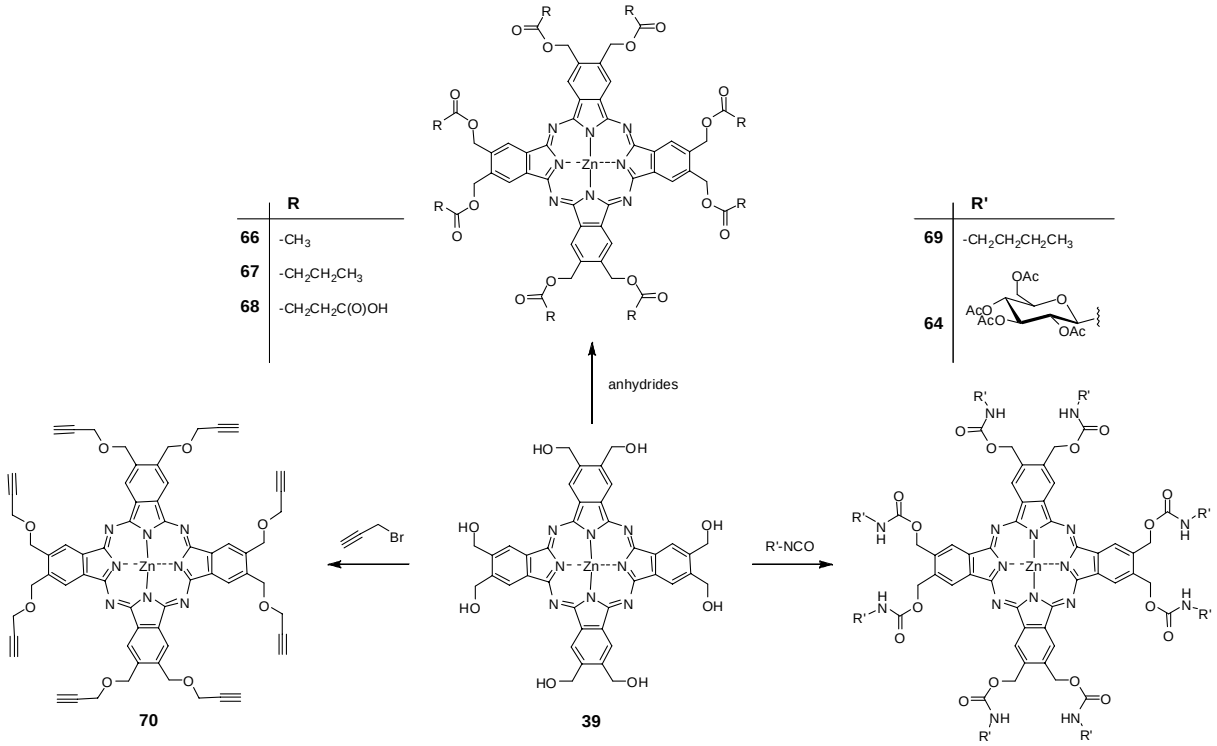

Scheme 19 **Derivatives of ZnPc-scaffold 39 derived from anhydrides, isocyanates and prop-2-yn bromide.**

Undeniable prerequisites for all subsequent derivatisation of this scaffold are regio-and stereospecifity and completeness of the reactions, in order to avoid the formation of intractable isomeric mixtures. Peracylation by anhydrides in pyridine is well known to fulfill these criterions and was applied effectually. Formation of carbamates from isocyanates was found to work excellent too and in addition has a much higher stability towards aqueous hydrolysis than esters. This permitted successful deacetylation of carbamate-linked peracetylated pyranoses as shown in Scheme 18. Finally, alkylation as described above opened new perspectives for diverse substitutions and modifications.

"CLICK-CHEMISTRY", A TOOL FOR DIVERSITY[162]

Intentionally, with the octapropargyloxy derivative **70** in hand, a plethora of cycloaddition reactions falls in place. In particular, the 1,3-dipolar cycloaddition of azides to alkynes, recently well recognized as "Sharpless-Click-Chemistry" has been established as a mild, robust and high-yielding method for the regio- and stereoselective functionalization of biologically interesting molecules.[163]

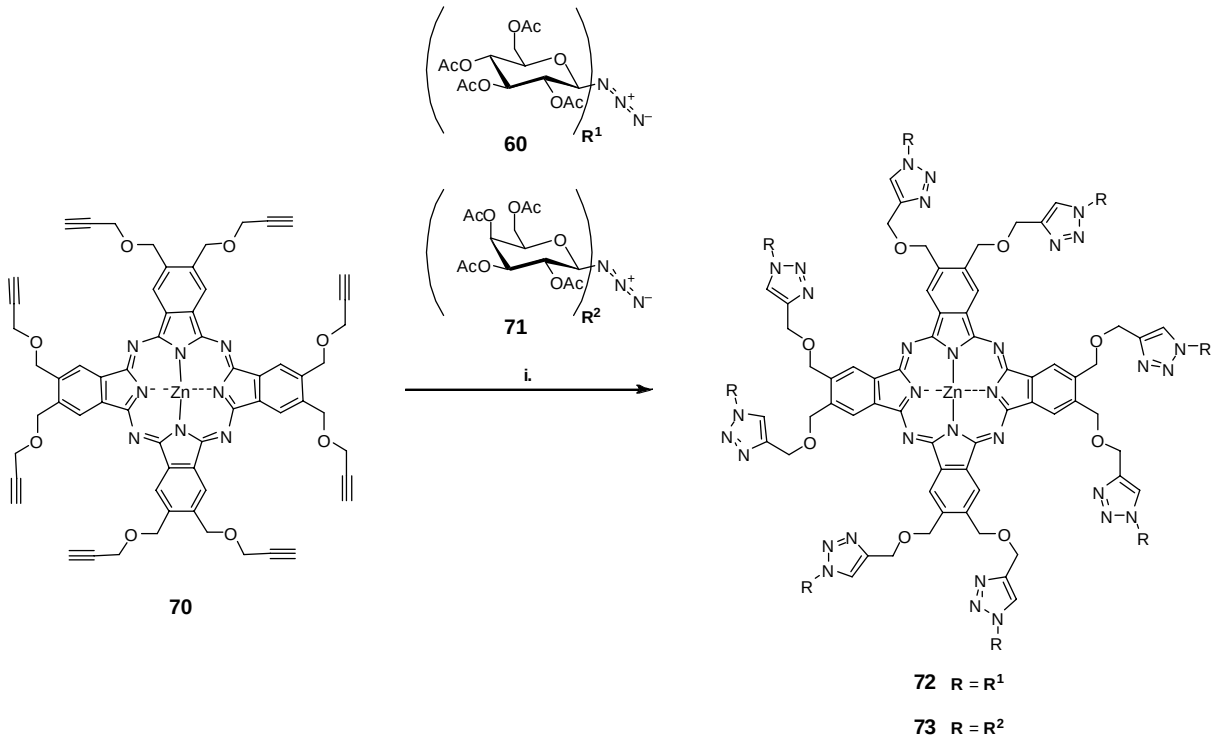

Scheme 20 **"Click-chemistry" → 1,3-dipolar cycloaddition reaction of glucosyl azide 60 and galactosyl azide 71 with ZnPc-*op*-$CH_2OCH_2C{\equiv}CH$ (70).[164] Conditions for i.) a) ZnPc 70, THF/EtOH = 2:1, 0.16 equiv. $CuSO_4{\bullet}H_2O$, 0.5 equiv. (+) sodium L-ascorbate, 3 equiv. glucosyl azide 60, r.t., light shielded, 5 d, 81%; b) ZnPc 70, THF/EtOH = 2:1, 0.3 equiv. $CuSO_4{\bullet}H_2O$, 0.8 equiv. (+) sodium L-ascorbate, 5 equiv. galactosyl azide 71, r.t., light shielded, 4 d, 72%.[146]**

A broad range of carbohydrate azides is either commercially available or quite simply to synthesize. For cell-cell interaction and recognition in biological systems, carbohydrates are of tremendous importance. Carbohydrate recognizing domains (CRD) interact specifically with sugars (glucose, mannose, galactose, etc.). In an interesting *in vivo* study on γ-imaging in Wistar rats, M. I. M. Prata *et al.*[165] monitored biodistribution and pharmacokinetics of

antennary $[^{153}Sm]^{3+}$-labeled glycoconjugates. Convincingly, the galactosylated derivative was rapidly internalized by the target organ liver, which strongly expresses the ASGP-receptor. In contrast, very little hepatic uptake was observed for compounds with terminal glucosyl groups. Blocking the receptor *in vivo* reduced liver uptake by 90%, strongly suggesting that the liver uptake of these compounds is mediated by their binding to the ASGP-receptor.[59]

Synthesis of Glycosyl Azides

Peracetylated azides of glucose **60** and galactose **71** (Scheme 20) were synthesized as described in the literature[166, 167] for triazole-coupling in a subsequent 1,3-dipolar-cycloaddition reaction.

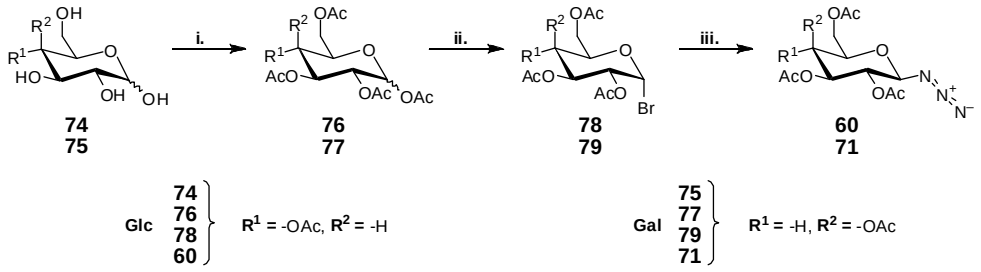

Scheme 21 **Synthesis of peracetylated azides of glucose 60 and galactose 71: i.) Py., Ac_2O, r.t., 24 h, 99%; ii.) 33% HBr/HOAc, r.t., 17 h, 65%;[168, 169] iii.) DMF, NaN_3, 50 °C, 2 h, 85%.[170]**

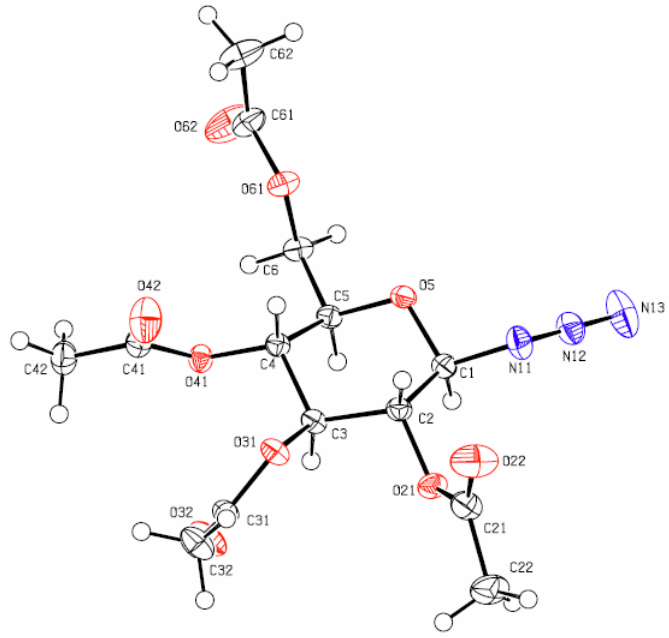

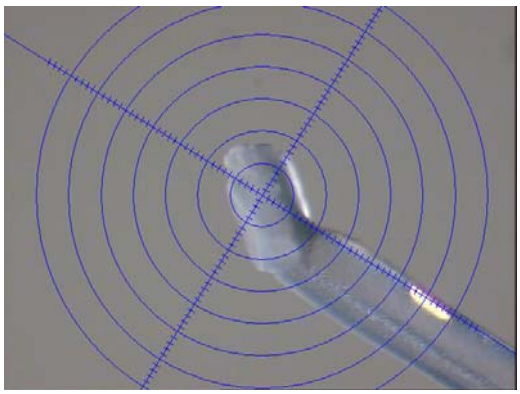

Image 5 **Single crystal for X-ray analysis of 2,3,4,6-tetra-*O*-acetyl-*β*-D-gluco-pyranosyl azide (60) from EA/Et_2O.**

Figure 13 **X-ray structure of 2,3,4,6-tetra-*O*-acetyl-*β*-D-glucopyranosyl azide (60). Numbered atoms: carbon C = black, oxygen O = red, nitrogen N = blue.[171]**

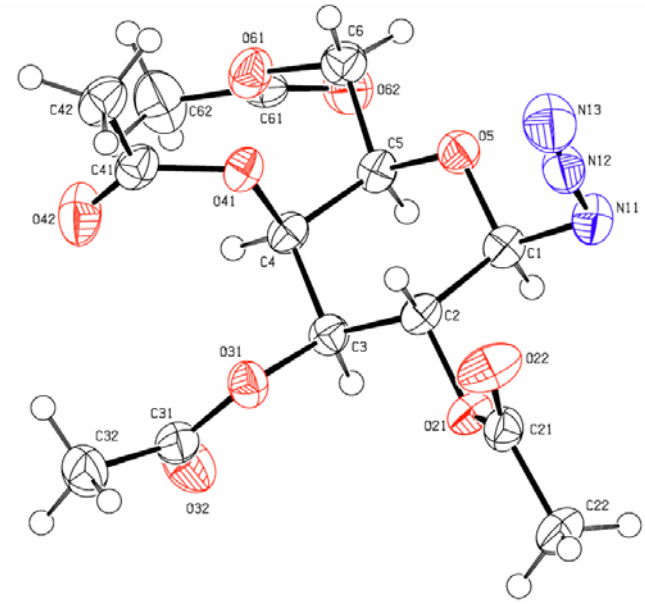

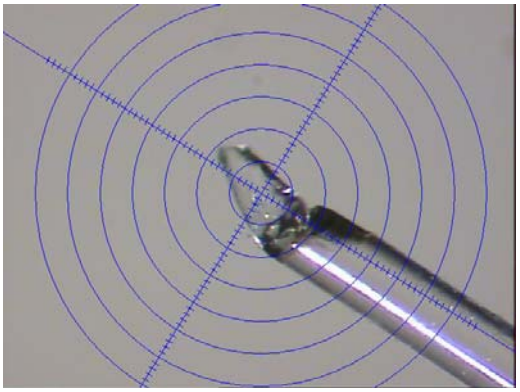

Image 6 **Single crystal for X-ray analysis of 2,3,4,6-tetra-*O*-acetyl-*β*-D-galacto-pyranosyl azide (71) from EA/Et_2O.**

Figure 14 **X-ray structure of 2,3,4,6-tetra-*O*-acetyl-*β*-D-galactopyranosyl azide (71). Numbered atoms: carbon C = black, oxygen O = red, nitrogen N = blue.**

Encouraged by the results of the carbamoylation with glucosyl isocyanate **62**, sterical bulk of the target molecule was not longer considered to be critical. Actually, the coupling reaction smoothly proceeded to completeness. After simple flash chromatography, the isomerically pure eightfold glycosylated triazole substituted ZnPcs **72** and **73** were isolated in good yields. MALDI-TOF and NMR analyses were in full agreement with the expected structures. NOESY-NMR and coupling constants unambiguously allowed the assignment of the distincive stereocenter at C-4 of the pyranose units.[172]

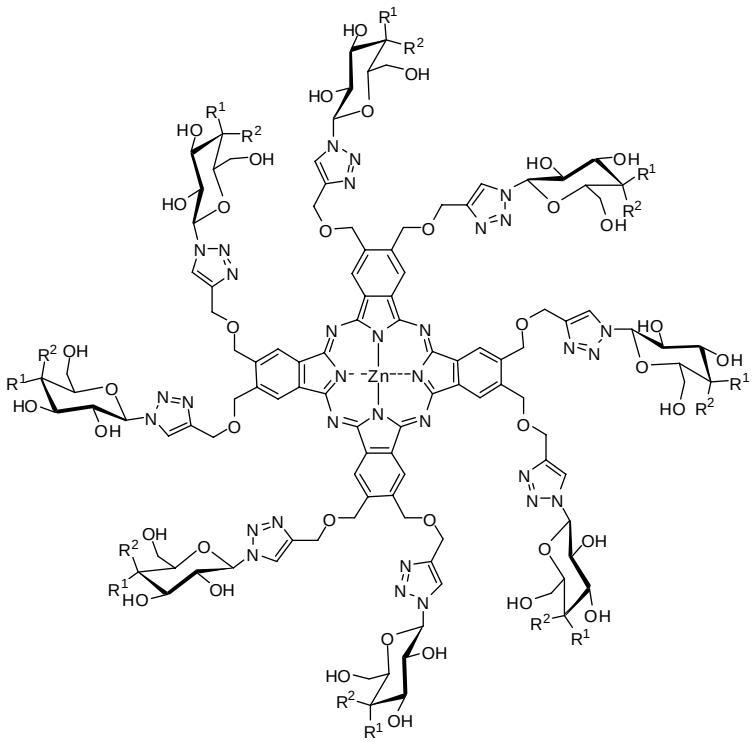

80 R^1 = - OH, R^2 = - H

81 R^1 = - H, R^2 = - OH

Figure 15 **Structure of glucosylated triazole ZnPc 80 and galactosylated triazole ZnPc 81.**

The fully deprotected glycosylated triazole ZnPcs **80** and **81** were obtained employing Zemplén[173] conditions. After centrifugation and lyophilization, they were isolated in almost quantitative yields and in analytically pure quality according to NMR spectroscopy (Figure 46 – Figure 51).

SPIRO-ANNELATED PC

With the intermediate **22** from the synthesis of ZnPc-*op*-CH_2OTBDPS (**33**) in hand, the primary rationale of a spiro annelated Pc as outlined in Scheme 8 was resurrected, since **22** was supposed to be an ideal candidate for this purpose.

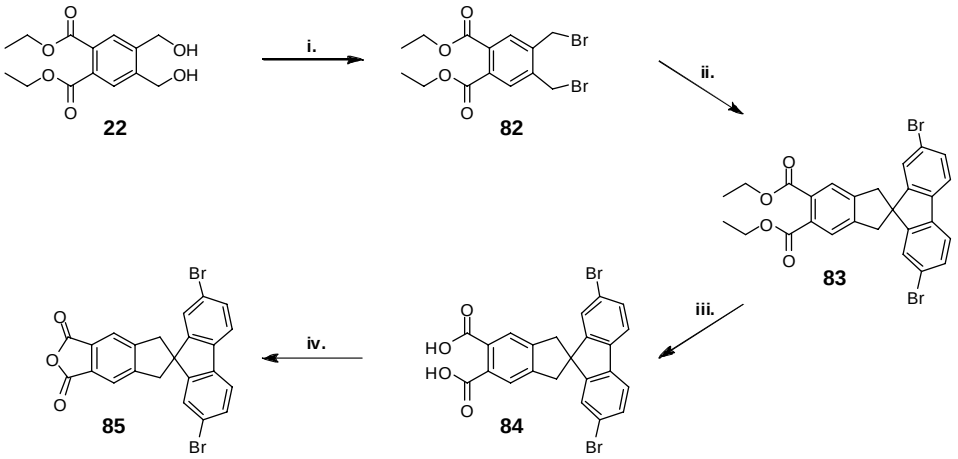

Scheme 22 **First strategy to a spiro linked phthalic anhydride: i.) LiBr, DMF, PBr_3, 0 °C / 2 h → r.t. / 24 h, 70%;[174] ii.) THF, 2,7-dibromofluorene, NaOEt, r.t., 24 h, 61%; iii.) THF, 2N NaOH, 50 °C, 12 h, 95%; vi.) Ac_2O, 150 °C, 3 h, 85%.[132]**

Starting from the diester intermediate **22,** prepared as already described in Scheme 10, bromination of the benzylic hydroxy group was achieved by LiBr/PBr_3 in DMF. Unsubstituted α,α'-dibromo xylene has been employed incidentally for the synthesis of spiro-annelated indanes under strongly basic conditions, usually in excellent yields.[175, 176, 177, 178] However, the liability of the ester functionalities to transesterification or saponification under these conditions had to be considered.

Coming along with these drawbacks during the course of this synthesis (Scheme 22), the limited performance in selectivity at the reduction of the tetra ester **21** (Scheme 10) made this route unattractive.

In general, synthetic strategies to densely substituted, highly functionalized aromatic systems *via* a lengthy sequence of functional group transformations can be challenging. Alternatively, distinct substitution patterns may be achieved straightforward by *de novo* synthesis of the aromatic ring from adequate building blocks.[179]

Alkyne Cyclotrimerization

A totally different route to the anhydride **85** was chosen when alkyne trimerization was found to be an elegant, short and efficient way. The key-step was the alkyne cyclotrimerisation to **87** in acceptable yields.

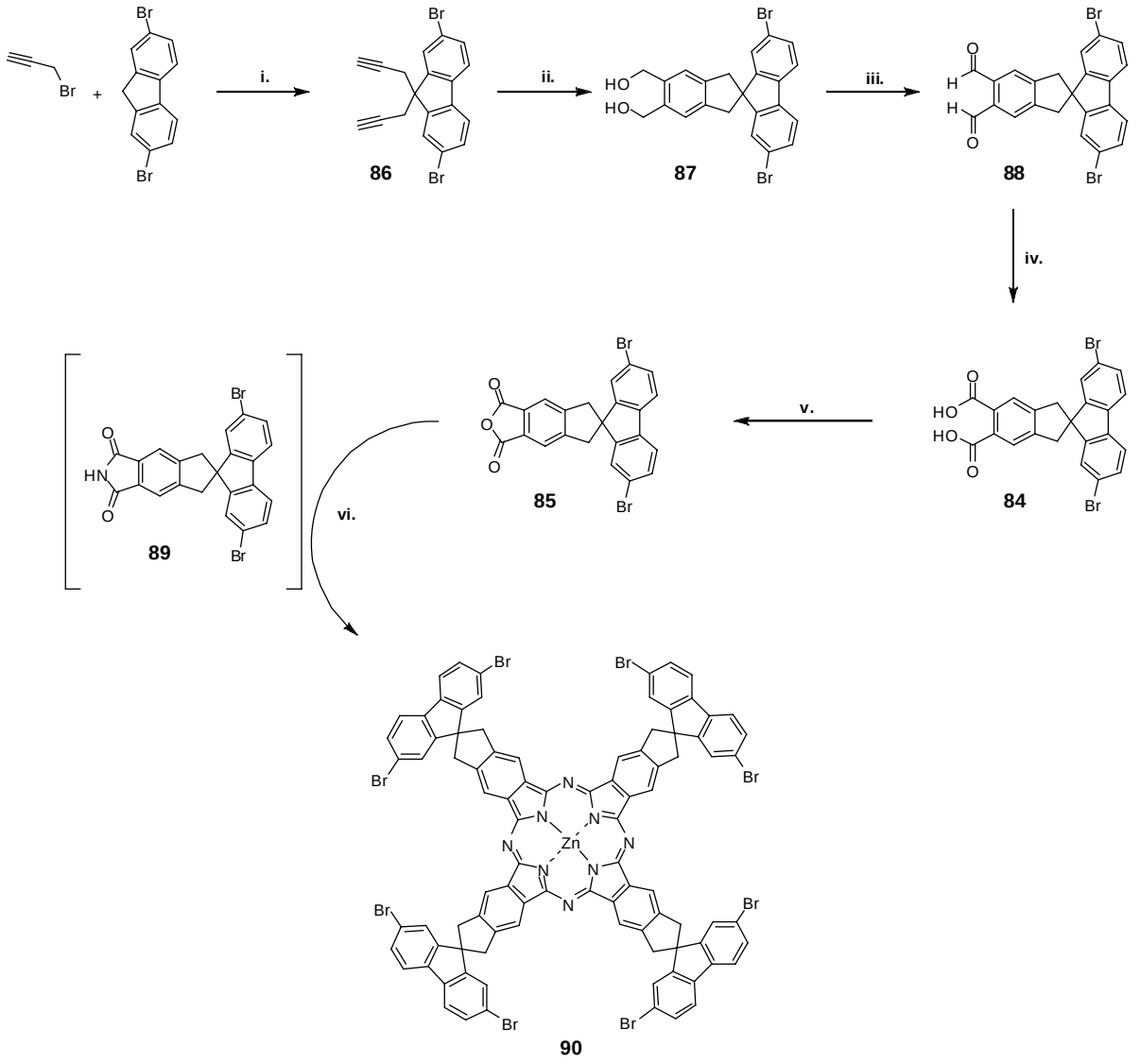

Scheme 23 **Synthesis of spiro-annelated ZnPc 90: i.) 1.5 equiv. propargyl bromide 80 wt.% in xylene, 2,7-dibromofluorene, BTEA$^+$Cl$^-$, 50% aq. NaOH, ultrasound, 60 °C, 12 h, 90%;[178] ii.) EtOH, 7 equiv. 2-butyne-1,4-diol, Wilkinson's catalyst, 70 °C, 48 h, 46%;[180] iii.) Swern oxidation, 92%;[130] iv.) HOAc, $NaBO_3$•$4H_2O$, 50 °C, 36 h, 88%;[131] v.) Ac_2O, 150 °C, 23 h, 93%;[132] vi.) HMDS, DMF, *p*-TsOH, $Zn(OAc)_2$, 100→130 °C then 130 °C / 10 h after evaporation HMDS, DMF, *p*-TsOH, $Zn(OAc)_2$, 130 °C / 48 h, 22%.**

By optimizing the procedure of Tregre *et al.*[178], the bispropargylated fluorene derivative **86** was obtained in excellent yield and in high purity after crystallization (Table 3). Sonication was successfully chosen in order to achieve sufficient agitation of the highly viscose biphasic mixture. During 12 hours of sonication, the water bath heated up to 50 °C. In all experiments, the precipitated organic substance was isolated from the heterogeneous reaction mixture by simply scraping with a spatula. After acidic extraction, the crude solid product was crystallized from DCM. However, ultrasonic effected self-heating to 50 °C was insufficient and resulted in diminished yields (Table 3, entry 1-2). Additional external heating to 60 °C gave reproducibly almost quantitative yields, independent of the concentration of aq. NaOH (Table 3, entry 3-4).

Table 3 Optimized reaction conditions of bispropargylation in a phase-transfer-catalyzed biphasic mixture.

entry	aq. NaOH [wt.%]	Temp. [°C]	Time [h]	Yield [% o.th.]
1	33	20→50	12	30
2	50	20→50		60
3	33	60		95
4	50	60		95

Several catalysts have been successfully used for alkyne trimerization, *e.g.* the well known η^5-cyclopentadienyl cobalt(I) dicarbonyl [$CpCo(CO)_2$] originally described by K. Peter C. Vollhardt.[181] However, Vollhardt's catalyst does not tolerate various functionalities, and its sensitivity to air and moisture makes handling difficult, especially on upscaling.

Alternatively, tris(triphenylphosphine)rhodium(I) chloride, known as Wilkinson's catalyst, was found to promote the [2+2+2] alkyne cyclotrimerization, as it has been exemplified extensively by Kotha *et al.*[180, 182] and Witulski *et al.*[183], and tolerates a wide varity of functional groups. The latter catalyst was successfully applied in the alkyne cyclotrimerization of the diyne substituted fluorene **86** with 7 equivalents of 2-butyne-1,4-diol to form the desired 4,5-substituted indane, spiro-annelated to 2,7-dibromofluorene **87** (Scheme 23).

Interestingly, different alcoholic solvents, like MeOH, EtOH, *i*-PrOH, or *n*-butanol work equally well. However, purity of the 2-butyne-1,4-diol used in the reaction seemed critical and prior purification is recommended. Less pure material, containing colored unidentified impurities (*e.g.* lot 13423/1 from Fluka, Table 4, first row) caused a significant drop in yield of the alkyne cyclotrimerization product **87** to mere 10% of the theory.

Table 4 **Quality check of two lots of 2-butyne-1,4-diol purchased from Fluka by mp. and TLC.**

Lot & Filling code:	Appearance	Labeled Mp [°C]	Measured Mp [°C]	TLC [R_f] *(EA)*
13423/1 40503377	bulky, orange crystals	54-57	54-57	0.37 → $KMnO_4$ 0.0 → UV
053795/1 22905143	fine, off-white, needles	54-57	62	0.37 → $KMnO_4$

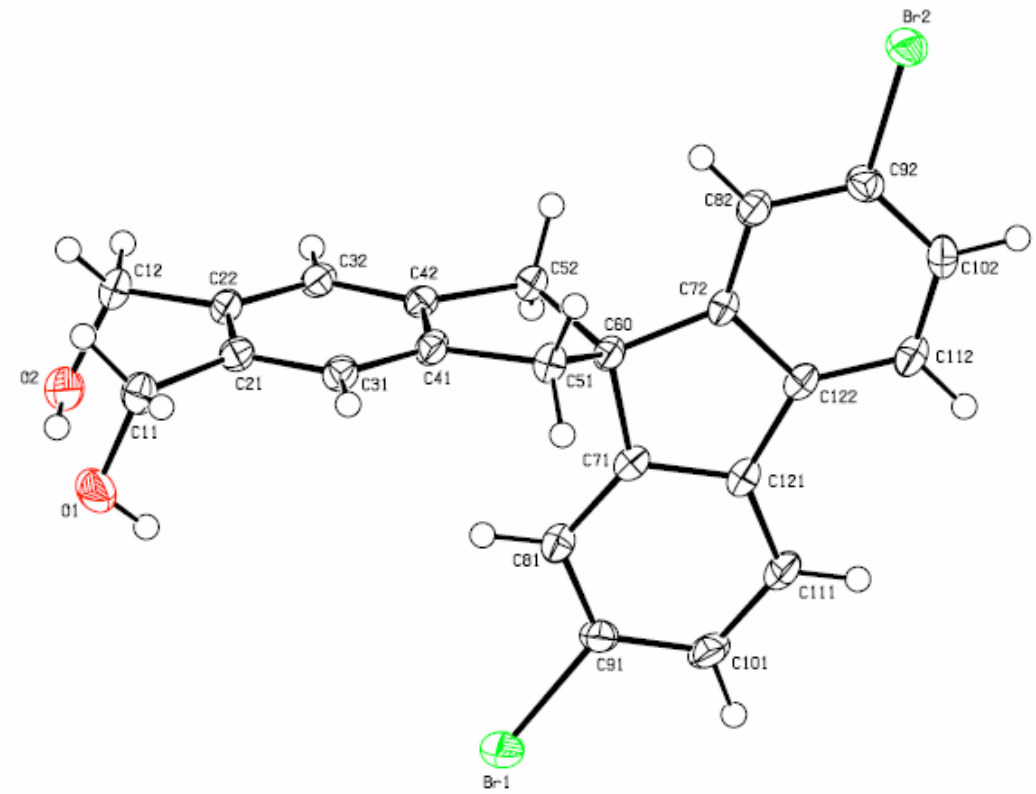

Figure 16 **X-ray structure of spiro fluorene phthalyl alcohol 87; Numbered atoms: carbon C = black, oxygen O = red, brom Br = green.**

The established two-stage oxidation sequence, employing Swern-oxidation followed by treatment with perborate (Scheme 10), and subsequent transformation to the anhydride as already described for **29** was used in order to obtain the spiro-annelated building block **85**.

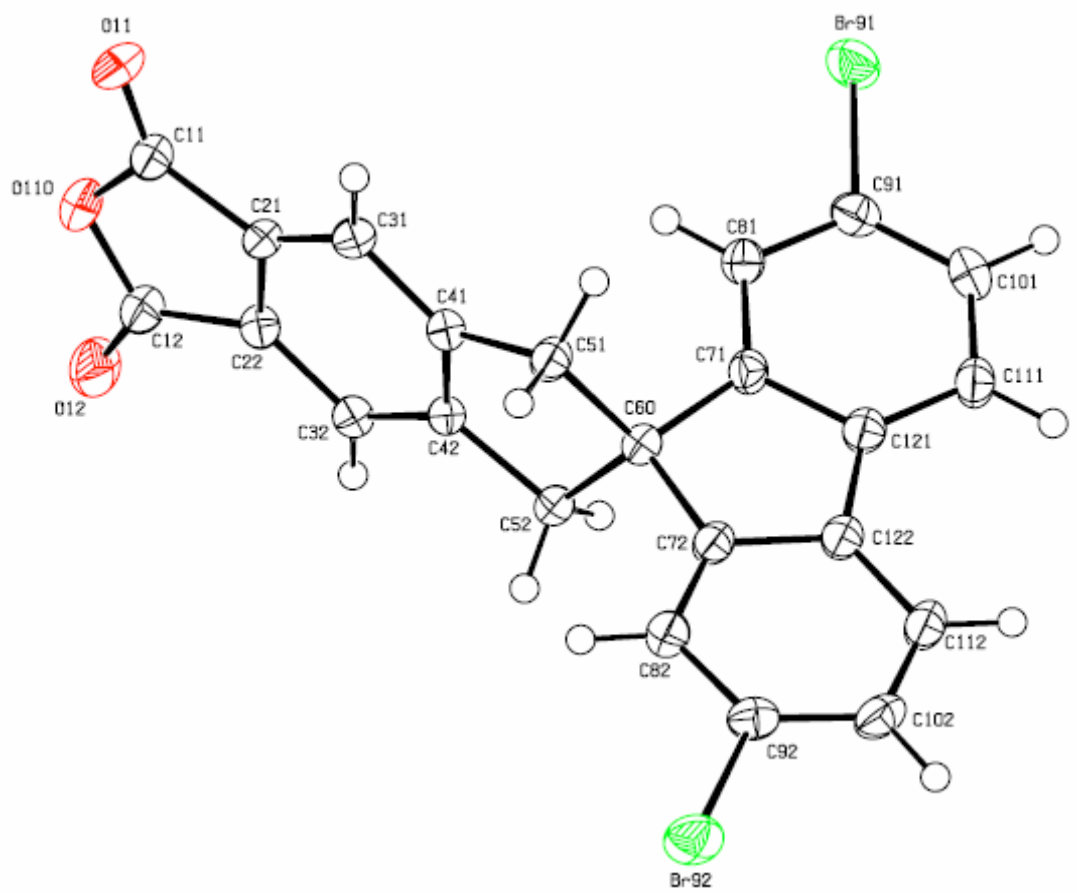

Figure 17 **X-ray structure of spiro fluorene phthalanhydride 85; Numbered atoms: carbon C = black, oxygen O = red, brom Br = green.**

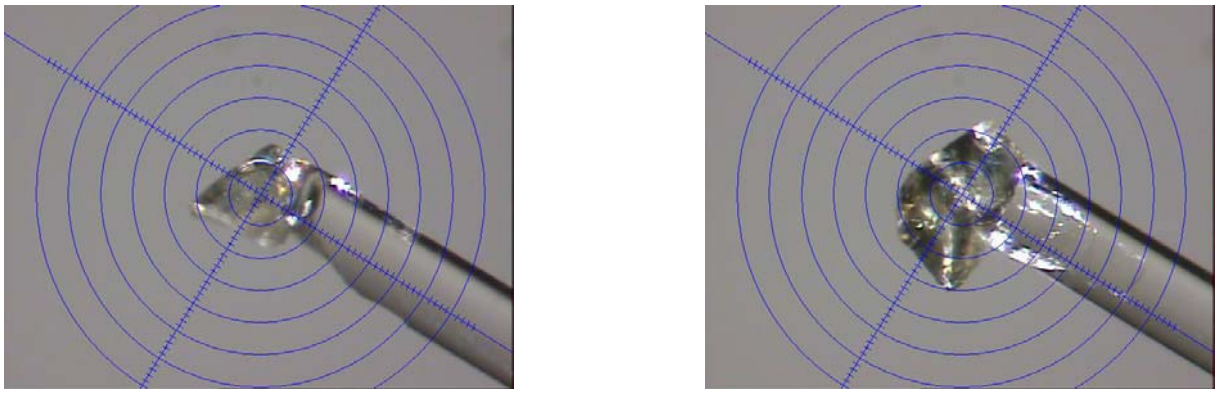

Image 7 **Single crystal for X-ray analysis of spiro fluorene phthalanhydride 85; (viewing angle 0° and 90°).**

Dibromofluorenyl Spiro-Annelated ZnPc

The protocol of Uchida *et al.*,[24] optimized for the synthesis of the silylated ZnPc-*op*-CH_2OTBDPS (**33**, **34**) and H_2Pc-*op*-CH_2OTBDPS (**35**) (Scheme 11) was applied to the 2,7-dibromofluorenyl spiro-annelated phthalanhydride **85**. However, several attempts in a scale of 300–500 mg of **85** yielded only traces of a blue solid, supposed to be the spiro fluorene ZnPc **90**. After column chromatography and size exclusion chromatography (SEC) on polystyrol resin (Biorad 12; exclusion mass 1100 g/mol) minimal amounts (ca. 10–20 mg) of a characteristic blue-colored material was isolated, showing the expected mass peak pattern according to MALDI-TOF. As a main by-product, a colorless crystalline solid was isolated and identified as the corresponding imide **89** (Scheme 23). Another finding was made when DMF and HMDS were combined at room temperature. A release of ammonia was observed, effectuated by decomposition of HMDS. So far, by Uchida *et al.*[24, 184, 185, 186], the role of DMF was only described as co-solvent, in order to facilitate solubilisation.

Upon this observation, the dark solid formed in a similar experiment (2.0 g of **85**) after 10 hours at standard conditions was redissolved in DCM, evaporated to dryness, and recharged with DMF, HMDS, $Zn(OAc)_2$ and *p*-TsOH in a tube. The tube was argon flushed and sealed, and after 48 hours at 130 °C a biphasic mixture was formed. At r.t., the upper colorless, clear phase was discarded and the lower black phase was evaporated and subjected to meticulous column chromatography on silica gel. Evaporation of the corresponding fractions afforded a blue-green residue, which was dissolved in THF and precipitated by dropwise addition into a mixture of EA/MeOH/THF (40:40:20). The composition of the solvent mixture was crucial in order to remove impurities. Thereby, filtration and washing with this solvent mixture successfully yielded the new spiro-linked ZnPc **90** in a spectroscopic pure form.

Due to poor solubility in a range of deuterated solvents or solvent mixtures, ^{13}C-NMR characterization was not possible. Nevertheless, the detected proton shifts were characteristic for Pcs[187] and in correlation with ^{13}C-shifts according to HSQC experiments. MALDI-TOF mass spectroscopy (Figure 62) and UV-vis spectroscopy (Figure 70) were in good agreement with the expected structure. UV-vis absorption spectra of spiro-annelated ZnPc **90** and the corresponding anhydride **85** in 1,4-dioxane did not indicate the formation of an "electronic coupling" from the Pc-π-system to the fluorene-π-system upon tetramerisation of **85** (Figure 71).

Dinitrofluorene-Precursor for a Spiro-Annelated Pc

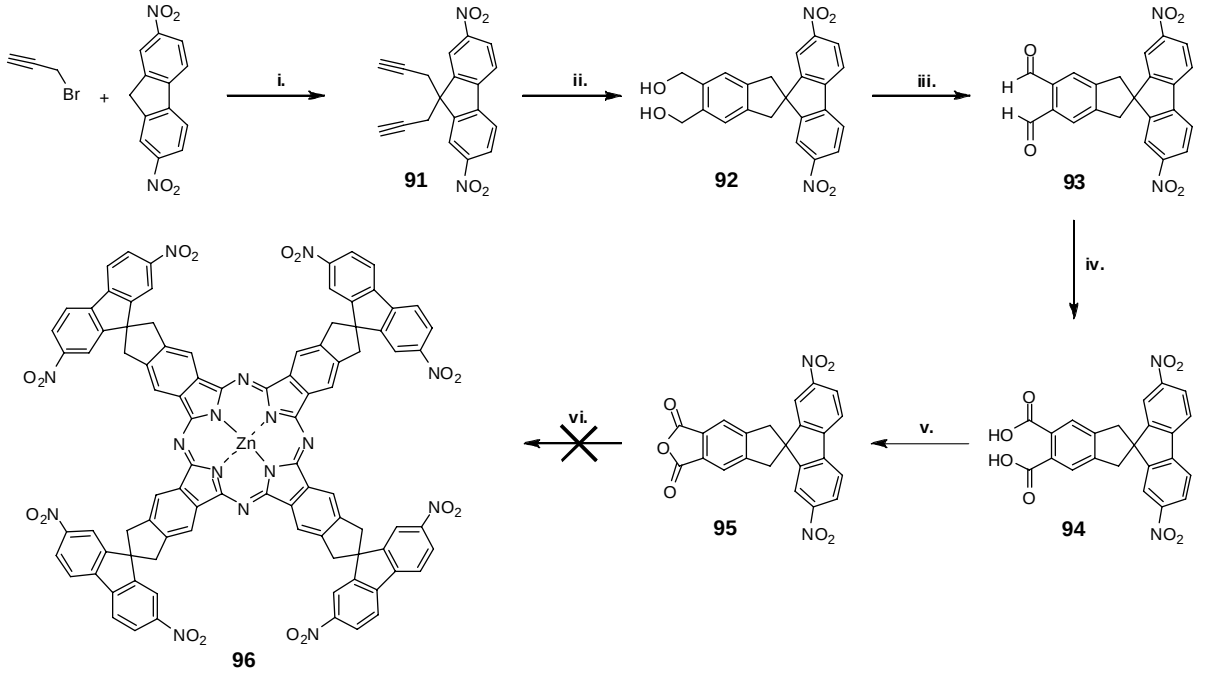

Scheme 24 **Attempted synthesis of spiro-annelated ZnPc 96: i.) 1.5 equiv. propargyl bromide 80 wt.% in xylene, 2,7-dinitrofluorene, $BTEA^+Cl^-$, 50% aq. NaOH, ultrasound, 5.5 h, 69%; ii.) EtOH, 8 equiv. 2-butyne-1,4-diol, Wilkinson's catalyst, 70 °C, 48 h, 34%;[180] iii.) Swern oxidation, 80%;[130] iv.) HOAc, $NaBO_3 \cdot 4H_2O$, 50 °C, 29 h, 88%;[131] v.) Ac_2O, 141 °C, 27 h, 84%;[132] vi.) HMDS, DMF, *p*-TsOH, $Zn(OAc)_2$, 100→130 °C then 130 °C / 48 h.**

The procedure developed for the 2,7-dibromofluorene was slightly modified and successfully applied to the corresponding 2,7-dinitrofluorene derivatives. The nitro functionality was chosen as a synthon for future transformation sequences, *e.g.* $-NO_2 \rightarrow -NH_2 \rightarrow -NHC(=O)R$ *etc.* Due to the strong electron withdrawing properties, alkylation by sonication was achieved without external heating within 6 hours. Considerable formation of tarry matter required the treatment with charcoal during work-up to isolate the bisalkyne **91**. Yields in the subsequent alkyne cyclotrimerization of the dinitro derivative were also remarkably reduced compared to the analogous dibromo derivative **92**. Even after excessive column chromatography, the spiro-derivative **92** still contained up to 15 mol% 2-butyne-1,4-diol as calculated from ^{1}H-NMR. The established oxidation sequence and formation of anhydride **95** could be performed as previously described (Scheme 10). Several attempts for the final tetramerization in order to form the desired dinitrofluorenyl spiro-annelated ZnPc **96** applying the established conditions failed so far. Further optimization may be done with good prospect.

TESTS FOR APPLICATIONS

PRELIMINARY PHYSICOCHEMICAL APPLICATIONS[188]

A plethora of intriguing applications of Pcs has been pointed out in the introduction (p. 9).

The physicochemical properties of the new ZnPc-*op*-CH_2OTBDPS (**33**, **34**) were kindly investigated in cooperation with Dr. Stephan Benning, from Prof. Dr. Heinz-Siegfried Kitzerow's group at the University of Paderborn.
The goal of these studies was a potential application of **33** and **34** in OLEDs and as light harvesting molecules as crucial components in photovoltaic cells.

As already mentioned, the preparation of thin-films *via* spin coating stringently requires Pcs, highly soluble in volatile organic solvents. The remarkable solubility of **33** and **34** made these structures excellent candidates for this technology, thus allowing their further testing in technical applications. It should be noted that all following physicochemical experiments were conducted on thin-film preparations.

The parameters necessary for the construction of a prototype OLED and a photovoltaic test unit respectively were processed according to the following *modus operandi*:

1. preparation of thin-film.
2. recording UV-vis absorption spectra.
3. graphical determination of E_g according to Tauc *et al.*[189]
4. cyclic voltammogram → HOMO.[190]
5. $E_{LUMO} = E_{HOMO} - (-E_{Tauc})$ → LUMO.
6. frontier MO engery diagram.

Due to the similarity of compound **33** and **34** the results obtained from one compound were deployed for any purpose regarding the other and *vice versa*. Thin-films of **33** and **34** were prepared by applying the established protocols for spin coating (c = 0.5 wt.% in 1,4-dioxane; 2000 rpm) and the absorption spectra were recorded:

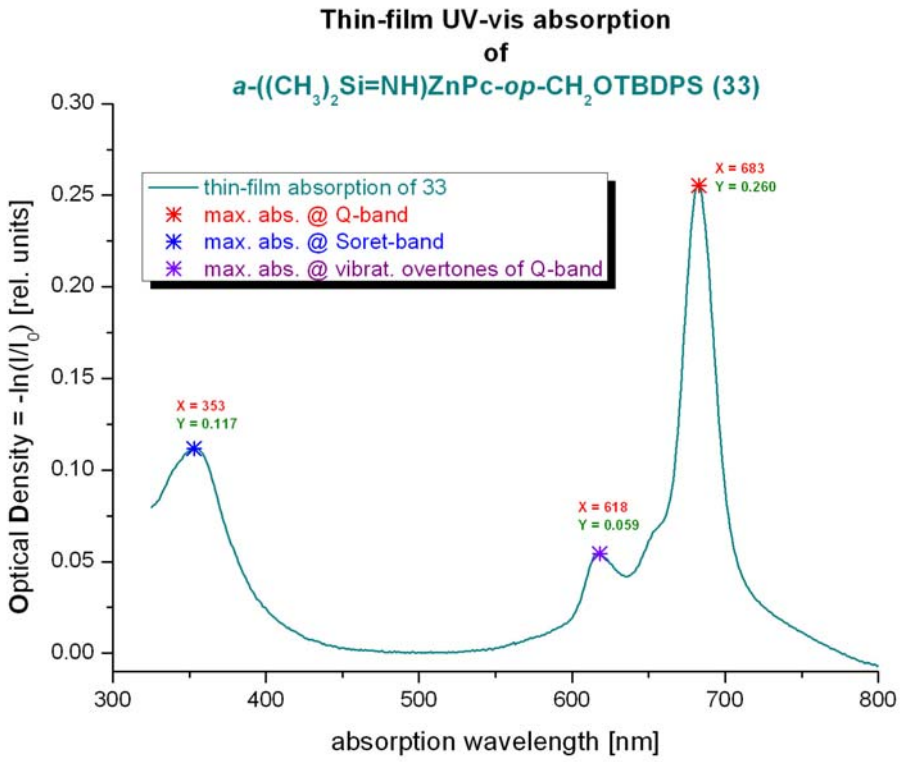

Figure 18 **UV-vis absorption spectrum of 33 derived from thin-film after spin coating.**

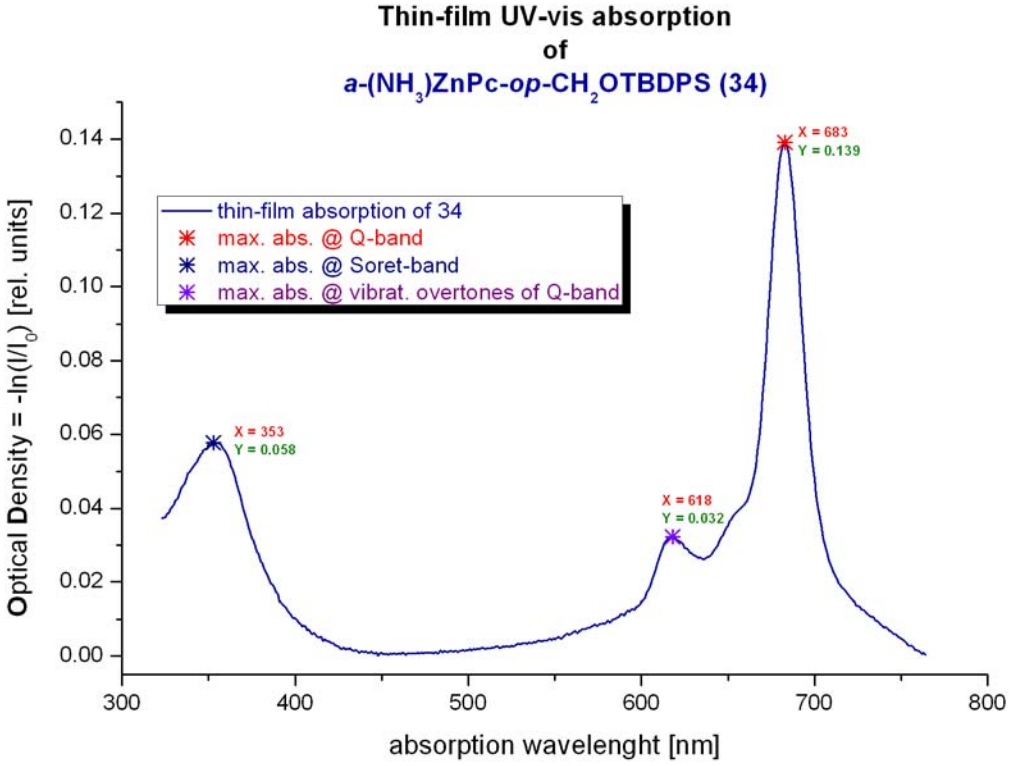

Figure 19 **UV-vis absorption spectrum of 34 derived from thin-film after spin coating.**

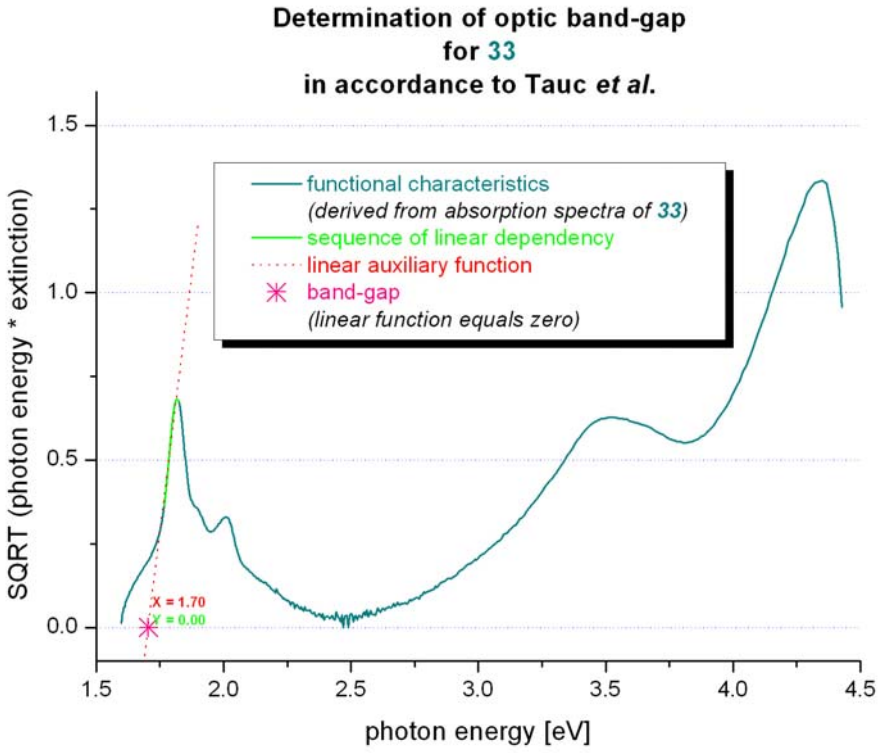

Figure 20 **Determination of band-gap energy (E_g = 1.70 eV) from 33 according to Tauc *et al.*[189]; functional characteristics derived from absorption spectra Figure 18.**

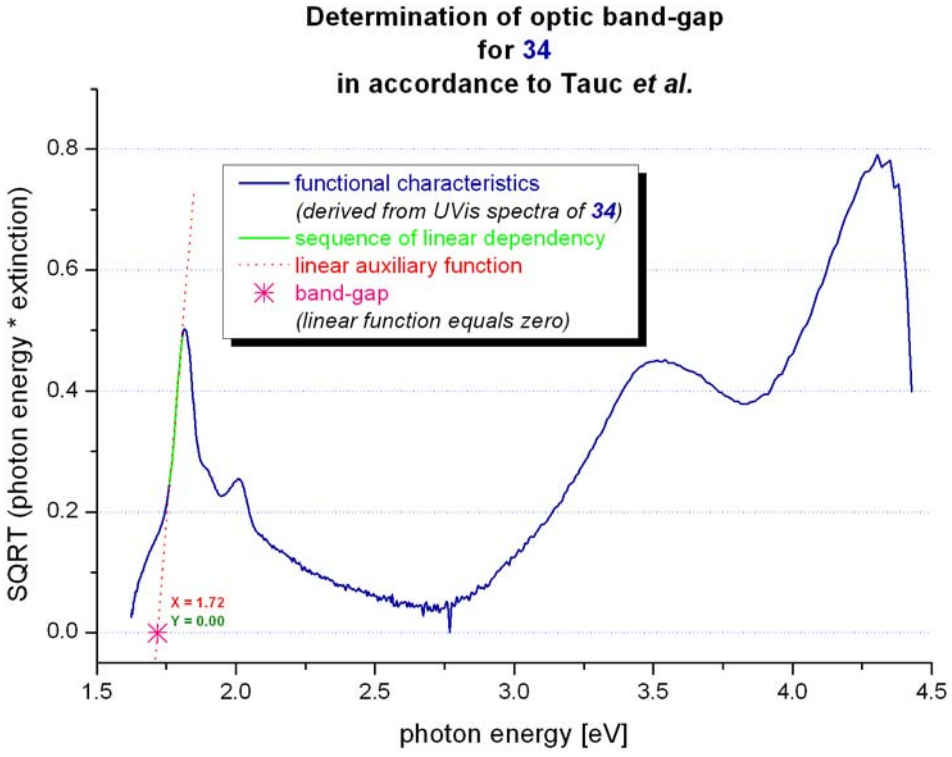

Figure 21 **Determination of band-gap energy (E_g = 1.72 eV) from 34 according to Tauc *et al.*[189]; functional characteristics derived from absorption spectra Figure 19.**

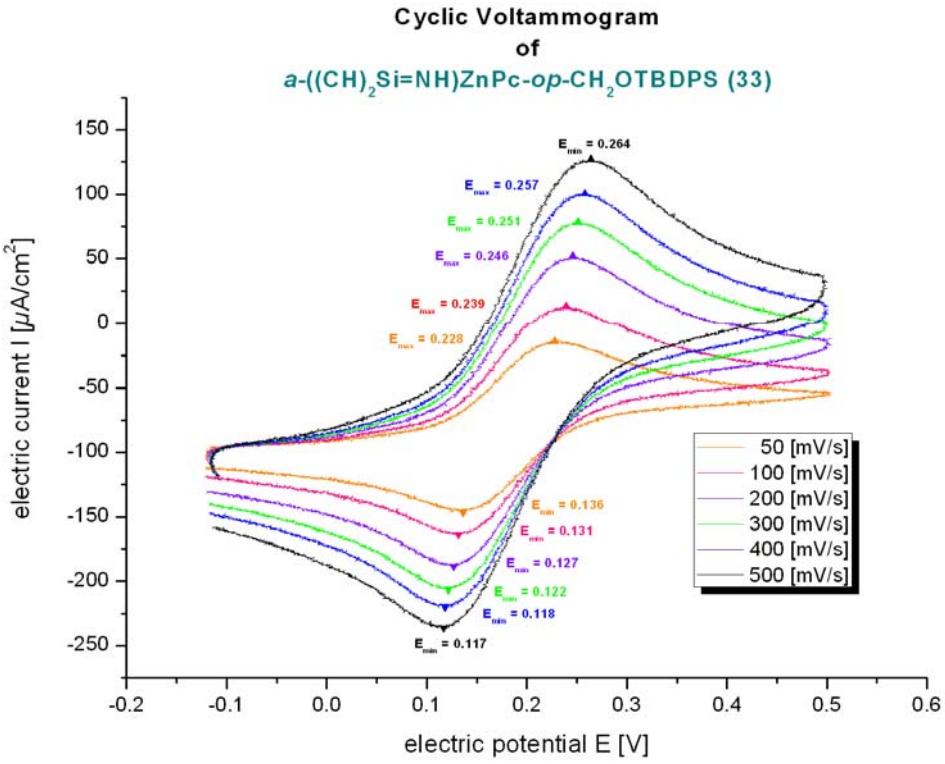

Figure 22 **CV of 33 obtained from a DCM solution at 22 °C: Pt-electrode, scan rate 50 – 500 [mV/s], [Bu_4N^+ PF_6^-] as the supporting electrolyte (0.4 M).**

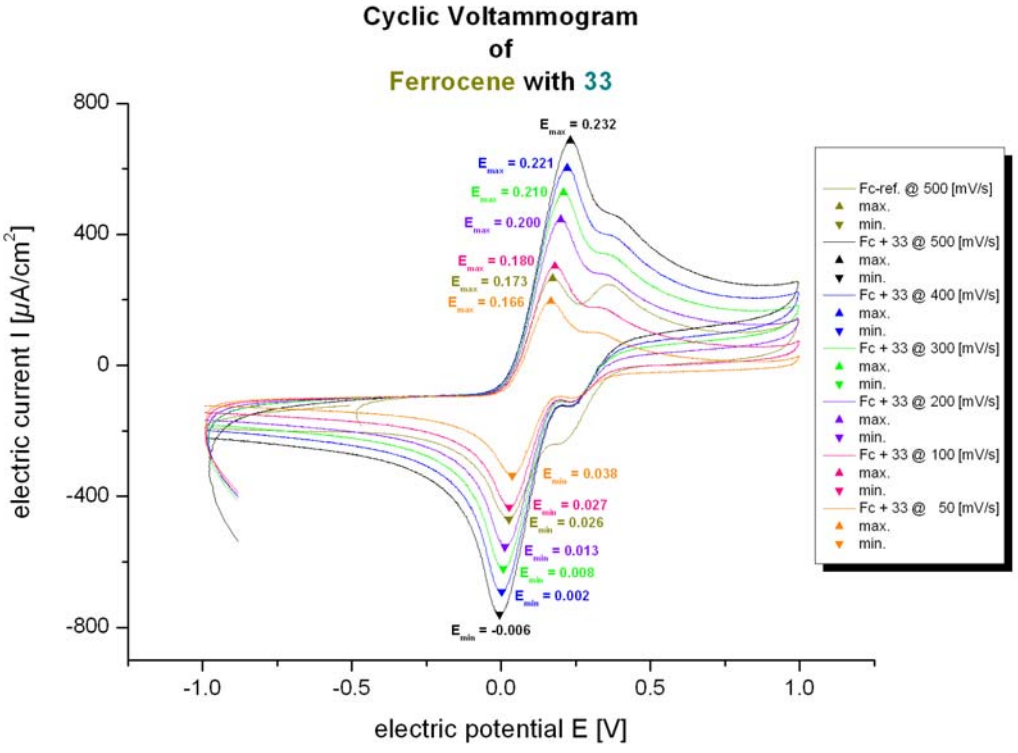

Figure 23 **CV of 33 obtained from a DCM solution at 22 °C: Pt-electrode, scan rate 50 – 500 [mV/s], [Bu_4N^+ PF_6^-] as the supporting electrolyte (0.4 M) and with ferrocenium/ferrocene (Fc^+/Fc) couple used as internal standard.[190]**

Table 5 **Calculation of HOMO and LUMO values of 33; raw data derived from CV-measurements (Figure 22 and Figure 23)[190]**

Cyclic Voltammogram of 428 + (Fc^+/Fc)	Fc (428 added) dwn	up	av.
Fc-ref. @ 500 mV/s	0.02600	0.17275	0.09938
Fc+428 @ 500 mV/s	-0.00550	0.23200	0.11325
Fc+428 @ 400 mV/s	0.00175	0.22100	0.11138
Fc+428 @ 300 mV/s	0.00750	0.20950	0.10850
Fc+428 @ 200 mV/s	0.01300	0.19975	0.10638
Fc+428 @ 100 mV/s	0.02700	0.18025	0.10363
Fc+428 @ 50 mV/s	0.03775	0.16625	0.10200
		av. of Fc	*0.10636*

Cyclic Voltammogram of 428	428 dwn	up	av.
428 @ 500 mV/s	0.11675	0.26425	0.19050
428 @ 400 mV/s	0.11800	0.25775	0.18788
428 @ 300 mV/s	0.12175	0.25100	0.18638
428 @ 200 mV/s	0.12675	0.24575	0.18625
428 @ 100 mV/s	0.13150	0.23925	0.18538
428 @ 50 mV/s	0.13600	0.22800	0.18200
		av. of 428	0.18640
		corr. av. of 428	**0.29275**

Calculation			
desired value (lit.) Ferrocene	0.40000		
actual value Ferrocene	*0.10636*		
difference	**0.29364**		
corr. by add. of Ferrocene av. actual value	**0.29275**	sum of corr. Ferrocene + corr. 428 CV-data → U_{CV}	***0.58640***
E_{HOMO} = -(4.6 +/- 0.1)eV - U_{CV}			-5.18640
$E_{LUMO} = E_{HOMO} - (-E_{Tauc})$			-3.47640

The calculated energy values of the frontier orbitals (HOMO, LUMO) of **33** justified the assembly of an OLED (Figure 25) using the similar compound **34**, and demonstrated its property of electroluminescence (Figure 26 and Figure 27). The wavelength – 688 nm – of the emitted light was in accordance with the demands for Pcs.

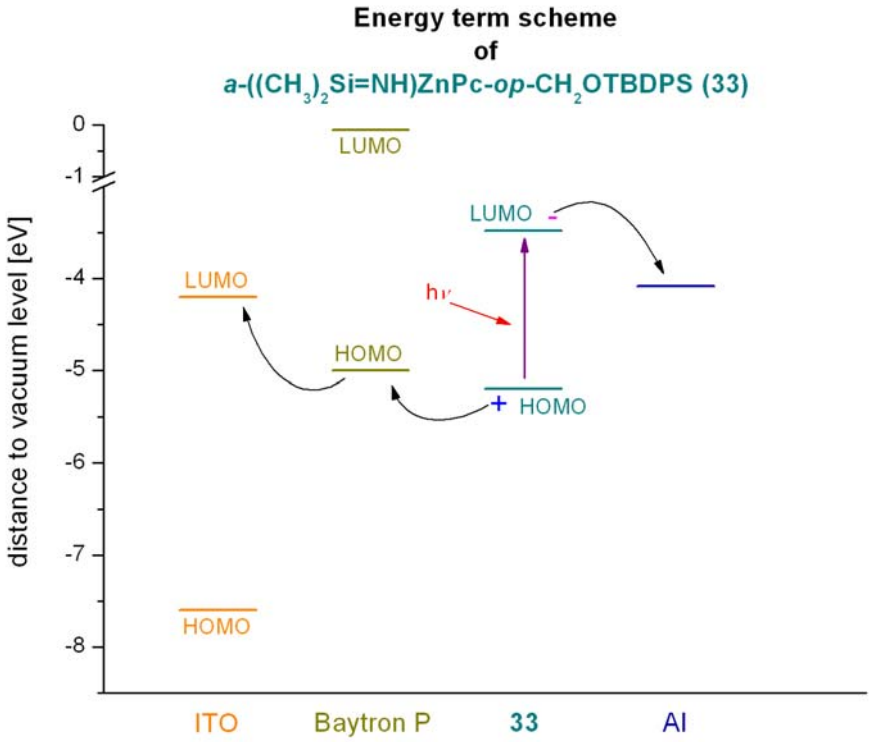

Figure 24 **Schematic energy band diagram for multilayer OLED before the electrical contact is shown, where all the energy values are relative to the vacuum level. HOMO level was obtained from CV data (Table 5) and LUMO level was calculated from the optical band-gap extracted from Tauc *et al.*[189] plots (Figure 20 and Figure 21).[191]**

A further point of interest was the expected ability of these new compounds to generate electricity. Due to the fact that the photovoltaic effect is based on the same electrophysical principles as electroluminescence, a further OLED-unit was irradiated with artificial light.

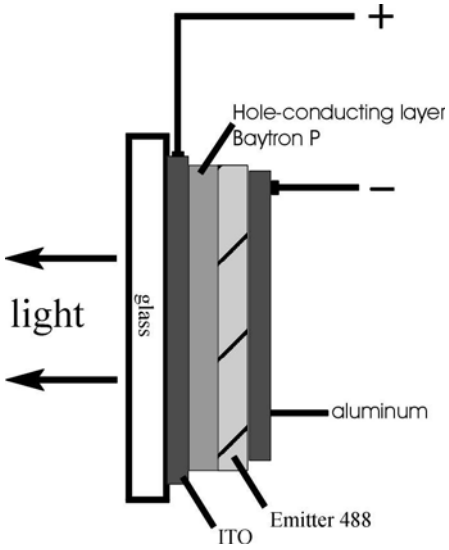

Figure 25 **Characteristic design of an OLED which was used to test 34 as an emitter. This assembly has also been used to test the photovoltaic effect of 33 and 34.**

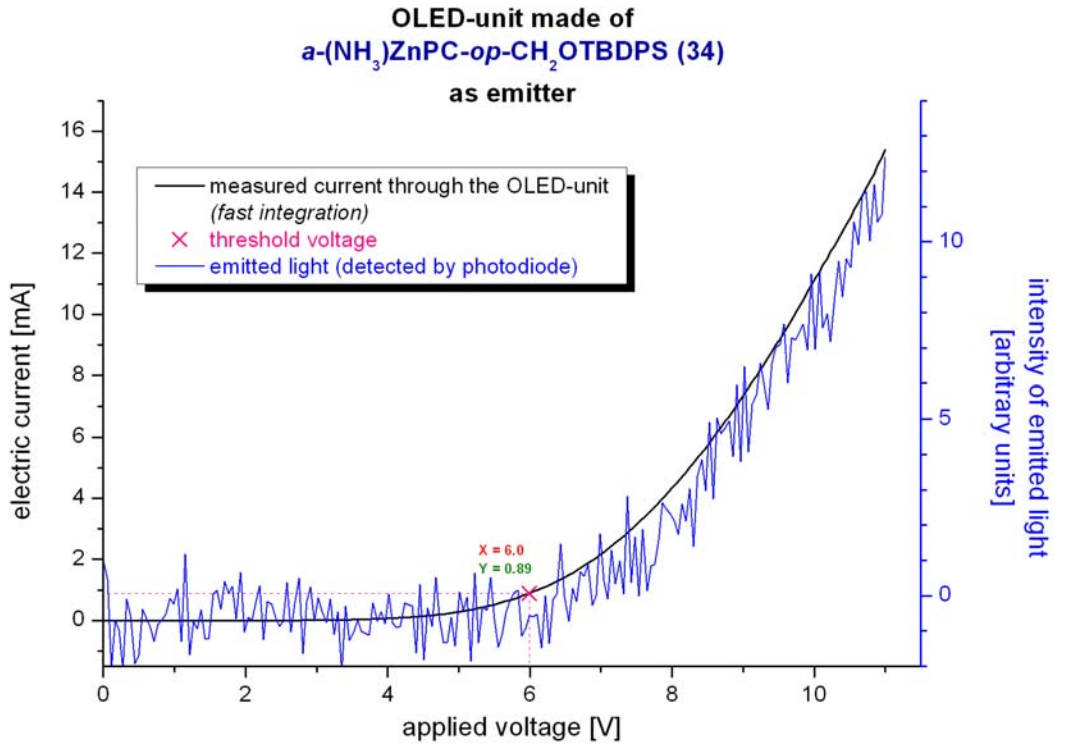

Figure 26 **Current *vs.* voltage characteristic of an OLED using 34 as emitter. The emitted light was recorded current independent *via* a photo diode. The voltage was rapidly increased (fast integration).**

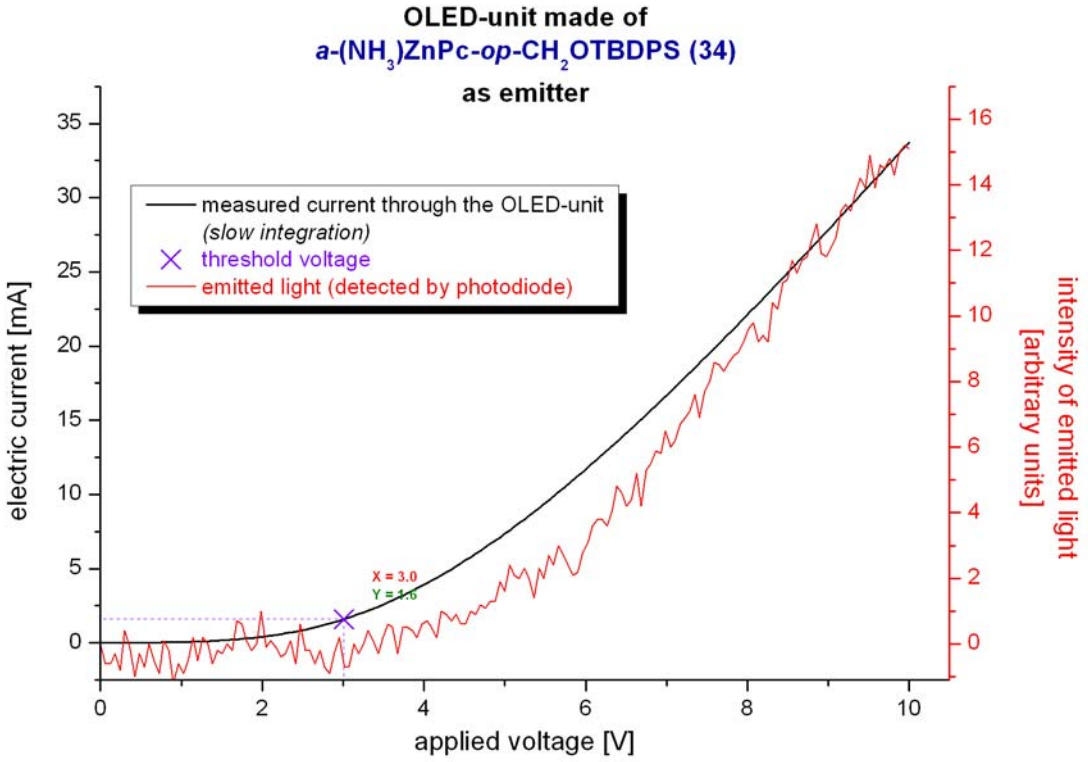

Figure 27 **Current *vs.* voltage characteristic of an OLED using 34 as emitter. The emitted light was recorded current independent *via* a photo diode. The voltage was slowly increased (slow integration).**

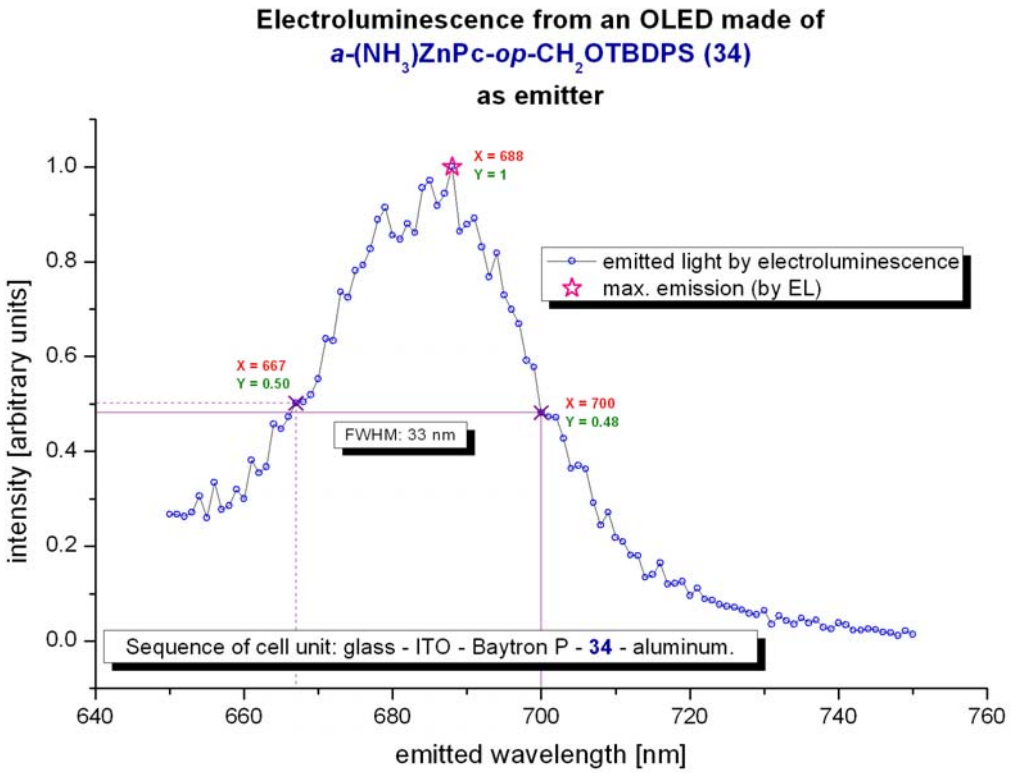

Figure 28 **Spectrum of emitted light obtained from OLED assembled as shown in Figure 25.**

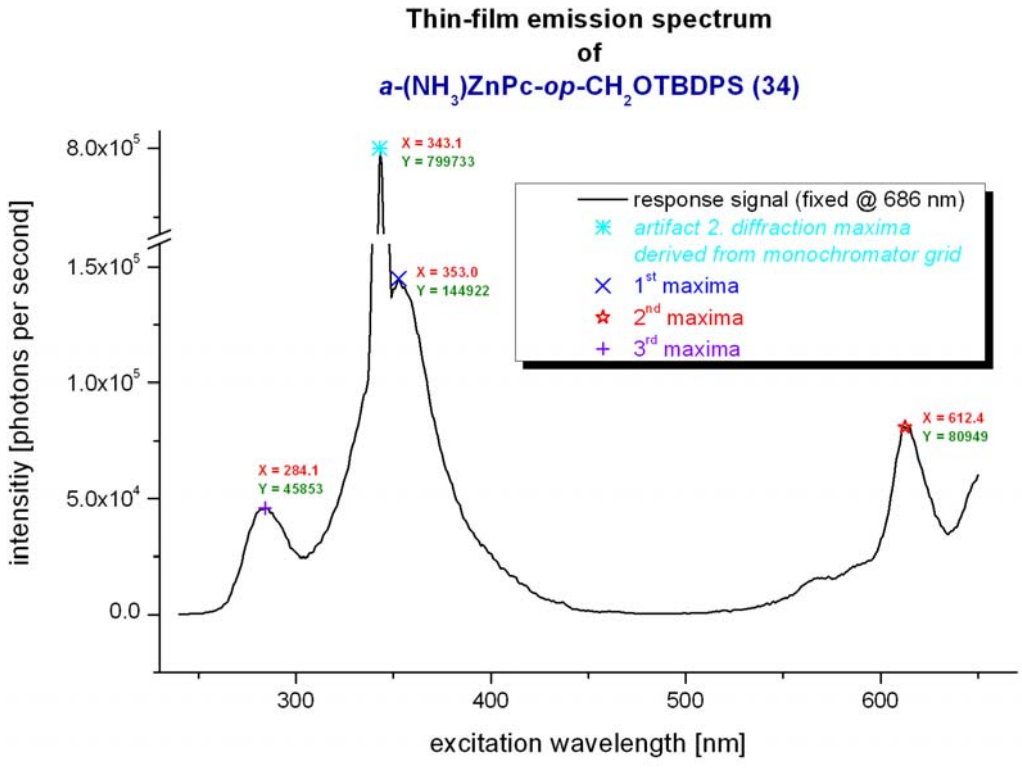

Figure 29 **Emission spectrum of 34 obtained from thin-film upon variation of the exciting wavelength; recorded response signal at 686 nm.**

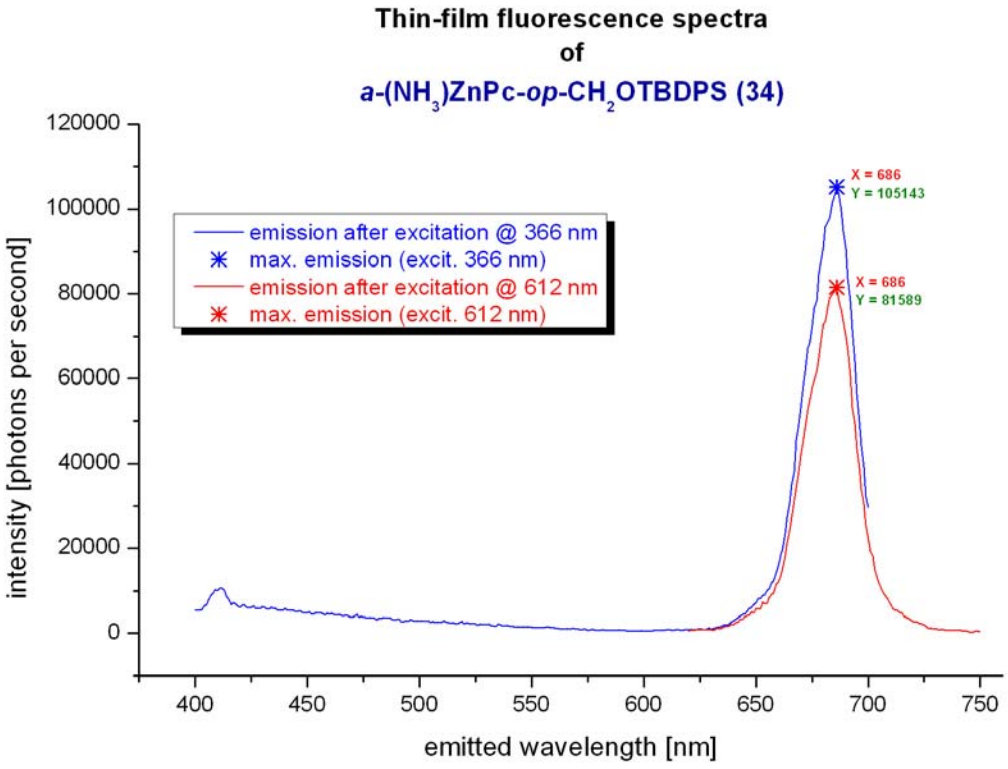

Figure 30 **Fluorescence spectra of 34 obtained from thin-film upon excitation at 366 and 612 nm.**

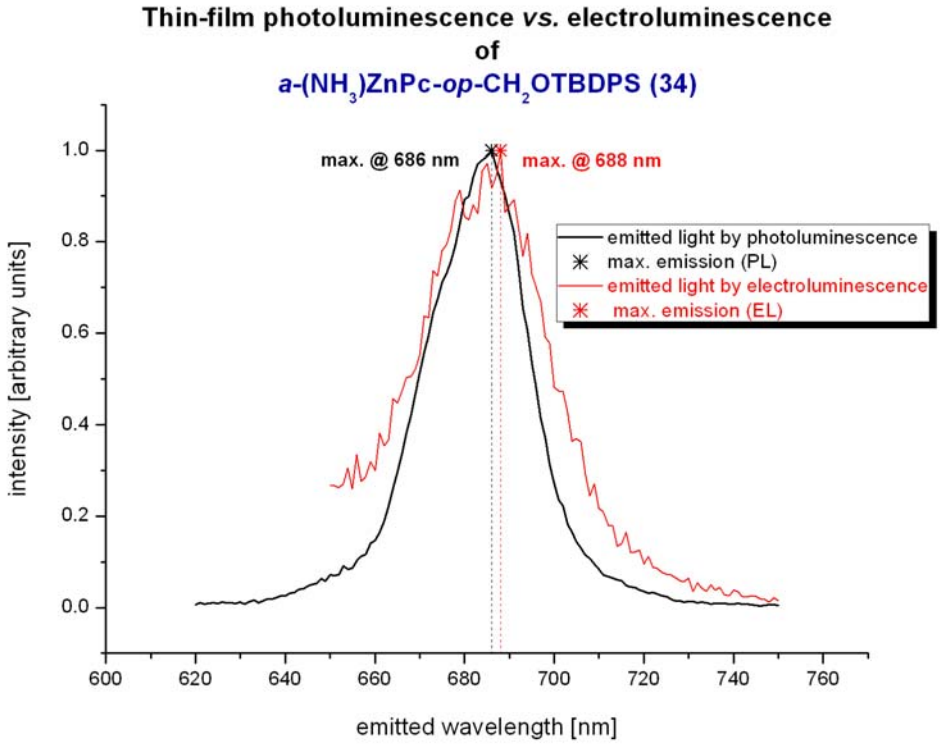

Figure 31 **Superposition of emitted light upon electroluminescence (OLED, Figure 28) and photoluminescence (fluorescence, Figure 30).**

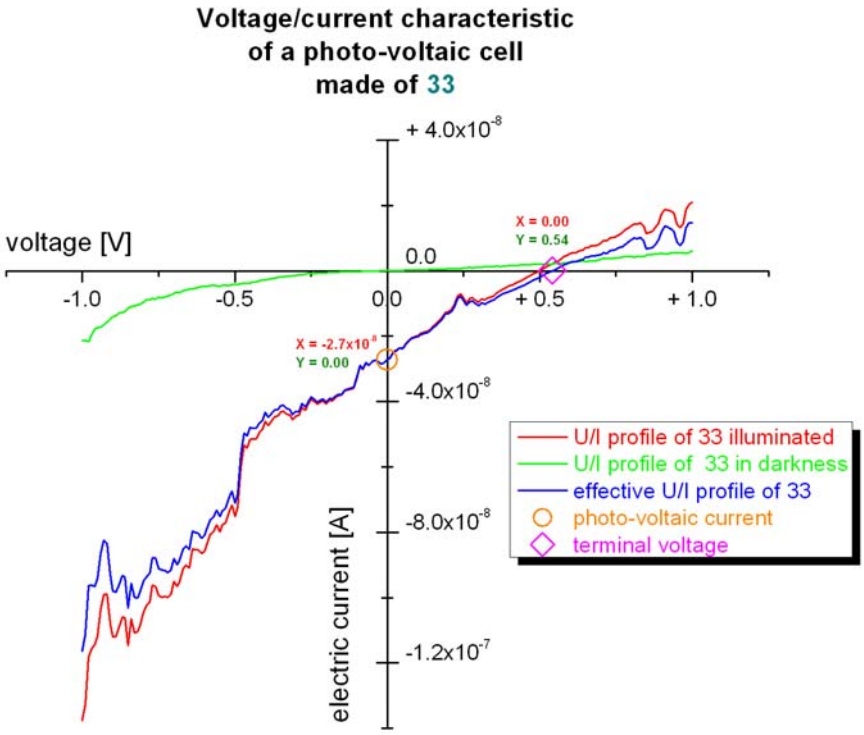

Figure 32 **Voltage-current plot of a photovoltaic cell assembled in accordance to Figure 25 with 33.**

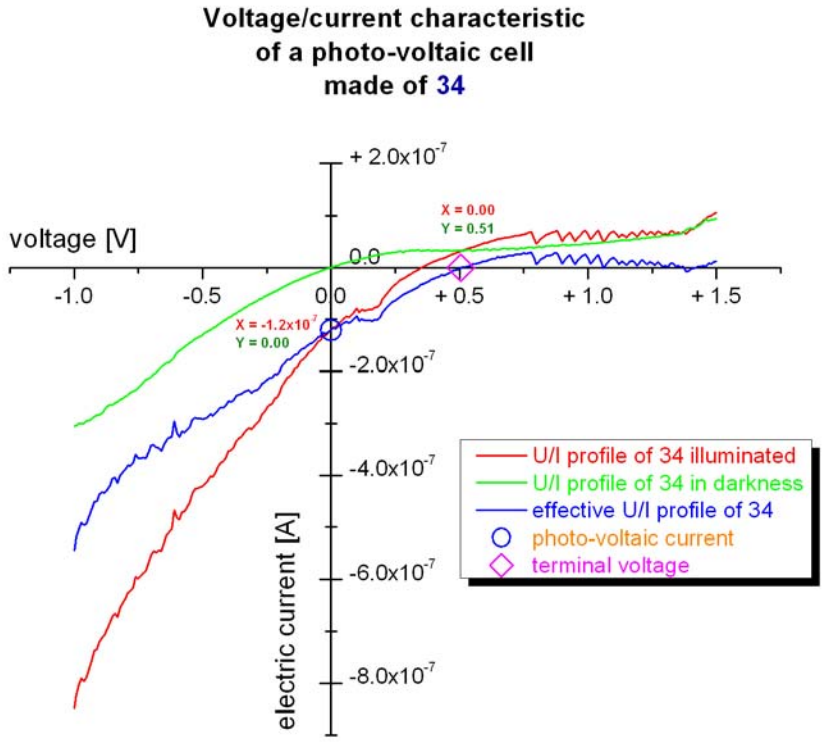

Figure 33 **Voltage-current plot of a photovoltaic cell assembled in accordance to Figure 25 with 34.**

It is well established that the HOMO and LUMO energies of Pc derivatives correlate well with their first oxidation and reduction potentials.[192, 193, 194] The measurement of electrochemical data is important, therefore, in determining the origins of the red-shifts of the Q-band wavelength. Figure 22 and Figure 23 display cyclic voltammograms of **33** in DCM with 0.4 M TBAP as the supporting electrolyte. The redox potential data are tabulated in Table 5. Only one oxidation and reduction couple was observed. From the differences between the various redox potentials (Table 5), all processes are clearly one-electron and can be assigned to either ring oxidation or ring reduction, since Zn^{+II} does not undergo redox processes within this potential window.[195, 196, 197]
The energy gap between the first oxidation and reduction potential (Q-band, lowest-energy band) of **33** was found to be 1.71 eV (HOMO → LUMO) which corresponds to the calculated wavelength of 725 nm, while the experimentally observed emitted wavelength is 688 nm, that is comparable to the absorption of the parent system (CuPc: 678 nm in solution).

However, an OLED-unit applying **34** verified the assumption to act as a red light emitter. Under unoptimized and atmospheric conditions, this test unit showed a different performance depending on the ramp time for the applied potential. A steep ramp time (fast integration) led to a higher threshold voltage (6 V) and the signal noise was high but the emitted light was in good correlation to the electric current. At a more flat ramp time (slow integration), the threshold voltage (3 V) was lower and the signal noise was low too but the emitted light with respect to the electric current was delayed. The observed electric current – almost 35 mA – determines the limited life time, thus the OLED test units could only be used once.
The same assembly as for the OLED was used to examine the photovoltaic effect. As shown in Figure 32 and Figure 33 a photovoltaic effect could be demonstrated for both lots – **33** and **34**. The photovoltaic cells were of small frame size and a commercial halogen lamp served as light source. In this arrangement the expected photovoltaic effect could be demonstrated, but was not extraordinary. The results were validated to exclude any unspecific effect. Consequently, the same unit was assembled once without Baytron P as a conductive polymer and another time without the ZnPc **33** and **34** respectively – as expected, no photovoltaic effect could be observed in both cases.

BIOLOGICAL TESTS

As outlined above, one objective of this thesis was biological testing with regard to specific receptor mediated uptake *via* the ASGP-R, and hence suitability of the Pcs for molecular imaging.

In cooperation with Prof. Dr. med. Michael Schaefer at the Department of Molecular Pharmacology and Cell Biology of the Charité / FU-Berlin the galactosylated triazole ZnPc **81** was tested on HepG2 cells *in vitro*.

Preparation of the cell assay was in accordance to standard procedure for HepG2 cells as described by Ng *et al.*[9, 28, 91] and Zheng *et al.*[198] A second cell culture was grown to serve as reference for for the 'blank'-sample in the course of spectroscopic measurements.

After 12 hours of incubation with ZnPc **81** those and the untreated reference were separately lysed by the means of ultrasound. The filtrates were sprectroscopically investigated.

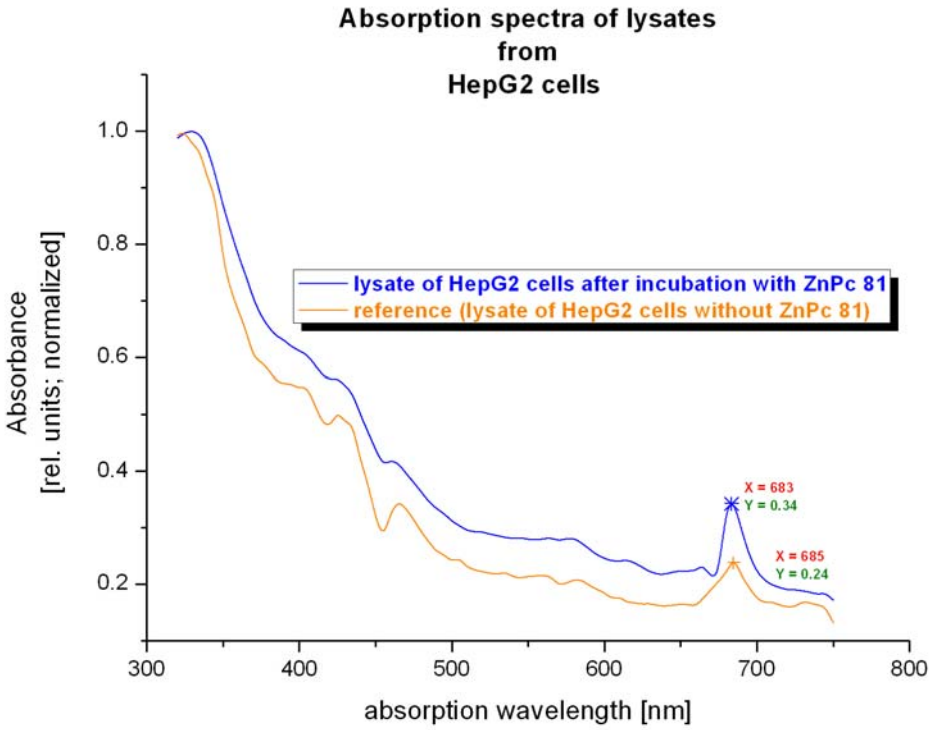

Figure 34 **Absorption spectra of lysates from HepG2 cells, once incubated with ZnPc 81 and as reference without ZnPc 81 (negative control sample).**

Unfortunately, absorption spectra gave no indicative result. Therefore fluorescence spectroscopy was further used in order to decide, whether ZnPc **81** exhibits specific affinity to HepG2 cells, or not.

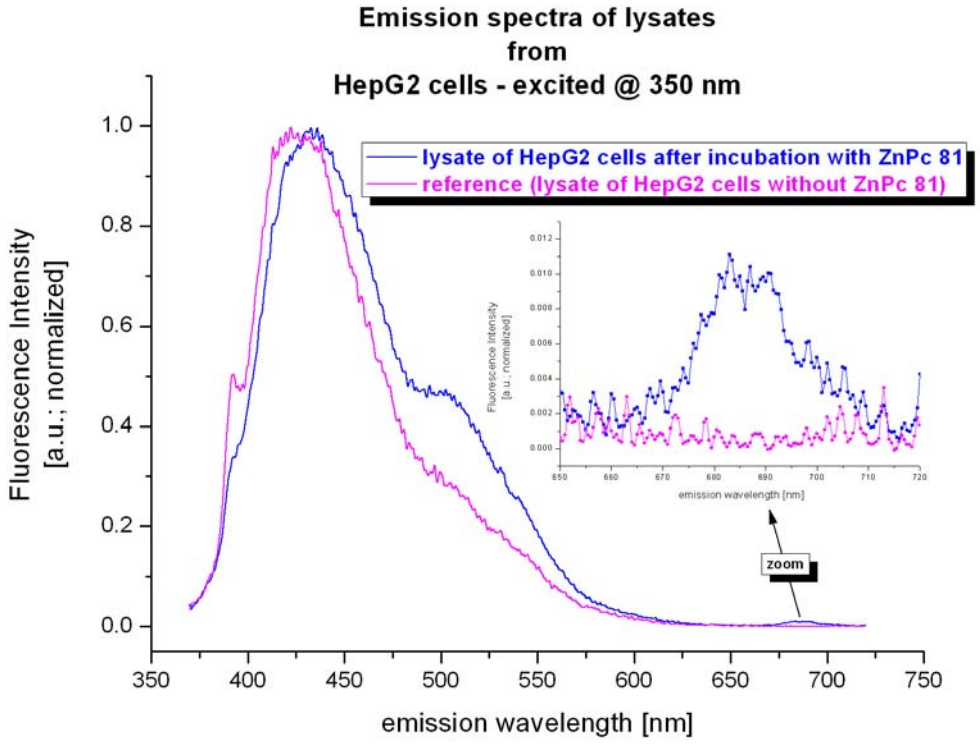

Figure 35 **Emission spectra of lysates from HepG2 cells after excitation at 350 nm; once incubated with ZnPc 81 and as reference without ZnPc 81. The inset plots the area which is significant for fluorescence emission of Pcs.**

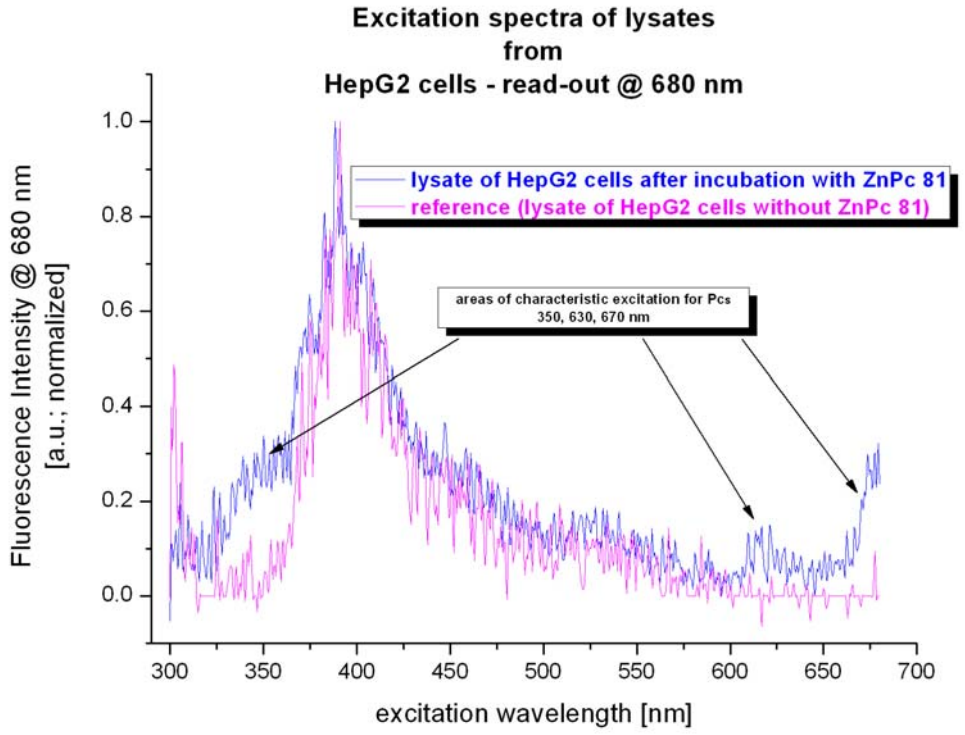

Figure 36 **Excitation spectra of lysates from HepG2 cells derived from response signal at 680 nm; once incubated with ZnPc 81 and as reference without ZnPc 81.**

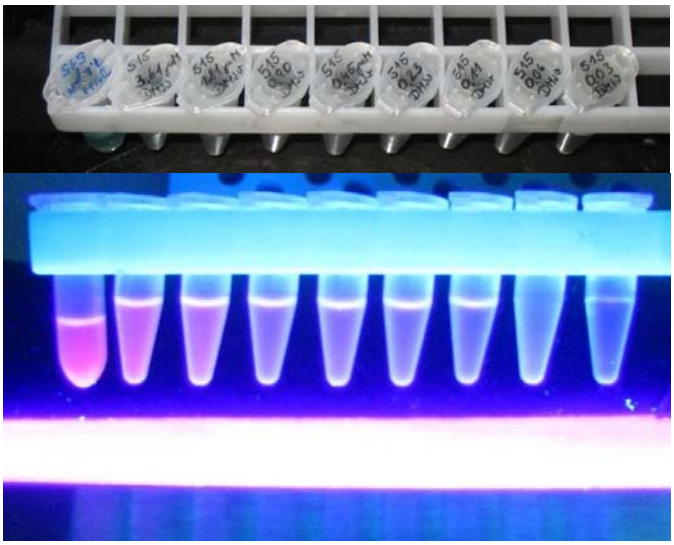

Image 8 **Dilution series of ZnPc 81 in DMSO of various concentrations from 7.2 μM to 0.03 μM. Fluorescence emission (red light) upon excitation with 302 nm by the means of an UV-table (UVT 2020 Herolab).**

At this dilution series the detection limit for the naked eye is 1.8 μM of **81** in DMSO (third sample from left). This concentration is at a scale as it has been used in the course of incubation of cell-based assays (10-8 μM).[9]

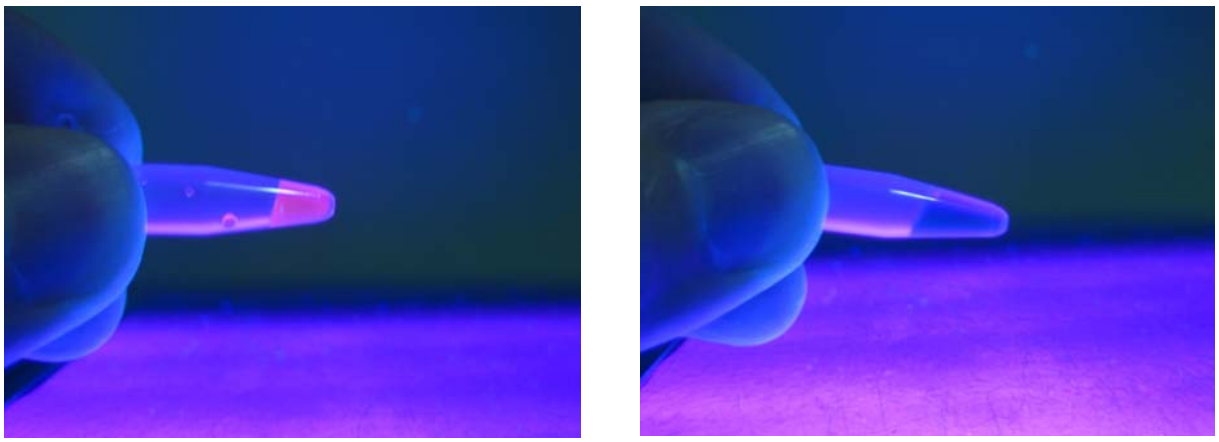

Image 9 **Fluorescence of ZnPc 81 in DMSO (44 μM, 0.1 mL) (left image). Quenching of fluorescence by aggregation caused upon dilution with 70 μL PBS: ZnPc 81 (25.5 μM in DMSO/PBS, 59:41).**

During the biological tests, a simple and effective check regarding quenching by aggregation due to solvent issues was carried out. It was found that without any formulation agent, the tolerated ratio of PBS was 37% at maximum and no fluorescence was observed at 41% of PBS. A potential solution will be mentioned at the chapter ‘Discussion & Outlook’ (p. 88).

DISCUSSION & OUTLOOK

The herein reported convergent synthesis towards the novel ZnPc-*op*-CH_2OTBDPS (**33**, **34**) has several advantages. First of all, it starts from inexpensive PMDA and can be conducted in multi-gram scale. Column chromatography is not needed and purification can rather be done simply by precipitation of the acid derivative **28** and crystallization of the anhydride **29** prior to cyclotetramerization. The crude Pc product can be purified by filtration through silica gel and subsequent crystallization of **33** and **34** or precipitation of **35** from acetone. The whole sequence seems to be adaptable for industrial production. For this purpose, the low temperature oxidation step at -78 °C needs to be re-engineered.

Whereas the most hitherto known substituted *op*-Pcs do not allow diversification in a final step, the eightfold substitution by hydroxymethylene groups – exemplified in the novel ZnPc-*op*-CH_2OH (**39**) – introduced a Pc-scaffold of unrivaled synthetic flexibility for a wide field of applications. Those derivatives can be "tailored" on customers' demands by further divergent synthetic approaches.[199] For instance, on their pursuit of supramolecular architecture, Bryce *et al.*[122, 200] generated Pcs, symmetrically functionalized with eight tetrathiafulvalene units attached *via* hydroxymethylene linkers in a conventional convergent synthesis. Hence, a divergent approach employing **39** would conveniently permit a wider variety of further optimized structures.[201]
Alkynylation, as an example, of **39** was successfully performed and it can be predicted that alkylation in general can be comprehensively applied to produce libaries of octaperipheral substituted Pcs.

Alkynylation along with the formation of triazoles *via* "Click-chemistry" opens the field for introducing a plenitude of complex, sensitive functionalities in a stereocontrolled fashion. This, as well as carbamoylation – as exemplified with **64** – will enable facile diversification in the final step, thus satisfying a central requirement of contemporary drug development. Consequently, the synthetic concept as outlined here, may further stimulate progress in the optimization of 2nd generation photosensitizer and other bioactive chemical entities.
A first biological *in vitro* assay with galactosylated triazole ZnPc **81** failed. This can be reasoned by aggregation[202] of **81** under physiological conditions, which makes detection *via*

fluorescence microscopy almost impossible. In order to prevent this phenomenon, addition of pluronic acid is recommended in the literature[91], but was in vain. Unfortunately, Cremophor® EL, which may be an even more promising formulation additive, was not accessible during the cooperation with Prof. Dr. med. M. Schaefer's group. However, the results of the second assay – investigated by UV-vis and fluorescence spectroscopy – in context with the published results by Ng. *et al.*[9, 28, 91] raised hope that formulation with Cremophor® EL will afford molecular imaging in hepatic cells.

The still unresolved aggregation – caused by π-stacking under physiological conditions – might be eliminated by introduction of axial substituents. This can be achieved by changing the coordinating metal from Zn^{+II} to *e.g.* Si^{+IV}.

I have shown that metal-free H_2Pc-*op*-CH_2OTBDPS (**35**) can be synthesized. After deprotection, treatment with $SiCl_4$ and further alkynylation with subsequent "Click"-reaction would form a 'spheric' shell of glycosyl adducts. Even simple substitution at the axial position (PEGylation, alkylation, *etc.*) may supress π-stacking under physiological conditions. The synthetic intermediate **70** may be further reacted with azides of various linker lengths. A broad range of lipohilic or hydrophilic spacers will be conceivable in between the carbohydrate and the azide moiety. This optimization potential will accomodate the findings of Biessen *et al.*[203] that a cluster galactosides with a 20 Å spacer had a 2000-fold higher affinity for the hepatic ASGP-receptor than a 4 Å one.

As the final invention of this thesis, the novel concept to a fourfold fluorenyl spiro-annelated ZnPc was demonstrated by the successful synthesis of **90**. Structural assignment was done *via* ^{1}H-NMR and HSQC experiments, supported by MALDI-TOF and UV-vis data. ^{13}C-NMR as well as ^{15}N-HMBC failed due to remarkably reduced solubility in deuterated solvent mixtures compared to the identical but non-deuterated compositions. For example, ZnPc **90** was soluble in a mixture of 1,4-dioxane and DMSO, but the same lot and the same quantity of **90** was almost insoluble in a mixture of 1,4-dioxane and DMSO-d_6. This surprising isotope effect could not be explained so far. The ^{1}H-NMR displayed some peculiarities: In several proton NMRs only two doublets appeared and could be assigned to the ortho-coupling protons (H-10 and H-11). Curiously, the integrals of these signals were accounted as for three protons rather than for two. Hence, either the missing signal set of H-8 was broadened along the aromatic shifts, or the H-8 protons became anisotropic due to the geometry of ZnPc **90**.

This finding is interpreted by the well known aromatic ring current effect which emerges in the course of NMR spectroscopy and generates an electromagnetic field in opposite to the inducing one. This aromatic ring current effect causes a down-field shift of aromatic protons that are outside of this aromatic ring, whereas protons inside the aromatic system are shifted up-field, as shown for NH-protons of H_2Pc (Figure 41). The generated electromagnetic field will have effects on protons that extend into the induced electromagnetic field during the NMR spectroscopy – above and below the aromatic plane of the Pc-core – and should cause a shift down-field or up-field, depending on the protrusion into the induced electromagnetic field. In the case of ZnPc **90** the spiro annelation creates a "teeter-totter" like arrangement of the protons H-8a and H-8b. Thus, whenever H-8a approaches proximity to the Pc-core, the opposit H-8b gains distance, and *vice versa*. As a result, the protons may be broadened and/or separated. A computer simulation of possible conformations of a hypothetical 2,7-diphenylfluorenyl spiro-annelated ZnPc illustrates this hypothesis (Figure 37).

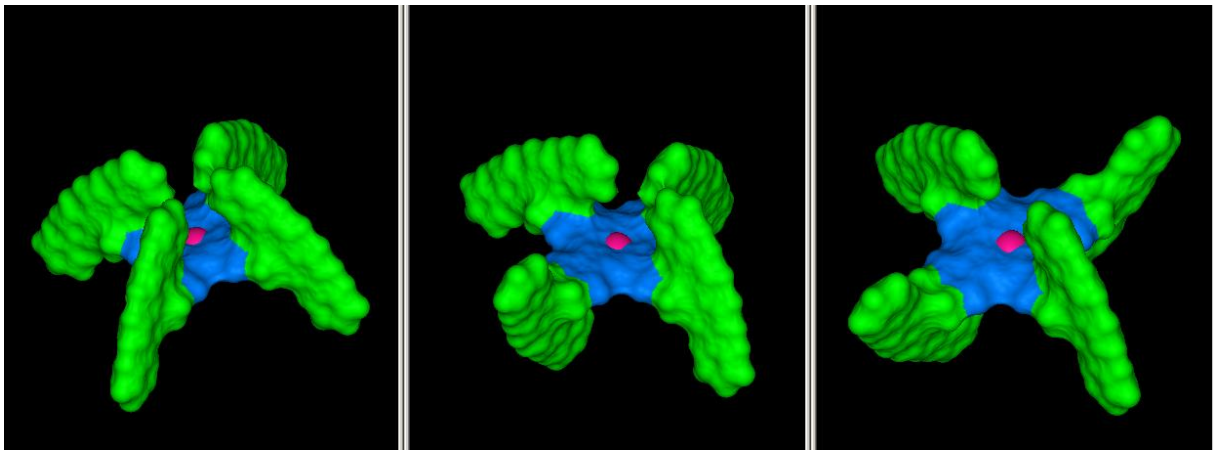

Figure 37 **Computer animated model of a hypothetical 2,7-diphenylfluorenyl spiro-annelated ZnPc.**

The observations made with this unique compound suggest, a surprisingly high tendency to aggregate. A possible explanation might be found, if considering the π-system perpendicular to the π-system of the Pc-core as an additional moiety that can show π-stacking.

As an every-day experience, quadratic stacking tables can be piled up in this manner. If this assumption is correct, this pile of molecules may show a helical self-organization. X-ray data of this compound, either from a single crystal or from powder, in combination with electric conductivity experiments may shed light on this interesting question.

Figure 38 Helical "self-organization" of quadratic stacking tables.

Whereas planar arrangements of Pcs have been thoroughly explored in the literature, there are only very few examples of ordered threedimensional assemblies of Pcs described. The synthetic potential of the aromatic bromine of **90** towards C-C coupling reactions, like Suzuki, Heck or Sonogashira[204] may stimulate further research on the pursuit of 3D molecular architecture of Pcs. The symmetry, the molecular geometry, the non-conjugated aromatic systems, as well as the rigidity are characteristic for this structure. These properties will sustainable influence the properties of any derivative emerged from this structure. Generally, thin-films of phthalocyanines are of interest for applications in photovoltaic, electronic, and sensing devices.[4] The self-assembled monolayer (SAM) technique developed in the groups of Whitesides[205], Ulman[206], and Nuzzo[207] offers great advantages in that the monolayer films are chemically bound to substrates so that reproducible, stable films can be formed.

Cook and Russell *et al.* used this approach to make monolayer films of phthalocyanines on gold and SiO_2 by reacting the surfaces with phthalocyanines that contain pendant thiols and trichlorosilanes. Additionally, besides the applications mentioned above, the conformational restrictions suggest applications as molecular tweezers[208] or clamps[209].

SUMMARY

The major goal of this thesis was to explore a synthetic pathway to a manifold carbohydrate decorated phthalocyanine, potentially of dendritic structure, with prospect to be soluble under physiological conditions and a promising candidate for *in vitro* tests regarding the cellular uptake.

The first synthetic strategy to a substituted tetra-spiro-annelated Pc failed because of insufficient thermal stability in solution of the trispiro-cyclotriphosphazene precursor probably due to ring strain.
In pursuing this aim, a decisive result of the first strategy was a benzene-1,2-dimethanol subunit as part of the Pc-precursor from which the cyclotetramerization should be performed. To get access to this subunit, an efficient multi-gram synthesis to a highly soluble Si-protected Pc starting from PMDA was developed, after the dissatisfactory bromination route (p. 45).

This highly soluble ZnPc-*op*-CH_2OTBDPS (**33**, **34**) was isolated from two experiments. According to X-ray analysis the two lots – 428 and 488 – differ with regard to a fifth ligand coordinated to the central atom of the Pc. As outlined in the introduction solubility is a crucial factor to explore Pcs'properties and for industrial applications, apart from the use as pigment (p. 14).
Some physicochemical properties such as photoluminescence and electroluminescence from thin-films of the new ZnPc-*op*-CH_2OTBDPS (**33**, **34**) were kindly investigated in cooperation by Dr. Stephan Benning, from Prof. Dr. Heinz-Siegfried Kitzerow's group at the University of Paderborn. Unoptimized tests affirmed – in principle – the applicability as emitter substance for red light OLEDs and as photovoltaic device (p. 74).

After promising preliminary tests the desired tetra-spiro annelated Pc (**10**) *via* an *in situ* deprotection-substitution-sequence could not be achieved. Instead, a novel, auspicious octahydroxymethylene ZnPc was obtained after deprotection. The minimal structural differences in relation to the nearly insoluble parent Pc were fortunately sufficient to improve remarkably solubility properties in DMSO and pyridine.

Severall substitution/addition reactions were successfully processed, from which alkylation is estimated to be the most promising for future developments. In particular, alkynylation made the wide field of "Click-chemistry" accessible.
Thus, glycosylation of ZnPc-*op*-CH_2OH (**39**) was accomplished by two different linker chemistries: Firstly, *via* carbamates by reaction with glucosyl isocyanate, and secondly, formation of triazoles from glycosyl azides – in accordance to "Click-chemistry" (p. 63) – after alkynylation of ZnPc-*op*-CH_2OH (**39**).

In cooperation with Prof. Dr. med. Michael Schaefer at the Department of Molecular Pharmacology and Cell Biology of the Charité / FU-Berlin galactosylated triazole ZnPc **81** was tested on HepG2 cells *in vitro*. On the basis of the results published by the workgroup of Prof. Dennis Ng,[9, 28, 91] microscopic fluorescence studies of the incubated cells on coverslips (2 mL culture medium) were examined with a multiwavelength illuminator (Polychrome IV, TILL Photonics) as excitation light source (at 357 nm).
Disappointingly, no significant fluorescence could be observed, obviously due to quenching in aqueous buffers. Therefore, in a final attempt HepG2 cells (10 mL culture medium) were incubated with **81** and the lysate was investigated in a cuvette with a standard UV-vis and fluorescence spectrometer. In comparison to a negative control experiment, a weak indication for the presence of Pc was found as shown in Figure 34 – Figure 36. A positive control experiment with the glucosylated triazole ZnPc **80** was not performed. This possibly could have ruled out artifacts, caused either by carryover during the washing sequence or by unspecific physisorption instead of endocytosis (p. 85).

The primary rationale of a spiro linked Pc was resurrected during the course of synthesis of ZnPc-*op*-$CH_2OTBDPS$ (**33**) starting from PMDA. Intermediate **22** was presumed to be an ideal candidate for the spiro annelation with fluorene derivatives. However, this synthesis was of limited success. A more elegant synthetic sequence was realized with the *de novo* synthesis of the symmetrically tetra-substituted benzene key building block *via* alkyne cyclotrimerisation to eventually yield the unique fluorenyl spiro-annelated ZnPc **90**. NMR elucidation was incomplete due to the poor solubility in deuterated solvents; hence, ^{13}C-NMR characterization was not possible. Nevertheless, the expected structure could be corroborated by ^{1}H-NMR, HSQC, mass- (MALDI-TOF), UV-vis and fluorescence spectroscopy data, which were in full agreement with the proposed structure of ZnPc **90**.

ZUSAMMENFASSUNG

Das Hauptziel dieser Dissertation war es, einen Syntheseweg zu einem mehrfach mit Kohlenhydraten dekoriertem Phthalocyanin (Pc) auszuarbeiten. Zudem sollte das Pc eine dendritische Geometrie aufweisen, unter physiologischen Bedingungen löslich sein und einen aussichtsreichen Kandidaten bezüglich der zellulären Aufnahme in biologischen *in vitro* Tests darstellen.

Die erste Synthesestrategie zu einem vierfach spiroverknüpftem Pc schlug wegen unzureichender thermischer Stabilität in Lösung fehl. Ein anzunehmender Grund ist die Ringspannung der Vorstufe, des dreifach spiroverknüpften Cyclotriphosphazens.

Beim Verfolgen der ersten Synthesestrategie stellte sich die Struktureinheit des 1,2-Benzendimethanols als ein entscheidendes Synthon für den Pc-Vorläufer heraus, von dem die Cyclotetramerisierung ausgehen sollte. Nachdem eine Bromierungsroute (S. 45) nicht zufriedenstellend verlief, wurde eine effektive Multigramm Synthese, ausgehend von PMDA, zu einem Pc mit Si-Schutzgruppen entwickelt, das hervorragende Löslichkeitseigenschaften zeigt (S. 46).

Dieses ausgezeichnet lösliche ZnPc-*op*-CH_2OTBDPS (**33**, **34**) wurde aus zwei Reaktionsansätzen isoliert. Die Einkristallröntgenstrukturanalyse dieser beiden Chargen – 428 und 488 – unterscheiden sich lediglich durch den fünften Liganden der an das Zentralatom des Phthalocyanins koordiniert ist. Wie schon in der Einleitung ausgeführt, kommt der Löslichkeit von Phthalocyaninen eine entscheidende Bedeutung zu, sowohl wenn es um die Bestimmung der Eigenschaften neuartiger Phthalocyanine geht, als auch für die industrielle Anwendung, abseits der Verwendung als Pigmentfarbstoff (S. 14).
In einer Kooperation mit der Universität Paderborn wurden einige physikochemische Eigenschaften wie Photolumineszenz und Elektrolumineszenz von Dünnfilmschichten des neuen ZnPc-*op*-CH_2OTBDPS (**33**, **34**) dankenswerterweise von Dr. Stephan Benning aus dem Arbeitskreis von Prof. Dr. Heinz-Siegfried Kitzerow untersucht. Erste, nicht optimierte Versuche bestätigten die erwarteten Eigenschaften der neuen Phthalocyanine als Emitter für OLEDs und als aktive Schicht in einer photovoltaischen Zelle (S. 74).

Trotz vielversprechender Vorversuche konnte das angestrebte, vierfach spiroverknüpfte Pc **10** nicht über eine *in situ* Entschützungs-Substitutions-Sequenz erreicht werden. Dafür konnte aber nach vollständiger Entschützung ein vielversprechendes Oktahydroxymethylen-ZnPc **39** isoliert werden. Der minimale strukturelle Unterschied im Vergleich zum beinahe unlöslichen Phthalocyaningrundkörper ist glücklicherweise ausreichend, um die Löslichkeit in DMSO und Pyridin entscheidend zu verbessern.

Von den diversen Substitutions- und Additions-Reaktionen, die erfolgreich angewendet werden konnten, scheint die Alkylierung die Vielversprechendste für zukünftige Anwendungen zu sein. Die Alkinylierung im Speziellen stößt das Tor zum weiten Feld der „Click-Chemie“ auf und macht dieses zugänglich.
Demzufolge konnte über zwei unterschiedliche Linker-Verfahren die Glycosylierung von ZnPc-*op*-CH_2OH (**39**) erreicht werden: Zum Einen durch die Bildung von Carbamaten in der Reaktion mit Isocyanaten und zum Anderen über die Bildung von Triazolen aus Aziden – gemäß der „Click-Chemie“ – nach Alkinylierung von ZnPc-*op*-CH_2OH (**39**).

In Kooperation mit Herrn Prof. Dr. med. Michael Schäfer vom Department der Molekularen Pharmakologie und Zellbiologie der Charité / FU-Berlin wurde die Verbindung ZnPc **81** *in vitro* an HepG2 Zellen getestet. Basierend auf den veröffentlichten Ergebnissen der Arbeitsgruppe um Prof. Dennis Ng[9, 28, 91] wurden HepG2 Zellen auf coverslips (2 mL Kulturmedium) mit ZnPc **81** inkubiert und mit einem Breitbandstrahler mit Monochromatoreinheit (Polychrom IV, TILL Photonics mit einer Xeno-Hochdrucklampe) bei einer Anregungswellenlänge von 357 nm untersucht.
Enttäuschenderweise konnte keine signifikante Fluoreszenz beobachtet werden, was sich am ehesten durch Quenching im wäßrigen Puffer zurückführen läßt. Aus diesem Grund wurden beim letzten Versuch HepG2 Zellen (10 mL Kulturmedium) mit **81** inkubiert und das Lysat in einer Küvette mit einem Standardspektrometer für UV-vis und Fluoreszenz untersucht. Im Vergleich zu einer Negativkontrolle konnte ein schwaches Indiz für die Anwesenheit von **81** im Lysat gefunden werden, wie in Figure 34 – Figure 36 gezeigt wird. Eine Positivkontrolle mit dem glucosylierten Triazol-ZnPc **80** wurde nicht ausgeführt. Dieser Vergleich hätte wahrscheinlich ausschließen können, daß es sich bei den detektierten Signalen eher um Artefakte handelt, die durch die Verschleppung während des Aufreinigungsprozesses oder

durch unspezifische Physisorption hervorgerufen wurden, als durch Endozytose aufgenommenes **81** (S. 85).

Der ursprüngliche Gedanke an ein spiroverknüpftes Pc wurde auf der Syntheseroute zum ZnPc-*op*-CH_2OTBDPS (**33**), ausgehend von PMDA, wieder aufgegriffen. Das Intermediate **22** wurde als idealer Kandidat für eine Spiroverknüpfung mit einem Fluorenderivat angesehen. Aus welchen Gründen auch immer, der Synthese war geringer Erfolg beschieden. Eine wesentlich elegantere Strategie wurde über die *de novo* Synthese einer Schlüsselverbindung, nämlich einem vierfach, symmetrisch substituierten Benzens über eine [2+2+2]-Alkincyclotrimerisierung, verwirklicht. Schließlich wurde daraus in weiterer Folge das einzigartige, mit 2,7-Dibromfluoren spiroannelierte ZnPc **90** gewonnen. Die NMR-Aufklärung war, bedingt durch die schlechte Löslichkeit in deuterierten Solventien, unvollständig. Folglich war eine ^{13}C-NMR Charakterisierung unmöglich. Nichtsdestotrotz konnten die Daten von ^{1}H-NMR, HSQC, Massenspektrometrie (MALDI-TOF), UV-vis und Fluoreszenzespektroskopie mit der vorgeschlagenen Struktur von ZnPc **90** in Einklang gebracht werden.

EXPERIMENTAL

Chemistry: Organic solvents used for reactions were of *p.a.* quality and used as purchased from Fisher Scientific, Merck, Acros or SAF. Commercial available starting compounds and reagents were used directly without further purification from SAF, Lancaster and Acros.
Column chromatography was performed on Fluka silica gel 60 Å (40-63 μm). Bulk solvents used for chromatography and extraction were of technical grade.

TLC: Analytic thin-layer chromatography were performed on aluminium sheets pre-coated with silica gel 60 Å with a fluorescent indicator (Merck 60 F_{254}), and detection was effected by UV light at 254 and 366 nm and/or visualized with various spray reagents such as 10% sulphuric acid in ethanol, acidic aq. solution of Cer(IV) ammonium nitrate and ninhydrin in ethanol followed by heating; or by a dipping bath of alkaline potassium permanganate.

NMR: Nuclear magnetic resonance spectra for protons and carbons were recorded on Bruker-AMX400, DRX500 or AV400 NMR spectrometer.
The positions of signals are reported in δ units (ppm) with respect to the deuterated solvent residual peak as internal standard. For proton and carbon NMRs respectively calibration of the spectra depending on the solvent was done at 2.50/39.5 ppm for DMSO-d_6, at 7.26/77.0 ppm for $CDCl_3$, at 7.20/128.0 ppm for C_6D_6, at 3.50/66.5 ppm for 1,4-dioxane-d_8, at 8.7/149.8 ppm for pyridine-d_5 and at 2.7/30.1 ppm for DMF-d_7.
Multiplicities of coupling protons are abbreviated as follows: s (singlet), d (doublet), dd (doublet of doublet), t (triplet), q (quartet), quint (quintet), sext (sextet), sept (septet), m (multiplet), m_c (centered multiplet); b is used as prefix for broadened signals.
Two-dimensional NMR technique such as HH-COSY, TOCSY, NOESY, edited HSQC and HMBC were used to assign the relative positions of protons and their carbons.
^{13}C NMR resonances are reported as the proton-decoupled chemical shifts, and in most cases the JMOD, PENDANT or/and DEPT ^{13}C-NMR technique was used to differentiate carbons.

HRMS-FAB: The fast atom bombardment (FAB) positive ion mass spectra were obtained on a VG 70S mass spectrometer with a xenon FAB-gun and *m*-nitrobenzyl alcohol as matrix at 5000 resolution.

MALDI-TOF: Matrix-assisted laser desorption ionization time-of-flight mass spectrometric analysis were performed on a Bruker Biflex III, positive mode (matrix: 1,8,9-anthracenetriol).

X-ray: 3D-molecular structures from single crystals were obtained after X-ray diffraction (XRD) analysis that was performed on a Bruker SMART APEX 1 CCD irradiated with a diffraction ceramic tube KFF-Mo-2K-90 ($Mo_{K\alpha}$ radiation, λ = 71.073 pm) at 157 K (Oxford Cryosystem, 700 series Cryostream Cooler). The raw data were processed by Brukers' AXS software package SMART APEX 5.0.

UV-vis: The ultraviolet-visible spectra were recorded on a Perkin-Elmer dual-beam Bio50.

Fluorescence: Emission spectra were recorded on Photon Technology Inc. Quantum Master Fluorometer, using a 1 cm × 1 cm quartz cuvette.

Optical rotation: Perkin-Elmer-Polarimeter at 546 nm (Hg), cuvette 10 cm, 20 °C.

FT-IR: Perkin-Elmer 1720 spectrometer using KBr disks.

Melting points (uncorrected)**:** determined in an open capillary tube on an APOTEC – Otto Stein Inc. melting point apparatus.

Microscopy: An Olympus BH optical polarising microscope equipped with a Mettler FP 82 hot stage and a Mettler FP 80 central processor was used to characterise anisotropic textures.

Cyclic Voltammetry: Cyclic voltammograms were obtained from the electrochemical computerized "Amel System 5000" with a high-speed function generator HSF-02 and Pt-electrodes.

Tetraethyl benzene-1,2,4,5-tetracarboxylate (**21**)[125]

$C_{18}H_{22}O_8$ (366.36 g/mol)

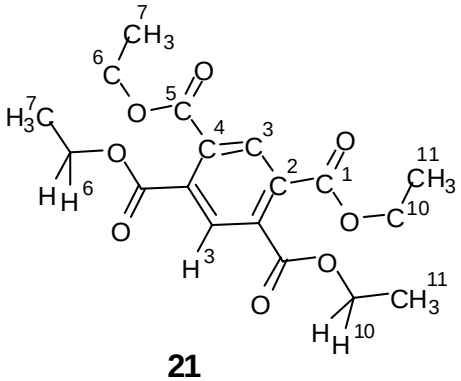

21

HRMS-FAB$^+$ (*m*-nitrobenzyl alcohol)
(calc. mono-isotopic 366,1315 amu)
m/z (%): 321.0982 (100) $[M - OCH_2CH_3]^+$
367.1399 (30) $[M + H]^+$

Mp. 54 °C (Lit. 53-54 °C)[125]

^{1}H-NMR (400 MHz, DMSO-d_6):
δ = 8.06 (s, 2H, H-3), 4.33 (q, 8H, H-6 = H-10, $^3J_{H\text{-}6,H\text{-}7} = {}^3J_{H\text{-}10,H\text{-}11}$ = 7.1 Hz), 1.30 (t, 12H, H-7 = H-11, $^3J_{H\text{-}6,H\text{-}7} = {}^3J_{H\text{-}10,H\text{-}11}$ = 7.1 Hz).

^{13}C-NMR (100 MHz, DMSO-d_6):
δ = 165.3 (C-1 = C-5), 133.9 (C-2 = C-4), 129.0 (C-3), 62.0 (C-6 = C-10), 13.8 (C-7 = C-11).

PMDA (50.0 g, 0.23 mol) was suspended in abs. EtOH (500 mL) and refluxed until a solution was formed. Conc. H_2SO_4 (30 mL, 1.1 mol) was added dropwise and refluxed for 18 hours. At atmospheric pressure, EtOH (350 mL) was distilled off from the reaction. The remaining solution was actively cooled to room temperature and poured into cold (0 °C) 2N NaOH (400 mL), while the internal temperature raised to 10 °C and a white precipitate was formed immediately. The aqueous phase was washed with MTBE (2 × 300 mL). To the acidic water phase 2N NaOH was added (pH > 9) and washed with MTBE (100 mL). The combined organic phases were washed subsequently with water, sat. aq. NaCl and dried over Na_2SO_4. Filtration and evaporation gave a slightly yellowish, highly viscous sirup. Upon standing at room temperature, white crystals were formed (80.5 g, 0.22 mol, 96% o.th.).

Diethyl 4,5-bis(hydroxymethyl)phthalate (**22**)

$C_{14}H_{18}O_6$ (282.29 g/mol)

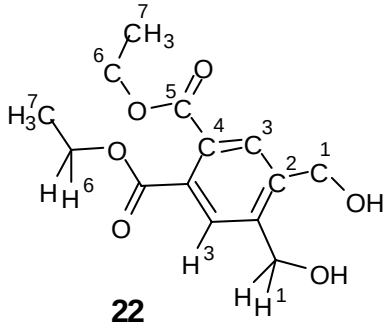

22

HRMS-FAB$^+$ (*m*-nitrobenzyl alcohol)
(calc. mono-isotopic 282.1103 amu)
m/z (%): 237.0766 (100) $[M - OCH_2CH_3]^+$
283.1184 (50) $[M + H]^+$

R$_f$ = 0.24 (PE/EA, 60:40)

^{1}H-NMR (400 MHz, DMSO-d_6):
δ = 7.76 (s, 2H, H-3), 5.27 (bs, 2H, -OH), 4.58 (s, 4H, H-1), 4.28 (q, 4H, H-6, $^3J_{H\text{-}6,H\text{-}7}$ = 7.0 – 7.3 Hz), 1.28 (t, 6H, H-7, $^3J_{H\text{-}6,H\text{-}7}$ = 7.0 – 7.3 Hz).

^{13}C-NMR (100 MHz, DMSO-d_6):
δ = 167.1 (C-5), 142.7 (C-2), 129.8 (C-4), 126.0 (C-3), 61.1 (C-6), 59.2 (C-1), 23.4 (C-13), 13.9 (C-7).

To a well-stirred solution of tetraethyl ester **21** (133 g, 362 mmol) in Et_2O (860 mL) was added a suspension of $LiAlH_4$ (16.5 g, 435 mmol) in Et_2O (600 mL) at a rate that maintained a steady reflux. After addition, the yellow mixture was refluxed 2.5 h. The progress of the reduction was monitored *via* LC-MS (tetraethyl ester R_t = 3.21 min, target R_t = 2.25 min) after micro workup. Since the starting material was still predominant a second portion of $LiAlH_4$ (5.7 g, 150 mmol) in Et_2O (200 mL) was added as before and reflux continued over night. After tetra ester was consumed completely, the yellow, heterogeneous mixture was cooled to room temperatur and carefully quenched by adding it to freshly prepared well-stirred sat. aq. Na_2SO_4. Salts were removed by filtration and washed with THF (500 mL). The organic phase was separated and the water phase was washed with ether (500 mL). The combined organic phases were evaporated to dryness, redissolved in chloroform (500 mL), dried over Na_2SO_4 and concentrated to yield an orange oil (60 g). According to proton NMR,

the oil consisted of the desired diester **22** (73 mol%, 41 g, 145 mmol) still containing the tetra ester **21** (27 mol%, 19 g, 52 mmol).

Analytically pure diester **22** was obtained from a sample of the crude oil (3.6 g) by column chromatography on silica gel (gradient from PE → 80% EA) as pale yellow oil (2.14 g, 7.58 mmol).

Diethyl 3,3-dimethyl-1,5-dihydrobenzo[*f*][2,4]dioxepine-7,8-dicarboxylate (**23**)

$C_{17}H_{22}O_6$ (322.35 g/mol)

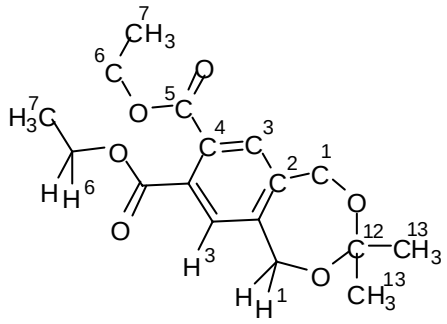

23

HRMS-FAB$^+$ (*m*-nitrobenzyl alcohol):
(calc. mono-isotopic 322.1416 amu)
m/z: 323.1503 $[M + H]^+$

R$_f$ = 0.66 (PE/EA, 60:40)

Mp. 85 °C

^{1}H-NMR (500 MHz, DMSO-d_6):
δ = 7.50 (s, 2H, H-3), 4.87 (s, 4H, H-1), 4.26 (q, 4H, H-6, $^3J_{H\text{-}6,H\text{-}7}$ = 6.9 - 7.3 Hz), 1.42 (s, 6H, H-13), 1.27 (t, 6H, H-7, $^3J_{H\text{-}6,H\text{-}7}$ = 7.3 Hz).

^{13}C-NMR (125 MHz, DMSO-d_6):
δ = 166.7 (C-5), 142.0 (C-2), 129.9 (C-4), 126.6 (C-3), 102.0 (C-12), 63.3 (C-1), 61.2 (C-6), 23.4 (C-13), 13.9 (C-7).

The crude orange oil of diester **22** (34.6 g) was dissolved in THF (240 mL) and stirred with 2,2-dimethoxypropane (100 mL, 816 mmol) and *p*-toluenesulfonic acid (1 g, 5.3 mmol) for 24 h. The reaction was quenched by addition of TEA (1.5 mL, 11 mmol). Volatiles were removed in vacuo and the resulting red-brown oil was dissolved in chloroform (300 mL) and washed consecutively with water (2 × 100 mL), sat. aq. $NaHCO_3$ (2 × 200 mL), sat. aq. NaCl, dried over Na_2SO_4 and concentrated to yield orange waxy crystals (41.4 g), which were used without further purification in the next reaction. Proton NMR of the intermediate product **23** still revealed a contamination with tetra ester **21** in a ratio identical to the starting mixture.
Analytically pure isopropylidene derivative **23** was obtained by reacting a sample of the purified dieester **22** (1.07 g, 3.80 mmol) in THF (12 mL, dried over MS) with

2,2-dimethoxypropane (3 mL, 24.5 mmol) and *p*-toluenesulfonic acid (25 mg, 0.13 mmol) for 24 h. The reaction was quenched by addition of TEA (0.5 mL, 3.6 mmol). The clear solution was evaporated to dryness, dissolved in EA, consecutively washed with aq. 0.5 N NaOH, sat. aq. $NaHCO_3$, brine and dried over Na_2SO_4 to yield after evaporation **23** as pale yellow crystals (1.16 g, 3.64 mmol, 96% o.th.).

7,8-bis(hydroxymethyl)-3,3-dimethyl-1,5-dihydrobenzo[*f*][2,4]dioxepine (**24**)[125]

$C_{13}H_{18}O_4$ (238.28 g/mol)

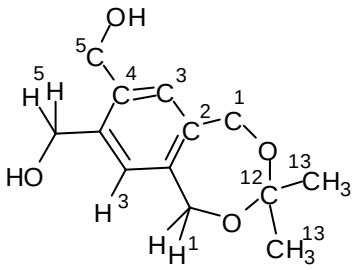

24

Mp. 137 °C (Lit. 137-138 °C)[125]

^{1}H-NMR (400 MHz, DMSO-d_6):

δ = 7.11 (s, 2H, H-3), 5.02 (t, 2H, -OH, $^3J_{\text{-OH,H-5}}$ = 5.4 Hz), 4.76 (s, 4H, H-1), 4.48 (d, 4H, H-5, $^3J_{\text{-OH,H-5}}$ = 5.5 Hz), 1.41 (s, 6H, H-13).

^{13}C-NMR (100 MHz, DMSO-d_6):

δ = 137.5 (C-4), 136.3 (C-2), 124.6 (C-3), 101.5 (C-12), 63.9 (C-1), 60.0 (C-5), 23.7 (C-13).

The crude product (40.5 g, orange, waxy crystals) of the diester-isopropylidene derivative **23** was dissolved in Et_2O (300 mL) and a suspension of $LiAlH_4$ (8.48 g, 223 mmol) in Et_2O (300 mL) was added at a rate that maintained a steady reflux. After addition, the yellow mixture was refluxed 3 h. Small samples were taken and worked up in order to monitor the progress of the reduction by LC-MS (tetraethyl ester **21** R_t = 3.21 min, diester-isopropylidene derivative **23** R_t = 3.06 min, diol-isopropylidene derivative **24** R_t = 2.02 min).

After completion of the reduction, the yellow, heterogeneous mixture was cooled to room temperatur and carefully quenched by adding it to a well-stirred sat. aq. solution of $NaHCO_3$. The organic phase was separated and the water phase was washed with EA (2 × 100 mL). The combined organic phases were concentrated and dried over Na_2SO_4. Evaporation of the solvent yielded an orange solid. Repeated recrystallization from MeOH gave four crops of fine, white needles of **24** (22.5 g, 94.3 mmol, 33% o.th. after 3 steps).

An analytical pure sample of diester-isopropylidene derivative **23** (2.03 g, 6.30 mmol) in Et_2O (50 mL) was subjected to the process described above using $LiAlH_4$ (0.50 g, 13 mmol) in Et_2O (30 mL). After work up the remaining solid (1.29 g, 5.42 mmol, 86% o.th.) was suspended in Et_2O by the means of ultrasound, chilled in a fridge, filtered and washed with cold Et_2O to give fine, white needles of **24** (1.16 g, 4.89 mmol, 78% o.th.).

7,8-Bis((*tert*-butyldiphenylsilyloxy)methyl)-3,3-dimethyl-1,5-dihydrobenzo[*f*][2,4]dioxepine (**25**)

$C_{45}H_{54}O_4Si_2$ (715.08 g/mol)

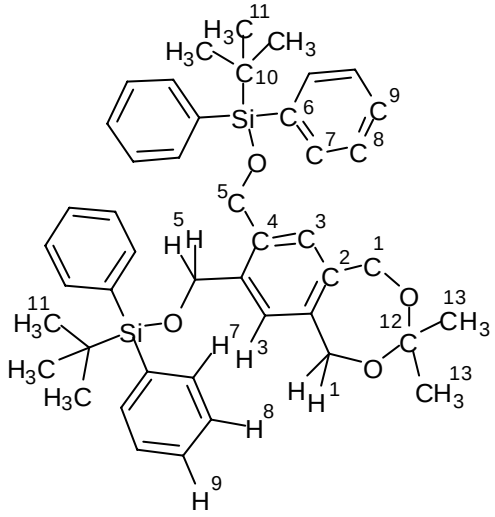

25

HRMS-FAB$^+$ (*m*-nitrobenzyl alcohol):

(calc. mono-isotopic 714.3561 amu)

m/z (%): 713.3510 (100) $[M - H]^+$

714.3556 (65) $[M]^{\bullet+}$

715.3549 (26) $[M + H]^+$

R$_f$ = 0.76 (PE/EA, 80:20)

^{1}H-NMR (400 MHz, DMSO-d_6):

δ = 7.54 (dd, 8H, H-7, $^3J_{H\text{-}7,H\text{-}8}$ = 8.0 Hz, $^4J_{H\text{-}7,H\text{-}9}$ = 1.3 – 1.5 Hz), 7.43 (tt, 4H, H-9, $^3J_{H\text{-}8,H\text{-}9}$ = 7.4 Hz, $^4J_{H\text{-}7,H\text{-}9}$ = 1.3 – 2.3 Hz), 7.35 (dd, 8H, H-8, $^3J_{H\text{-}7,H\text{-}8}$ = 8.1 Hz, $^3J_{H\text{-}8,H\text{-}9}$ = 7.4 Hz), 7.10 (s, 2H, H-3), 4.77 (s, 4H, H-1), 4.70 (s, 4H, H-5), 1.42 (s, 6H, H-13), 0.91 (s, 18H, H-11).

^{13}C-NMR (100 MHz, DMSO-d_6):

δ = 137.1 (C-2), 135.8 (C-4), 134.9 (C-7), 132.6 (C-6), 129.8 (C-9), 127.8 (C-8), 124.7 (C-3), 101.6 (C-12), 63.9 (C-1), 63.0 (C-5), 26.5 (C-11), 23.6 (C-13), 18.7 (C-10).

To a solution of the hydroxy-isopropylidene derivative **24** (20.4 g, 85.5 mmol) in dry DMF (150 mL) was added imidazole (35.1 g, 516 mmol) in portions. An endothermic enthalpy of solvation was observed. To the clear, colorless solution, TBDPS-Cl (53.0 mL, 207 mmol) was added dropwise with a syringe through a septum. A mild exothermic reaction occurred. After stirring for 24 h at room temperature, M*t*BE (500 mL) was added to the clear, yellow solution in order to precipitate imidazolium•HCl as colorless solid. The organic layer was filtered and consecutively washed with water (2 × 300 mL), aq. 2N HCl (2 × 200 mL), buffer (~ pH 5,

100 mL), sat. aq. $NaHCO_3$ (100 mL), sat. aq. NaCl and dried over Na_2SO_4. Concentration yielded a clear, slightly yellow residue (67.9 g). The crude product was further purified by column chromatography on silica gel (gradient from PE → 20% EA, with 1 vol.% TEA) to yield the TBDPS protected isopropylidene derivative **25** as clear, colorless, highly viscous oil (59.2 g, 82.7 mmol, 97% o.th.).

(4,5-Bis((*tert*-butyldiphenylsilyloxy)methyl)-1,2-phenylene) dimethanol (**26**)

$C_{42}H_{50}O_4Si_2$ (675.02 g/mol)

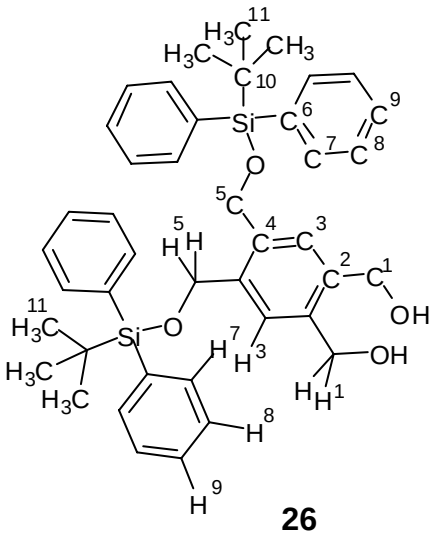

26

HRMS-FAB$^+$ (*m*-nitrobenzyl alcohol):
(calc. mono-isotopic 674.3248 amu)
m/z (%): 655.3078 (100) $[M - H_2O]^{\bullet+}$
673.3147 (50) $[M - H]^+$
674.3195 (22) $[M]^{\bullet+}$

$\mathbf{R}_f$ = 0.42 (PE/EA, 60:40)

^{1}H-NMR (400 MHz, DMSO-d_6):
δ = 7.57 (dd, 8H, H-7, $^3J_{H\text{-}7,H\text{-}8}$ = 8.0 Hz, $^4J_{H\text{-}7,H\text{-}9}$ = 1.3 – 1.5 Hz), 7.51 (s, 2H, H-3), 7.44 (tt, 4H, H-9, $^3J_{H\text{-}8,H\text{-}9}$ = 7.4 – 7.6 Hz, $^4J_{H\text{-}7,H\text{-}9}$ = 1.3 – 2.3 Hz), 7.35 (dd, 8H, H-8, $^3J_{H\text{-}7,H\text{-}8}$ = 8.1 Hz, $^3J_{H\text{-}8,H\text{-}9}$ = 7.4 Hz), 5.09 (t, 2H, -OH, $^3J_{OH,H\text{-}1}$ = 5.3 Hz), 4.74 (s, 4H, H-5), 4.56 (d, 4H, H-1, $^3J_{OH,H\text{-}1}$ = 4.6 Hz), 0.92 (s, 18H, H-11).

^{13}C-NMR (100 MHz, DMSO-d_6):
δ = 138.2 (C-2), 135.7 (C-4), 134.9 (C-6), 132.7 (C-7), 129.8 (C-9), 127.8 (C-8), 125.8 (C-3), 63.3 (C-5), 60.3 (C-1), 26.5 (C-11), 18.7 (C-10).

The TBDPS protected isopropylidene derivative **25** (2.54 g, 3.55 mmol) was completely dissolved in acetone (134 mL). Water (ca. 37 mL) was added slowly in portions until opacity of the solution persisted. To this mixture, *p*-TsOH•H_2O (86 mg) was added at once and stirred at room temperature for 24 h. After 10 min the liquid already began to clarify. The reaction was terminated by addition of TEA until ~ pH 7-8. Evaporation to half of the volume (ca. 80 mL) caused turbidity again. The mixture was washed with Et_2O (3 × 100 mL). The combined organic phases were washed consecutively with aq. citric acid (0.5 wt.%, ~ pH 3),

sat. aq. $NaHCO_3$, sat. aq. NaCl, dried over Na_2SO_4 and concentrated to yield the benzene-1,2-dimethanol derivative **26** as colorless, highly viscous oil (2.38 g, 3.47 mmol, 98% o.th.).

4,5-Bis((*tert*-butyldiphenylsilyloxy)methyl)phthalaldehyde (**27**)

$C_{42}H_{46}O_4Si_2$ (670.98 g/mol)

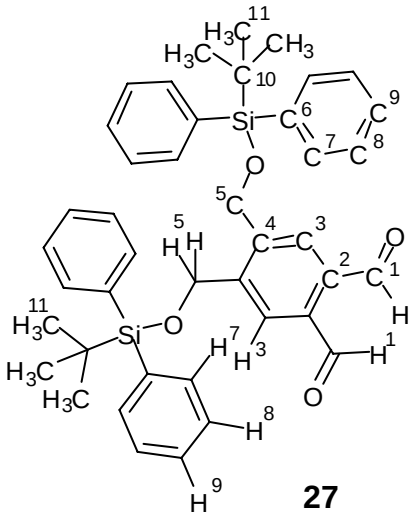

27

HRMS-FAB$^+$ (*m*-nitrobenzyl alcohol):
(calc. mono-isotopic 670.2935 amu)
m/z (%): 655.3119 (100) $[M + H - O]^+$
656.3141 (49) $[M - H_2O]^+$
671.3027 (48) $[M + H]^+$

R$_f$ = 0.80 (PE/EA, 80:20)

^{1}H-NMR (400 MHz, DMSO-d_6):
δ = 10.5 (s, 2H, H-1), 8.07 (s, 2H, H-3), 7.54 (dd, 8H, H-7, $^3J_{H\text{-}7,H\text{-}8}$ = 8.0 Hz, $^4J_{H\text{-}7,H\text{-}9}$ = 1.3 – 1.5 Hz), 7.44 (tt, 4H, H-9, $^3J_{H\text{-}8,H\text{-}9}$ = 7.4 Hz, $^4J_{H\text{-}7,H\text{-}9}$ = 1.3 – 2.3 Hz), 7.35 (dd, 8H, H-8, $^3J_{H\text{-}7,H\text{-}8}$ = 8.1 Hz, $^3J_{H\text{-}8,H\text{-}9}$ = 7.4 Hz), 4.84 (s, 4H, H-5), 0.94 (s, 18H, H-11).

^{13}C-NMR (100 MHz, DMSO-d_6):
δ = 192.5 (C-1), 143.5 (C-4), 135.2 (C-2), 134.9 (C-7), 132.2 (C-6), 130.0 (C-9), 127.9 (C-8), 127.7 (C-3), 62.6 (C-5), 26.5 (C-11), 18.7 (C-10).

According to the procedure of Farooq[130], oxalyl chloride (0.65 mL, 7.70 mmol) was dissolved in DCM (6 mL) and cooled to -78 °C. A solution of DMSO (1.20 mL, 16.9 mmol) in DCM (11.0 mL) was added dropwise. The solution was stirred for 20 minutes and the benzene-1,2-dimethanol derivative **26** (2.03 g, 3.00 mmol) dissolved in DCM (6 mL) was added dropwise. The mixture was stirred at -78 °C for 3 h and then TEA (5.0 mL, 35.9 mmol) was slowly added at -78 °C. The mixture was allowed to reach room temperature over night before the yellow, heterogeneous mixture was diluted with DCM (200 mL) extracted with aq. 2N HCl, sat. aq. $NaHCO_3$, sat. aq. NaCl, and dried over Na_2SO_4. On evaporation a yellow, highly viscous oil of the *o*-phthalaldehyde derivative **27** (1.95 g, 2.91 mmol, 97% o.th.) was

obtained. For analytical characterization, adsorption on silica gel and subsequent column chromatography on silica gel (gradient from PE → 20% EA) yielded the *o*-phthalaldehyde derivative **27** as colorless, highly viscous oil (1.03 g, 1.53 mmol, 51% o.th.).

4,5-Bis((*tert*-butyldiphenylsilyloxy)methyl)phthalic acid (**28**)

$C_{42}H_{46}O_6Si_2$ (702.98 g/mol)

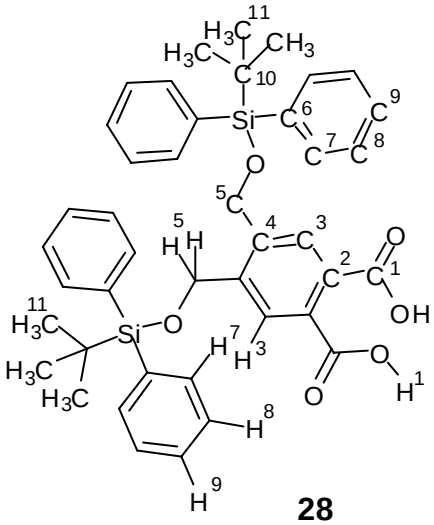

28

HRMS-FAB$^+$ (*m*-nitrobenzylalcohol)
(calc. mono-isotopic 702.2833 amu)
m/z: 703.2913 $[M + H]^+$

R$_f$ = 0.74 (*t*-butanol/water/HOAc, 60:20:20)

Mp. 137 °C

^{1}H-NMR (400 MHz, DMSO-d_6):
δ = 13.1 (bs, 2H, H-1), 7.77 (s, 2H, H-3), 7.54 (dd, 8H, H-7, $^3J_{H\text{-}7,H\text{-}8}$ = 8.0 Hz, $^4J_{H\text{-}7,H\text{-}9}$ = 1.5 Hz), 7.44 (tt, 4H, H-9, $^3J_{H\text{-}8,H\text{-}9}$ = 7.3 – 7.5 Hz, $^4J_{H\text{-}7,H\text{-}9}$ = 1.3 – 2.3 Hz), 7.35 (dd, 8H, H-8, $^3J_{H\text{-}7,H\text{-}8}$ = 8.0 Hz, $^3J_{H\text{-}8,H\text{-}9}$ = 7.5 Hz), 4.77 (s, 4H, H-5), 0.93 (s, 18H, H-11).

^{13}C-NMR (100 MHz, DMSO-d_6):
δ = 168.5 (C-1), 140.2 (C-4), 134.9 (C-7), 132.3 (C-6), 131.6 (C-2), 129.9 (C-9), 127.9 (C-8), 126.5 (C-3), 62.5 (C-5), 26.4 (C-11), 18.7 (C-10).

To a solution of the *o*-phthalaldehyde derivative **27** (21.8 g, 32.4 mmol) in glacial acetic acid (133 mL) was added sodium perborate tetrahydrate (14.0 g, 91.0 mmol) in one portion and stirred for 16 h at 50 °C. The acetic acid was removed by evaporation under reduced pressure. The remaining white, crystalline residue was first sonificated with EA (3 × 100 mL) and decanted. The remaining insoluble mass was dissolved in aqueous citric acid (200 mL, 0.5 wt.%, ~ pH 3) and extracted with EA (100 mL). The combined organic phases were washed consecutively with aq. citric acid (~ pH 3), sat. aq. NaCl, dried over Na_2SO_4 and concentrated to yield a white, crystalline solid (21.7 g, 30.9 mmol, 95% o.th.) Recrystallisation from EA/PE at 60 °C gave several crops of the *o*-phthalic acid derivative **28** after storage in a fridge (20.3 g, 28.9 mmol, 89% o.th.).

4,5-Bis((*tert*-butyldiphenylsilyloxy)methyl)phthalic anhydride (**29**)

$C_{42}H_{44}O_5Si_2$ (684.97 g/mol)

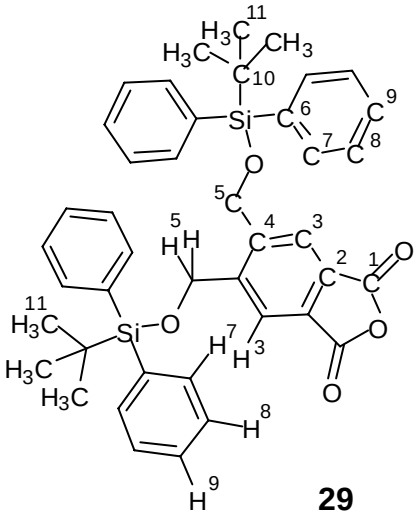

29

HRMS-FAB$^+$ (*m*-nitrobenzyl alcohol)
(calc. mono-isotopic 684.2727 amu)
m/z: 685.2817 $[M + H]^+$

X-ray: successful (see Figure 8)

Mp. 118 °C

^{1}H-NMR (400 MHz, DMSO-d_6):
δ = 8.05 (s, 2H, H-3), 7.54 (dd, 8H, H-7, $^3J_{H\text{-}7,H\text{-}8}$ = 7.9 Hz, $^4J_{H\text{-}7,H\text{-}9}$ = 1.5 Hz), 7.45 (tt, 4H, H-9, $^3J_{H\text{-}8,H\text{-}9}$ = 7.3 – 7.6 Hz, $^4J_{H\text{-}7,H\text{-}9}$ = 1.2 – 2.1 Hz), 7.36 (dd, 8H, H-8, $^3J_{H\text{-}7,H\text{-}8}$ = 7.9 Hz, $^3J_{H\text{-}8,H\text{-}9}$ = 7.6 Hz), 4.89 (s, 4H, H-5), 0.95 (s, 18H, H-11).

^{13}C-NMR (100 MHz, DMSO-d_6):
δ = 163.0 (C-1), 146.7 (C-4), 134.9 (C-7), 132.1 (C-6), 130.5 (C-2), 130.0 (C-9), 127.9 (C-8), 122.5 (C-3), 62.7 (C-5), 26.5 (C-11), 18.7 (C-10).

A degassed and argon flushed suspension of the *o*-phthalic acid derivative **28** (15.5 g, 22.0 mmol) in acetic anhydride (300 mL) was stirred for 3 h at 145-150 °C (oil bath) under exclusion of moisture. After cooling to 60 °C all volatiles were removed under reduced pressure. The amorphous residue (16.2 g) was washed with dry PE. Recrystallization from dry EA in a fridge gave **29** as pale yellow crystals, used for X-ray analysis (14.5 g, 21.1 mmol, 95% o.th.).

[2,3,9,10,16,17,23,24-Octakis((*tert*-butyldiphenylsilyloxy)methyl) phthalocyaninato] zinc(II) (**33**, **34**)

$C_{168}H_{176}N_8O_8Si_8Zn$ (2725.34 g/mol)

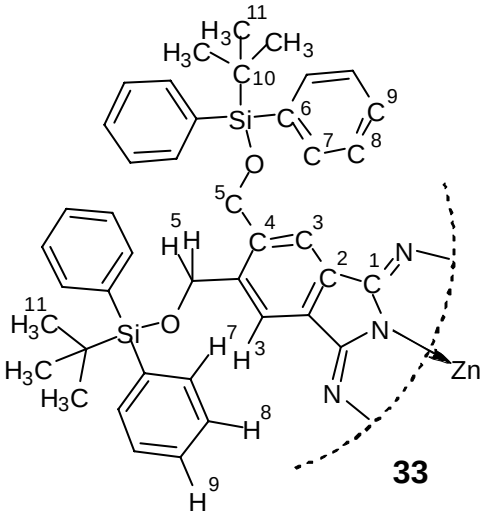

33

34

MS MALDI-TOF (1,8,9-anthracenetriol)
(calc. mono-isotopic 2721.1057 amu)
m/z (%): 2722.12 (100), 2723.14 (93), 2721.20 (93), 2724.10 (82), 2720.25 (74), 2725.08 (63), 2719.27 (47) $[M]^{\cdot+}$.

UV-vis (1,4-dioxane)
λ_{max} (log ε): 676 nm (2.8-4.3×10^5 [L/cm·mol])

X-ray: successful (Figure 9 and Figure 10)

Mp. 285 °C (dec.)

^{1}H-NMR (400 MHz, acetone-d_6):
δ = 9.60 (s, 8H, H-3), 7.87 – 7.85 (m, 32H, H-7), 7.41 – 7.40 (m, 48H, H-8/H-9), 5.58 (s, 16H, H-5), 1.18 (s, 72H, H-11).

^{1}H-NMR (400 MHz, DMSO-d_6/$CDCl_3$, 6:2):
δ = 9.42 (s, 8H, H-3), 7.73 – 7,71 (m, 32H, H-7), 7.35 – 7.31 (m, 48H, H-8/H-9), 5.34 (bs, 16H, H-5), 1.08 (s, 72H, H-11).

^{13}C-NMR (100 MHz, DMSO-d_6/$CDCl_3$, 6:2):
δ = 153.2 (C-1), 139.9 (C-4), 137.2 (C-2), 134.9 (C-7), 132.6 (C-6), 129.6 (C-9), 127.6 (C-8), 120.8 (C-3), 64.4 (C-5), 26.5 (C-11), 18.8 (C-10).

A screw cap vial was charged in the following order: *o*-phthalic anhydride derivative **29** (3.95 g, 5.76 mmol), $Zn(OAc)_2$ (0.264 g, 1.43 mmol), HMDS (7.25 mL, 34.8 mmol) and DMF (0.45 mL, 5.81 mmol). A vigorous stream of argon was bubbled through the stirred suspension for 5 minutes before *p*-TsOH•H_2O (0.117 mg, 0.615 mmol) was added. The vial was sealed and placed in a pre-heated (100 °C) aluminum block when the temperture was rised to 130 °C. The mixture was stirred at this temperature for 63 h. The pressurized, sealed vial was carefully opened after cooling to ambient temperature and the sticky, solid product (5.1 g) was dissolved in DCM and subjected to flash chromatography on silica gel, using DCM, followed by gradients of PE/EA (60:40 → 40:60). Evaporation of the solvents and recrystallization from PE/DCM (90:10) in the fridge gave two crops of ZnPc-*op*-CH_2OTBDPS (**33**) appearing as blue shiny crystals (2.84 g, 1.04 mmol, 72% o.th.).

NOTE: In order to prevent light induced decomposition of the substance, protection from light is strongly recommended!

2,3,9,10,16,17,23,24-Octakis((*tert*-butyldiphenylsilyloxy)methyl) phthalocyanine (**35**)

$C_{168}H_{178}N_8O_8Si_8$ (2661.94 g/mol)

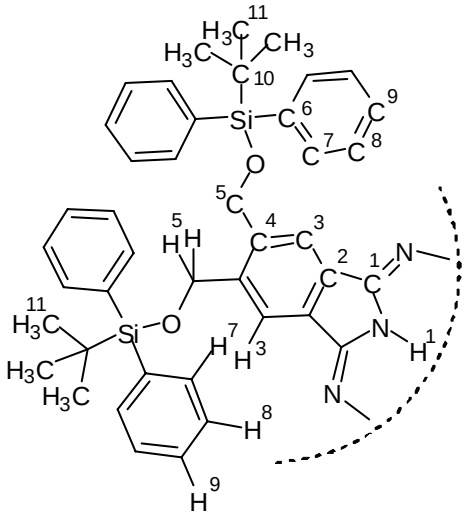

35

UV-vis (THF)

λ_{max} (log ε): 700 nm (1.5×10^5 [L/cm·mol])

MS MALDI-TOF (1,8,9-anthracenetriol)

(calc. mono-isotopic 2659.1922 amu)

m/z (%): 2661.19 (100), 2662.18 (90), 2660.22 (87), 2663.14 (60), 2659.25 (50), 2664.12 (37), 2665.12 (23) $[M + H]^+$.

Mp. 268 °C

^{1}H-NMR (400 MHz, $CDCl_3$):

δ = 9.51 (s, 8H, H-3), 7.80 – 7.78 (m, 32H, H-7), 7.36 – 7.31 (m, 48H, H-8/H-9), 5.35 (s, 16H, H-5), 1.16 (s, 72H, H-11), -0.17 (bs, 2H, NH).

^{13}C-NMR (100 MHz, $CDCl_3$):

δ = 150.4 (C-1), 141.4 (C-4), 136.1 (C-2), 135.6 (C-7), 133.4 (C-6), 129.8 (C-9), 127.8 (C-8), 122.1 (C-3), 65.4 (C-5), 27.0 (C-11), 19.4 (C-10).

A screw cap vial was charged in the following order: *o*-phthalic anhydride derivative **29** (3.91 g, 5.71 mmol), HMDS (7.5 mL, 36 mmol) and DMF (0.44 mL, 5.7 mmol). A vigorous stream of argon was bubbled through the stirred suspension for 5 minutes before *p*-TsOH•H_2O (0.116 mg, 0.608 mmol) was added. The vial was sealed and placed in a pre-heated (100 °C) aluminum block when the temperture was rised to 130 °C. The mixture was stirred at this temperature for 10 h. The pressurized, sealed vial was carefully opened after cooling to ambient temperature and the sticky, solid product was dissolved in DCM and

subjected to flash chromatography on silica gel, using DCM, followed by gradients of PE/EA (60:40 → EA) and THF. Evaporation of the solvents and precipitation from acetone gave two crops of the H_2Pc-*op*-CH_2OTBDPS (**35**) appearing as turquoise powder (2.50 g, 0.94 mmol, 66% o.th.).

NOTE: In order to prevent light induced decomposition of the substance, protection from light is strongly recommended!

[2,3,9,10,16,17,23,24-Octakis(hydroxymethyl)phthalocyaninato] zinc(II) (**39**)

$C_{40}H_{32}N_8O_8Zn$ (818.14 g/mol)

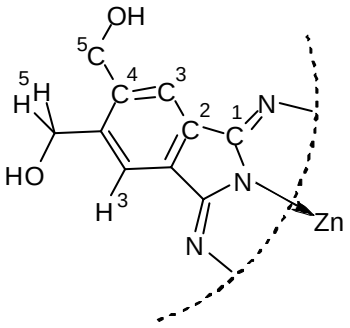

39

UV-vis (DMSO)

λ_{max} (log ε): 681 nm (6.7×10^5 [L/cm·mol])

MS MALDI-TOF (1,8,9-anthracenetriol)

(calc. mono-isotopic 816.1635 amu)

m/z (%): 816.80 (100), 818.80 (60), 817.81 (56),

820.79 (46), 819.80 (38), 821.80 (18) $[M]^{+\bullet}$.

Mp. > 360 °C

^{1}H-NMR (500 MHz, DMSO-d_6):

δ = 9.40 (s, 8H, H-3), 5.72 (t, 8H, -OH, $^3J_{OH,H-5}$ = 5.4 – 5.7 Hz), 5.12 (d, 16H, H-5, $^3J_{OH,H-5}$ = 5.4 Hz).

^{13}C-NMR (125 MHz, DMSO-d_6):

δ = 153.0 (C-1), 141.7 (C-4), 136.6 (C-2), 120.0 (C-3), 60.9 (C-5).

To a stirred solution of the ZnPc-*op*-CH_2OTBDPS (**33**, **34**) (2.31 g, 0.848 mmol) and BTAF•H_2O (4.05 g, 21.6 mmol) in THF (50 mL) at room temperature was added water (10 mL) and DMSO (50 mL) in order to maintain homogeneity of the solution and to prevent precipitation. After 24 h at r.t. a second portion of BTAF•H_2O (4.11 g, 22.0 mmol) and DMSO (20 mL) was added. Additional amounts of TFA were added after 27 h (0.2 mL), 30 h (0.2 mL), and 33 h (1.8 mL) and stirring continued in the dark for 3 days, until the starting material was consumed, as monitored *via* TLC (THF). After evaporation of the volatiles, the cleaved protecting groups TBDPS-F (**40**) and TBDPS-OH (**41**) were removed by dissolving the residue in a minimum of DMSO (50 mL) and extracting with PE (5 × 75 mL). The DMSO

phase was dropped into water and the precipitate thus formed was collected by centrifugation. The wet slurry was rinsed with AcN in order to remove traces of BTAF and collected by centrifugation. The resulting sticky, deeply blue paste was suspended in water by the aid of ultrasound and finally lyophilized to get the pure product **39** as free flowing, fine flakes (0.673 g, 0.823 mmol, 97% o.th.).

Deprotection was remarkably facilitated when using TEA•3HF instead of BTAF•H_2O with similar yields.

O,O'-(4,5-dimethyl-1,2-phenylene)bis(methylene) bis(*N*-(3-chloropropyl)carbamate) (**45**)

$C_{18}H_{26}Cl_2N_2O_4$ (405.32 g/mol)

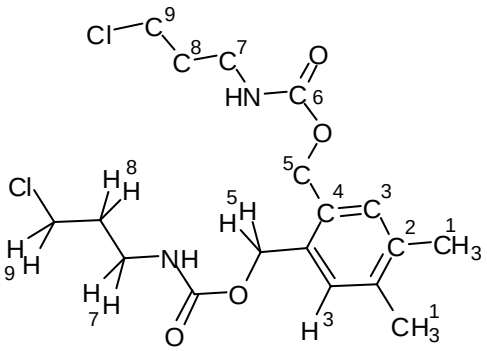

45

^{1}H-NMR (400 MHz, DMSO-d_6):

δ = 7.28 (t, 2H, NH, $^3J_{NH,H\text{-}7}$ = 5.3 – 5.5 Hz), 7.13 (s, 2H, H-3), 5.01 (s, 4H, H-5), 3.63 (t, 4H, H-9, $^3J_{H\text{-}8,H\text{-}9}$ = 6.5 Hz), 3.11 (q, 4H, H-7, $^3J_{NH,H\text{-}7}$ = $^3J_{H\text{-}7,H\text{-}8}$ = 6.0 – 6.5 Hz), 2.20 (s, 6H, H-1), 1.85 (quint, 4H, H-8, $^3J_{H\text{-}7,H\text{-}8}$ = $^3J_{H\text{-}8,H\text{-}9}$ = 6.5 – 6.8 Hz).

^{13}C-NMR (100 MHz, DMSO-d_6):

δ = 156.0 (C-6), 135.8 (C-2), 132.4 (C-4), 130.1 (C-3), 62.7 (C-5), 42.8 (C-9), 37.6 (C-7), 32.3 (C-8), 18.9 (C-1).

A screw cap vial was charged with a solution of 4,5-dimethylbenzene-1,2-dimethanol (**42**) (68 mg, 0.41 mmol) in dry pyridine (5.0 mL, 62 mmol) and 3-chloropropyl isocyanate (0.12 mL, 1.12 mmol) was quickly added. The mixture was stirred at room temperature for 6 d. The solvent was evaporated and the remaining residue was dissolved in Et_2O and consecutively washed with 1N HCl, water, sat. aq. $NaHCO_3$, sat. aq. NaCl and dried over Na_2SO_4. Evaporation of the solvent afforded the 3-chloropropyl carbamate **45** as a white crystalline solid (0.13 g, 0.32 mmol, 78% o.th.).

O,O'-(4,5-Dimethyl-1,2-phenylene)bis(methylene) bis(*N*-(2,3,4,6-tetra-*O*-acetyl-*β*-D-glucopyranosyl)carbamate) (**47**)

$C_{40}H_{52}N_2O_{22}$ (912.84 g/mol)

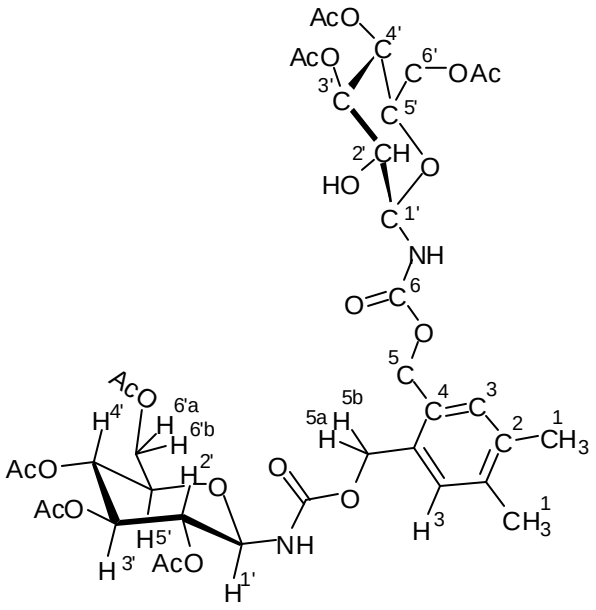

47

HRMS-FAB$^+$ (*m*-nitrobenzyl alcohol):
(calc. mono-isotopic 912.3012 amu)
m/z: 913.3095 $[M+H]^+$

R$_f$ = 0.84 (EA)

$[\alpha]_{546nm}^{20°C}$ = -0.16 ° (c = 1, $CHCl_3$)

Mp. = 132-133 °C

^{1}H-NMR (500 MHz, DMSO-d_6):
δ = 8.28 (d, 2H, -NH, $^3J_{NH,H\text{-}1'}$ = 9.5 Hz), 7.13 (s, 2H, H-3), 5.33 (dd, 2H, H-3', $^3J_{H\text{-}2',H\text{-}3'}$ = $^3J_{H\text{-}3',H\text{-}4'}$ = 9.5 Hz), 5.18 (dd, 2H, H-1', $^3J_{H\text{-}1',H\text{-}2'}$ = $^3J_{NH,H\text{-}1'}$ = 9.5 Hz), 5.08 (d, 2H, H-5a, $^2J_{H\text{-}5a,H\text{-}5b}$ = 12.6 Hz), 5.05 (d, 2H, H-5b, $^2J_{H\text{-}5a,H\text{-}5b}$ = 13.2 Hz), 4.85 (dd, 4H, H-2'/H-4', $^3J_{H\text{-}1',H\text{-}2'}$ = $^3J_{H\text{-}2',H\text{-}3'}$ = $^3J_{H\text{-}3',H\text{-}4'}$ = $^3J_{H\text{-}4',H\text{-}5'}$ = 9.1 – 9.5 Hz), 4.14 (dd, 2H, H-6'a, $^2J_{H\text{-}6'a,H\text{-}6'b}$ = 12.3 Hz, $^3J_{H\text{-}5',H\text{-}6'a}$ = 4.4 Hz), 4.07 (ddd, 2H, H-5', $^3J_{H\text{-}4',H\text{-}5'}$ = 9.9 Hz, $^3J_{H\text{-}5',H\text{-}6'a}$ = 4.4 Hz, $^3J_{H\text{-}5',H\text{-}6'b}$ = 2.1 Hz), 3.96 (dd, 2H, H-6'b, $^2J_{H\text{-}6'a,H\text{-}6'b}$ = 12.5 Hz, $^3J_{H\text{-}5',H\text{-}6'b}$ = 1.6 – 1.9 Hz), 2.20 (s, 6H, H-1), 1.98 (s, 12H, 2 × -OC(O)C$\underline{H}_3$), 1.91 (s, 12H, 2 × -OC(O)C$\underline{H}_3$).

^{13}C-NMR (100 MHz, DMSO-d_6):
δ = 169.9, 169.4, 169.2, 168.9 (4 × -O$\underline{C}$(O)CH_3), 155.4 (C-6), 136.0 (C-2), 131.9 (C-4), 130.1 (C-3), 79.6 (C-1'), 72.9 (C-3'), 71.7 (C-5'), 70.4 (C-2'), 67.7 (C-4'), 61.7 (C-5), 59.7 (C-6'), 20.4, 20.3, 20.23, 20.21 (4 × -OC(O)$\underline{C}H_3$), 18.9 (C-1).

To a solution of 4,5-dimethylbenzene-1,2-dimethanol (**42**) (48 mg, 0.29 mmol) in dry pyridine (10.0 mL, 124 mmol) was quickly added 2,3,4,6-tetra-*O*-acetyl-*β*-D-glucopyranosyl

isocyanate (**62**) (0.426 g, 1.14 mmol) and the mixture was stirred in a screw cap vial in a pre-heated aluminum block at 50 °C for 48 h. The solvent was evaporated and the remaining residue (0.59 g) was subjected to column chromatography on silica gel (gradient from PE/EA = 80:20 → 100% EA) in order to separate the excess of peracetylated glucosamine (resulting from hydrolyzed isocyanate during silica gel chromatography). After evaporation of the solvent, the target compound **47** was isolated as a white, crystalline solid (0.26 g, 0.29 mmol, 99% o.th.).

(4,5-Dimethyl-1,2-phenylene)bis(methylene) bis(1,2,3,4-tetra-*O*-acetyl-*β*-D-glucopyranuronylat) (**48**)

$C_{38}H_{38}O_{22}$ (846.70 g/mol)

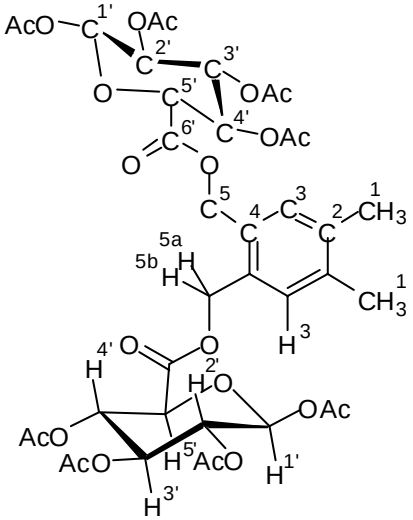

48

R_f = 0.84 (EA)

$[\alpha]_{546nm}^{20°C}$ = +17.4 ° (c = 1, $CHCl_3$)

Mp. = 151 °C

^{1}H-NMR (400 MHz, DMSO-d_6):

δ = 7.15 (s, 2H, H-3), 5.99 (d, 2H, H-1', $^3J_{H\text{-}1',H\text{-}2'}$ = 8.2 Hz), 5.47 (dd, 2H, H-3', $^3J_{H\text{-}2',H\text{-}3'}$ = 9.4 Hz, $^3J_{H\text{-}3',H\text{-}4'}$ = 9.7 Hz), 5.15 (d, 2H, H-5a, $^2J_{H\text{-}5a,H\text{-}5b}$ = 12.2 Hz), 5.05 (d, 2H, H-5b, $^2J_{H\text{-}5a,H\text{-}5b}$ = 13.2 Hz), 5.03 (dd, 2H, H-4', $^3J_{H\text{-}3',H\text{-}4'}$ = $^3J_{H\text{-}4',H\text{-}5'}$ = 9.7 Hz), 4.98 (dd, 2H, H-2', $^3J_{H\text{-}1',H\text{-}2'}$ = 8.1 Hz, $^3J_{H\text{-}2',H\text{-}3'}$ = 9.4 Hz,), 4.69 (d, 2H, H-5', $^3J_{H\text{-}4',H\text{-}5'}$ = 9.9 Hz), 2.21 (s, 6H, H-1), 2.07, 2.00, 1.95, 1.76, (s, 6H, 4 × -OAc).

^{13}C-NMR (100 MHz, DMSO-d_6):

δ = 169.4, 169.1, 169.0, 168.7 (4 × -OAc), 166.2 (C-6'), 137.1 (C-2), 131.3 (C-3), 130.9 (C-4), 90.6 (C-1'), 71.5 (C-5'), 71.0 (C-3'), 69.7 (C-2'), 68.7 (C-4'), 64.3 (C-5), 20.7, 20.4, 20.2, 19.9 (4 × -OC(O)<u>C</u>H$_3$), 18.9 (C-1).

4,5-Dimethylbenzene-1,2-dimethanol (**42**) (106 mg, 0.64 mmol) was dissolved in Pyridin (5 mL), placed on an ice-bath (≤ 0 °C) and acid chloride **59** (1.08 g, 2.85 mmol) was added in portions. The mixture was allowed to reach room temperature and was stirred for 48 h. The solvent was removed *in vacuo*. The residue was dissolved in a minimum of DCM and subjected to flash chromatography on silica gel. Upon changing the eluent from DCM to EA, the coupling product **48** was isolated after evaporation of the solvent (EA) as white solid (628 mg, 0.735 mmol, 99% o. th.).

1,2-dimethyl-4,5-bis((prop-2-ynyloxy)methyl)benzene (**49**)

$C_{16}H_{18}O_2$ (242.31 g/mol)

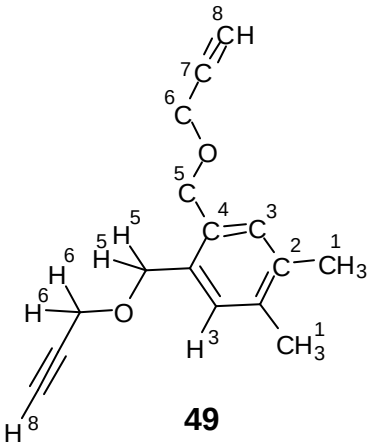

49

^{1}H-NMR (500 MHz, DMSO-d_6):

δ = 7.12 (s, 2H, H-3), 4.52 (s, 4H, H-5), 4.16 (d, 4H, H-6, $^4J_{H\text{-}6,H\text{-}8}$ = 2.2 Hz), 3.47 (t, 2H, H-8, $^4J_{H\text{-}6,H\text{-}8}$ = 2.4 Hz), 2.22 (s, 6H, H-1).

^{13}C-NMR (100 MHz, DMSO-d_6):

δ = 135.5 (C-2), 133.1 (C-4), 130.2 (C-3), 80.2 (C-7), 77.2 (C-8), 68.1 (C-5), 56.8 (C-6), 18.9 (C-1).

To a vigorously stirred solution of 4,5-dimethylbenzene-1,2-dimethanol (**42**) (0.10 g, 0.60 mmol) in DMSO (1.5 mL) was added aq. NaOH (50 wt.%, 0.11 mL, 2.1 mmol) to form a gel-like suspension. Immediately, propargyl bromide (80 wt.% in xylene, 0.2 mL, 1.8 mmol) was added dropwise and stirring continued for 2 d at room temperature. The clear, orange, viscous mixture thus obtained was diluted with Et_2O (100 mL) and extracted consecutively with water (100 mL), aq. 2N HCl (2 × 50 mL), sat. aq. $NaHCO_3$, sat. aq. NaCl. Drying over Na_2SO_4 and concentration yielded a crude orange oil (154 mg). After column chromatography using silica gel (gradient from PE → EA) the bispropargylated derivative **49** was isolated as slightly yellow, viscous oil (0.124 g, 0.513 mmol, 85% o.th.).

1,2-Dimethyl-4,5-bis(((*N*-1-(2,3,4,6-tetra-*O*-acetyl-*β*-D-glucopyranosyl)-1*H*-1,2,3-triazol-4-yl)methoxy)methyl)benzene (**50a**)

$C_{44}H_{56}N_6O_{20}$ (988.94 g/mol)

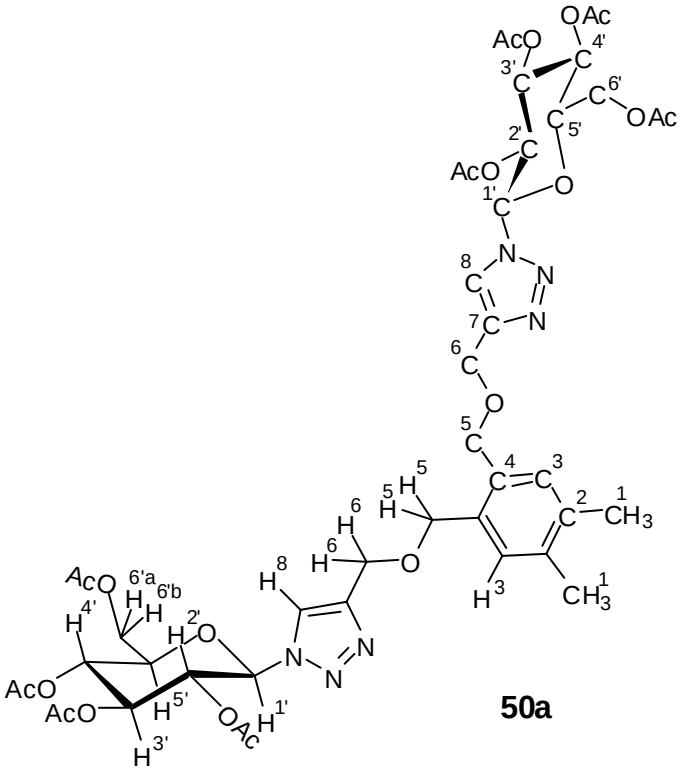

50a

^{1}H-NMR (500 MHz, DMSO-d_6):

δ = 8.45 (s, 2H, H-8), 7.13 (s, 2H, H-3), 6.35 (d, 2H, H-1', $^3J_{H\text{-}1',H\text{-}2'}$ = 9.1 Hz), 5.68 (dd, 2H, H-2', $^3J_{H\text{-}1',H\text{-}2'}$ = 9.4, $^3J_{H\text{-}2',H\text{-}3'}$ = 9.5 Hz), 5.56 (dd, 2H, H-3', $^3J_{H\text{-}2',H\text{-}3'}$ = 9.5 Hz, $^3J_{H\text{-}3',H\text{-}4'}$ = 9.8 Hz), 5.19 (dd, 2H, H-4', $^3J_{H\text{-}3',H\text{-}4'}$ = $^3J_{H\text{-}4',H\text{-}5'}$ = 9.8 Hz), 4.54 (s, 4H, H-6), 4.49 (s, 4H, H-5), 4.37 (ddd, 2H, H-5', $^3J_{H\text{-}4',H\text{-}5'}$ = 10.1 Hz, $^3J_{H\text{-}5',H\text{-}6'a}$ = 5.4 Hz, $^3J_{H\text{-}5',H\text{-}6'b}$ = 2.5 – 2.8 Hz), 4.13 (dd, 2H, H-6'a, $^2J_{H\text{-}6'a,H\text{-}6'b}$ = 12.5 Hz, $^3J_{H\text{-}5',H\text{-}6'a}$ = 5.4 – 5.7 Hz), 4.07 (dd, 2H, H-6'b, $^2J_{H\text{-}6'a,H\text{-}6'b}$ = 12.3 Hz, $^3J_{H\text{-}5',H\text{-}6'a}$ = 2.2 Hz), 2.21 (s, 6H, H-1), 2.03, 1.99, 1.97, 1.79 (s, 24H, 4 × -OC(O)C$\underline{H}_3$).

^{13}C-NMR (100 MHz, DMSO-d_6):

δ = 170.0, 169.5, 169.3, 168.5 (4 × -O$\underline{C}$(O)CH_3),, 144.7 (C-7), 135.3 (C-2), 133.4 (C-4), 130.0 (C-3), 122.9 (C-8), 83.8 (C-1'), 73.2 (C-5'), 72.1 (C-3'), 70.2 (C-2'), 68.7 (C-5), 67.5 (C-4'), 62.6 (C-6), 61.7 (C-6'), 20.4, 20.3, 20.2, 19.8 (4 × -OC(O)$\underline{C}H_3$), 19.0 (C-1).

To a vigorously stirred solution of bisalkynylated derivative **49** (50 mg, 0.21 mmol) in THF (4 mL) and EtOH (2 mL) was added consecutively $CuSO_4 \bullet 5H_2O$ (7.5 mg, 30 μmol), (+) sodium L-ascorbate (18 mg, 93 μmol) and 2,3,4,6-tetra-*O*-acetyl-β-D-glucopyranosyl azide (**60**) (230 mg, 0.61 mmol). After 42 h stirring at r.t., the solvents were removed and the residue (340 mg) was purified *via* column chromatography on silica gel (gradient from PE → EA). The combined fractions containing the coupling product were evaporated to yield **50a** as a white solid (169 mg, 0.171 mmol, 83% o.th.).

1,2-Dimethyl-4,5-bis(((*N*-1-(2,3,4,6-tetra-*O*-acetyl-*β*-D-galactopyranosyl)-1*H*-1,2,3-triazol-4-yl)methoxy)methyl)benzene (**50b**)

$C_{44}H_{56}N_6O_{20}$ (988.94 g/mol)

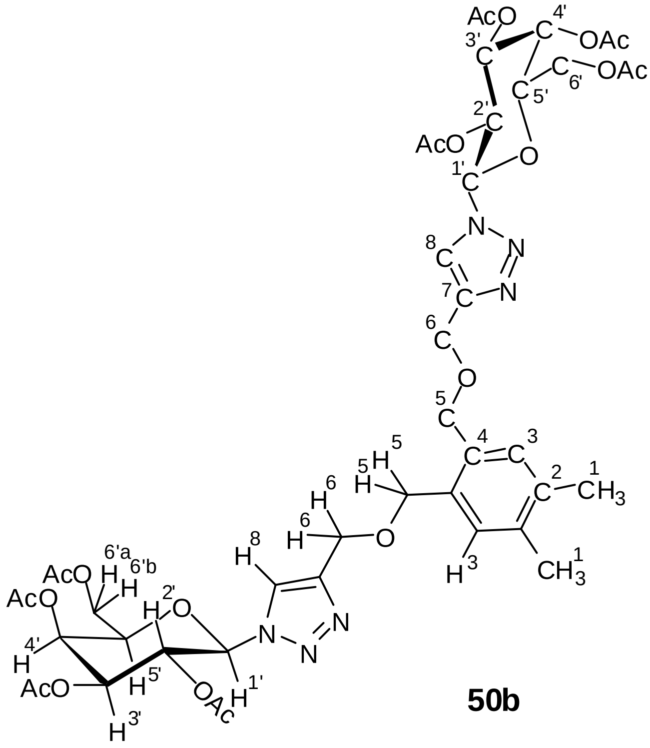

50b

^{1}H-NMR (400 MHz, DMSO-*d$_6$*):

δ = 8.37 (s, 2H, H-8), 7.13 (s, 2H, H-3), 6.27 (d, 2H, H-1’, $^3J_{H-1’,H-2’}$ = 9.2 Hz), 5.61 (dd, 2H, H-2’, $^3J_{H-1’,H-2’}$ = 9.4, $^3J_{H-2’,H-3’}$ = 9.9 Hz), 5.47 (dd, 2H, H-3’, $^3J_{H-2’,H-3’}$ = 10.2 Hz, $^3J_{H-3’,H-4’}$ = 3.3 Hz), 5.42 (dd, 2H, H-4’, $^3J_{H-3’,H-4’}$ = 3.6 Hz, $^3J_{H-4’,H-5’}$ = 0.8 Hz), 4.59 (dd, 2H, H-5’, $^3J_{H-5’,H-6’a}$ = 6.0 Hz, $^3J_{H-5’,H-6’b}$ = 6.4 Hz), 4.55 (s, 4H, H-6), 4.49 (s, 4H, H-5), 4.13 (dd, 2H, H-6’a, $^2J_{H-6’a,H-6’b}$ = 11.6 Hz, $^3J_{H-5’,H-6’a}$ = 5.1 – 5.3 Hz), 4.02 (dd, 2H, H-6’b, $^2J_{H-6’a,H-6’b}$ = 11.6 Hz, $^3J_{H-5’,H-6’a}$ = 7.1 – 7.4 Hz), 2.20 (s, 6H, H-1), 2.18, 1.98, 1.95, 1.81 (s, 24H, 8 × -OC(O)C<u>H</u>$_3$).

^{13}C-NMR (100 MHz, DMSO-*d$_6$*):

δ = 169.93, 169.85, 169.4 168.5 (4 × -O<u>C</u>(O)CH$_3$), 144.5 (C-7), 135.3 (C-2), 133.4 (C-4), 130.0 (C-3), 123.3 (C-8), 84.2 (C-1’), 72.9 (C-5’), 70.4 (C-3’), 68.7 (C-5), 67.8 (C-2’), 67.3 (C-4’), 62.4 (C-6), 61.5 (C-6’), 20.4, 20.31, 20.26, 19.9 (4 × -OC(O)<u>C</u>H$_3$), 18.9 (C-1).

To a vigorously stirred solution of bisalkynylated derivative **49** (57 mg, 0.24 mmol) in THF (4 mL) and EtOH (2 mL) was added consecutively $CuSO_4 \cdot 5H_2O$ (11 mg, 43 μmol), (+) sodium L-ascorbate (20 mg, 100 μmol) and 2,3,4,6-tetra-*O*-acetyl-β-D-galactopyranosyl azide (**71**) (260 mg, 0.70 mmol). After 24 h stirring at 50 °C the solvents were removed and the residue (375 mg) was subjected to column chromatography on silica gel (gradient from PE → EA). The combined fractions containing the coupling product were evaporated to yield **50b** as a white solid (160 mg, 0.162 mmol, 69% o.th.).

Acetic 1,2,3,4-tetra-*O*-acetyl-*β*-D-glucopyranuronic anhydride (**57**)[152]

$C_{16}H_{20}O_{12}$ (404.32 g/mol)

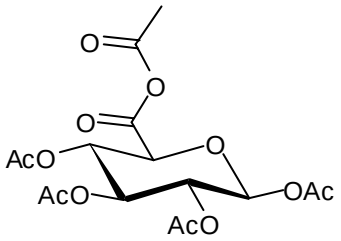

57

$[\alpha]_{546nm}^{20°C}$ = +2.6 ° (c = 1, $CHCl_3$)

Mp. = 129 °C

^{1}H-NMR (400 MHz, $CDCl_3$):

δ = 5.80 (d, 1H, H-1, $^3J_{H\text{-}1,H\text{-}2}$ = 6.9 Hz), 5.37 (dd, 1H, H-4, $^3J_{H\text{-}3,H\text{-}4}$ = $^3J_{H\text{-}4,H\text{-}5}$ = 9.2 Hz), 5.28 (dd, 1H, H-3, $^3J_{H\text{-}2,H\text{-}3}$ = 8.4 Hz, $^3J_{H\text{-}3,H\text{-}4}$ = 9.2 Hz), 5.11 (dd, 1H, H-2, $^3J_{H\text{-}2,H\text{-}3}$ = 8.4 Hz, $^3J_{H\text{-}1,H\text{-}2}$ = 6.9 Hz), 4.31 (d, 1H, H-5, $^3J_{H\text{-}4,H\text{-}5}$ = 9.2 Hz), 2.27 (s, 3H, -C(O)OC(O)CH_3), 2.12, 2.053, 2.047, 2.03 (s, 12H, 4 × -OAc).

^{13}C-NMR (100 MHz, C_6D_6):

δ = 169.6, 169.1, 169.8, 168.4, (4 × -OAc), 164.8, 163.0 (-C(O)OC(O)CH_3), 91.8 (C-1), 73.2 (C-5), 72.0 (C-3), 70.8 (C-2), 68.5 (C-4), 21.3 -C(O)OC(O)CH_3), 20.04, 19.98, 19.95, 19.92 (4 × -OAc).

The anomeric mixture of D-glucuronic acid (**56**) (5.03 g, 26.0 mmol) was suspended in acetic anhydride (75 mL) and stirred at 0 °C. Iodine (353 mg, 1.39 mmol) was added in portions and the orange suspension was stirred for 2 h on ice and for further 3 h at room temperature. Acetic anhydride was removed *in vacuo* and the remaining residue taken up in dichloromethane (70 mL). The organic layer was then washed twice with $Na_2S_20_3$ (1.0 M, 2 × 80 mL), dried over Na_2SO_4, filtered and concentrated to afford a yellow oil from which the crystalline, white crude product was obtained upon standing. Recrystallization from DCM (40 mL) and PE (20 mL) at RT isolated the *β*-anomer **57** from its *α*-anomer, present as minor impurity (8.48 g, 20.8 mmol, 80% o.th.).

1,2,3,4-Tetra-*O*-acetyl-*β*-D-glucopyranuronic acid (**58**)[152]

$C_{14}H_{18}O_{11}$ (362.29 g/mol)

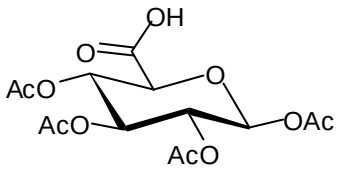

58

$[\alpha]_{546nm}^{20°C}$ = +18.5 ° (c = 1, $CHCl_3$)

Mp. = 151 °C

^{1}H-NMR (400 MHz, DMSO-d_6):
δ = 13.3 (bs, 1H, -C(O)OH), 5.99 (d, 1H, H-1, $^3J_{H\text{-}1,H\text{-}2}$ = 7.9 Hz), 5.47 (dd, 1H, H-3, $^3J_{H\text{-}2,H\text{-}3}$ = 9.7 Hz, $^3J_{H\text{-}3,H\text{-}4}$ = 9.4 Hz), 5.05 (dd, 1H, H-4, $^3J_{H\text{-}3,H\text{-}4}$ = $^3J_{H\text{-}4,H\text{-}5}$ = 9.7 Hz), 4.94 (dd, 1H, H-2, $^3J_{H\text{-}1,H\text{-}2}$ = 8.1 Hz, $^3J_{H\text{-}2,H\text{-}3}$ = 9.7 Hz), 4.51 (d, 1H, H-5, $^3J_{H\text{-}4,H\text{-}5}$ = 9.9 Hz), 2.07, 2.00, 1.97, 1.96, (s, 12H, 4 × -OAc).

^{13}C-NMR (100 MHz, DMSO-d_6):
δ = 169.5 (-OAc), 169.1(2 × -OAc), 168.7 (-OAc), 167.9 (-C(O)OH), 90.6 (C-1), 71.6 (C-5), 71.2 (C-3), 69.9 (C-2), 68.7 (C-4), 20.5, 20.32, 20.28, 20.26 (4 × -OAc).

The anhydride **57** (4.02 g, 9.89 mmol) was dissolved in water/THF (180 mL, 1:2) and stirred overnight. The solution was concentrated and the product extracted into DCM (2 × 50 mL). The organic phase was extracted with sat. aq. NaCl, dried over Na_2SO_4 and filtered. After evaporation *in vacuo* a white fluffy material was obtained and identified as **58** (3.66 g, 9.72 mmol, 98% o.th.). Compound **58** can also be obtained more quickly stirring **57** in water/THF for 3 hours and evaporating the solvents directly from the reaction mixture without any workup.

1,2,3,4-Tetra-*O*-acetyl-*β*-D-glucopyranuronoyl chloride (**59**)[154]

$C_{14}H_{17}ClO_{11}$ (380.73 g/mol)

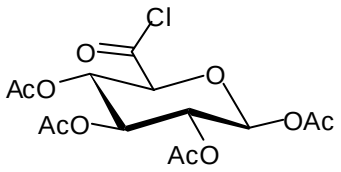

59

Mp. = 141 °C (Lit.: 120 – 123 °C)[154]

$[\alpha]_{546nm}^{20°C}$ = +15.3 ° (c = 1, $CHCl_3$) (Lit.: $[\alpha]_{589nm}$ = +6.4 °, c = 1, DCM)[154]

^{1}H-NMR (400 MHz, $CDCl_3$):

δ = 5.87 (d, 1H, H-1, $^3J_{H\text{-}1,H\text{-}2}$ = 6.4 Hz), 5.39 (dd, 1H, H-4, $^3J_{H\text{-}3,H\text{-}4}$ = $^3J_{H\text{-}4,H\text{-}5}$ = 8.6 Hz), 5.26 (dd, 1H, H-3, $^3J_{H\text{-}2,H\text{-}3}$ = 8.1, $^3J_{H\text{-}3,H\text{-}4}$ = 8.9 Hz), 5.09 (dd, 1H, H-2, $^3J_{H\text{-}1,H\text{-}2}$ = 6.4 Hz, $^3J_{H\text{-}2,H\text{-}3}$ = 7.9 Hz), 4.45 (d, 1H, H-5, $^3J_{H\text{-}4,H\text{-}5}$ = 8.6 Hz), 2.14, 2.07, 2.06, 2.04 (s, 3H, 4 × -OAc).

^{13}C-NMR (100 MHz, $CDCl_3$):

δ = 169.8 (-C(O)Cl), 169.7, 169.1, 169.0, 168.5 (4 × -OAc), 91.1 (C-1), 78.8 (C-5), 70.8 (C-3), 69.8 (C-2), 67.6 (C-4), 20.7 (-OAc), 20.5 (2 × -OAc), 20.4 (-OAc).

A solution of 1,2,3,4-tetra-*O*-acetyl-*β*-D-glucopyranuronic acid (**58**) (1.00 g, 2.63 mmol) in DCM (50 mL, 0.02 g/mL) was cooled to 0 °C and oxalyl chloride (0.50 mL, 5.8 mmol) was added. Dry DMF (21 μL, 10 mol% with respect to **58**) was slowly added to the stirring solution and evolution of gas was observed. The pale yellow solution was allowed to stir for 30 min at 0 °C and then for 2 h at rt. The solution was evaporated to leave a off-white chalky solid (0.95 g, 2.50 mmol, 95% o.th.), which was stored in a desiccator over P_4O_{10}.

2,3,4,6-Tetra-*O*-acetyl-*β*-D-glucopyranosyl azide (**60**)[166]

$C_{14}H_{19}N_3O_9$ (373.31 g/mol)

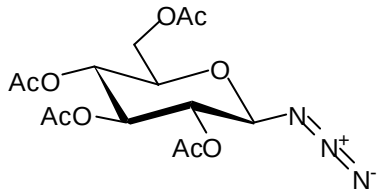

60

X-ray: successful (Figure 13)

$[\alpha]_{546nm}^{20°C}$ = -31.5 ° (c = 1, $CHCl_3$) (Lit.: $[\alpha]_{589nm}^{27°C}$ = -29 °, c = 2, $CHCl_3$)[166]

Mp. 127 °C (Lit.: 126 – 127 °C)[166]

IR: $\tilde{\nu}$ [$-N_3$] = 2118 cm^{-1} (Lit.: 2140 cm^{-1})[210]

^{1}H-NMR (500 MHz, C_6D_6):
δ = 5.29 (dd, 1H, H-3, $^3J_{H\text{-}2,H\text{-}3}$ = $^3J_{H\text{-}3,H\text{-}4}$ = 9.5 Hz), 5.18 (dd, 1H, H-4, $^3J_{H\text{-}3,H\text{-}4}$ = 8.8 Hz, $^3J_{H\text{-}4,H\text{-}5}$ = 9.8 Hz), 5.15 (dd, 1H, H-2, $^3J_{H\text{-}1,H\text{-}2}$ = 8.8 Hz, $^3J_{H\text{-}2,H\text{-}3}$ = 9.5 Hz), 4.21 (dd, 1H, H-6a, $^2J_{H\text{-}6a,H\text{-}6b}$ = 12.6 Hz, $^3J_{H\text{-}5,H\text{-}6a}$ = 4.7 Hz), 4.07 (d, 1H, H-1, $^3J_{H\text{-}1,H\text{-}2}$ = 8.8 Hz), 4.00 (dd, 1H, H-6b, $^2J_{H\text{-}6a,H\text{-}6b}$ = 12.6 Hz, $^3J_{H\text{-}5,H\text{-}6b}$ = 1.9 Hz), 3.21 (ddd, 1H, H-5, $^3J_{H\text{-}4,H\text{-}5}$ = 10.1 Hz, $^3J_{H\text{-}5,H\text{-}6a}$ = 4.7 Hz, $^3J_{H\text{-}5,H\text{-}6b}$ = 2.2 Hz), 1.711 (s, 3H, -OC(O)C$\underline{H}_3$), 1.707 (s, 6H, 2 × -OC(O)C$\underline{H}_3$), 1.69 (s, 3H, -OC(O)C$\underline{H}_3$).

^{13}C-NMR (100 MHz, C_6D_6):
δ = 170.0, 169.8, 168.9, 168.7 (4 × -O$\underline{C}$(O)CH_3), 87.9 (C-1), 74.3 (C-5), 73.0 (C-3), 71.0 (C-2), 68.1 (C-4), 61.5 (C-6), 20.12, 20.07, 20.0, 20.0 (4 × -OC(O)$\underline{C}H_3$).

Sodium azide (17.1 g, 263 mmol) and 2,3,4,6-tetra-*O*-acetyl-*α*-D-glucopyranosyl bromide (35.4 g, 86.2 mmol) were suspended in dry DMF (270 mL) and stirred at 50 °C (internal glass coated thermometer) for 2 h. During heating-up, the internal temperature rose rapidly to 55 °C indicating an exothermic process. Evaporation to dryness (temp. ≤ 50 °C) afforded a yellow-white residue that was dissolved in chloroform (500 mL) and water (200 mL). The phases were separated and the organic layer was washed consecutively with dist. water (300 mL),

sat. aq. $NaHCO_3$ (400 mL), sat. aq. NaCl (200 mL) and dried over Na_2SO_4. The crude yellowish mass (33.3 g), obtained after filtration and evaporation was washed with cold Et_2O to yield the azide **60** as white crystals (27.5 g, 73.6 mmol, 85% o.th.). For X-ray analysis, the product was recrystallized from EA/Et_2O (Figure 13).

2,3,4,6-Tetra-*O*-acetyl-*β*-D-glucopyranosyl amine (**61**)[166]

$C_{14}H_{21}NO_9$ (347.32 g/mol)

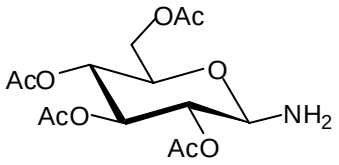

61

X-ray: successful (Figure 12)

$[\alpha]_{546nm}^{20°C}$ = +16.7 ° (c = 1, $CHCl_3$) (Lit.: $[\alpha]_{589nm}^{20°C}$ = +28 °, c = 0.04, $CHCl_3$)[166]

Mp. 111 °C (Lit.: 115 – 116 °C)[166]

^{1}H-NMR (400 MHz, C_6D_6):
δ = 5.44 (dd, 1H, H-3, $^3J_{H\text{-}2,H\text{-}3}$ = 9.7 Hz, $^3J_{H\text{-}3,H\text{-}4}$ = 9.4 Hz), 5.26 (dd, 1H, H-4, $^3J_{H\text{-}3,H\text{-}4}$ = 9.4 Hz, $^3J_{H\text{-}4,H\text{-}5}$ = 9.9 Hz), 4.96 (dd, 1H, H-2, $^3J_{H\text{-}1,H\text{-}2}$ = 8.9 Hz, $^3J_{H\text{-}2,H\text{-}3}$ = 9.7 Hz), 4.29 (dd, 1H, H-6a, $^2J_{H\text{-}6a,H\text{-}6b}$ = 12.2 Hz, $^3J_{H\text{-}5,H\text{-}6a}$ = 4.8 Hz), 4.10 (dd, 1H, H-6b, $^2J_{H\text{-}6a,H\text{-}6b}$ = 12.0 Hz, $^3J_{H\text{-}5,H\text{-}6b}$ = 2.3 Hz), 3.72 (d, 1H, H-1, $^3J_{H\text{-}1,H\text{-}2}$ = 8.9 Hz), 3.24 (ddd, 1H, H-5, $^3J_{H\text{-}4,H\text{-}5}$ = 10.1 Hz, $^3J_{H\text{-}5,H\text{-}6a}$ = 4.6 – 4.8 Hz, $^3J_{H\text{-}5,H\text{-}6b}$ = 2.3 – 2.4 Hz), 1.78, 1.76 (s, 6H,2 × -OC(O)C$\underline{H}_3$), 1.75 (s, 6H, 2 × -OC(O)C$\underline{H}_3$), 1.46 (bs, 2H, -NH_2).

^{1}H-NMR (500 MHz, DMSO-d_6):
δ = 5.23 (dd, 1H, H-3, $^3J_{H\text{-}2,H\text{-}3}$ = 9.5 Hz, $^3J_{H\text{-}3,H\text{-}4}$ = 9.8 Hz), 4.83 (dd, 1H, H-4, $^3J_{H\text{-}3,H\text{-}4}$ = $^3J_{H\text{-}4,H\text{-}5}$ = 9.8 Hz), 4.63 (dd, 1H, H-2, $^3J_{H\text{-}1,H\text{-}2}$ = 9.1 Hz, $^3J_{H\text{-}2,H\text{-}3}$ = 9.5 Hz), 4.29 (d, 1H, H-1, $^3J_{H\text{-}1,H\text{-}2}$ = 9.2 Hz), 4.09 (dd, 1H, H-6a, $^2J_{H\text{-}6a,H\text{-}6b}$ = 12.1 Hz, $^3J_{H\text{-}5,H\text{-}6a}$ = 5.1 – 5.4 Hz), 3.97 (dd, 1H, H-6b, $^2J_{H\text{-}6a,H\text{-}6b}$ = 12.0 Hz, $^3J_{H\text{-}5,H\text{-}6b}$ = 2.2 Hz), 3.88 (ddd, 1H, H-5, $^3J_{H\text{-}4,H\text{-}5}$ = 9.9 Hz, $^3J_{H\text{-}5,H\text{-}6a}$ = 5.1 – 5.4 Hz, $^3J_{H\text{-}5,H\text{-}6b}$ = 2.4 Hz), 2.55 (bs, 2H, -NH_2), 2.00 (s, 3H,-OC(O)C$\underline{H}_3$), 1.97 (s, 6H, 2 × -OC(O)C$\underline{H}_3$), 1.93 (s, 3H,-OC(O)C$\underline{H}_3$).

^{13}C-NMR (100 MHz, C_6D_6):
δ = 170.0, 169.8, 169.6, 169.3 (4 × -O$\underline{C}$(O)CH_3), 85.3 (C-1), 73.7 (C-3), 73.0 (C-5), 72.4 (C-2), 69.3 (C-4), 62.4 (C-6), 20.4, 20.3, 20.23, 20.18 (4 × -OC(O)$\underline{C}H_3$).

^{13}C-NMR (125 MHz, DMSO-d_6):
δ = 170.0, 169.5, 169.32, 169.29 (4 × -O<u>C</u>(O)CH_3), 84.1 (C-1), 72.9 (C-3), 72.2 (C-2), 71.1 (C-5), 68.7 (C-4), 62.3 (C-6), 20.54, 20.52, 20.35, 20.28 (4 × -OC(O)<u>C</u>H_3).

2,3,4,6-Tetra-*O*-acetyl-*β*-D-glucopyranosyl azide (**60**) (10.1 g, 270 mmol) was dissolved in a mixture of EA (300 mL) and TEA (4 mL) by gentle warming. The clear, colorless solution was degassed before a freshly prepared suspension of dry Pd/C (1.0 g, 0.94 mmol) in EA (10 mL) was added. The flask was sealed with a septum, evacuated and flushed with hydrogen, bubbling through the solution *via* a capillary. The reaction was monitored by TLC (PE/EA = 60:40). After 12 h the slowly stirred solution was evacuated, recharged with hydrogen and stirred for further 12 h. For hydrogenation, a glass apparatus was used, applying moderate positive hydrostatic pressure (500 mm) The suspension was filtered through a short pad of Na_2SO_4 (2 cm). Evaporation of the clear, solution gained a slightly yellow solid of 2,3,4,6-tetra-*O*-acetyl-*β*-D-glucopyranosyl amine (**61**) (7.90 g, 23.0 mmol, 85% o.th.). Recrystallization from EA at room temperature afforded an analytically pure sample of fine, white needles appropriate for X-ray analysis (Figure 12).

2,3,4,6-Tetra-*O*-acetyl-*β*-D-glucopyranosyl isocyanate (**62**)[157, 160]

$C_{15}H_{19}NO_{10}$ (373.31 g/mol)

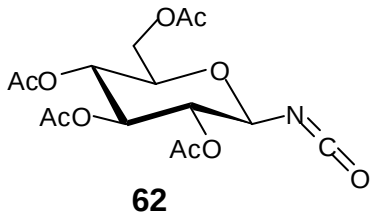

62

$[\alpha]_{546nm}^{20°C}$ = -7.4 ° (c= 1 mol/L) (Lit.: $[\alpha]_{589nm}^{20°C}$ -6.7 °)[160]

Mp. 117 °C (Lit.: 117 – 119°C)[157]

IR $\tilde{\nu}$ [-NCO] = 2246 cm^{-1} (Lit.: 2260 cm^{-1})[160]

^{1}H-NMR (500 MHz, $CDCl_3$):
δ = 5.18 (dd, 1H, H-3, $^3J_{H\text{-}2,H\text{-}3}$ = $^3J_{H\text{-}3,H\text{-}4}$ = 9.5 Hz), 5.10 (dd, 1H, H-4, $^3J_{H\text{-}3,H\text{-}4}$ = 9.5 Hz, $^3J_{H\text{-}4,H\text{-}5}$ = 10.1 Hz), 4.99 (dd, 1H, H-2, $^3J_{H\text{-}1,H\text{-}2}$ = 8.8 Hz, $^3J_{H\text{-}2,H\text{-}3}$ = 9.5 Hz), 4.80 (d, 1H, H-1, $^3J_{H\text{-}1,H\text{-}2}$ = 8.8 Hz), 4.24 (dd, 1H, H-6a, $^2J_{H\text{-}6a,H\text{-}6b}$ = 12.5 Hz, $^3J_{H\text{-}5,H\text{-}6a}$ = 4.7 – 5.0 Hz), 4.14 (dd, 1H, H-6b, $^2J_{H\text{-}6a,H\text{-}6b}$ = 12.6 Hz, $^3J_{H\text{-}5,H\text{-}6b}$ = 2.2 Hz), 3.76 (ddd, 1H, H-5, $^3J_{H\text{-}4,H\text{-}5}$ = 9.9 Hz, $^3J_{H\text{-}5,H\text{-}6a}$ = 4.7 – 5.0 Hz, $^3J_{H\text{-}5,H\text{-}6b}$ = 2.2 Hz), 2.10, 2.08, 2.02, 2.01 (s, 12H, 4 × -OC(O)C$\underline{H}_3$).

^{1}H-NMR (400 MHz, C_6D_6):
δ = 5.22 (dd, 1H, H-3, $^3J_{H\text{-}2,H\text{-}3}$ = 8.9 Hz, $^3J_{H\text{-}3,H\text{-}4}$ = 9.4 Hz), 5.16 (dd, 1H, H-4, $^3J_{H\text{-}3,H\text{-}4}$ = 9.4 Hz, $^3J_{H\text{-}4,H\text{-}5}$ = 9.7 Hz), 5.06 (dd, 1H, H-2, $^3J_{H\text{-}1,H\text{-}2}$ = 8.6 Hz, $^3J_{H\text{-}2,H\text{-}3}$ = 9.2 Hz), 4.19 (dd, 1H, H-6a, $^2J_{H\text{-}6a,H\text{-}6b}$ = 12.5 Hz, $^3J_{H\text{-}5,H\text{-}6a}$ = 4.8 Hz), 4.08 (d, 1H, H-1, $^3J_{H\text{-}1,H\text{-}2}$ = 8.6 Hz), 3.98 (dd, 1H, H-6b, $^2J_{H\text{-}6a,H\text{-}6b}$ = 12.5 Hz, $^3J_{H\text{-}5,H\text{-}6b}$ = 2.0 Hz), 3.76 (ddd, 1H, H-5, $^3J_{H\text{-}4,H\text{-}5}$ = 7.2 Hz, $^3J_{H\text{-}5,H\text{-}6a}$ = 4.8 Hz, $^3J_{H\text{-}5,H\text{-}6b}$ = 2.2 – 2.5 Hz), 1.72, 1.70, 1.69, 1.68 (s, 12H, 4 × -OC(O)C$\underline{H}_3$).

^{13}C-NMR (125 MHz, $CDCl_3$):
δ = 170.6, 170.1, 169.23, 169.18 (4 × -O$\underline{C}$(O)CH_3), 127.1 (-N$\underline{C}$O), 82.7 (C-1), 74.1 (C-5), 72.5 (C-2, C-3), 67.8 (C-4), 61.6 (C-6), 20.7 (-OC(O)$\underline{C}H_3$), 20.50 (2 × -OC(O)$\underline{C}H_3$), 20.46 (-OC(O)$\underline{C}H_3$).

A biphasic mixture of a solution of 2,3,4,6-tetra-*O*-acetyl-*β*-D-glucopyranosyl amine (**61**) (0.515 g, 1.48 mmol) in DCM (17 mL) and sat. aq. $NaHCO_3$ (10 mL) was constantly stirred at 500 rpm in a single neck round bottomed flask (50 mL) using a Teflon® coated stirring bar (oval, 2 cm) and cooled. When the internal temperature of the heterogeneous mixture reached -10 to 0 °C, triphosgene (0.461 g, 1.55 mmol) was added in one portion. The biphasic mixture was stirred for exactly 30 minutes while cooling was continued. Within the first three minutes, formation of a massive solid at the phase interfaces was observed. The heterogeneous mixture was transferred in a separation funnel, diluted with DCM (50 mL) and the organic phase was separated without agitation. The organic phase was quickly washed with sat. aq. NaCl (50 mL) and dried over Na_2SO_4. Prior to filtration, toluene (2 mL) was added and DCM was removed by evaporation at ≤ 30 °C. From the resulting clear toluene solution crystallization was accomplished upon addition of *n*-hexane at room temperature, to yield 2,3,4,6-tetra-*O*-acetyl-*β*-D-glucopyranosyl isocyanate (**62**) (0.45 g, 1.2 mmol, 81% o.th.) as colorless crystals.

O,O'-(4,5-Dimethyl-1,2-phenylene)bis(methylene)) bis(*N*-(*β*-D-glucopyranosyl)carbamate) (**63**)

$C_{24}H_{36}N_2O_{14}$ (576.55 g/mol)

R$_f$ = 0.42 (*n*-butanol/HOAc/water, 60:20:20)

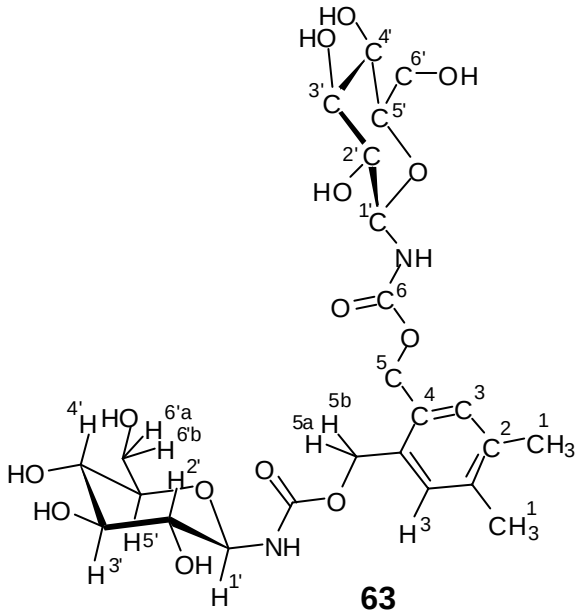

63

^{1}H-NMR (DMSO-d_6/MeOH-d_4, 400 MHz):

δ = 7.13 (s, 2H, H-3), 5.08 (d, 2H, H-5a, $^2J_{H\text{-}5a,H\text{-}5b}$ = 12.7 Hz), 5.04 (d, 2H, H-5b, $^2J_{H\text{-}5a,H\text{-}5b}$ = 12.5 Hz), 4.52 (dd, 2H, H-1', $^3J_{H\text{-}1',H\text{-}2'}$ = 8.9 Hz), 3.65 (dd, 2H, H-6'a, $^2J_{H\text{-}6'a,H\text{-}6'b}$ = 11.7 Hz, $^3J_{H\text{-}5',H\text{-}6'a}$ = 1.8 Hz), 3.45 (dd, 2H, H-6'b, $^2J_{H\text{-}6'a,H\text{-}6'b}$ = 11.8 Hz, $^3J_{H\text{-}5',H\text{-}6'b}$ = 5.1 – 5.3 Hz), 3.20 (dd, 2H, H-3', $^3J_{H\text{-}2',H\text{-}3'}$ = 8.6 Hz, $^3J_{H\text{-}3',H\text{-}4'}$ = 8.9 Hz), 3.11 (ddd, 2H, H-5', $^3J_{H\text{-}4',H\text{-}5'}$ = 9.4 Hz, $^3J_{H\text{-}5',H\text{-}6'a}$ = 1.9 Hz, $^3J_{H\text{-}5',H\text{-}6'b}$ = 4.8 – 5.1 Hz), 3.09 (dd, 2H, H-2', $^3J_{H\text{-}1',H\text{-}2'}$ = 9.2 Hz, $^3J_{H\text{-}2',H\text{-}3'}$ = 8.9 Hz), 3.07 (dd, 2H, H-4', $^3J_{H\text{-}3',H\text{-}4'}$ = 8.7 Hz, $^3J_{H\text{-}4',H\text{-}5'}$ = 9.4 Hz), 2.18 (s, 6H, H-1).

NH-signals do not appear due to proton/deuterium exchange.

^{1}H-NMR (DMSO-d_6, 500 MHz):

δ = 7.87 (d, 2H, NH, $^3J_{NH,H\text{-}1'}$ = 9.1 Hz), 7.17 (s, 2H, H-3), 5.06 (dd, 4H, H-5a/H-5b, $^2J_{H\text{-}5a,H\text{-}5b}$ = 12.6 – 13.2 Hz), 4.94 (d, 2H, OH, ^3J = 4.7 Hz), 4.86 (dd, 4H, OH, ^3J = 4.4 Hz, ^3J = 4.7 Hz), 4.46 – 4.50 (m, 4H, H-1'/OH), 3.63 (dd, 2H, H-6'a, $^2J_{H\text{-}6'a,H\text{-}6'b}$ = 10.6 Hz, $^3J_{H\text{-}5',H\text{-}6'a}$ = 5.4 – 5.7 Hz), 3.42 – 3.37 (m, 2H, H-6'b), 3.18 – 3.13 (m, 2H, H-3'), 3.09 – 3.06 (m, 4H, H-2'/H-5'), 3.04 – 2.99 (m, 2H, H-4'), 2.21 (s, 6H, H-1).

^{13}C-NMR (DMSO-d_6/MeOH-d_4, 100 MHz):
δ = 157.0 (C-6), 137.2 (C-2), 133.3 (C-4), 131.6 (C-3), 83.2 (C-1'), 79.0 (C-5'), 78.2 (C-3'), 72.9 (C-2'), 70.7 (C-4'), 64.2 (C-5), 61.8 (C-6'), 19.2 (C-1).

^{13}C-NMR (DMSO-d_6, 100 MHz):
δ = 155.8 (C-6), 136.0 (C-2), 132.3 (C-4), 130.5 (C-3), 82.4 (C-1'), 78.4 (C-5'), 77.5 (C-3'), 72.0 (C-2'), 69.9 (C-4'), 63.0 (C-5), 60.9 (C-6'), 19.0 (C-1).

Deprotection was accomplished under Zemplén conditions by dissolving the peracetylated bisglucosyl carbamate **47** (54 mg, 59 μmol) in a freshly prepared solution of NaOMe/MeOH (20 mL, ~ pH 9). The reagent was prepared by diluting 5mL of a 0.01M methanolic stock solution (prepared from 5.6 mg of NaOMe in 100 mL of MeOH) with 95 mL of MeOH. Deprotection was completed after 96 h at room temperature according to TLC (*n*-butanol/HOAc/water = 60:20:20). Excess of acidic ion exchange resin (Amberlite® IR 120) was added, and after filtration and evaporation, the remaining residue was dissolved in deionized water and lyophilized. The deprotected carbamate **63** was obtained as a faintly yellowish, voluminous residue (32 mg, 55 μmol, 93% o.th.).

[2,3,9,10,16,17,23,24-Octakis(*O*-(*N*-1-(2,3,4,6-tetra-*O*-acetyl-*β*-D-glucopyranosyl)carbamoyloxy)methyl)phthalocyaninato] zinc(II) (**64**)

$C_{160}H_{184}N_{16}O_{88}Zn$ (3804.64 g/mol)

MS-MALDI-TOF (1,8,9-anthracenetriol):
(calc. mono-isotopic 3800.9706 amu)
m/z (%): 3807.00 (100), 3807.98 (96),
3806.09 (95), 3808.96 (84),
3805.15 (69), 3809.87 (61) $[M]^{+\cdot}$

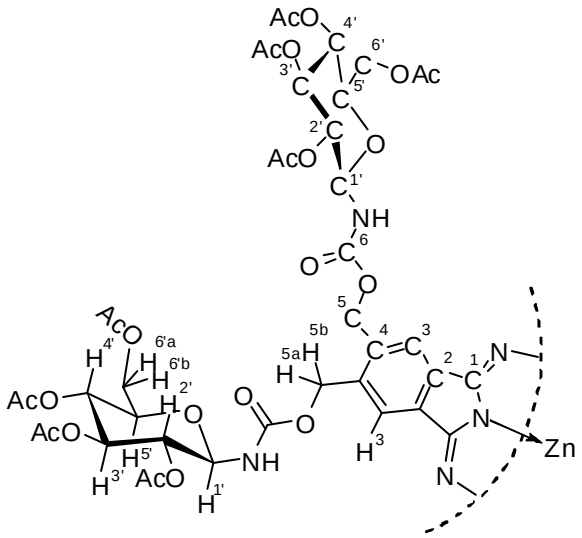

64

R_f = 0.22 (EA)

Mp. 284 °C

^{1}H-NMR (400 MHz, DMSO-d_6):
δ = 9.55 (bs, 8H, H-3), 8.64 (bd, 8H, NH, $^3J_{H\text{-}1',NH}$ = 8.9 Hz), 5.83 (d, 8H, H-5a, $^2J_{H\text{-}5a,H\text{-}5b}$ = 12.7 Hz), 5.77 (d, 8H, H-5b, $^2J_{H\text{-}5a,H\text{-}5b}$ = 14.5 Hz), 5.39 (dd, 8H, H-3', $^3J_{H\text{-}2',H\text{-}3'}$ = 9.4 Hz, $^3J_{H\text{-}3',H\text{-}4'}$ = 9.7 Hz), 5.32 (dd, 8H, H-1', $^3J_{H\text{-}1',NH}$ = $^3J_{H\text{-}1',H\text{-}2'}$ = 9.4 Hz), 4.97 (dd, 8H, H-2', $^3J_{H\text{-}1',H\text{-}2'}$ = 9.2 Hz, $^3J_{H\text{-}2',H\text{-}3'}$ = 9.4 Hz), 4.90 (dd, 8H, H-4', $^3J_{H\text{-}3',H\text{-}4'}$ = $^3J_{H\text{-}4',H\text{-}5'}$ = 9.7 Hz), 4.19 – 4.13 (m, 16H, H-5'/H-6'a), 3.99 (d, 8H, H-6'b, $^2J_{H\text{-}6'a,H\text{-}6'b}$ = 10.7 Hz), 1.98, 1.96, 1.95, 1.92 (s, 96H, 4 × -OC(O)C<u>H</u>$_3$).

^{13}C-NMR (100 MHz, DMSO-d_6):
δ = 169.9, 169.5, 169.2, 169.0 (4 × -O<u>C</u>(O)CH_3), 155.6 (C-6), 153.1 (C-1), 137.7 (C-2), 137.1 (C-4), 123.6 (C-3), 79.8 (C-1'), 72.9 (C-3'), 71.9 (C-5'), 70.5 (C-2'), 67.8 (C-4'), 64.3 (C-5), 61.7 (C-6'), 20.4, 20.3, 20.24, 20.23 (4 × -OC(O)<u>C</u>H_3).

ZnPc-*op*-CH_2OH **39** (51 mg, 60 μmol) was dissolved in dry pyridine (5.0 mL, 62 mmol) in a screw cap vial by means of sonification and 2,3,4,6-tetra-*O*-acetyl-*β*-D-glucopyranosyl isocyanate (**62**) (0.38 g, 1.0 mmol) was quickly added. The mixture was stirred in a pre-

heated aluminum block at 50 °C for 64 h. The solvent was evaporated and the remaining residue (0.46 g) was purified by column chromatography on silica gel (gradient from EA → 10% AcN). Evaporation of the solvent yielded the peracetylated glucosyl carbamate ZnPc **64** as blue, shiny plates (190 mg, 50 μmol, 82% o.th.).

[2,3,9,10,16,17,23,24-Octakis(*O*-(*N*-1-(*β*-D-glucopyranosyl)carbamoyloxy)methyl)phthalocyaninato] zinc(II) (**65**)

$C_{96}H_{120}N_{16}O_{56}Zn$ (2459.46 g/mol)

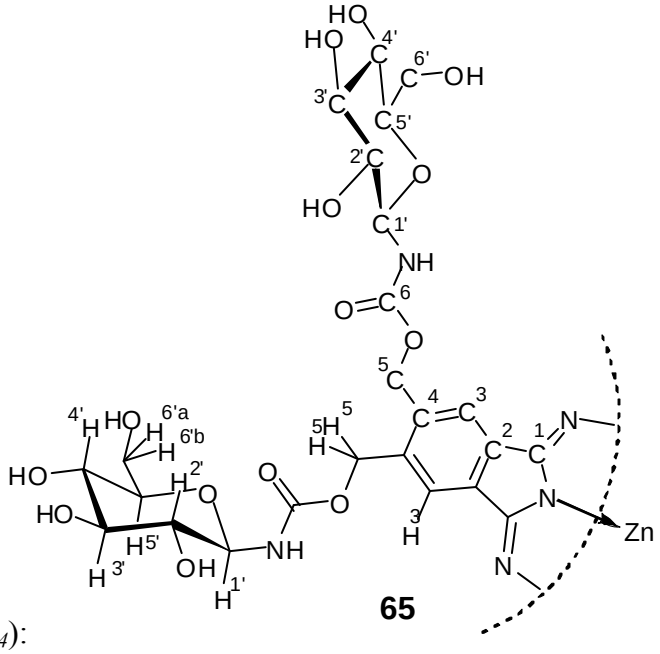

65

MS MALDI-TOF (1,8,9-anthracenetriol)
(calc. mono-isotopic 2456.6326 amu)
m/z: …attempts failed

^{1}H-NMR (400 MHz, DMSO-d_6 / MeOH-d_4):
δ = 9.55 (bs, 8H, H-3), 5.81 (bs, 16H, H-5), 4.68 (d, 8H, H-1', $^{3}J_{H\text{-}1',H\text{-}2'}$ = 8.4 Hz), 3.67 (d, 8H, H-6'a, $^{2}J_{H\text{-}6'a,H\text{-}6'b}$ = 11.2 Hz), 3.45 (dd, 8H, H-6'b, $^{2}J_{H\text{-}6'a,H\text{-}6'b}$ = 11.6 Hz, $^{3}J_{H\text{-}5',H\text{-}6'b}$ = 4.8 – 5.1 Hz), 3.28 – 3.09 (m, 32H, H-3'/H-2'/H-5'/H-4').
NH-protons appeared in neat DMSO-d_6 at 8.30 (d, 8H, NH, $^{3}J_{H\text{-}1',NH}$ = 8.7 Hz).

^{13}C-NMR (100 MHz, DMSO-d_6):
δ = 156.1 (C-6), 153.2 (C-1), 137.6 (C-2), 137.4 (C-4), 123.7 (C-3), 82.6 (C-1'), 78.5 (C-5'), 77.6 (C-3'), 72.1 (C-2'), 69.9 (C-4'), 60.9 (C-6').

Deprotection was accomplished under Zemplén conditions by dissolving the peracetylated glucosyl carbamate ZnPc **64** (21 mg, 5.5 μmol) in a freshly prepared solution of NaOMe/MeOH (20 mL, ~ pH 9). The reagent was prepared by diluting 5 mL of a 0.01M methanolic stock solution (prepared from 5.6 mg of NaOMe in 100 mL of MeOH) with 95 mL of MeOH. After stirring at room temperature for 3 d in the dark the precipitate thus formed was collected by centrifugation and washed several times with MeOH. The pellet was sonificated in deionized water and lyophilized. Glucosyl carbamate ZnPc **65** was isolated as a blue voluminous solid (14 mg, 5.5 μmol, 99% o.th.).

[2,3,9,10,16,17,23,24-Octakis(acetoxymethyl)phthalocyaninato] zinc(II) (**66**)

$C_{56}H_{48}N_8O_{16}Zn$ (1154.43 g/mol)

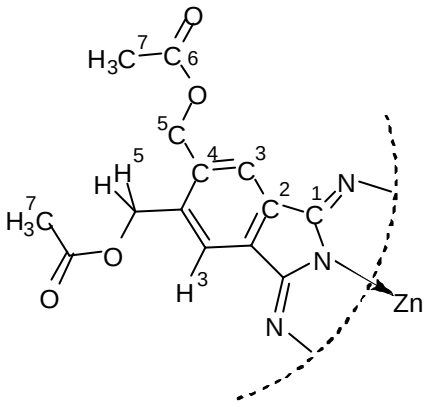

66

MS MALDI-TOF (1,8,9-anthracenetriol):
(calc. mono-isotopic 1152.2480 amu)
m/z (%): 1153.09 (100), 1154.07 (99.7), 1155.06 (87),
1152.11 (82), 1156.05 (80), 1157.05 (61),
1158.04 (33), 1159.04 (17) $[M + H]^+$.

^{1}H-NMR (400 MHz, DMSO-d_6):
δ = 8.77 (bs, 8H, H-3), 5.73 (bs, 16H, H-5), 2.33 (s, 24H, H-7).

^{13}C-NMR (100 MHz, DMSO-d_6):
δ = 170.4 (C-6), 151.2 (C-1), 136.9 (C-2), 135.5 (C-4), 122.7 (C-3), 63.9 (C-5), 20.8 (C-7).

Upon sonification, ZnPc-*op*-CH_2OH (**39**) (0.109 g, 0.133 mmol) was dissolved in dry pyridine (10.0 mL. 124 mmol), and acetic anhydride (3.0 mL, 32 mmol) was added dropwise. The mixture was stirred in the dark for 3 d at room temperature. Evaporation of the solvent and column chromatography on silica gel (gradients from PE/EA = 40:60 → EA → THF) yielded the peracetylated ZnPc derivative **66** (0.125 g, 0.108 mmol, 81% o.th.) after drying.
Alternatively, instead of column chromatography, purification was carried out by extraction with EA. The organic phase was washed with citric acid (~ pH 3) followed by sat. aq. $NaHCO_3$, sat. aq. NaCl and dried over Na_2SO_4. Evaporation yielded analytically pure **66**.

[2,3,9,10,16,17,23,24-Octakis(butyryloxymethyl)phthalocyaninato] zinc(II) (**67**)

$C_{72}H_{80}N_8O_{16}Zn$ (1378.86 g/mol)

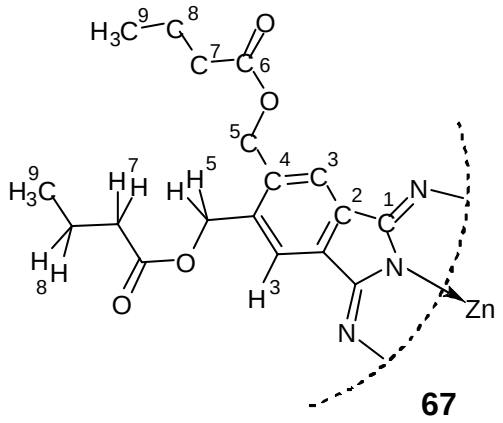

67

^{1}H-NMR (400 MHz, DMSO-d_6):

δ = 8.72 (bs, 8H, H-3), 5.74 (bs, 16H, H-5), 2.60 (t, 16H, H-7, $^3J_{H\text{-}7,H\text{-}8}$ = 7.0 – 7.3 Hz), 1.79 (sext, 16H, H-8, $^3J_{H\text{-}7,H\text{-}8}$ = $^3J_{H\text{-}8,H\text{-}9}$ = 7.3 – 7.5 Hz), 1.07 (quint, 24H, H-9, $^3J_{H\text{-}8,H\text{-}9}$ = 6.3 – 7.5 Hz).

^{13}C-NMR (100 MHz, DMSO-d_6):

δ = 172.7 (C-6), 151.1 (C-1), 136.8 (C-2), 135.5 (C-4), 122.4 (C-3), 63.8 (C-5), 35.5 (C-7), 18.1 (C-8), 13.5 (C-9).

To a sonificated solution of ZnPc-*op*-CH_2OH (**39**) (0.11 g, 0.13 mmol) in dry pyridine (10.0 mL. 124 mmol) was added dropwise butyric anhydride (2.20 mL, 13.4 mmol) and the mixture was stirred in the dark for 6 d at room temperatur. The solvent was evaporated, the remaining residue dissolved in a minimum of THF (3 mL), precipitated by dropwise addition to PE (40 mL) and centrifuged. The supernatant was discarded and the precipitate was washed with MeOH and dried under vaccuum to give the perbutyrylated ZnPc **67** (0.16 g, 0.12 mmol, 92% o.th.).

[2,3,9,10,16,17,23,24-Octakis((3-carboxypropanoyloxy)methyl) phthalocyaninato] zinc(II) (**68**)

$C_{71}H_{62}N_8O_{32}Zn$ (1604.70 g/mol)

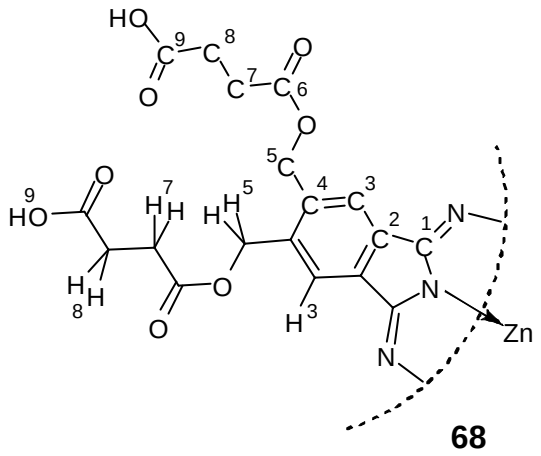

68

^{1}H-NMR (400 MHz, DMSO-d_6):

δ = 12.3 (bs, 8H, H-9), 8.96 (bs, 8H, H-3), 5.76 (bs, 16H, H-5), 2.83 (t, 16H, H-7, $^3J_{H\text{-}7,H\text{-}8}$ = 6.0 – 6.8 Hz), 2.67 (t, 16H, H-8, $^3J_{H\text{-}7,H\text{-}8}$ = 6.3 – 6.8 Hz).

^{13}C-NMR (100 MHz, DMSO-d_6):

δ = 173.4 (C-9), 172.2 (C-6), 151.7 (C-1), 137.1 (C-2), 135.8 (C-4), 123.1 (C-3), 64.1 (C-5), 28.82 (C-7), 28.77 (C-8).

Upon sonification, ZnPc-*op*-CH_2OH (**39**) (100 mg, 124 μmol) was dissolved in dry pyridine (10.0 mL, 124 mmol) and succinic anhydride (1.05 g, 10.5 mmol) was added and the mixture was stirred in the dark for 6 d at room temperature. After evaporation of the solvent, the remaining residue was washed with EA and centrifuged to remove the excess of anhydride. The residue was dissolved in a minimum of DMSO (3 mL) and dropwise added to AcN (40 mL). The precipitate thus obtained was dissolved again in DMSO (3 mL) and added dropwise to deionized water (50 mL). The mixture was lyophilized and dried in an evacuated desiccator over P_4O_{10} for 5 d to yield the target compound **68** as blue, free flowing powder (170 mg, 105 μmol, 85% o.th.).

[2,3,9,10,16,17,23,24-Octakis((*N*-butylcarbamoyloxy)methyl) phthalocyaninato] zinc(II) (**69**)

$C_{80}H_{104}N_{16}O_{16}Zn$ (1611.19 g/mol)

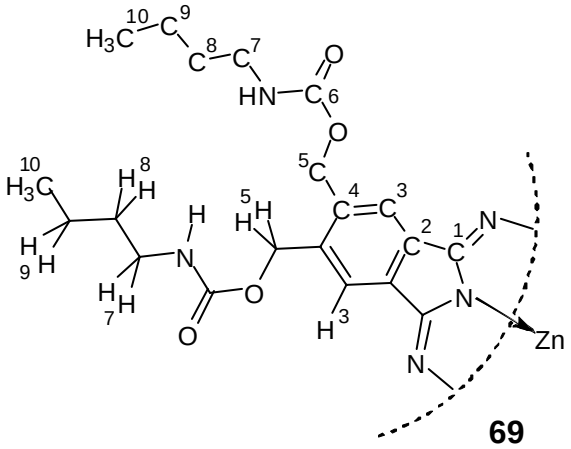

69

Mp. > 295 °C (dec.)

^{1}H-NMR (400 MHz, DMSO-d_6):

δ = 9.20 (bs, 8H, H-3), 7.59 (t, 8H, NH, $^{3}J_{NH,H-7}$ = 5.1 Hz), 5.70 (bs, 16H, H-5), 3.19 (bd, 16H, H-7, $^{3}J_{NH,H-7}$ = 5.6 Hz), 1.55 (quint, 16H, H-8, $^{3}J_{H-7,H-8}$ = $^{3}J_{H-8,H-9}$ = 6.9 – 7.1 Hz), 1.41 (sext, 16H, H-9, $^{3}J_{H-8,H-9}$ = 6.9 Hz, $^{3}J_{H-9,H-10}$ = 7.1 – 7.4 Hz), 0.92 (dd, 24H, H-10, $^{3}J_{H-9,H-10}$ = 7.1 – 7.4 Hz).

^{13}C-NMR (100 MHz, DMSO-d_6):

δ = 156.2 (C-1/C-6, *two overlapping signals*), 137.1 (C-4), 136.8 (C-2), 122.2 (C-3), 63.6 (C-5), 40.3 (C-7, *overlap with DMSO-d_6; derived from HSQC*), 31.6 (C-8), 19.5 (C-9), 13.6 (C-10).

^{1}H-NMR (400 MHz, Pyridine-d_5):

δ = 9.49 (bs, 8H, H-3), 8.09 (bs, 8H, NH), 6.20 (bs, 16H, H-5), 3.54 (bs, 16H, H-7), 1.75 (bs, 16H, H-8), 1.49 (bd, 16H, H-9, $^{3}J_{H-9,H-10}$ = 6.8 Hz), 0.92 (t, 24H, H-10, $^{3}J_{H-9,H-10}$ = 6.8 – 7.1 Hz).

^{13}C-NMR (100 MHz, Pyridine-d_5):

δ = 157.4 (C-1/C-6), 123.7 (C-3), 65.3 (C-5), 41.3 (C-7), 32.5 (C-8), 20.3 (C-9), 13.9 (C-10) (*C-2 and C-4 overlapping with pyridine-d_5 signals*).

ZnPc-*op*-CH_2OH (**39**) (0.10 g, 0.13 mmol) was dissolved in dry pyridine (10.0 mL, 124 mmol) by using ultrasound before *n*-butyl isocyanate (0.5 mL, 4.4 mmol) was added and stirred in the dark at r. t. for 4 d. Additional amounts of *n*-butyl isocyanate were added after 4 d (0.3 mL, 2.7 mmol), 7 d (0.2 mL, 1.8 mmol), and 8 d (0.2 mL, 1.8 mmol), and one equivalent DMAP (0.1 g, 0.82 mmol) was added after 5 days. According to TLC (THF), the conversion was still unsatisfactory, hence after 8 days the mixture was warmed to 50 °C for 3 d. Volatiles were removed by evaporation. The residue was dissolved in a minimum of pyridine (4 mL) by the means of ultrasound, precipitated by dropwise addition to AcN (40 mL) and centrifuged, to yield deep blue crystals of **69** (0.15 g, 0.10 mmol, 77% o.th.).

[2,3,9,10,16,17,23,24-Octakis((prop-2-ynyloxy)methyl) phthalocyaninato] zinc(II) (**70**)

$C_{64}H_{48}N_8O_8Zn$ (1122.52 g/mol)

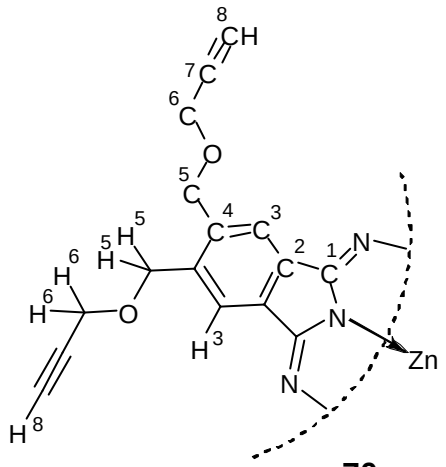

70

MS MALDI-TOF (1,8,9-anthracenetriol):
(calc. mono-isotopic 1120.2887 amu)
m/z (%): 1120.47 (100), 1122.43 (96), 1121.46 (87), 1123.41 (74), 1124.39 (73), 1125.39 (51), 1126.37 (24).

^{1}H-NMR (400 MHz, DMSO-d_6):
δ = 8.86 (bs, 8H, H-3), 5.18 (bs, 16H, H-5), 4.65 (d, 16H, H-6, $^4J_{H\text{-}6,H\text{-}8}$ = 2.3 Hz), 3.72 (t, 8H, H-8, $^4J_{H\text{-}6,H\text{-}8}$ = 2.3 Hz).

^{13}C-NMR (100 MHz, DMSO-d_6):
δ = 151.4 (C-1), 137.0 (C-4), 136.7 (C-2), 121.7 (C-3), 80.5 (C-7), 77.8 (C-8), 69.3 (C-5), 57.8 (C-6).

To a vigorously stirred solution of ZnPc-*op*-CH_2OH (**39**) (0.10 g, 0.12 mmol) in DMSO (9 mL) was added aq. NaOH (50 wt.%, 0.90 mL, 17 mmol) to form a gel-like suspension. Immediately, propargyl bromide (80 wt.% in xylene, 1.7 mL, 16 mmol) was added dropwise, and the mixture was further stirred for 3 d in the dark. The resulting suspension was diluted with THF (25 mL) and EA (75 mL), and poured into 100 mL of water. The organic phase was separated and consecutively washed with aq. 1N HCl, sat. aq. $NaHCO_3$, sat. aq. NaCl. After drying over Na_2SO_4 and concentration the crude material (450 mg) was purified by column chromatography using silica gel (PE/EA = 60:40 → EA → THF). Appropriate fractions were combined (180 mg) and evaporated. In order to remove still remaining impurities, the material was precipitated from THF in MeOH and isolated by centrifugation to yield the octakis-propargylated product **70** (72 mg, 64 μmol, 53% o.th.).

2,3,4,6-Tetra-O-acetyl-*β*-D-galactopyranosyl azide (**71**)[170]

$C_{14}H_{19}N_3O_9$ (373.32 g/mol)

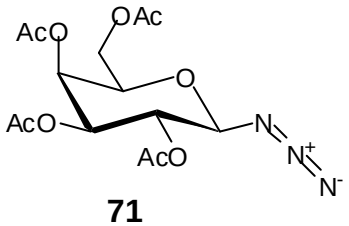

71

X-ray: successful (Figure 14)

^{1}H-NMR (400 MHz, DMSO-d_6):

δ = 5.32 (dd, 1H, H-4, $^3J_{H\text{-}3,H\text{-}4}$ = 3.6 Hz, $^3J_{H\text{-}4,H\text{-}5}$ = 1.0 Hz), 5.23 (dd, 1H, H-3, $^3J_{H\text{-}2,H\text{-}3}$ = 3.3 -3.6, $^3J_{H\text{-}3,H\text{-}4}$ = 10.3 Hz), 5.07 (d, 1H, H-1, $^3J_{H\text{-}1,H\text{-}2}$ = 8.9 Hz), 4.93 (dd, 1H, H-2, $^3J_{H\text{-}1,H\text{-}2}$ = 8.9 Hz, $^3J_{H\text{-}2,H\text{-}3}$ = 10.2 Hz), 4.35 (ddd, 1H, H-5, $^3J_{H\text{-}4,H\text{-}5}$ = 1.0 Hz, $^3J_{H\text{-}5,H\text{-}6a}$ = 5.6 Hz, $^3J_{H\text{-}5,H\text{-}6b}$ = 6.6 Hz), 4.09 (dd, 1H, H-6a, $^2J_{H\text{-}6a,H\text{-}6b}$ = 11.4 Hz, $^3J_{H\text{-}5,H\text{-}6a}$ = 5.6 Hz), 4.06 (dd, 1H, H-6b, $^2J_{H\text{-}6a,H\text{-}6b}$ = 11.4 Hz, $^3J_{H\text{-}5,H\text{-}6b}$ = 6.9 Hz), 2.13, 2.07, 2.02, 1.93 (s, 12H, 4 × -O(O)CC$\underline{H}_3$).

^{13}C-NMR (100 MHz, DMSO-d_6):

δ = 169.9 (2 × -O$\underline{C}$(O)CH_3), 169.4, 169.3 (2 × -O$\underline{C}$(O)CH_3), 86.6 (C-1), 72.1 (C-5), 69.9 (C-3), 67.8 (C-2), 67.2 (C-4), 61.4 (C-6), 20.5, 20.4, 20.33, 20.27 (4 × -OC(O)$\underline{C}H_3$).

Sodium azide (6.50 g, 100 mmol) and 2,3,4,6-tetra-*O*-acetyl-*α*-D-galactopyranosyl bromide (**79**) (13.4 g, 32.6 mmol) were suspended in dry DMF (100 mL) and stirred at 50 °C (internal glass coated thermometer) for 2 h. During heating, the internal temperature rose to 55 °C indicating an exothermic process. Evaporation to dryness (temp. ≤ 50 °C) afforded a yellowish residue, which was partitioned between chloroform (300 mL) and water (150 mL). The organic phase was separated and washed consecutively with water (150 mL), sat. aq. $NaHCO_3$, sat. aq. NaCl and dried over Na_2SO_4. After filtration and evaporation the crude pale yellow crystalline product (13 g) was recrystallized from EA/Et_2O to yield white crystals of 2,3,4,6-tetra-*O*-acetyl-*β*-D-galactopyranosyl azide (**71**) sufficiently pure for X-ray analysis (7.83 g, 21.0 mmol, 64% o.th.).

[2,3,9,10,16,17,23,24-Octakis(((*N*-1-(2,3,4,6-tetra-*O*-acetyl-*β*-D-glucopyranosyl)-1*H*-1,2,3-triazol-4-yl)methoxy)methyl) phthalocyaninato] zinc(II) (**72**)

$C_{176}H_{200}N_{32}O_{80}Zn$ (4109.05 g/mol)

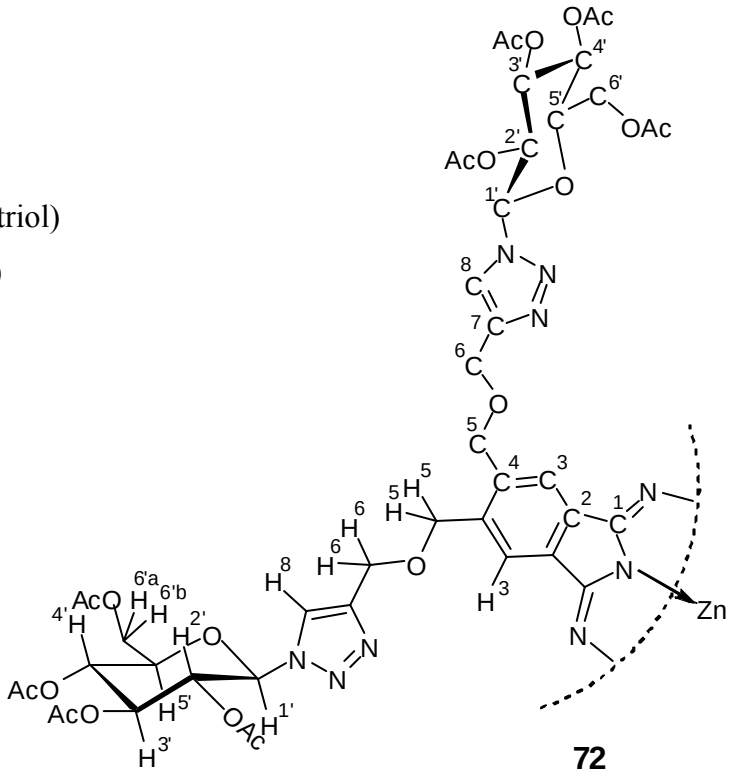

72

MS MALDI-TOF (1,8,9-anthracenetriol)

(calc. mono-isotopic 4105.1857 amu)

m/z: 4108.9 $[M]^{+\bullet}$ (Figure 60)

$[\alpha]_{546nm}^{20°C}$ = too low transmission

^{1}H-NMR (500 MHz, DMSO-d_6):

δ = 9.51 (bs, 8H, H-3), 8.66 (bs, 8H, H-8), 6.43 (d, 8H, H-1', $^{3}J_{H\text{-}1',H\text{-}2'}$ = 9.2 Hz), 5.76 (dd, 8H, H-2', $^{3}J_{H\text{-}1',H\text{-}2'} = {}^{3}J_{H\text{-}2',H\text{-}3'}$ = 9.5 Hz), 5.60 (dd, 8H, H-3', $^{3}J_{H\text{-}2',H\text{-}3'} = {}^{3}J_{H\text{-}3',H\text{-}4'}$ = 9.5 Hz), 5.21 (dd, 8H, H-4', $^{3}J_{H\text{-}3',H\text{-}4'} = {}^{3}J_{H\text{-}4',H\text{-}5'}$ = 9.8 Hz), 5.21 (bs, 16H, H-5), 4.95 (bs, 16H, H-6), 4.40 (ddd, 8H, H-5', $^{3}J_{H\text{-}4',H\text{-}5'}$ = 9.8 Hz, $^{3}J_{H\text{-}5',H\text{-}6'a}$ = 5.1 Hz, $^{3}J_{H\text{-}5',H\text{-}6'b}$ = 2.5 Hz), 4.16 (dd, 8H, H-6'a, $^{2}J_{H\text{-}6'a,H\text{-}6'b}$ = 12.3 Hz, $^{3}J_{H\text{-}5',H\text{-}6'a}$ = 5.1 – 5.7 Hz), 4.09 (bd, 8H, H-6'b, $^{2}J_{H\text{-}6'a,H\text{-}6'b}$ = 10.7 Hz), 2.02, 1.96, 1.95, 1.85 (s, 96H, 4 × -OC(O)C$\underline{H}_3$).

^{13}C-NMR (100 MHz, DMSO-d_6):

δ = 170.0, 169.5, 169.3, 168.6 (4 × -O$\underline{C}$(O)CH_3), 153.2 (C-1), 144.7 (C-7), 138.7 (C-4), 137.4 (C-2), 123.3 (C-8), 122.7 (C-3), 84.0 (C-1'), 73.3 (C-5'), 72.1 (C-3'), 70.3 (C-2'), 69.7 (C-5), 67.6 (C-4'), 63.3 (C-6), 61.7 (C-6'), 20.4, 20.3, 20.2, 19.9 (4 × -OC(O)$\underline{C}H_3$).

To a vigorously stirred solution of peralkynylated ZnPc **70** (29 mg, 26 μmol) in THF (6 mL) and EtOH (3 mL) was added consecutively $CuSO_4 \bullet 5H_2O$ (8.0 mg, 34 μmol), (+) sodium L-ascorbate (20 mg, 101 μmol) and 2,3,4,6-tetra-*O*-acetyl-β-D-glucopyranosyl azide (**60**) (220 mg, 0.60 mmol). Additional amounts of THF (3 × 2 mL) were added after 18 h, 2 d and 3 d in order to redissolve precipitated material. After 5 d of stirring in the dark at r.t. all solvents were removed and the residue (311 mg) was purified by column chromatography on silica gel (EA → THF → DMF). The combined fractions containing **72** were evaporated and the residue (120 mg) was dissolved in a minimum of THF (3 mL) and precipitated in MeOH to yield **72** after centrifugation (86 mg, 21 μmol, 81% o.th.).

[2,3,9,10,16,17,23,24-Octakis(((1-*N*-(2,3,4,6-tetra-*O*-acetyl-*β*-D-galactopyranosyl)-1*H*-1,2,3-triazol-4-yl)methoxy)methyl) phthalocyaninato] zinc(II) (**73**)

$C_{176}H_{200}N_{32}O_{80}Zn$ (4109.05 g/mol)

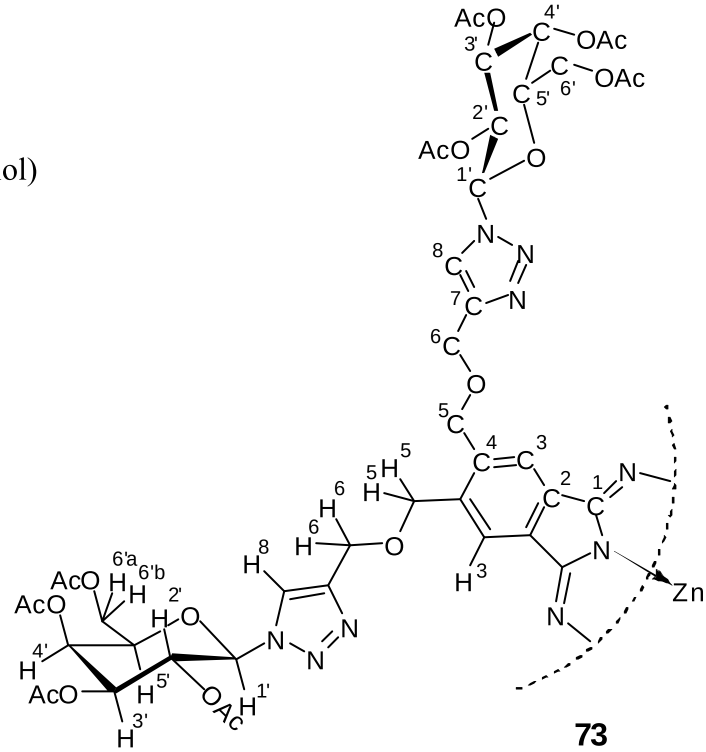

73

MS MALDI-TOF (1,8,9-anthracenetriol)

(calc. mono-isotopic 4105.1857 amu)

m/z: 4109.1 $[M]^{+\bullet}$

4132.2 $[M+Na]^{+}$ (Figure 61)

$[\alpha]_{546nm}^{20°C}$ = too low transmission

^{1}**H-NMR** (500 MHz, DMSO-d_6):

δ = 9.50 (bs, 8H, H-3), 8.59 (bs, 8H, H-8), 6.34 (d, 8H, H-1', $^{3}J_{H-1',H-2'}$ = 9.5 Hz), 5.68 (dd, 8H, H-2', $^{3}J_{H-1',H-2'}$ = $^{3}J_{H-2',H-3'}$ = 9.8 Hz), 5.50 (dd, 8H, H-3', $^{3}J_{H-2',H-3'}$ = 10.25 Hz, $^{3}J_{H-3',H-4'}$ = 3.2 – 3.5 Hz), 5.43 (bd, 8H, H-4', $^{3}J_{H-3',H-4'}$ = 2.84 Hz), 5.20 (bs, 16H, H-5), 4.95 (bs, 16H, H-6), 4.61 (dd, 8H, H-5', $^{3}J_{H-5',H-6'a}$ = 6.0 Hz, $^{3}J_{H-5',H-6'b}$ = 6.3 Hz), 4.13 (dd, 8H, H-6'a, $^{2}J_{H-6'a,H-6'b}$ = 11.5 Hz, $^{3}J_{H-5',H-6'a}$ = 4.7 – 5.0 Hz), 4.03 (dd, 8H, H-6'b, $^{2}J_{H-6'a,H-6'b}$ = 12.9 Hz, $^{3}J_{H-5',H-6'b}$ = 6.0 Hz), 2.15, 1.96, 1.93, 1.89 (s, 96H, 4 × -OC(O)C<u>H</u>$_3$).

^{13}**C-NMR** (100 MHz, DMSO-d_6):

δ = 169.9, 169.8, 169.4, 168.6 (4 × -O<u>C</u>(O)CH$_3$), 153.2 (C-1), 144.6 (C-7), 138.7 (C-4), 137.4 (C-2), 123.6 (C-8), 122.6 (C-3), 84.4 (C-1'), 72.9 (C-5'), 70.4 (C-3'), 69.6 (C-5), 67.9 (C-2'), 67.3 (C-4'), 63.1 (C-6), 61.5 (C-6'), 20.4, 20.3, 20.2, 20.0 (4 × -OC(O)<u>C</u>H$_3$).

To a vigorously stirred solution of peralkynylated ZnPc **70** (33 mg, 29 μmol) in THF (8 mL) and EtOH (4 mL) was added consecutively $CuSO_4 \bullet 5H_2O$ (17 mg, 68 μmol), (+) sodium L-ascorbate (36 mg, 180 μmol) and 2,3,4,6-tetra-*O*-acetyl-β-D-galactopyranosyl azide (**71**) (0.457 g, 1.22 mmol). A precipitate, formed after 2 d was redissolved by adding THF (2 mL). After 4 d of stirring at room temperature in the dark, the solvents were removed and the residue (611 mg) was purified by column chromatography on silica gel (EA → THF → DMF). The combined fractions containing **73** were evaporated and the residue (93 mg) was dissolved in a minimum of THF (3 mL) and precipitated in MeOH to yield **73** after centrifugation (86 mg, 21 μmol, 72% o.th.).

2,3,4,6-Tetra-*O*-acetyl-α-D-glucopyranosyl bromide (**78**)[211]

$C_{14}H_{19}BrO_9$ (411.20 g/mol)

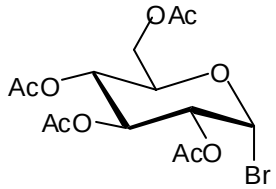

78

Mp. 89 °C (Lit.: 88 – 89 °C)[169]

$[\alpha]_{546\,nm}^{20°C}$ = +220.7 ° (c = 1, $CHCl_3$) (Lit.: $[\alpha]_{589\,nm}^{24°C}$ = +239.4 °, c = 1.2, $CHCl_3$)[211]

^{1}H-NMR (500 MHz, C_6D_6):
δ = 6.52 (d, 1H, H-1, $^3J_{H\text{-}1,H\text{-}2}$ = 4.1 Hz), 5.88 (dd, 1H, H-3, $^3J_{H\text{-}2,H\text{-}3}$ = $^3J_{H\text{-}3,H\text{-}4}$ = 9.8 Hz), 5.32 (dd, 1H, H-4, $^3J_{H\text{-}3,H\text{-}4}$ = $^3J_{H\text{-}4,H\text{-}5}$ = 9.8 Hz), 4.84 (dd, 1H, H-2, $^3J_{H\text{-}1,H\text{-}2}$ = 4.1 Hz, $^3J_{H\text{-}2,H\text{-}3}$ = 10.1 Hz), 4.29 – 4.23 (m, 2H, H-5/H-6b), 3.95 (d, 1H, H-6a, $^2J_{H\text{-}6a,H\text{-}6b}$ = 10.7 Hz), 1.72 (s, 6H, 2 × -OC(O)C$\underline{H}_3$), 1.70, 1.59 (s, 6H, 2 × -OC(O)C$\underline{H}_3$).

^{13}C-NMR (100 MHz, C_6D_6):
δ = 169.8, 169.4, 169.2, 169.1 (4 × -O$\underline{C}$(O)CH_3), 87.6 (C-1), 72.8 (C-5), 71.0 (C-2), 70.7 (C-3), 67.4 (C-4), 60.8 (C-6), 20.14, 20.12, 20.0, 19.9 (4 × -OC(O)$\underline{C}H_3$).

To a vigorously stirred solution of an anomeric mixture of peracetylated D-glucose **76** (α/β = 4:1, 67.5 g, 173 mmol) in glacial acetic acid (288 mL) was added carefully a solution of 33% hydrobromic acid in glacial acetic acid at room temperature. The yellow solution was stirred for 17 h in the dark. The clear orange solution was poured in ice-water (ca. 2.3 L), the white precipitate was filtered off and dissolved in chloroform (1 L). The filtrate was extracted with chloroform (600 mL). The combined organic phases were consecutively washed with sat. aq. $NaHCO_3$ (2 × 600 mL), dist. water (300 mL), sat. aq. NaCl (2 × 300 mL) and dried over Na_2SO_4. Filtration and evaporation (≤ 50 °C) gave the crude off-white product (69 g). Repeated recrystallization from boiling Et_2O yielded the anomerically pure bromide **78** as white, chalky solid. Column chromatography of the combined mother liquors (28 g) on silica gel (gradient from PE → EA, with 1 vol.% TEA) yielded a second crop of **78** (overall 46 g, 112 mmol, 65% o.th.).

[2,3,9,10,16,17,23,24-Octakis(((1-*N*-(*β*-D-glucopyranosyl)-1*H*-1,2,3-triazol-4-yl)methoxy)methyl)phthalocyaninato] zinc(II) (**80**)

$C_{112}H_{136}N_{32}O_{48}Zn$ (2763.87 g/mol)

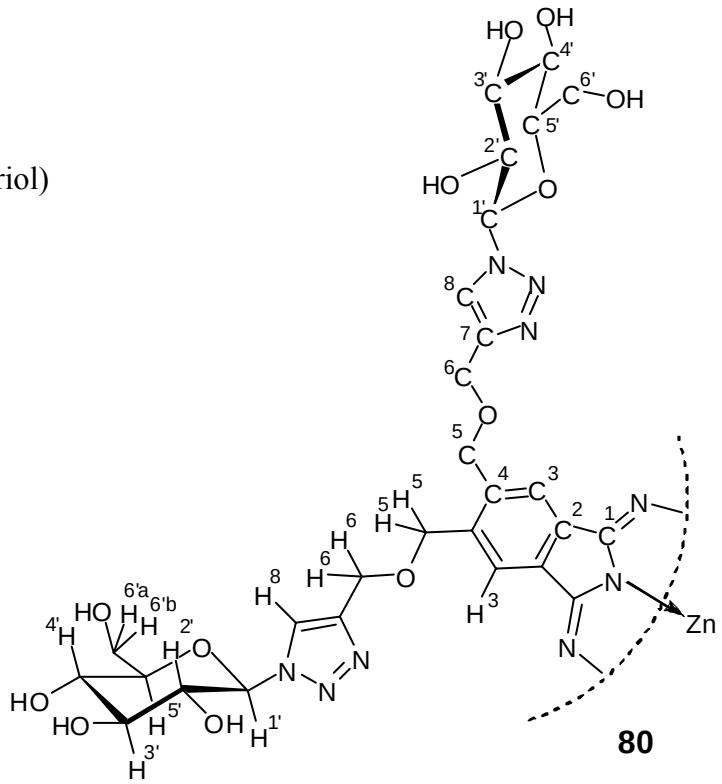

MS MALDI-TOF (1,8,9-anthracenetriol)

(calc. mono-isotopic 2760.8476 amu)

m/z:…attempts failed

HRMS-LCMS

…attempts failed

^{1}H-NMR (400 MHz, DMSO-d_6 / MeOH-d_4):

δ = 9.49 (bs, 8H, H-3), 8.54 (bs, 8H, H-8), 5.23 (bs, 16H, H-5), 4.94 (bs, 16H, H-6), 5.63 (d, 8H, H-1', $^{3}J_{H\text{-}1',H\text{-}2'}$ = 9.2 Hz), 3.87 (dd, 8H, H-2', $^{3}J_{H\text{-}1',H\text{-}2'} = {}^{3}J_{H\text{-}2',H\text{-}3'}$ = 8.9 Hz), 3.69 (d, 8H, H-6'a, $^{2}J_{H\text{-}6'a,H\text{-}6'b}$ = 10.2 Hz), 3.62 – 3.41 (m, 24H, H-5'/H-6'b/H-3'), 3.27 (dd, 8H, H-4', $^{3}J_{H\text{-}3',H\text{-}4'} = {}^{3}J_{H\text{-}4',H\text{-}5'}$ = 8.9 Hz).

^{13}C-NMR (100 MHz, DMSO-d_6):

δ = 153.2 (C-1), 143.9 (C-7), 138.8 (C-4), 137.3 (C-2), 123.62 (C-8), 123.57 (C-3), 87.6 (C-1'), 79.9 (C-5'), 76.9 (C-3'), 72.1 (C-2'), 69.8 (C-5), 69.6 (C-4'), 63.4 (C-6), 60.8 (C-6').

Deprotection was accomplished under Zemplén conditions by dissolving the peracetylated glucosyl triazole ZnPc **72** (42 mg, 10 μmol) in DMF (2 mL), followed by a freshly prepared 0.01M methanolic solution of NaOMe (15 mL, ~ pH 11). After stirring at room temperature

for 3 d in the dark, the precipitate thus formed was triturated with EA (5 mL) and isolated by centrifugation. The pellet was washed with MeOH (2 × 15 mL), sonificated in deionized water and lyophilized. Title compound **80** was isolated as a blue, voluminous solid (20 mg, 7.2 μmol, 71% o.th.).

[2,3,9,10,16,17,23,24-Octakis(((1-*N*-(*β*-D-galactopyranosyl)-1*H*-1,2,3-triazol-4-yl)methoxy)methyl)phthalocyaninato] zinc(II) (**81**)

$C_{112}H_{136}N_{32}O_{48}Zn$ (2763.87 g/mol)

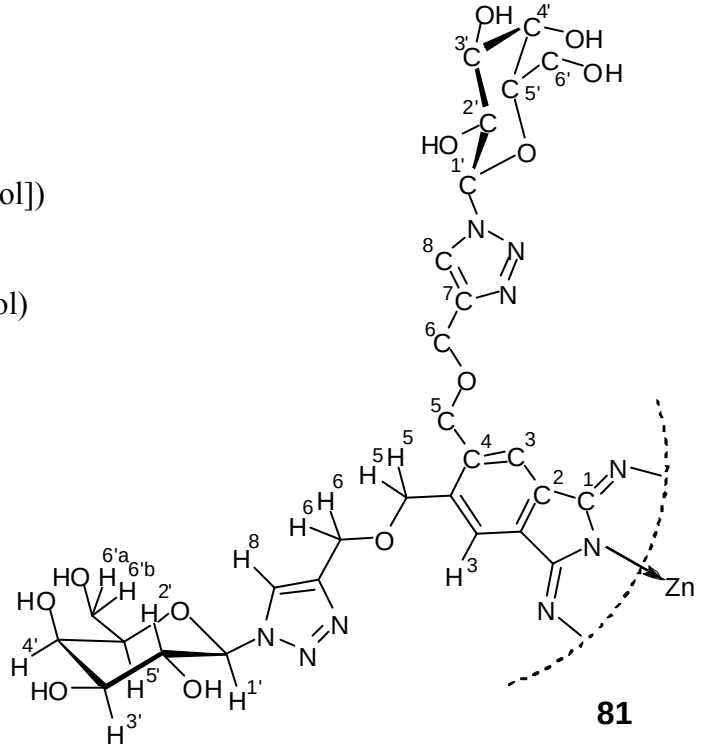

81

UV-vis (DMSO)

λ_{max} (log ε): 681 nm (2.3×10^5 [L/cm·mol])

MS MALDI-TOF (1,8,9-anthracenetriol)

(calc. mono-isotopic 2760.84762 amu)

m/z:…attempts failed

HRMS-LCMS

…attempts failed

^{1}H-NMR (400 MHz, DMSO-d_6 / MeOH-d_4):

δ = 9.48 (bs, 8H, H-3), 8.50 (bs, 8H, H-8), 5.60 (d, 8H, H-1', $^3J_{H\text{-}1',H\text{-}2'}$ = 9.0 Hz), 5.24 (bs, 16H, H-5), 4.97 (bs, 16H, H-6), 4.17 (dd, 8H, H-2', $^3J_{H\text{-}1',H\text{-}2'} = {}^3J_{H\text{-}2',H\text{-}3'}$ = 9.3 Hz), 3.81 (bd, 8H, H-4', $^3J_{H\text{-}3',H\text{-}4'}$ = 2.8 Hz), 3.77 (dd, 8H, H-5', $^3J_{H\text{-}5',H\text{-}6'a}$ = 6.0 Hz, $^3J_{H\text{-}5',H\text{-}6'b}$ = 6.3 Hz), 3.61 (dd, 8H, H-3', $^3J_{H\text{-}2',H\text{-}3'}$ = 9.4 Hz, $^3J_{H\text{-}3',H\text{-}4'}$ = 3.0 – 3.3 Hz), 3.58 – 3.54 (m, 16H, H-6'a/H-6'b).

^{13}C-NMR (100 MHz, DMSO-d_6):

δ = 153.3 (C-1), 144.0 (C-7), 138.4 (C-4), 137.1 (C-2), 123.4 (C-8), 122.7 (C-3), 88.2 (C-1'), 78.4 (C-5'), 73.7 (C-3'), 70.1 (C-5), 69.4 (C-2'), 68.8 (C-4'), 63.4 (C-6), 60.4 (C-6').

Deprotection was accomplished under Zemplén conditions by dissolving the peracetylated galactosyl triazole ZnPc **73** (55 mg, 13 μmol) in DMF (2.5 mL), followed by a freshly prepared 0.01M methanolic solution of NaOMe (20 mL, ~ pH 11). After stirring at room

temperature for 3 d in the dark, the precipitate thus formed was triturated with EA (5 mL) and isolated by centrifugation. The pellet was washed with MeOH (2 × 15 mL), sonificated in deionized water and lyophilized. Title compound **81** was isolated as a blue, voluminous solid (36 mg, 13 μmol, 99% o.th.).

2,7-Dibromo-1',3'-dihydrospiro[fluorene-9,2'-indene]-5',6'-dicarboxylic acid (**84**)

$C_{23}H_{14}Br_2O_4$ (514.16 g/mol)

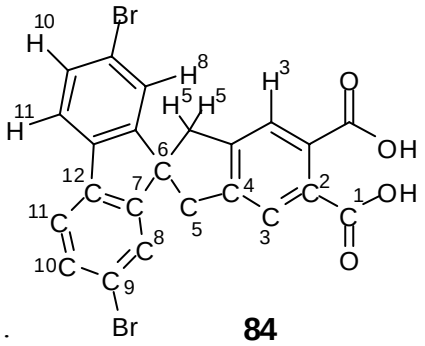

84

HRMS-FAB$^+$ (*m*-nitrobenzyl alcohol):
(calc. mono-isotopic 511.9259 amu)
m/z (%): 513.9245 (100), 511.9223 (62), 515.9145 (60) $[M]^{+\cdot}$.

^{1}H-NMR (400 MHz, DMSO-d_6):
δ = 12.99 (s, 2H, C(O)OH), 7.86 (d, 2H, H-11, $^3J_{H\text{-}10,H\text{-}11}$ = 8.1 Hz), 7.64 (s, 2H, H-3), 7.58 (dd, 2H, H-10, $^3J_{H\text{-}10,H\text{-}11}$ = 8.1 Hz, $^4J_{H\text{-}8,H\text{-}10}$ = 1.8 Hz), 7.42 (d, 2H, H-8, $^4J_{H\text{-}8,H\text{-}10}$ = 1.5 Hz), 3.43 (s, 4H, H-5).

^{13}C-NMR (100 MHz, DMSO-d_6):
δ = 168.8 (C-1), 153.3 (C-7), 145.2 (C-4), 137.2 (C-9), 132.0 (C-2), 130.8 (C-10), 125.4 (C-8), 124.5 (C-3), 122.3 (C-11), 121.0 (C-12), 57.5 (C-6), 44.0 (C-5).

To a solution of the spiro *o*-phthalaldehyde derivative **88** (10.3 g, 23.9 mmol) in glacial acetic acid (200 mL) was added sodium perborate tetrahydrate (11.1 g, 72.2 mmol) in one portion and the mixture was stirred for 36 h at 50 °C. The acetic acid was removed by evaporation under reduced pressure. The remaining white crystalline residue was first sonificated with EA (300 mL) and then dissolved in aq. 2N HCl (200 mL). The aqueous phase was extracted with EA (100 mL) and the combined organic phases were washed with sat. aq. NaCl, dried over Na_2SO_4, and concentrated to yield a yellow, solid residue. Recrystallization from boiling EA gave off-white crystals of the *o*-phthalic acid derivative **84** (8.58 g, 16.7 mmol, 78% o.th). A second crop of **84** (1.10 g, 2.13 mmol, 10% o.th) was obtained from EA/MeOH/water.

2,7-Dibromospiro[fluorene-9,6'-indeno[5,6-*c*]furan]-1',3'(5'*H*,7'*H*)-dione (**85**)

$C_{23}H_{12}Br_2O_3$ (496.15 g/mol)

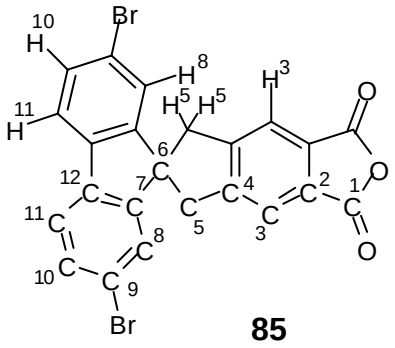

85

X-ray: successful (Figure 17)

HRMS-FAB$^+$ (*m*-nitrobenzylalcohol):
(calc. mono-isotopic 493.9153 amu)

m/z (%):495.9135 (100), 497.9177 (46), 493.9157 (44) $[M]^{\cdot+}$.

^{1}H-NMR (400 MHz, DMSO-d_6):
δ = 8.03 (s, 2H, H-3), 7.87 (d, 2H, H-11, $^3J_{H\text{-}10,H\text{-}11}$ = 8.1 Hz), 7.60 (dd, 2H, H-10, $^3J_{H\text{-}10,H\text{-}11}$ = 8.1 Hz, $^4J_{H\text{-}8,H\text{-}10}$ = 1.8 Hz), 7.47 (d, 2H, H-8, $^4J_{H\text{-}8,H\text{-}10}$ = 1.8 Hz), 3.57 (s, 4H, H-5).

^{13}C-NMR (100 MHz, DMSO-d_6):
δ = 163.3 (C-1), 152.8 (C-7), 151.8 (C-4), 137.2 (C-9), 131.0 (C-10), 130.8 (C-2), 125.4 (C-8), 122.4 (C-11), 121.3 (C-3), 121.1 (C-12), 57.5 (C-6), 44.1 (C-5).

A degassed and argon flushed suspension of the spiro *o*-phthalic acid derivative **84** (9.68 g, 18.8 mmol) in acetic anhydride (900 mL) was stirred for 23 h at 143 °C (internal glass coated thermometer) under exclusion of moisture. After cooling to 60 °C, all volatiles were removed under reduced pressure. The solid residue was washed with dry AcN and filtered to give a fine, beige, crystalline powder of **85** (8.64 g, 17.4 mmol, 93% o.th.).

2,7-Dibromo-9,9-di(prop-2-ynyl)fluorene (**86**)

$C_{19}H_{12}Br_2$ (400.11 g/mol)

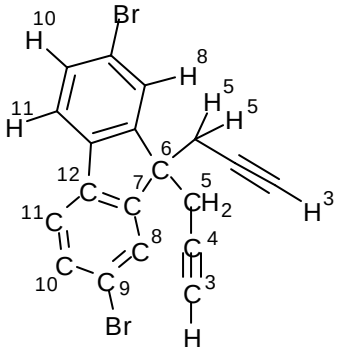

86

X-ray: successful (Figure 81)

HRMS FAB$^+$ (*m*-nitrobenzyl alcohol):
(calc. mono-isotopic 397.93058 amu)
m/z (%):399.9279 (100), 397.9297 (50), 401.9282 (50) $[M]^{+\cdot}$

^{1}H-NMR (400 MHz, DMSO-d_6):
δ = 7.93 (d, 2H, H-8, $^4J_{H\text{-}8,H\text{-}10}$ = 1.5 Hz), 7.82 (d, 2H, H-11, $^3J_{H\text{-}10,H\text{-}11}$ = 8.1 Hz), 7.58 (dd, 2H, H-10, $^3J_{H\text{-}10,H\text{-}11}$ = 8.1 Hz, $^4J_{H\text{-}8,H\text{-}10}$ = 1.8 Hz), 2.95 (d, 4H, H-5, $^4J_{H\text{-}3,H\text{-}5}$ = 2.5 Hz), 2.59 (t, 2H, H-3, $^4J_{H\text{-}3,H\text{-}5}$ = 2.5 Hz).

^{13}C-NMR (100 MHz, DMSO-d_6):
δ = 150.3 (C-7), 138.7 (C-9), 130.9 (C-10), 126.6 (C-8), 122.1 (C-11), 120.7 (C-12), 80.2 (C-4), 72.9 (C-3), 51.9 (C-6), 26.8 (C-5).

A stock solution of 2,7-dibromofluorene (23.4 g, 72.3 mmol), benzyltriethylammonium chloride (0.87 g, 3.8 mmol) and propargyl bromide 80 wt.% in xylene (24.0 mL, 216 mmol) was partitioned in 12 aliquots, sealed in screw cap vials, and sonificated for 5 minutes. To the suspensions was added aq. NaOH (50 wt.%, 10 mL each) and subjected to sonication for 12 h at 60 °C. The reaction was monitored by TLC (PE/EA = 80:20) and visualized by dipping in aqueous, basic solution of potassium permanganate. From the heterogeneous mixture, the liquid was decanted and the remaining yellow, sticky solid, collected from the reaction mixtures was dissolved in Et_2O (400 mL) and consecutively washed with aq. 2N HCl (200 mL), water (2 × 200 mL), sat. aq. NaCl and dried over Na_2SO_4. Evaporation and recrystallization from DCM yielded four crops of beige crystals **86** (26.0 g, 64.9 mmol, 90% o.th.).

(2,7-Dibromo-1',3'-dihydrospiro[fluorene-9,2'-indene]-5',6'-diyl) dimethanol (**87**)[180]

$C_{23}H_{18}Br_2O_2$ (486.20 g/mol)

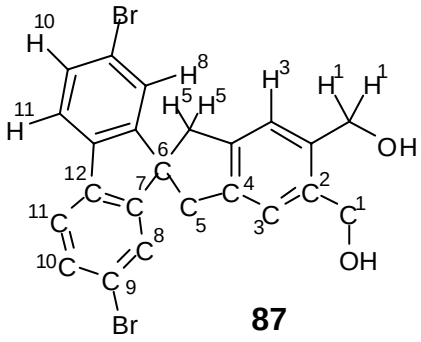

87

X-ray: successful (Figure 16)

HRMS-FAB$^+$(*m*-nitrobenzyl alcohol):
(calc. mono-isotopic 483.96736 amu)
m/z (%): 485.9657 (100), 483.9669 (58), 487.9639 (50) $[M]^{+\bullet}$.

^{1}H-NMR (400 MHz, DMSO-d_6):
δ = 7.85 (d, 2H, H-11, $^3J_{H\text{-}10,H\text{-}11}$ = 8.1 Hz), 7.56 (dd, 2H, H-10, $^3J_{H\text{-}10,H\text{-}11}$ = 8.1 Hz, $^4J_{H\text{-}8,H\text{-}10}$ = 1.8 Hz), 7.41 (d, 2H, H-8, $^4J_{H\text{-}8,H\text{-}10}$ = 1.8 Hz), 7.36 (s, 2H, H-3), 5.13 (t, 2H, -OH, $^3J_{OH,H\text{-}1}$ = 5.6 Hz), 4.59 (d, 4H, H-1, $^3J_{OH,H\text{-}1}$ = 5.3 Hz), 3.33 (s, 4H, H-5).

^{13}C-NMR (100 MHz, DMSO-d_6):
δ = 154.0 (C-7), 140.0 (C-4), 138.3 (C-2), 137.2 (C-9), 130.5 (C-10), 125.2 (C-8), 122.9 (C-3), 122.2 (C-11), 120.9 (C-12), 60.4 (C-1), 57.6 (C-6), 44.2 (C-5).

A suspension of 9,9-dipropargyl-2,7-dibromofluorene (**86**) (23.0 g, 57.5 mmol) and but-2-yn-1,4-diol (40.0 g, 465 mmol) in absolute EtOH (2.0 L) was degassed by consecutive evacuation and flushing with argon (3 cycles). Upon warming to 70 °C (internal temperature), the suspension dissolved to a pale yellow solution. At this temperature tris(triphenylphosphin)Rh(I)chloride (3.7 g, 4.0 mmol, 7 mol%) – Wilkinson's catalyst – from a freshly opened vial was added quickly. After 24 h at 73 °C under exclusion of moisture, a second portion of catalyst (0.36 g, 0.39 mmol, 3.2 mol%) was added and stirring continued for further 24 h at 70 – 73 °C under exclusion of moisture, until TLC monitoring indicated the consumption of the starting diyne **86** visualized by dipping in aqueous, basic solution of potassium permanganate. After removal of the solvent, the residue was dissolved in a minimum of boiling DCM. Excessive but-2-yn-1,4-diol (30 g) precipitated after slow cooling

to room temperature and storage in a fridge (at 0 °C) over night and was removed by suction. The mother liquor was evaporated and subjected to column chromatography on silica gel (gradient from PE → 40% EA). The product containing fractions were combined. Evaporation of the solvent and recrystallization from EA gave four crops of the spiro derivative **87** appropriate for X-ray analysis (12.8 g, 26.3 mmol, 46% o.th.).

2,7-Dibromo-1',3'-dihydrospiro[fluorene-9,2'-indene]-5',6'-dicarbaldehyde (**88**)

$C_{23}H_{14}Br_2O_2$ (482.16 g/mol)

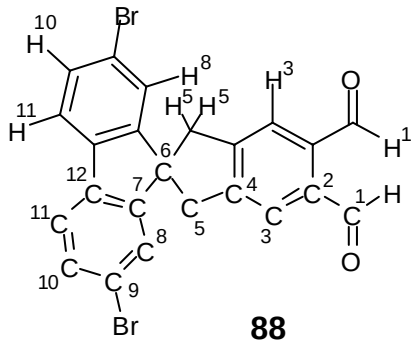

88

MS-FAB$^+$ (*m*-nitrobenzyl alcohol):
(calc. mono-isotopic 479.93605 amu)
m/z (%): 483.0 (100), 481.0 (56), 485.0 (42) $[M+H]^+$

^{1}H-NMR (400 MHz, DMSO-d_6):
δ = 10.54 (s, 2H, H-1), 7.98 (s, 2H, H-3), 7.87 (d, 2H, H-11, $^3J_{H\text{-}10,H\text{-}11}$ = 8.1 Hz), 7.59 (dd, 2H, H-10, $^3J_{H\text{-}10,H\text{-}11}$ = 8.1 Hz, $^4J_{H\text{-}8,H\text{-}10}$ = 1.8 Hz), 7.43 (d, 2H, H-8, $^4J_{H\text{-}8,H\text{-}10}$ = 1.5 Hz), 3.54 (s, 4H, H-5).

^{13}C-NMR (100 MHz, DMSO-d_6):
δ = 192.8 (C-1), 153.1 (C-7), 148.9 (C-4), 137.3 (C-9), 136.0 (C-2), 130.9 (C-10), 126.0 (C-3), 125.5 (C-8), 122.5 (C-11), 121.1 (C-12), 57.4 (C-6), 44.3 (C-5).

According to the procedure of Farooq, a solution of oxalyl chloride (6.6 mL, 78 mmol) in DCM (51 mL) was cooled to -78 °C and a solution of DMSO (13 mL, 183 mmol) in DCM (55 mL) was added dropwise over a periode of 25 minutes. Stirring was continued for 5 minutes and a solution of the spiro derivative **87** (11.3 g, 23.3 mmol) in a mixture of DCM (328 mL) and DMSO (23 mL) was added dropwise over a period of 90 minutes. After completion stirring was continued for 90 minutes at -78 °C, followed by addition of TEA (60 mL, 430 mmol). The stirred reaction mixture was then allowed to reach room temperature over night. The yellow heterogeneous mixture was dissolved in chloroform (400 mL) and consecutively washed with aq. 2N HCl (200 mL), aq. 1N HCl (200 mL), dist. water (200 mL), sat. aq. NaCl, dried over Na_2SO_4 and concentrated to a solid residue (11.5 g). Recrystallization from EA gave two crops of **88** as fine, beige, crystalline solid (10.3 g, 23.9 mmol, 92% o.th.).

2',7'-Dibromo-5,7-dihydro-1*H*-spiro[cyclopenta[*f*]isoindole-6,9'-fluorene]-1,3(2*H*)-dione (**89**)

$C_{23}H_{13}Br_2NO_2$ (495.16 g/mol)

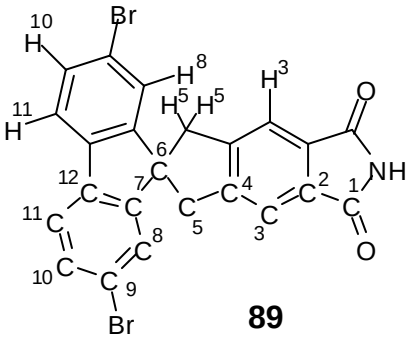

89

^{1}H-NMR (400 MHz, DMSO-d_6):

δ = 11.28 (bs, 1H, NH), 7.86 (d, 2H, H-11, $^3J_{H\text{-}10,H\text{-}11}$ = 8.1 Hz), 7.76 (s, 2H, H-3), 7.58 (dd, 2H, H-10, $^3J_{H\text{-}10,H\text{-}11}$ = 8.1 Hz, $^4J_{H\text{-}8,H\text{-}10}$ = 1.8 Hz), 7.45 (d, 2H, H-8, $^4J_{H\text{-}8,H\text{-}10}$ = 1.8 Hz), 3.50 (s, 4H, H-5).

^{13}C-NMR (125 MHz, DMSO-d_6):

δ = 130.7 (C-10), 125.0 (C-8), 122.5 (C-11), 119.2 (C-3), 44.0 (C-5).

Signals were obtained from an edited HSQC spectra.

The substance was isolated in analytical amouts (20 mg) during the chromatographic purification of the fluorenyl spiro-annelated ZnPc **90**.

{Tetrakis[2',7'-dibromo-1,3-dihydrospiro[fluorene-9',2-indeno]][5,6-*b*:5',6'-*g*:5'',6''-*l*:5''',6'''-*q*]-5,10,15,20-tetraazaporphyrinato} zinc(II) (**90**)

$C_{92}H_{48}Br_8N_8Zn$ (1970.06 g/mol)

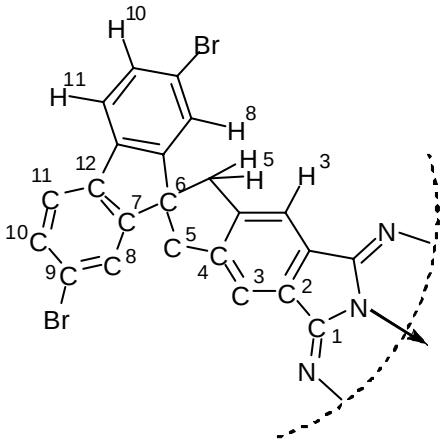

90

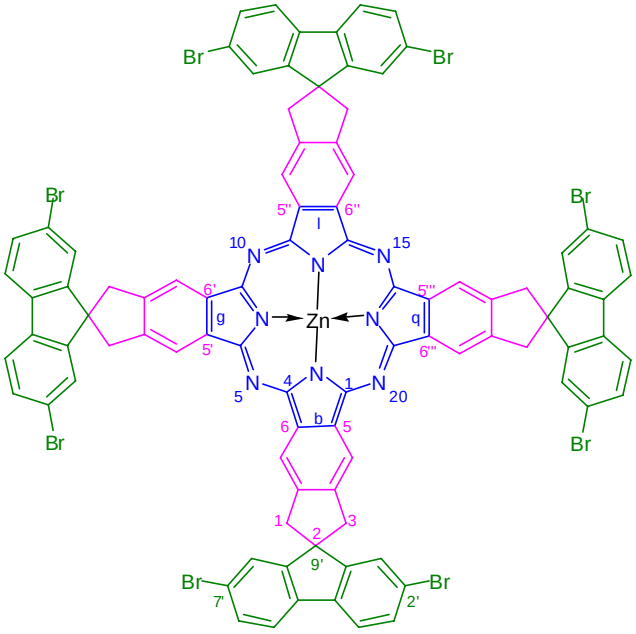

Figure 39 **Numbering according the IUPAC-nomenclatur for 5,10,15,20-tetraazaporphyrins (blue).**

MS MALDI-TOF (1,8,9-anthracenetriol)

(calc. mono-isotopic 1959.6760 amu)

m/z (%): 1970.0 (100), 1968.0 (92),1969.0 (91), 1971.0 (86), 1972.0 (82), 1967.1 (66), 1973.0 (64), 1966.1 (60), 1973.9 (51), 1974.9 (33), 1965.1 (32), 1964.1 (24), 1975.9 (23), 1976.9 (14) $[M]^{+\bullet}$

1890.0 (27), 1891.0 (26), 1892.0 (24), 1888.1 (23), 1889.0 (23), 1893.0 (21), 1894.0 (18), 1887.1 (17), 1886.1 (15), 1895.0 (15), 1896.0 (12) $[M - Br]^+$ (Figure 62).

Mp. > 360 °C

^{1}H-NMR (400 MHz, 1,4-dioxane/DMSO-d_6, 2:1):

δ = 9.18 (s, 8H, H-3), 7.92 – 7.65 (m, 24H, H-8, H-10, H-11).

Due to solvent suppression technique signals close to 1,4-dioxane could not be detected.

^{1}H-NMR (400 MHz, THF-d_8):
δ = 9.38 (s, 8H, H-3), 7.92 (bs, 8H, H-8), 7.74 (d, 8H, H-11, $^{3}J_{H\text{-}10,H\text{-}11}$ = 8.3 Hz), 7.54 (d, 8H, H-10, $^{3}J_{H\text{-}10,H\text{-}11}$ = 8.1 Hz), 4.05 (s, 16H, H-5).

^{1}H-NMR (300 MHz, Dioxan-d_8):
δ = 9.20 (s, 8H, H-3), 7.73 (m_c, 8H, H-8), 7.65 (m_c, 8H, H-11), 7.50 (m_c, 8H, H-10), 4.15 (s, 16H, H-5).

^{13}C-NMR (100 MHz, DMSO-d_6/THF-d_8)
δ = 130.2 (C-10), 121.8 (C-11), 118.4 (C-3), 44.6 (C-5).
Shifts were obtained from an HSQC experiment.

^{13}C-NMR (100 MHz, THF-d_8)
δ = 131.7 (C-10), 126.2 (C-8), 122.2 (C-11), 119.5 (C-3), 46.1 (C-5).
Shifts were obtained from an HSQC experiment (Figure 53).

A screw cap vial was charged in the following order: Fluorenyl spiro-annelated *o*-phthalic anhydride **85** (2.02 g, 4.06 mmol), HMDS (5.50 mL, 26.4 mmol), DMF (0.32 mL, 4.13 mmol), $Zn(OAc)_2$ (0.21 g, 1.1 mmol) and *p*-TsOH•H_2O (0.09 mg, 0.46 mmol). A vigorous stream of argon was bubbled through the stirred suspension before the vial was sealed and placed in a pre-heated (100 °C) aluminum block when the temperture was rised to 130 °C. The mixture was stirred at this temperature for 10 h. The pressurized, sealed vial was carefully opened after cooling to ambient temperature. The sticky dark solid formed was redissolved in DCM, evaporated to dryness, and recharged with DMF (6.0 mL, 77 mmol), HMDS (7.0 mL, 34 mmol), $Zn(OAc)_2$ (0.196 g, 1.07 mmol) and *p*-TsOH•H_2O (0.16 g, 0.83 mmol) in a tube. The tube was argon flushed and sealed, and after 48 hours at 130 °C a biphasic mixture was formed. The upper colorless, clear phase was discarded and the lower black phase was evaporated to dryness giving a dark residue (3.88 g) which was subjected to meticulous column chromatography on silica gel.
Evaporation of the corresponding fractions afforded a blue-green residue, which was dissolved in a minimum of THF and precipitated by dropwise addition into a mixture of

EA/MeOH/THF (40:40:20). Filtration and washing with this solvent mixture yielded the fluorenyl spiro-annelated ZnPc **90** in a spectroscopically pure form (0.440 g, 0.223 mmol, 22% o.th.).

2,7-Dinitro-9,9-di(prop-2-ynyl)fluorene (**91**)

$C_{19}H_{12}N_2O_4$ (332.31 g/mol)

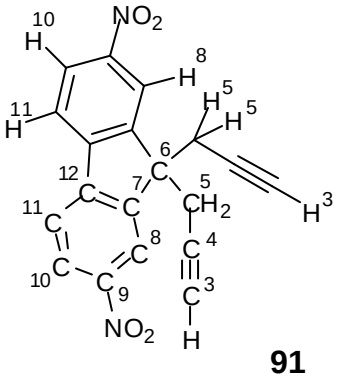

91

FAB$^+$-HRMS (*m*-nitrobenzyl alcohol):
(calc. mono-isotopic 332.0797 amu)
m/z: 333.0881 $[M+H]^+$

R_f = 0.68 (PE/EA = 60:40)

Mp. >268 °C (dec.)

^{1}H-NMR (400 MHz, DMSO-d_6):
δ = 8.74 (d, 2H, H-8, $^4J_{H\text{-}8,H\text{-}10}$ = 2.0 Hz), 8.39 (dd, 2H, H-10, $^3J_{H\text{-}10,H\text{-}11}$ = 8.4 Hz, $^4J_{H\text{-}8,H\text{-}10}$ = 2.0 - 2.3 Hz), 8.33 (d, 2H, H-11, $^3J_{H\text{-}10,H\text{-}11}$ = 8.5 Hz), 3.19 (d, 4H, H-5, $^4J_{H\text{-}3,H\text{-}5}$ = 2.5 Hz), 2.57 (t, 2H, H-3, $^4J_{H\text{-}3,H\text{-}5}$ = 2.5 Hz).

^{13}C-NMR (100 MHz, DMSO-d_6):
δ = 151.1 (C-7), 147.9 (C-9), 144.6 (C-12), 124.3 (C-10), 122.6 (C-11), 119.0 (C-8), 79.7 (C-4), 73.2 (C-3), 53.0 (C-6), 26.4 (C-5).

2,7-Dinitrofluorene (10.5 g, 41.1 mmol), benzyltriethylammonium chloride (0.50 g, 2.2 mmol) and propargyl bromide (80 wt.% in xylene, 16.8 mL, 151 mmol) was subdivided into seven screw cap vials and sonificated for 5 minutes. To the suspensions was added aqueous NaOH (50 wt.%, 10 mL each). The vials were sealed and sonification was continued for 5.5 h while the water of the ultrasound bath reached 58 °C without additional heating. The reaction was monitored by TLC (PE/EA = 60:40) and visualized by dipping in aqueous, basic solution of potassium permanganate. The heterogeneous mixture was decanted and the remaining yellow-green, sticky solid was dissolved in EA (700 mL) and consecutively washed with aq. 2N HCl (2 × 200 mL), water (2 × 200 mL), sat. aq. NaCl and dried over Na_2SO_4. The solution was evaporated to a small volume to give an opaque, brown solution,

which was treated with charcoal (10 g) at 70 °C for 10 minutes. Hot filtration over a plug of Na_2SO_4 on a sintered glass frit gave a clear, yellow solution. Evaporation and recrystallization from boiling EA yielded orange crystals of **91** (9.40 g, 28.3 mmol, 69% o.th.).

(2,7-Dinitro-1',3'-dihydrospiro[fluorene-9,2'-indene]-5',6'-diyl) dimethanol (**92**)

$C_{23}H_{18}N_2O_6$ (418.12 g/mol)

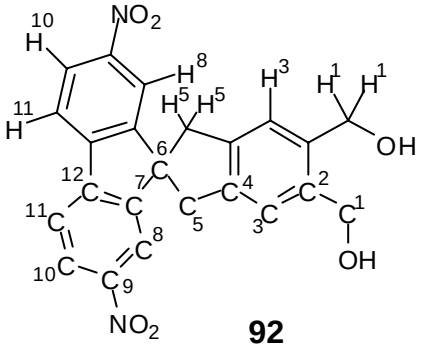

92

R_f = 0.46 (PE/EA = 40:60)

R_f = 0.13 (PE/EA = 60:40)

Mp. >263 °C (dec.)

^{1}H-NMR (400 MHz, DMSO-d_6):

δ = 8.34(3 (dd, 2H, H-10, $^3J_{H\text{-}10,H\text{-}11}$ = 8.5 Hz, $^4J_{H\text{-}8,H\text{-}10}$ = 1.6 – 1.7 Hz), 8.342 (dd, 2H, H-11, $^3J_{H\text{-}10,H\text{-}11}$ = 8.6 Hz, $^5J_{H\text{-}8,H\text{-}11}$ = 0.8 – 1.2 Hz), 8.16 (dd, 2H, H-8, $^4J_{H\text{-}8,H\text{-}10}$ = 1.6 Hz, $^5J_{H\text{-}8,H\text{-}11}$ = 1.1 Hz), 7.40 (s, 2H, H-3), 5.15 (t, 2H, -OH, $^3J_{\text{-}OH,H\text{-}1}$ = 5.3 – 5.6 Hz), 4.61 (d, 4H, H-1, $^3J_{\text{-}OH,H\text{-}1}$ = 5.3 Hz), 3.48 (s, 4H, H-5).

^{13}C-NMR (100 MHz, DMSO-d_6):

δ = 154.6 (C-7), 148.0 (C-9), 143.1 (C-12), 139.6 (C-4), 138.5 (C-2), 123.9 (C-10), 122.9 (C-3), 122.8 (C-11), 117.7 (C-8), 60.3 (C-1), 58.0 (C-6), 43.8 (C-5).

A suspension of 9,9-dipropargyl-2,7-dinitrofluorene (**91**) (9.04 g, 27.2 mmol) and but-2-yn-1,4-diol (18.8 g, 219 mmol) in absolute EtOH (1.5 L) was degassed by evacuation and flushing with argon (3 cycles). Heating to 70 °C (internal temperature) gave a clear yellow solution. At this temperature tris(triphenylphosphin)Rh(I) chloride (2.7 g, 2.9 mmol, 11 mol%) – Wilkinson's catalyst – was added quickly and stirring continued for 2 d at 70–73 °C under exclusion of moisture until TLC indicated the consumption of the but-2-yn-1,4-diol (detected by dipping in aqueous, basic solution of potassium permanganate). After removal of the solvent, the residue was dissolved in a minimum of boiling DCM, and cooled very slow to room temperature. Storage in a fridge over night precipitated most of the excess of but-2-yn-1,4-diol (11 g). The filtrate was evaporated and the residue washed with cold MeOH. Repeated recrystallization from boiling MeOH after storage at 0 °C yielded several

crops of the [2+2+2] cycloaddition product **92** as yellow crystalline solid (combined 3.83 g, 9.15 mmol, 34% o.th.). Analytical samples were obtained from column chromatography on silica gel (gradient from PE/EA = 60:40 → 100% EA).

2,7-Dinitro-1',3'-dihydrospiro[fluorene-9,2'-indene]-5',6'-dicarbaldehyde (**93**)

$C_{23}H_{14}N_2O_6$ (414.37 g/mol)

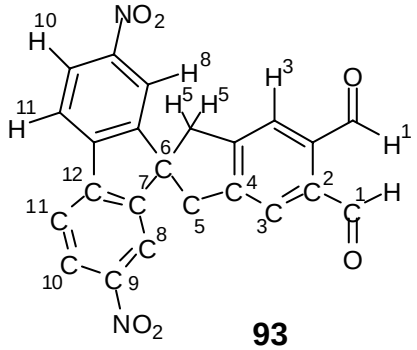

93

R_f = 0.78 (PE/EA, 40:60)

R_f = 0.50 (PE/EA, 60:40)

R_f = 0.28 ($CHCl_3$)

Mp. >275 °C (dec.)

^{1}H-NMR (400 MHz, DMSO-d_6):

δ = 10.58 (s, 2H, H-1), 8.368 (dd, 2H, H-10, $^3J_{H\text{-}10,H\text{-}11}$ = 8.5 Hz, $^4J_{H\text{-}8,H\text{-}10}$ = 1.7 Hz), 8.366 (dd, 2H, H-11, $^3J_{H\text{-}10,H\text{-}11}$ = 8.5 Hz, $^5J_{H\text{-}8,H\text{-}11}$ = 1.1 Hz), 8.20 (dd, 2H, H-8, $^4J_{H\text{-}8,H\text{-}10}$ = 1.6 Hz, $^5J_{H\text{-}8,H\text{-}11}$ = 1.0 – 1.1 Hz), 8.02 (s, 2H, H-3), 3.69 (s, 4H, H-5).

^{13}C-NMR (100 MHz, DMSO-d_6):

δ = 192.8 (C-1), 153.7 (C-7), 148.6 (C-4), 148.1 (C-9), 143.1 (C-12), 136.1 (C-2), 126.0 (C-3), 124.2 (C-10), 122.9 (C-11), 118.0 (C-8), 57.7 (C-6), 43.8 (C-5).

According to the procedure of Farooq, a solution of oxalyl chloride (2.80 mL, 33.1 mmol) in DCM (22 mL) was cooled to -78 °C and a solution of DMSO (5.60 mL, 78.8 mmol) in DCM (25 mL) was added dropwise over a periode of 20 minutes. Stirring was continued for 5 minutes and a solution of the spiro derivative **92** (3.70 g, 8.84 mmol) in a mixture of DCM (140 mL) and DMSO (20 mL) was added dropwise over a period of 90 minutes. After completion stirring was continued for 90 minutes at -78 °C followed by addition of TEA (23.0 mL, 165 mmol). The stirred reaction was allowed to reach room temperature over night. The yellow heterogeneous mixture was dissolved in chloroform (1400 mL) and was consecutively washed with aq. 2N HCl (300 mL), aq. 1N HCl (300 mL), dist. water (300 mL), sat. aq. NaCl, dried over Na_2SO_4 and concentrated to a solid residue (3.73 g). Leaching with a minimum of AcN by the means of ultrasound and filtration gave two crops of fine, beige

crystalline solid **93** (2.93 g, 7.08 mmol, 80% o.th.). For NMR spectroscopy, a sample was purified on silica gel (gradient from PE → 60% EA).

2,7-Dinitro-1',3'-dihydrospiro[fluorene-9,2'-indene]-5',6'-dicarboxylic acid (**94**)

$C_{23}H_{14}N_2O_8$ (446.37 g/mol)

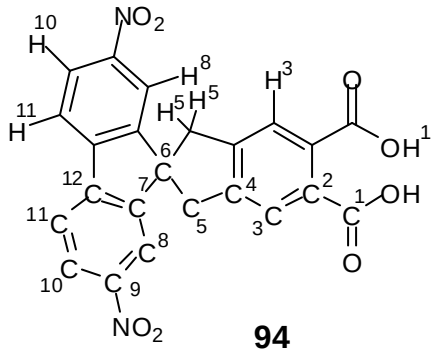

94

HRMS-FAB$^+$(*m*-nitrobenzyl alcohol):
(calc. mono-isotopic 446.0750 amu)
m/z: …failed

HRMS-LCMS:
m/z: …negative mode failed

Mp. >277 °C (dec.)

^{1}H-NMR (400 MHz, DMSO-d_6):
δ = 13.07 (bs, 2H, H-1), 8.35(7) (dd, 2H, H-10, $^3J_{H\text{-}10,H\text{-}11}$ = 8.5 Hz, $^4J_{H\text{-}8,H\text{-}10}$ = 1.7 – 1.8 Hz), 8.35(4) (dd, 2H, H-11, $^3J_{H\text{-}10,H\text{-}11}$ = 8.5 Hz, $^5J_{H\text{-}8,H\text{-}11}$ = 1.0 – 0.9 Hz), 8.19 (dd, 2H, H-8, $^4J_{H\text{-}8,H\text{-}10}$ = 1.7 Hz, $^5J_{H\text{-}8,H\text{-}11}$ = 1.0 – 0.9 Hz), 7.68 (s, 2H, H-3), 3.58 (s, 4H, H-5).

^{13}C-NMR (100 MHz, DMSO-d_6):
δ = 168.8 (C-1), 153.9 (C-7), 148.0 (C-9), 144.9 (C-4), 143.1 (C-12), 132.2 (C-2), 124.6 (C-3), 124.1 (C-10), 122.9 (C-11), 117.9 (C-8), 57.8 (C-6), 43.5 (C-5).

To a solution of the spiro *o*-phthalaldehyde derivative **93** (2.93 g, 7.08 mmol) in glacial acetic acid (70 mL) was added sodium perborate tetrahydrate (3.97 g, 25.8 mmol) in one portion and the mixture was stirred for 29 h at 50 °C. The acetic acid was removed by evaporation under reduced pressure. The remaining white crystalline residue was first sonificated with EA (700 mL) and dissolved in aq. 2N HCl (200 mL). The aqueous phase was extracted with EA (100 mL) and the combined organic phases were washed with sat. aq. NaCl, and dried over Na_2SO_4. Evaporation yielded a yellow-brown solid residue (3.10 g). Sonification in AcN and filtration gave **94** as a pale yellow crystalline solid (2.77 g, 6.20 mmol, 88% o.th).

2,7-Dinitrospiro[fluorene-9,6'-indeno[5,6-*c*]furan]-1',3'(5'*H*,7'*H*)-dione (**95**)

$C_{23}H_{12}N_2O_7$ (428.35 g/mol)

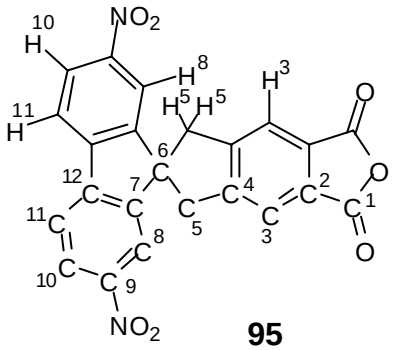

95

Mp. 282 °C (dec.)

^{1}H-NMR (400 MHz, DMSO-d_6):

δ = 8.37(3) (dd, 2H, H-10, $^3J_{H\text{-}10,H\text{-}11}$ = 8.4 Hz, $^4J_{H\text{-}8,H\text{-}10}$ = 1.6 Hz), 8.37(0) (dd, 2H, H-11, $^3J_{H\text{-}10,H\text{-}11}$ = 8.5 Hz, $^5J_{H\text{-}8,H\text{-}11}$ = 0.9 – 1.0 Hz), 8.22 (dd, 2H, H-8, $^4J_{H\text{-}8,H\text{-}10}$ = 1.7 Hz, $^5J_{H\text{-}8,H\text{-}11}$ = 0.9 – 1.0 Hz), 8.08 (s, 2H, H-3), 3.72 (s, 4H, H-5).

^{13}C-NMR (100 MHz, DMSO-d_6):

δ = 163.2 (C-1), 153.4 (C-7), 151.5 (C-4), 148.1 (C-9), 143.0 (C-12), 130.8 (C-2), 124.2 (C-10), 122.9 (C-11), 121.4 (C-3), 118.0 (C-8), 57.7 (C-6), 43.7 (C-5).

A degassed and argon flushed suspension of the spiro *o*-phthalic acid derivative **94** (2.57 g, 5.75 mmol) in acetic anhydride (300 mL) was stirred for 27 h at 141 °C (internal glass coated thermometer) under exclusion of moisture. After cooling to 60 °C, all volatiles were removed under reduced pressure. The solid residue was washed with dry AcN and filtered to give the anhydride **95** as beige, fine needles (2.07 g, 4.84 mmol, 84% o.th.).

ANALYTICAL DATA OF NOVEL PCS

NMR SPECTRA

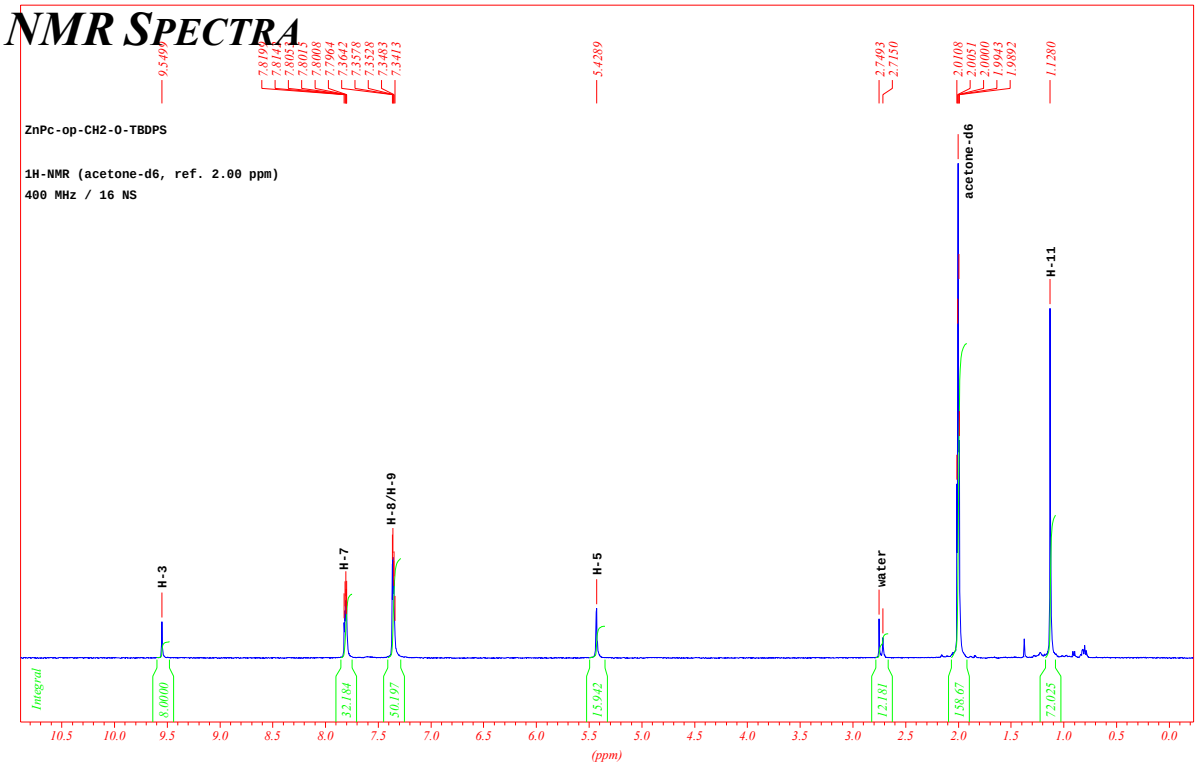

Figure 40 **^{1}H-NMR spectrum of ZnPc-*op*-CH$_2$OTBDPS (33) (proton assignment p. 113).**

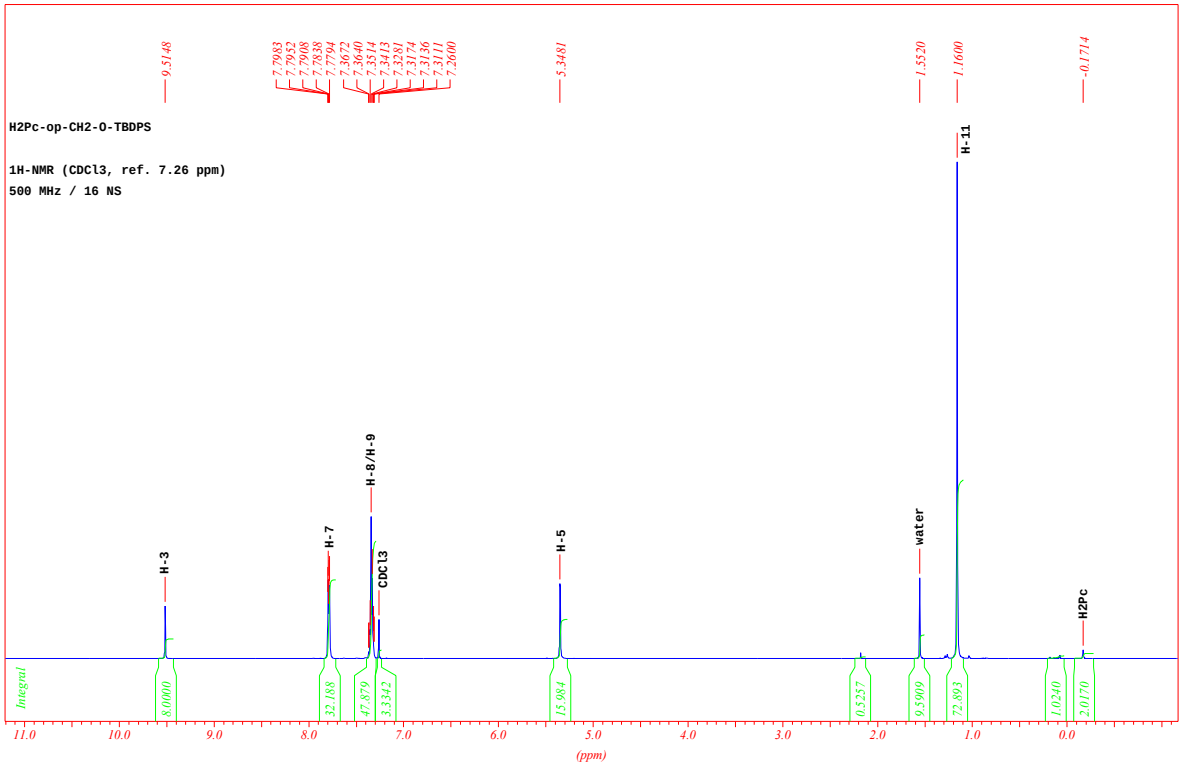

Figure 41 **^{1}H-NMR spectrum of H$_2$Pc-*op*-CH$_2$OTBDPS (35) (proton assignment p. 115)[187]**

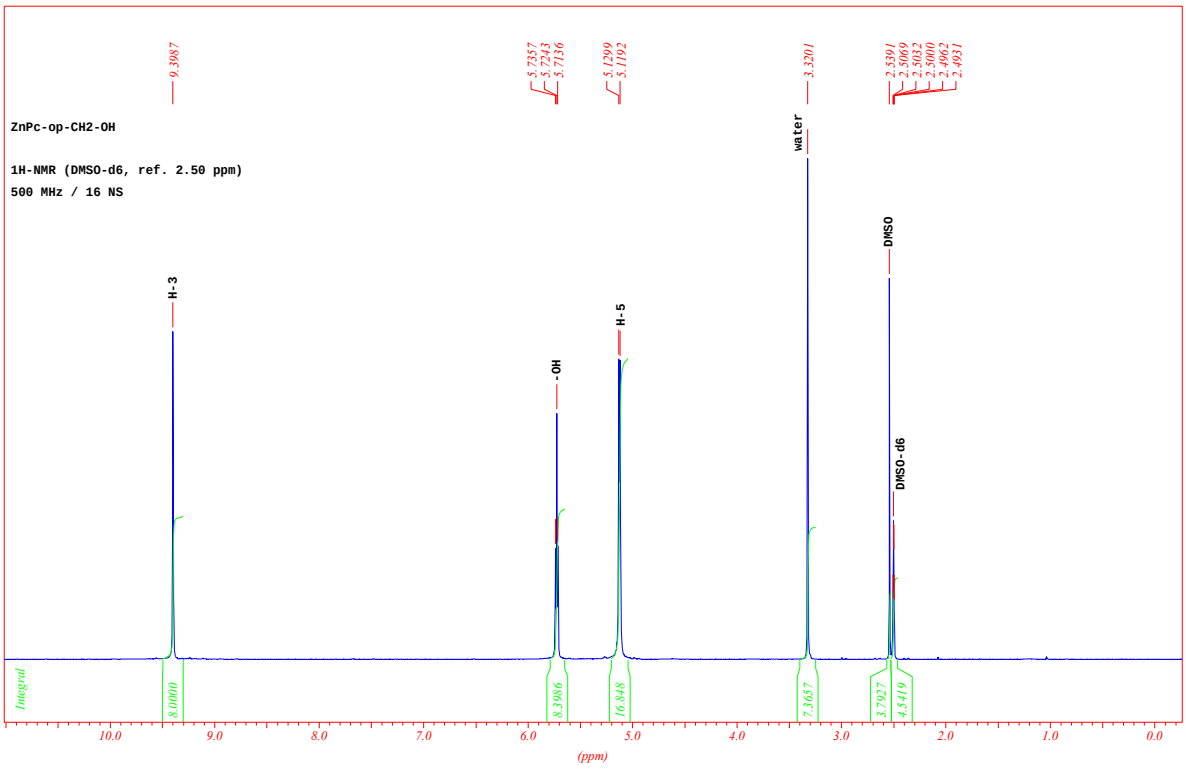

Figure 42 **^{1}H-NMR spectrum of ZnPc-*op*-CH_2OH (39) (proton assignment p. 117).**

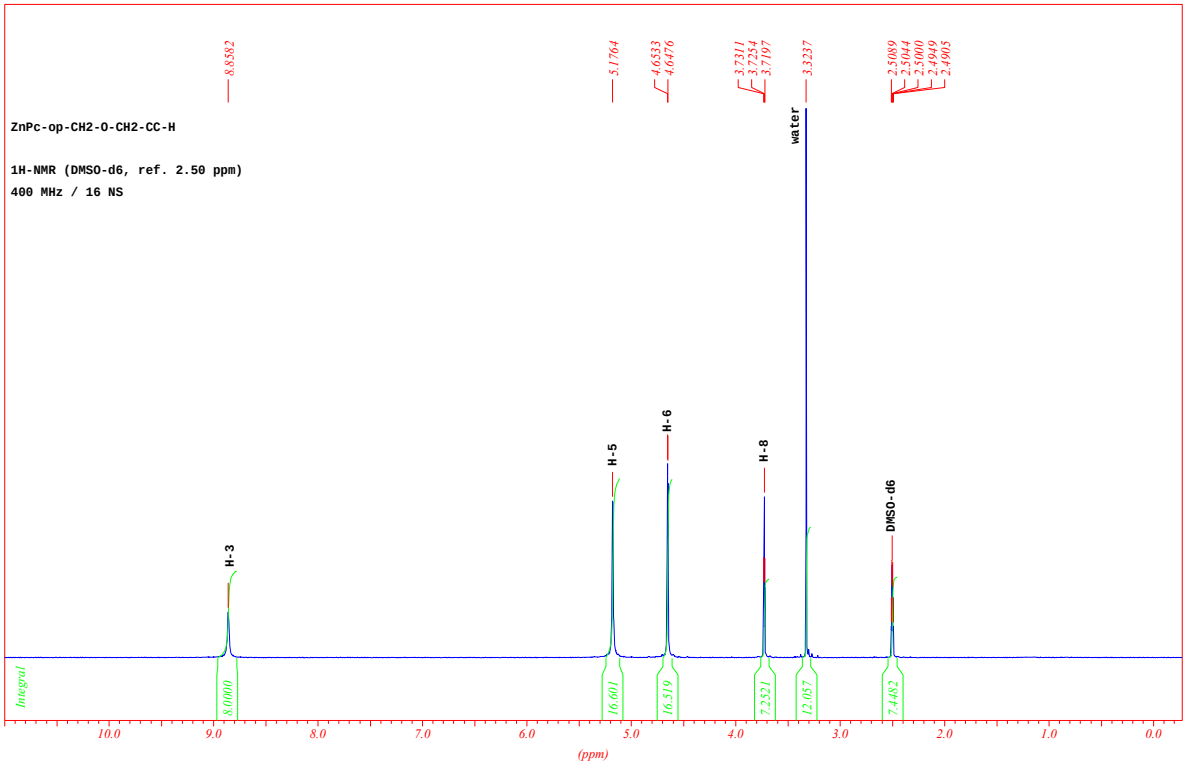

Figure 43 **^{1}H-NMR spectrum of ZnPc-*op*-$CH_2OCH_2C{\equiv}CH$ (70) (proton assignment p. 147).**

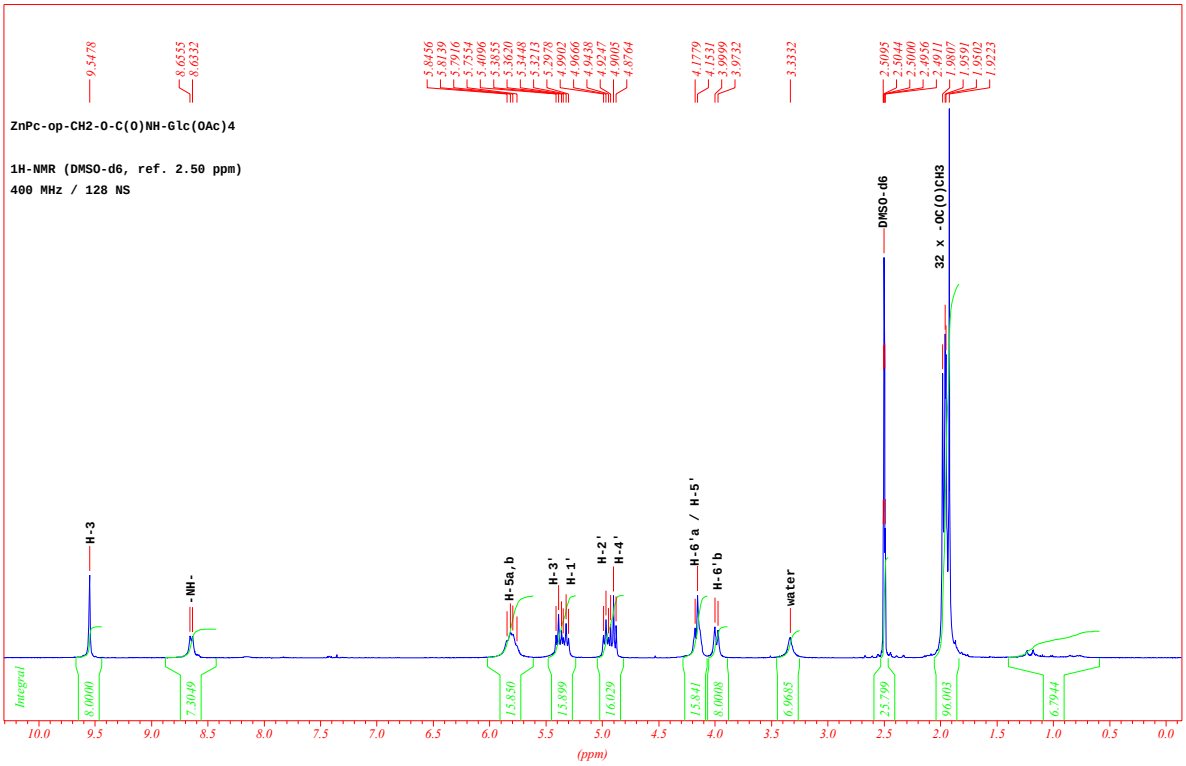

Figure 44 **[1]H-NMR spectrum of peracetylated glucosyl carbamate ZnPc 64. (proton assignment p. 139)**

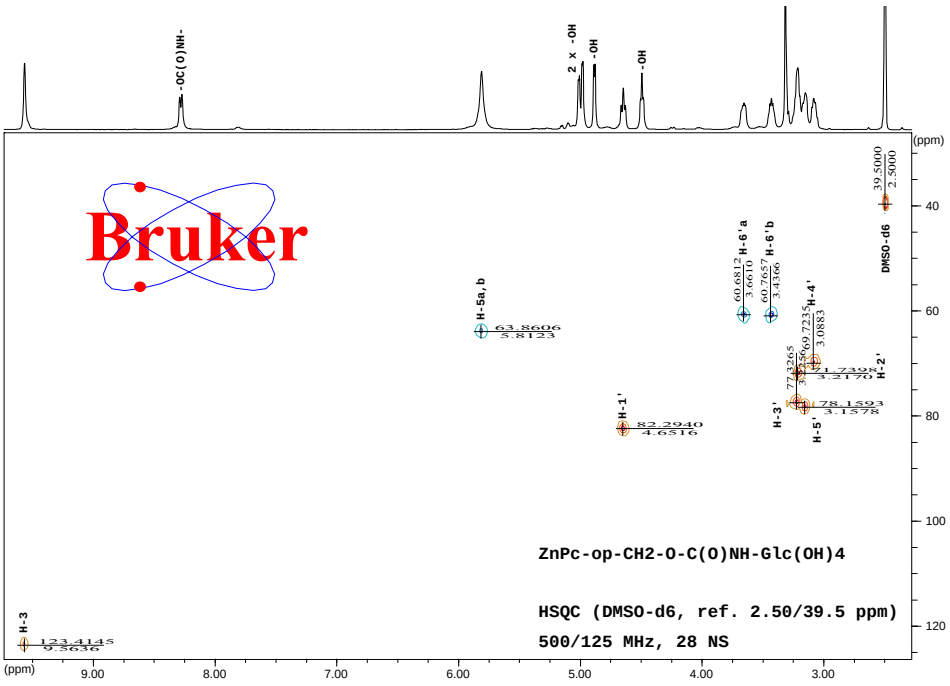

Figure 45 **HSQC spectrum of glucosyl carbamate ZnPc 65; blue colored signals correspond to -CH_2-, whereas red colored signals are refered to –CH- or –CH_3 (p. 141).**

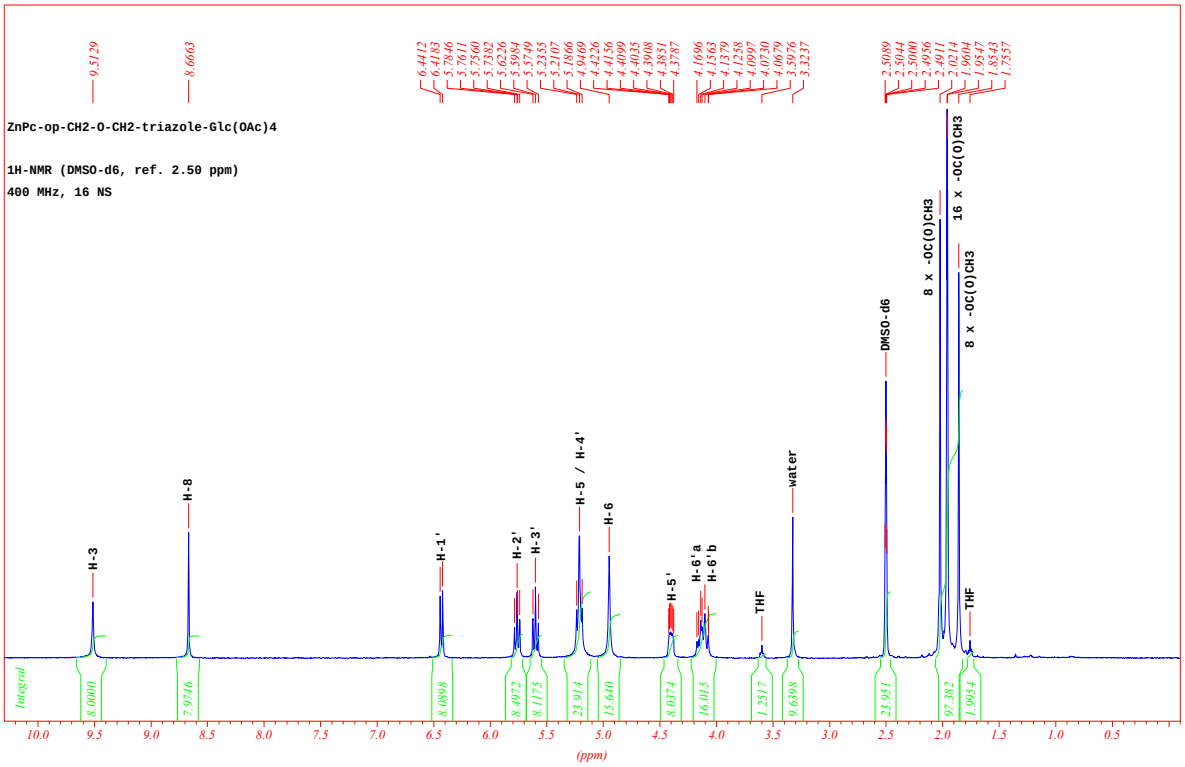

Figure 46 **[1]H-NMR spectrum of peracetylated glucosyl triazole ZnPc 72 (proton assignment p. 149).**

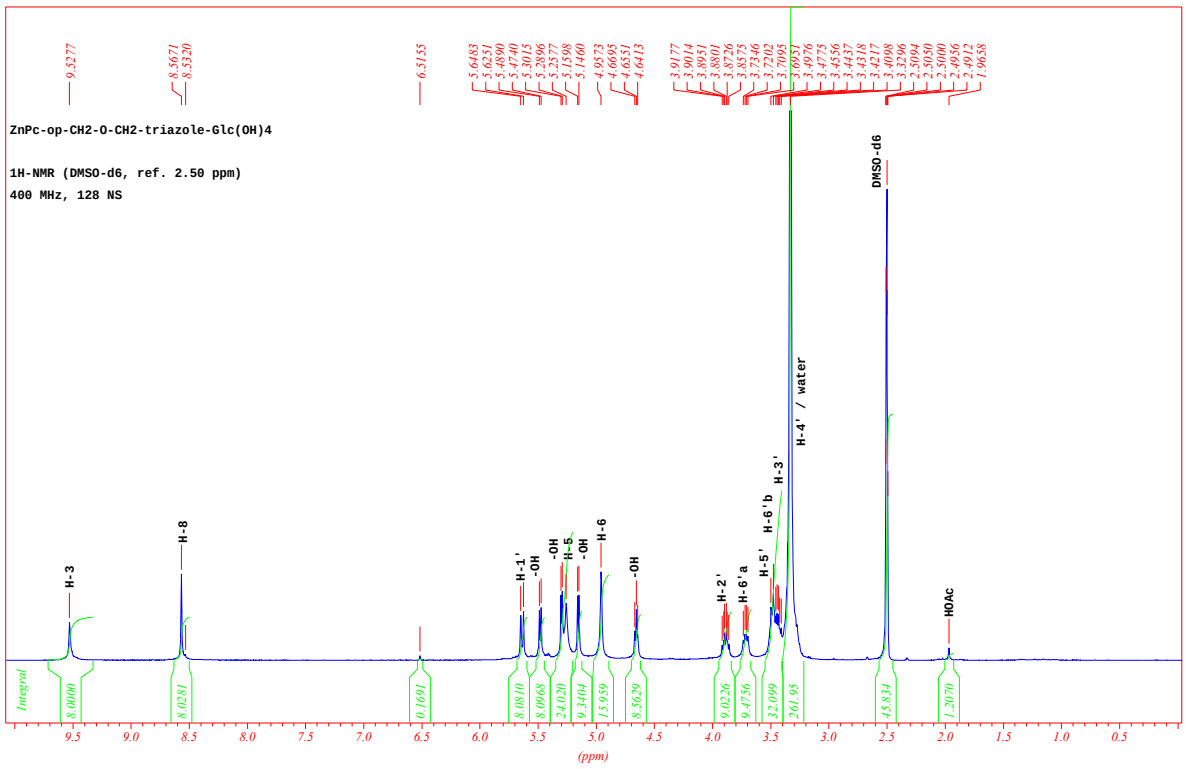

Figure 47 **[1]H-NMR spectrum of glucosyl triazole ZnPc 80 (proton assignment p. 154).**

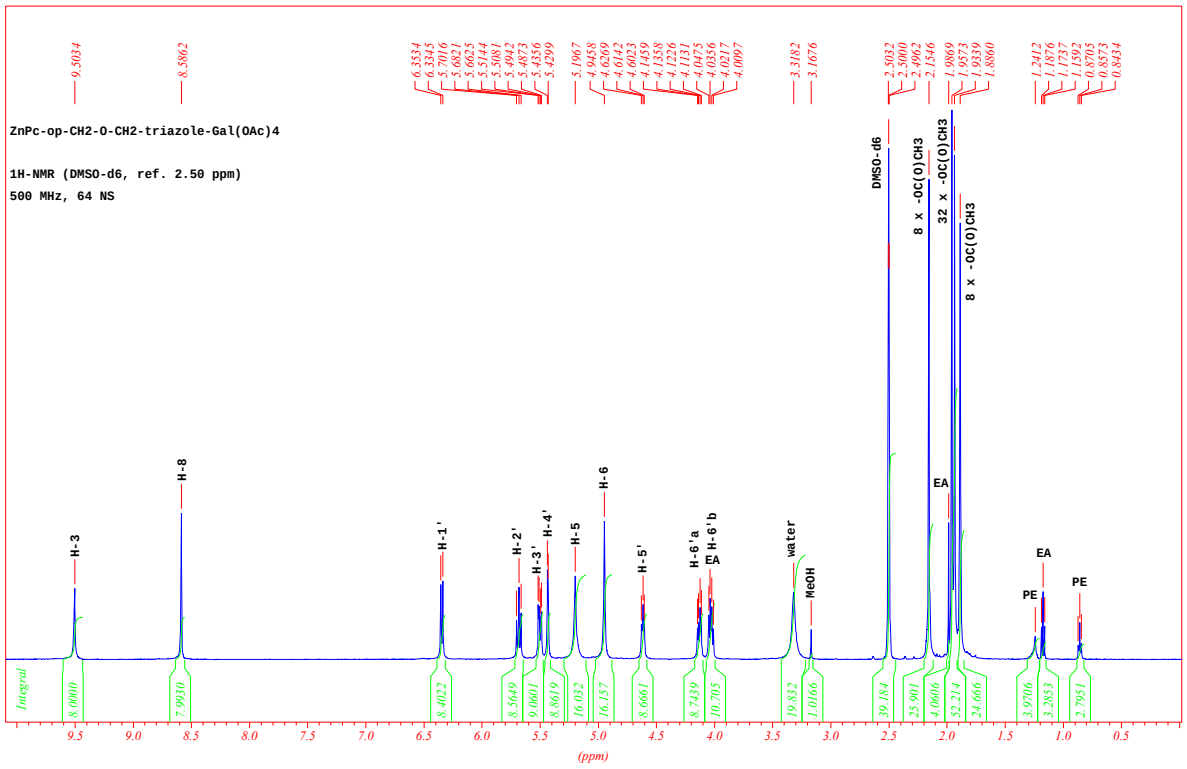

Figure 48 **[1]H-NMR spectrum of peracetylated galactosyl triazole ZnPc 73 (proton assignment p. 151).**

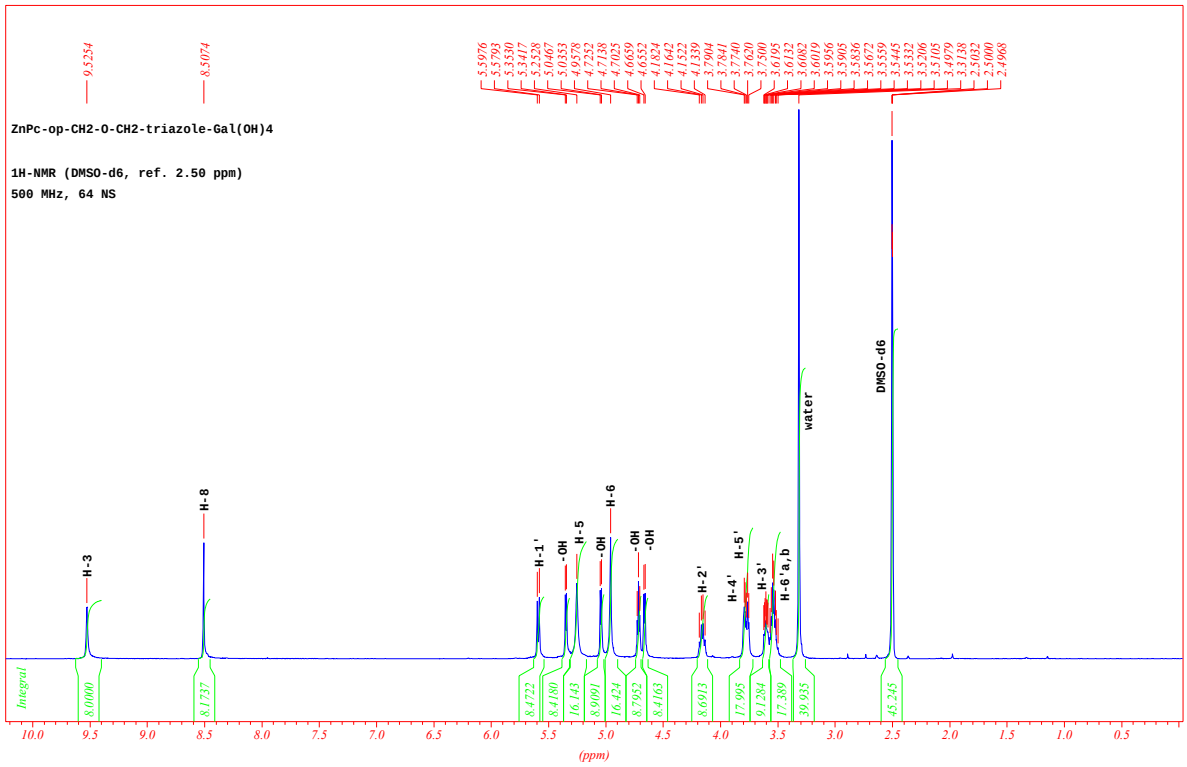

Figure 49 **[1]H-NMR spectrum of galactosyl triazole ZnPc 81 (proton assignment p. 156).**

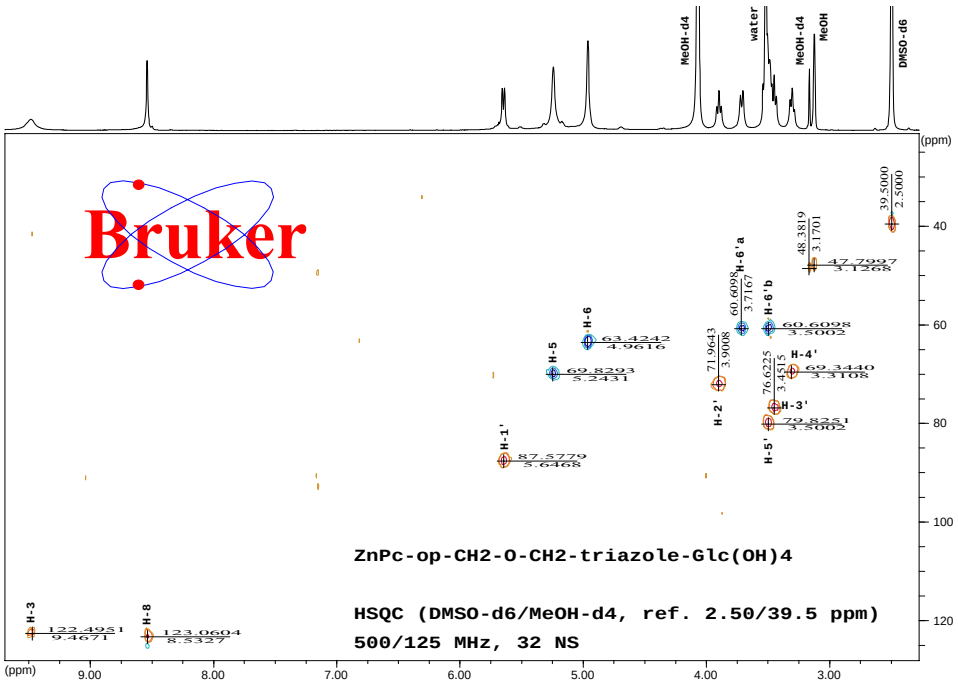

Figure 50 **HSQC spectrum of glucosyl triazole ZnPc 80 after deuterium-proton-exchange; blue colored signals correspond to -CH_2- whereas red colored signals refer to –CH- or –CH_3 (p. 154).**

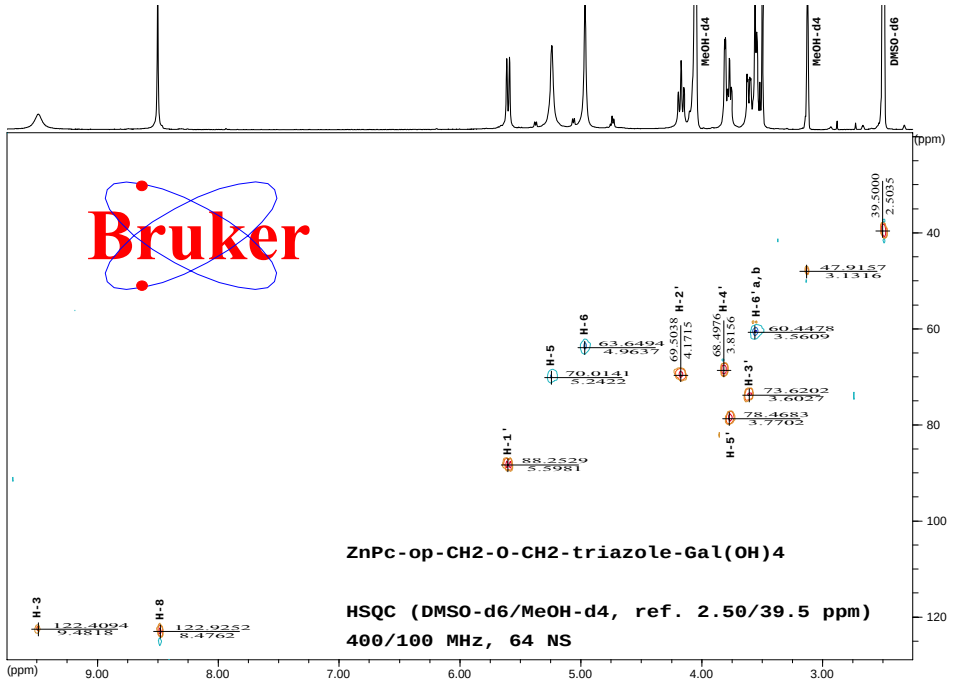

Figure 51 **HSQC spectrum of galactosyl triazole ZnPc 81 after deuterium-proton-exchange; blue colored signals correspond to -CH_2- whereas red colored signals refer to –CH- or –CH_3 (p. 156).**

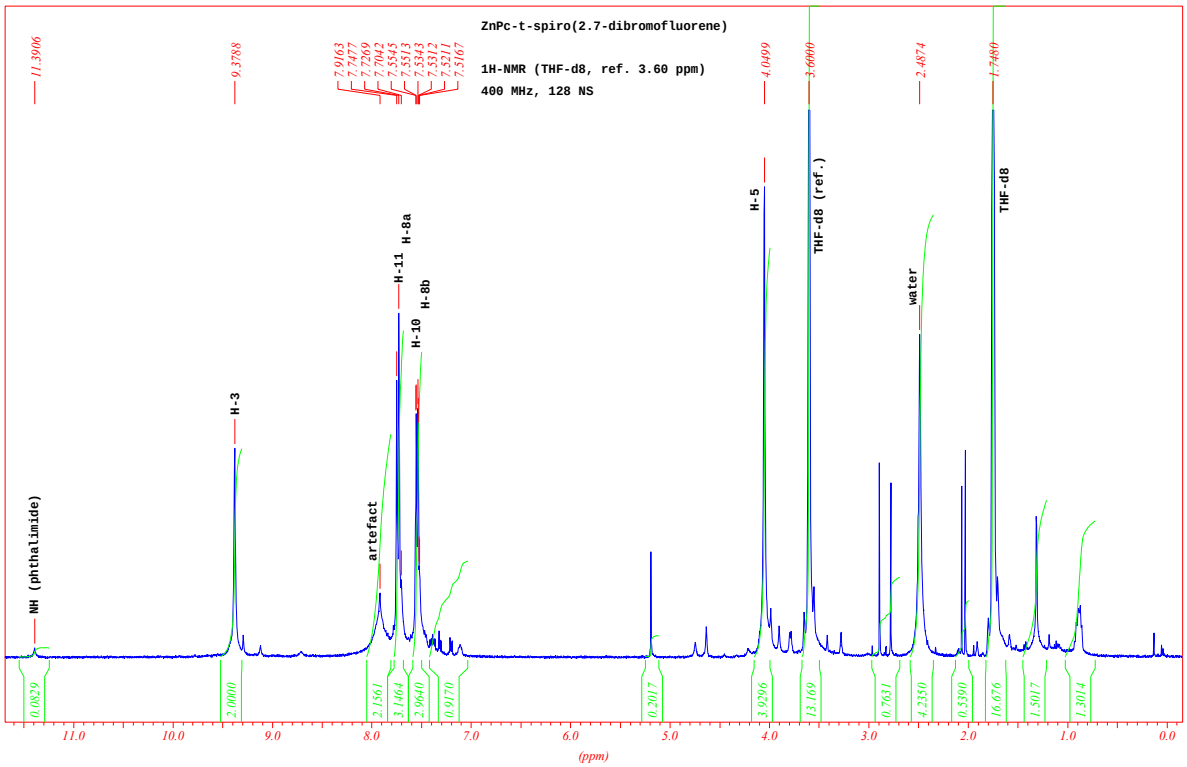

Figure 52 **^{1}H-NMR spectrum of dibromofluorenyl spiro-annelated ZnPc 90 (proton assignment p. 165).**

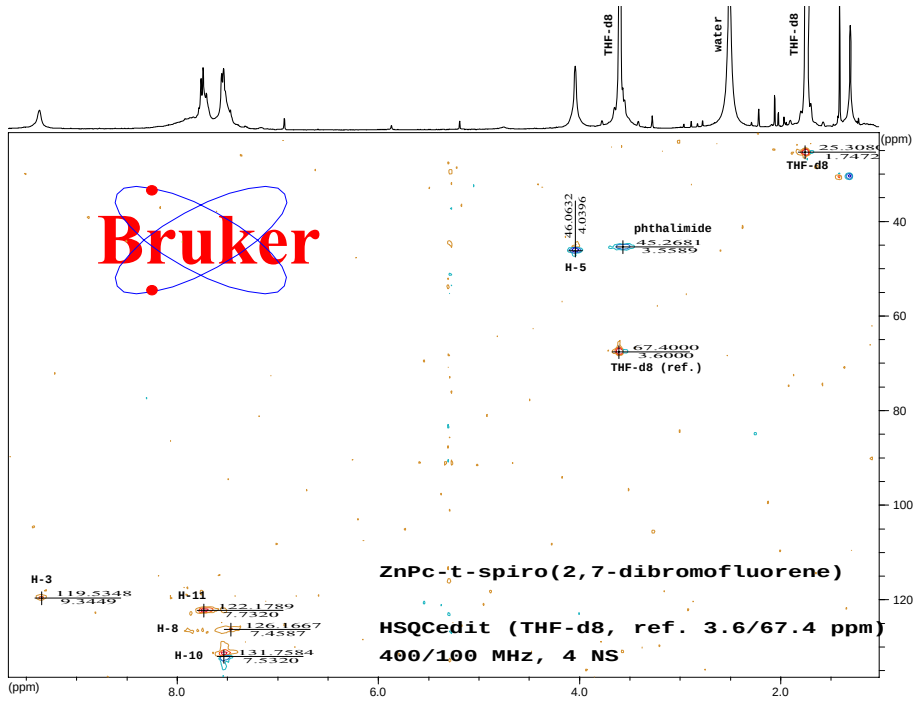

Figure 53 **HSQC spectrum of dibromofluorenyl spiro-annelated ZnPc 90; blue colored signals correspond to -CH_2- whereas red colored signals refer to –CH- or –CH_3 (proton assignment p. 165).**

MASS SPECTRA

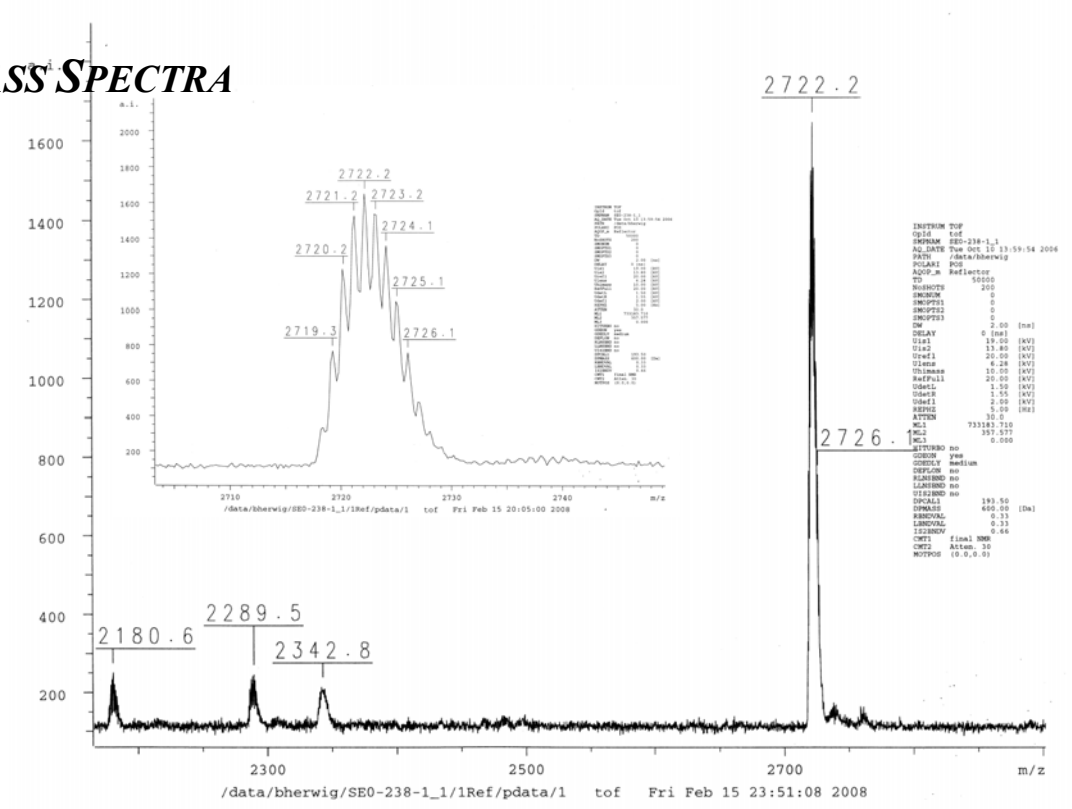

Figure 54 **MALDI-TOF spectrum of ZnPc-*op*-CH_2OTBDPS (34). The inset plots the isotopic pattern of the $[M]^{+\cdot}$ peak (2722.2 m/z).**

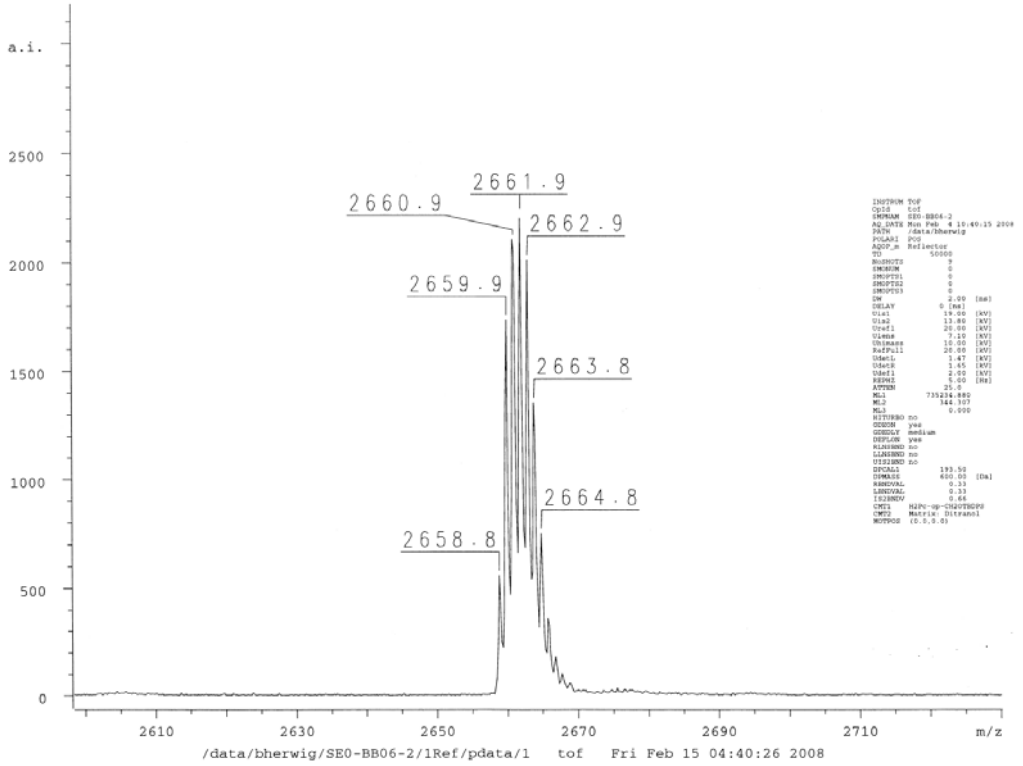

Figure 55 **MALDI-TOF spectrum of metal free H_2Pc-*op*-CH_2OTBDPS (35). The $[M+H]^+$ peak (2661.9 m/z) shows the characteristic isotopic pattern.**

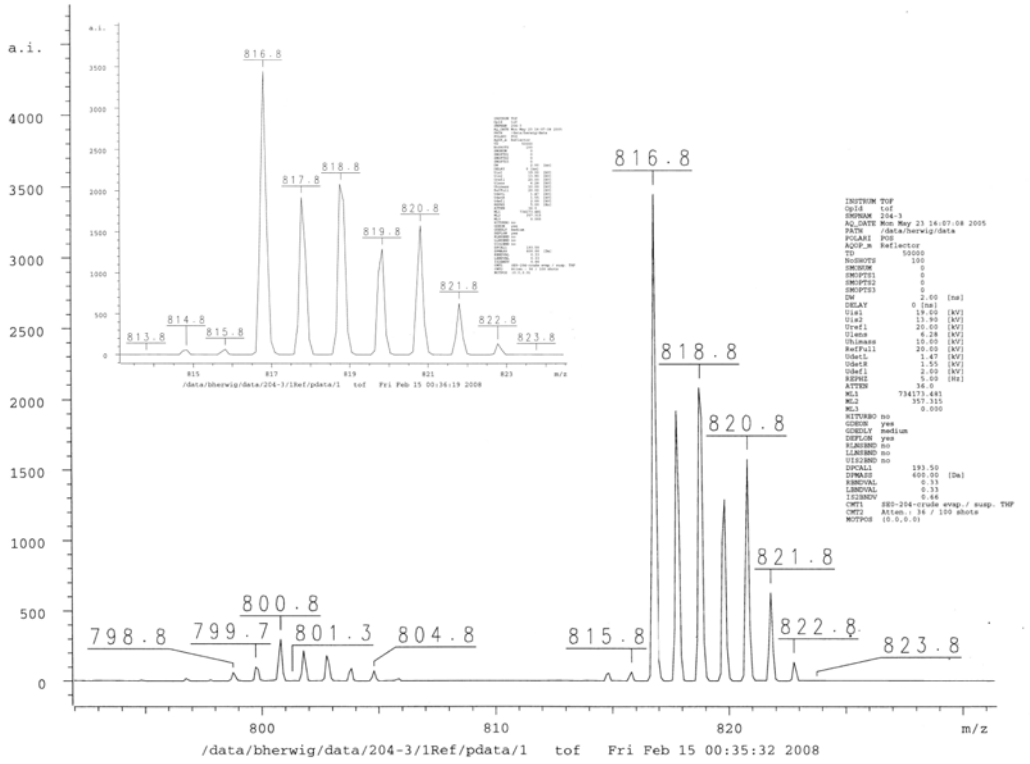

Figure 56 **MALDI-TOF spectrum of ZnPc-*op*-CH_2OH (39) The inset plots the isotopic pattern of the $[M]^{\cdot}$ peak (816.8 m/z).**

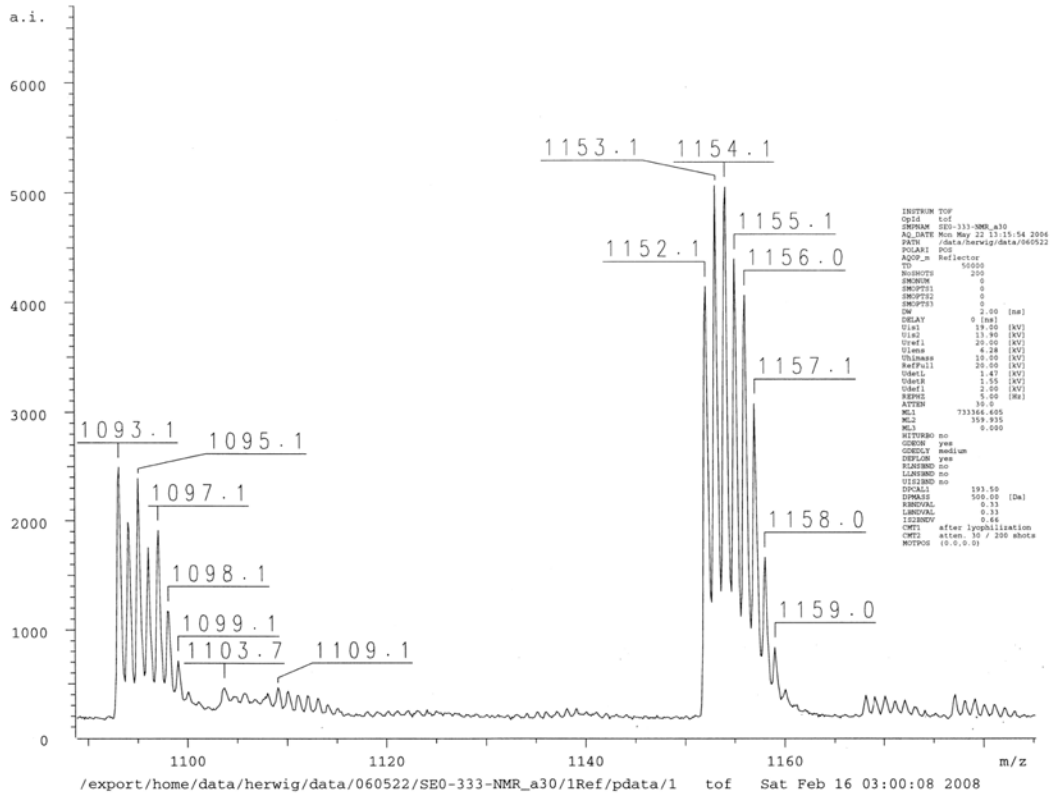

Figure 57 **MALDI-TOF spectrum of ZnPc-*op*-CH_2OAc (66). The $[M]^{\cdot}$ peak (1153.1 m/z) shows the characteristic isotopic pattern.**

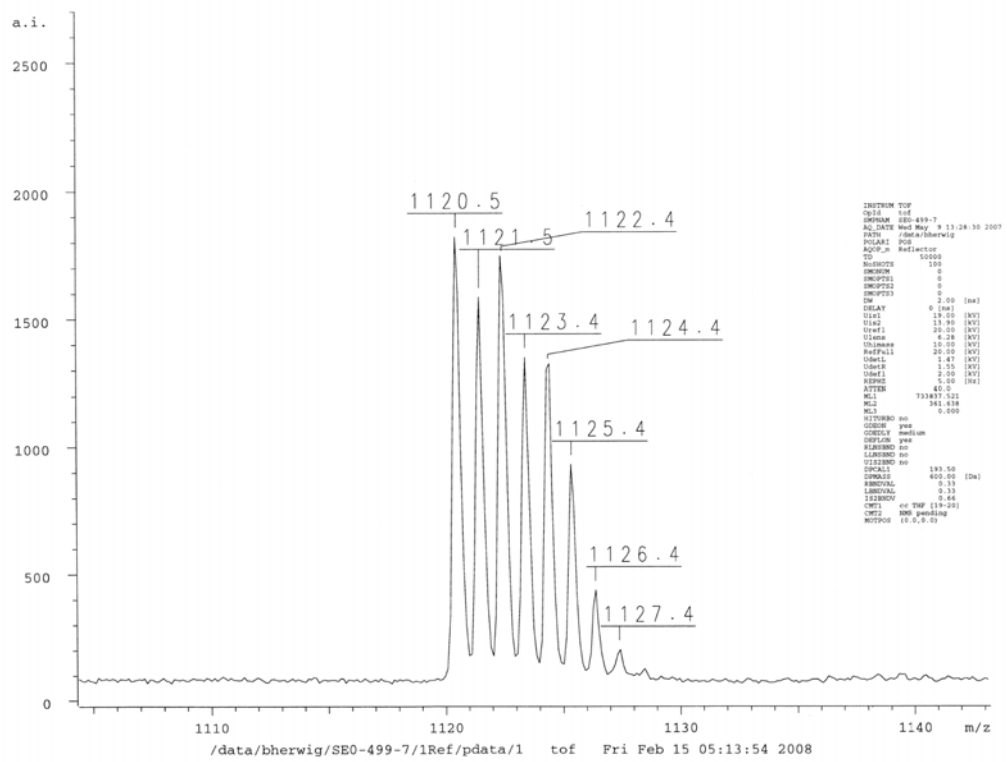

Figure 58 **MALDI-TOF spectrum of ZnPc-*op*-$CH_2OCH_2C{\equiv}CH$ (70). The $[M]^{\cdot+}$ peak (1120.5 m/z) shows the characteristic isotopic pattern.**

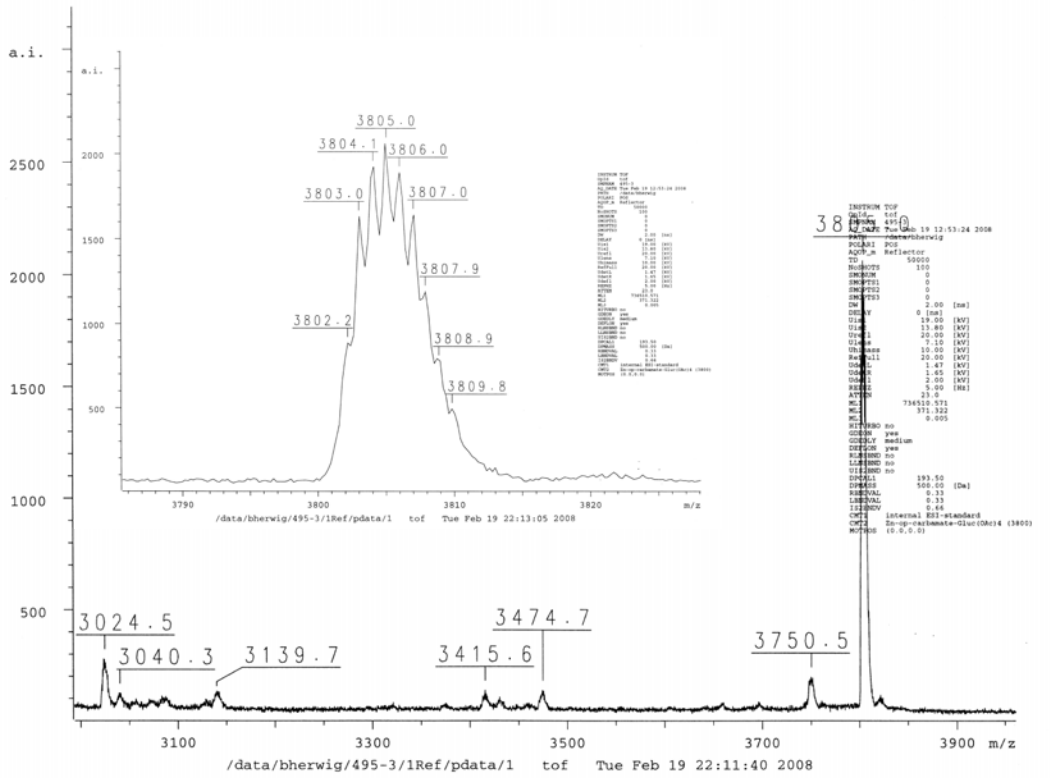

Figure 59 **MALDI-TOF spectrum of the peracetylated glucosyl carbamate ZnPc 64. The inset plots the isotopic pattern of the $[M]^{\cdot+}$ peak (3805.0 m/z).**

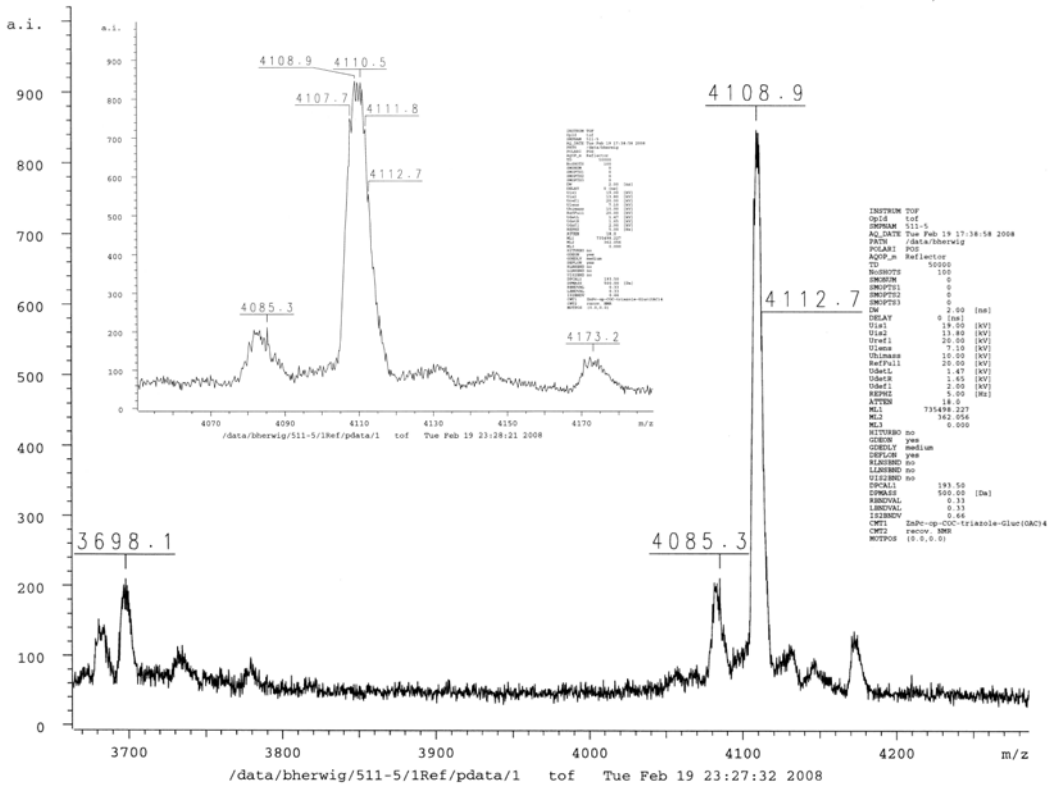

Figure 60 **MALDI-TOF spectrum of the peracetylated glucosyl triazole ZnPc 72. The inset plots partially the isotopic pattern of the $[M]^{+\cdot}$ peak (4108.9 m/z).**

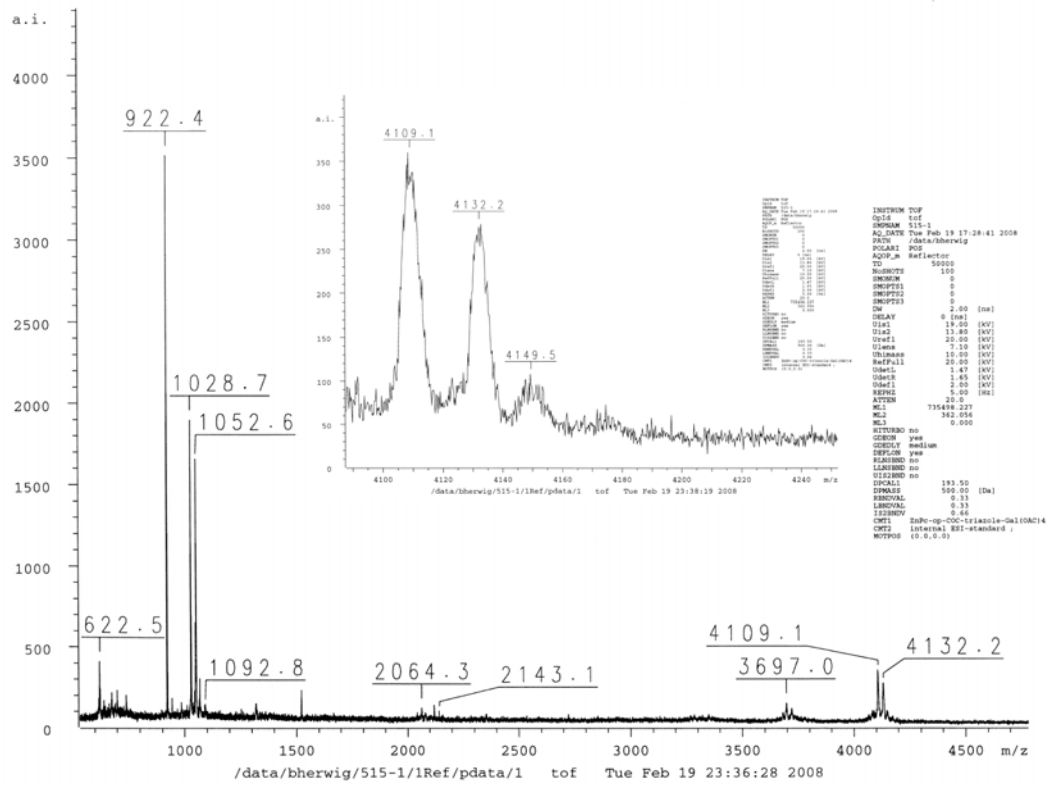

Figure 61 **MALDI-TOF spectrum of the peracetylated galactosyl triazole ZnPc 73. The inset plots the expansion of the $[M]^{+\cdot}$ peak (4109.1 m/z) and the $[M+Na]^{+}$ peak (4132.2 m/z). The peak at 922.4 m/z refers to the internal used ESI-standard.**

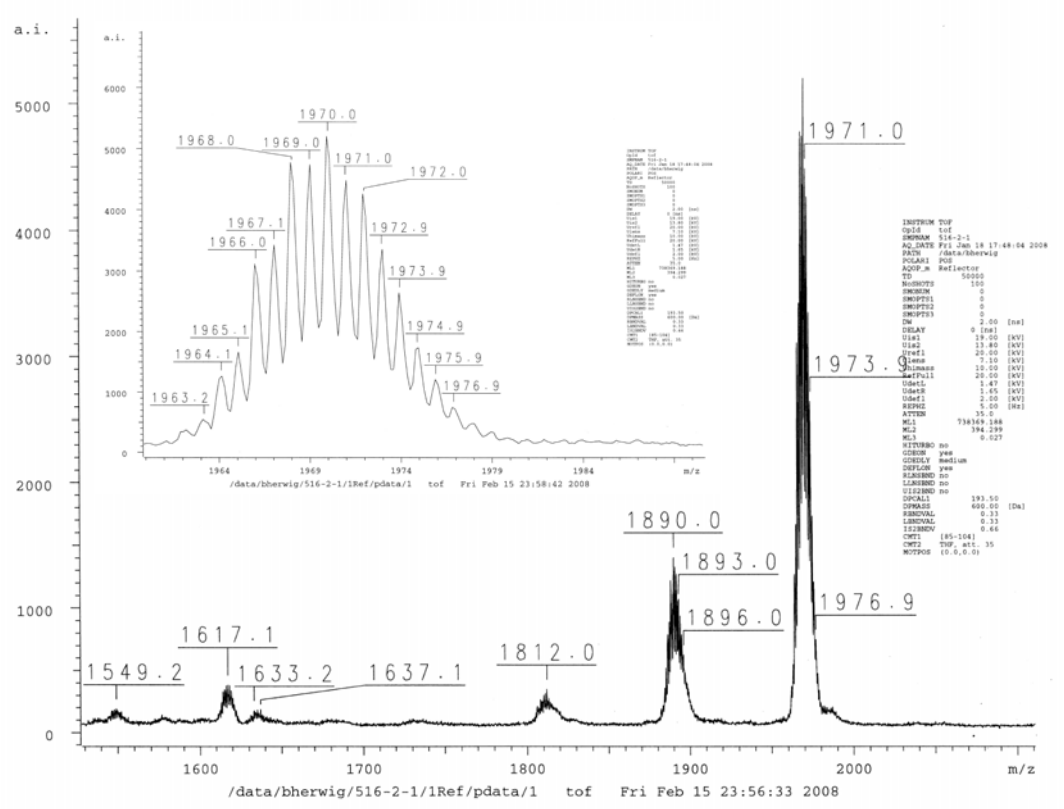

Figure 62 **MALDI-TOF spectrum of the dibromofluorenyl spiro-annelated ZnPc 90. The inset plots the isotopic pattern of the $[M]^{+\cdot}$ peak (1970.0 m/z), which results from eight Br-atoms and one Zn-atom.**

All mass spectra are in agreement with the predicted results calculated with the software ChemDraw Ultra 10.

UV-VIS SPECTRA

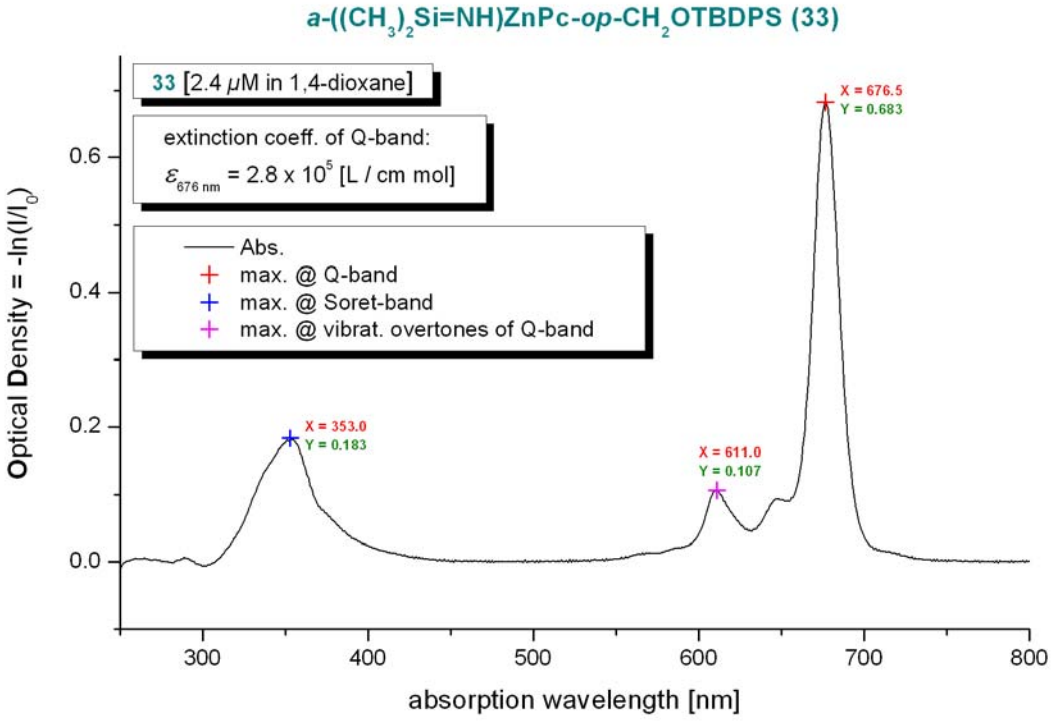

Figure 63 **UV-vis absorption spectrum of ZnPc 33 in 1,4-dioxane (2.4 μM).**

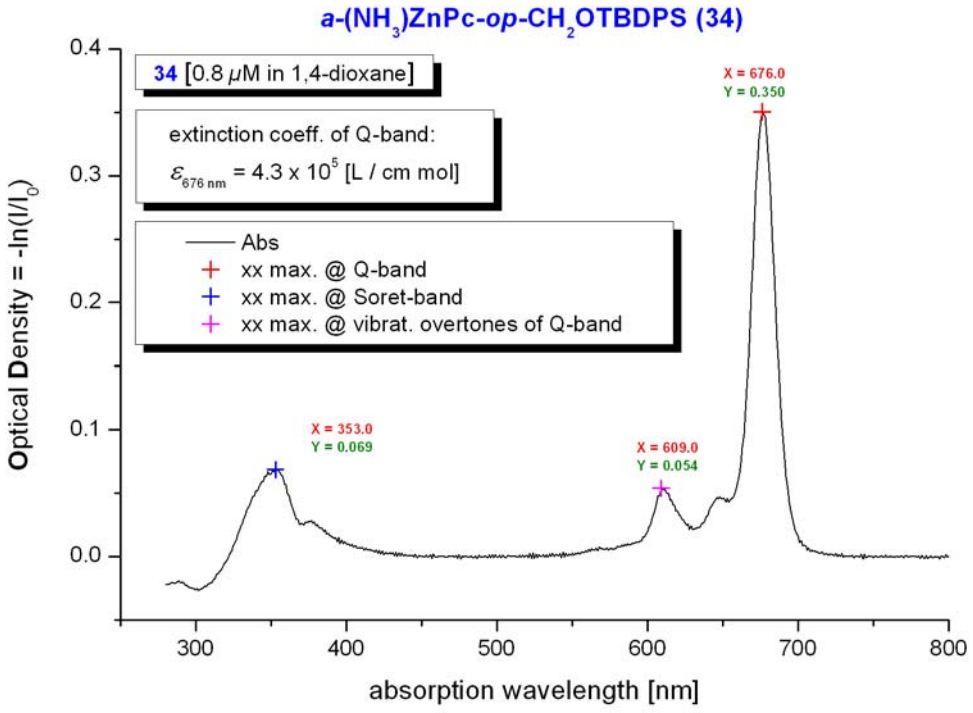

Figure 64 **UV-vis-absorption spectrum of ZnPc 34 in 1,4-dioxane (0.8 μM).**

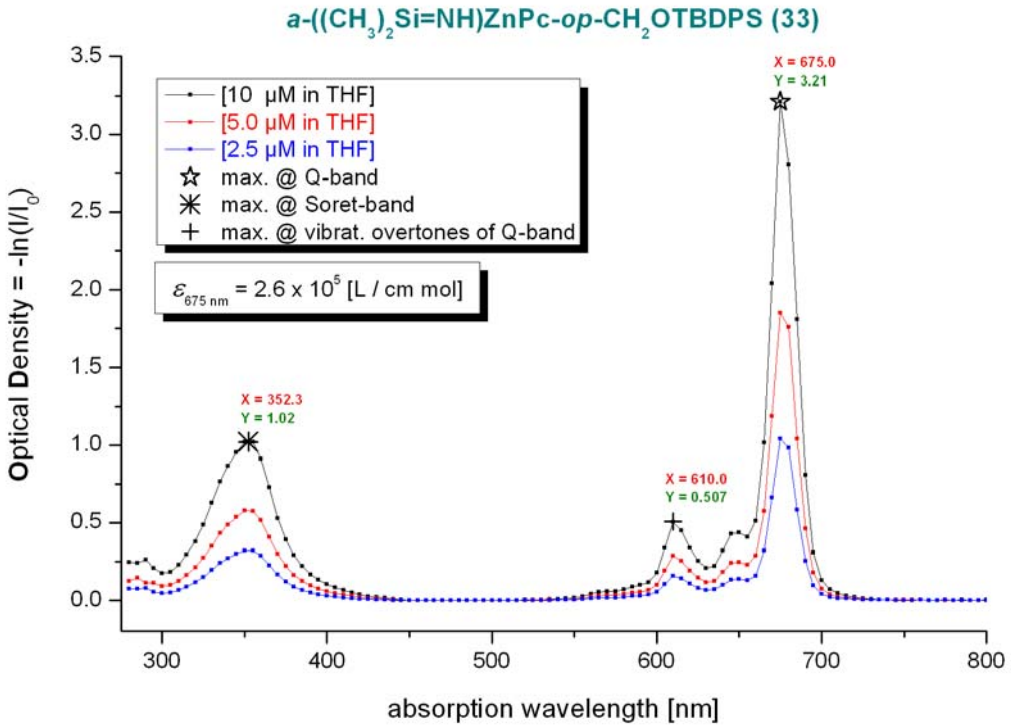

Figure 65 **UV-vis absorption spectra of ZnPc33 in THF of various concentrations (2.5, 5.0 and 10 μM).**

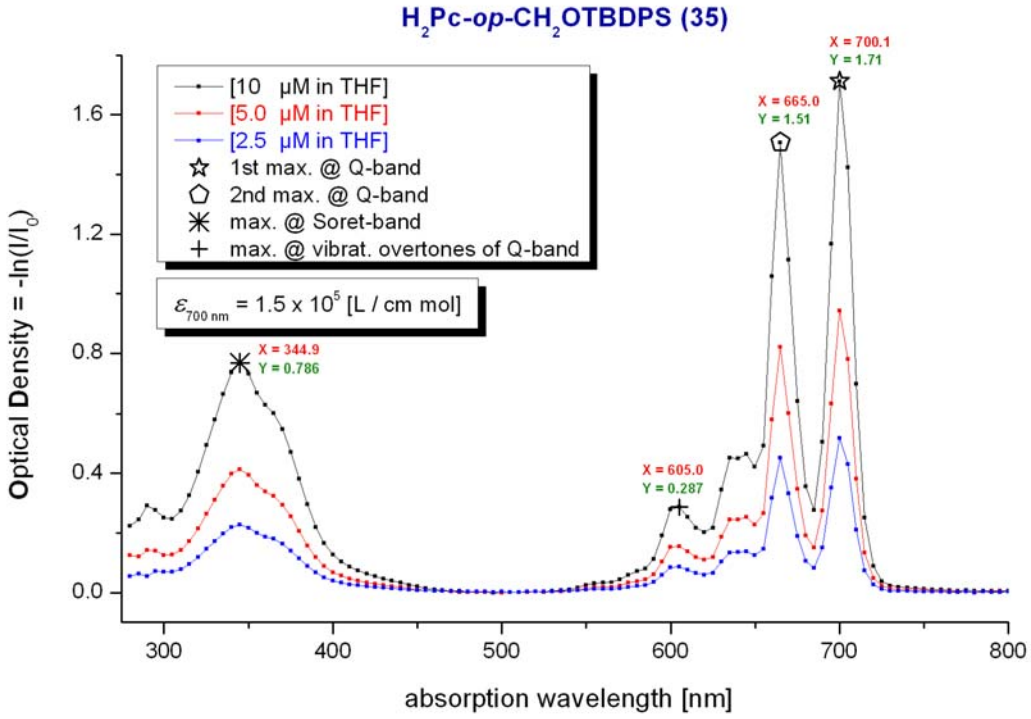

Figure 66 **UV-vis absorption spectra of metal free Pc 35 in THF of various concentrations (2.5, 5.0 and 10 μM).**

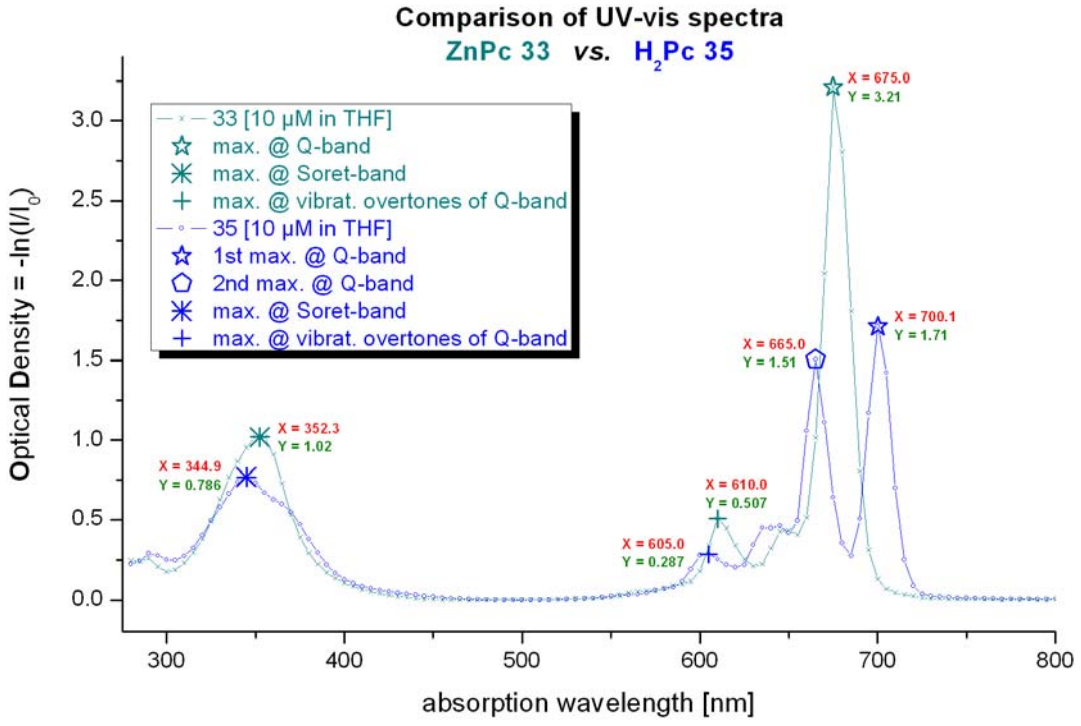

Figure 67 **Superposition of UV-vis absorption spectra of ZnPc 34 and H_2Pc 35 at 10 μM in THF.**

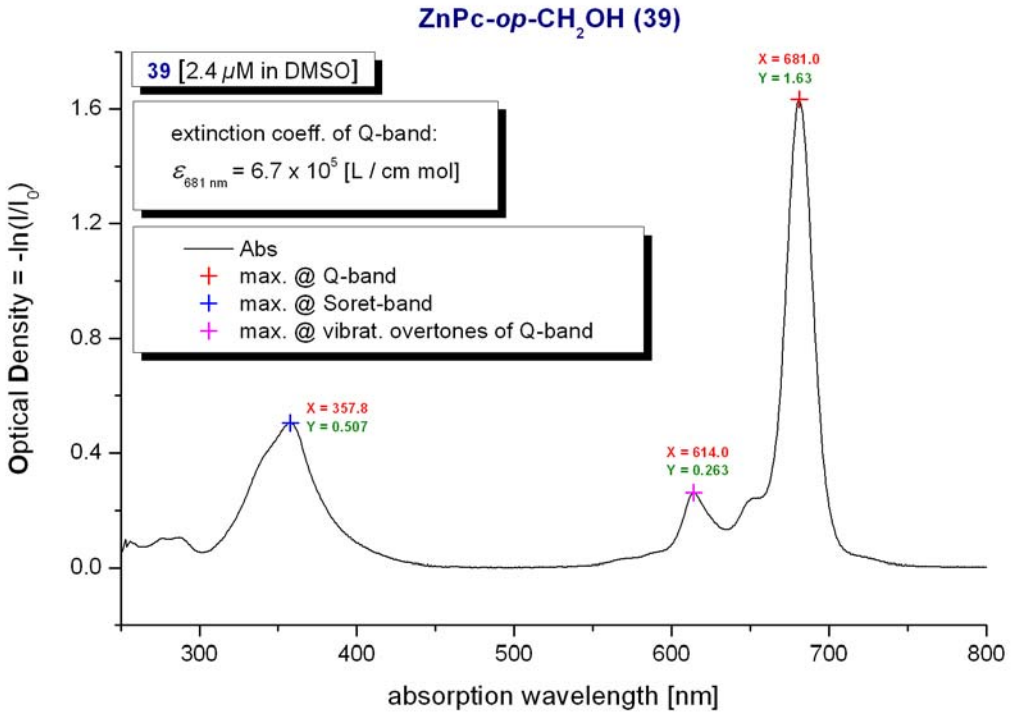

Figure 68 **UV-vis absorption spectrum of ZnPc-*op*-CH_2OH (39) in DMSO (2.4 μM).**

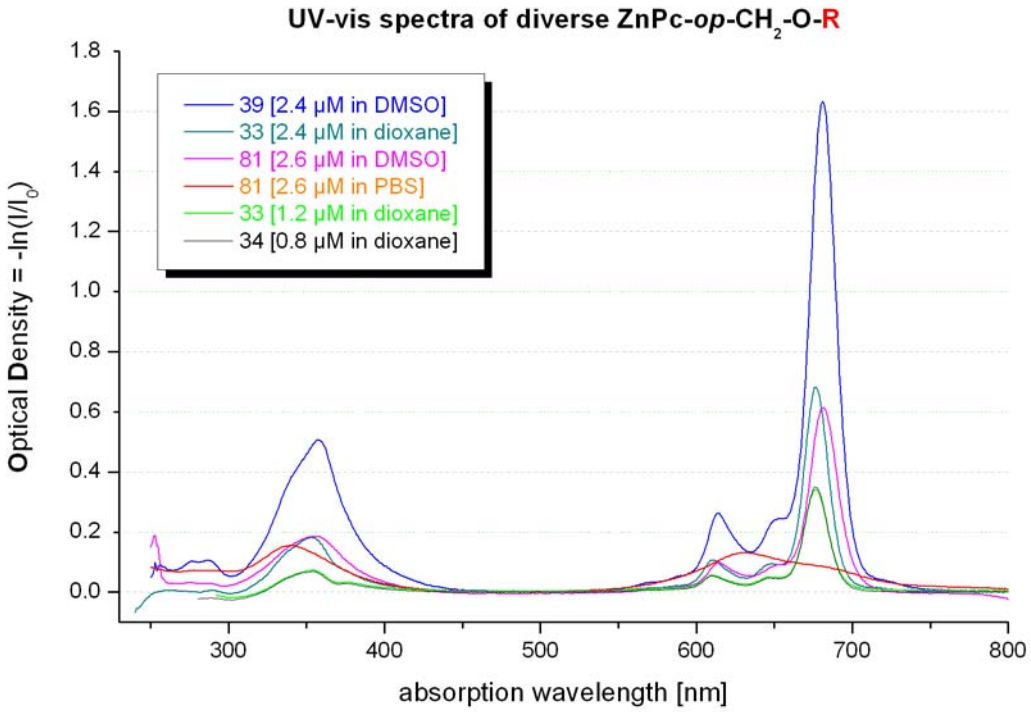

Figure 69 **Superposition of UV-vis spectra of diverse ZnPcs (33, 34, 39, 81).**

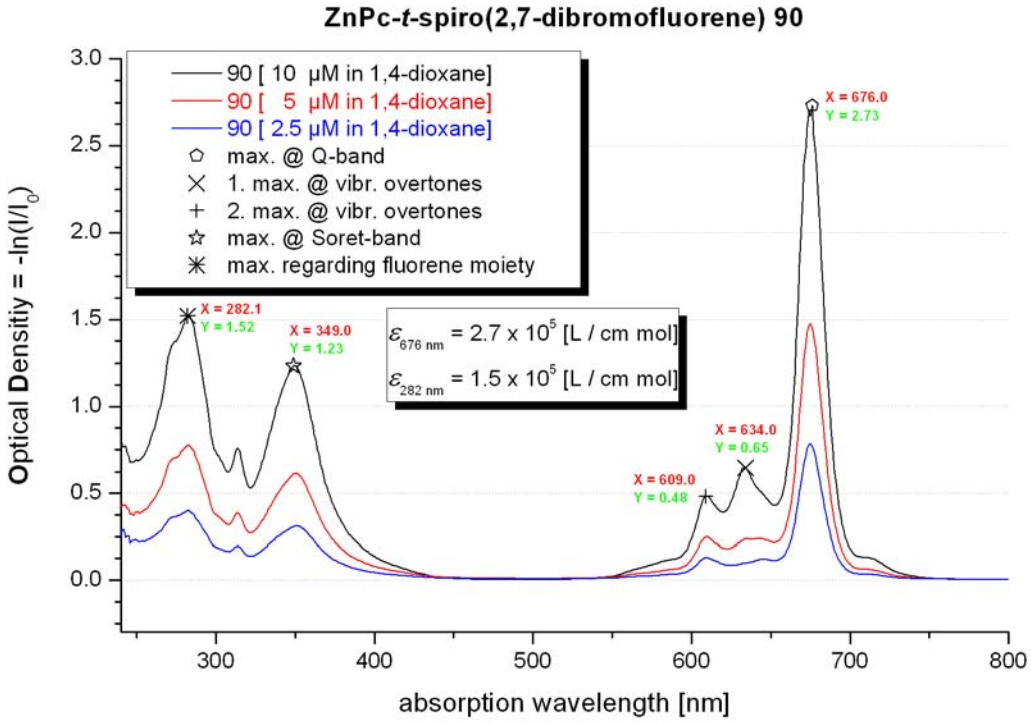

Figure 70 **UV-vis absorption spectra of dibromofluorenyl spiro-annelated ZnPc 90 in 1,4-dioxane of various concentrations (2.5, 5.0 and 10 μM).**

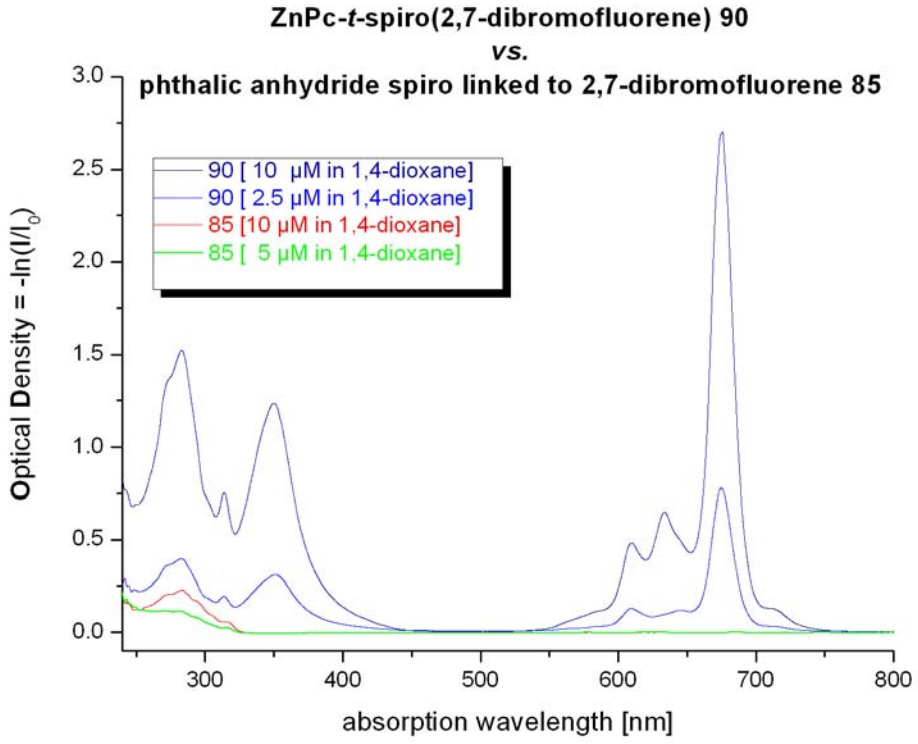

Figure 71 **UV-vis absorption spectra of dibromofluorenyl spiro-annelated ZnPc 90 and the corresponding anhydride 85 in 1,4-dioxane of various concentrations.**

All investigated Pc-derivatives (**33**, **34**, **35**, **39**, **81**, **90**) exhibited the characteristic absorption bands – Q-band (660-700 nm), Soret-band (340-360 nm) and in addition the vibrational overtones of the Q-band (~600 nm) – in solution.[212]

The split of the Q-band was clearly observed for the metal free Pc **35** as result of its lower symmetry (Figure 67). In the H_2Pc **35**, two of the isoindole nitrogens are carrying hydrogen atoms, whereas the other two are involved in iminic type functions, hence, giving two components of the split band.

Furthermore, a single absorption peak for the corresponding Q-band is specific for a symmetrically substituted Pc-scaffold. The high molar absorptivity (ε) of ~ 10^5 [L / cm·mol] of the Q-band is the origin of the purity and depth of the color of phthalocyanine dyes (Figure 68).[213]

Throughout, the Beer-Lamberts' law was fulfilled (Figure 65, Figure 66, and Figure 70).

FLUORESCENCE SPECTRA

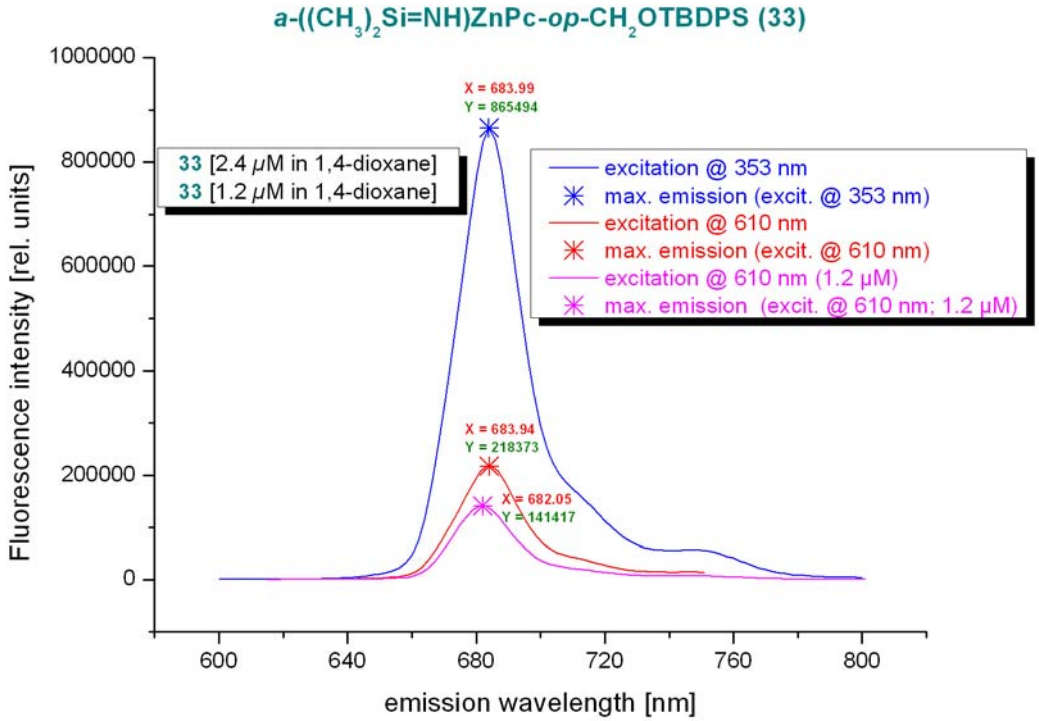

Figure 72 **Fluorescence emission spectra of ZnPc-*op*-CH_2OTBDPS (33) in obedience of molar concentration and the excitation wavelength.**

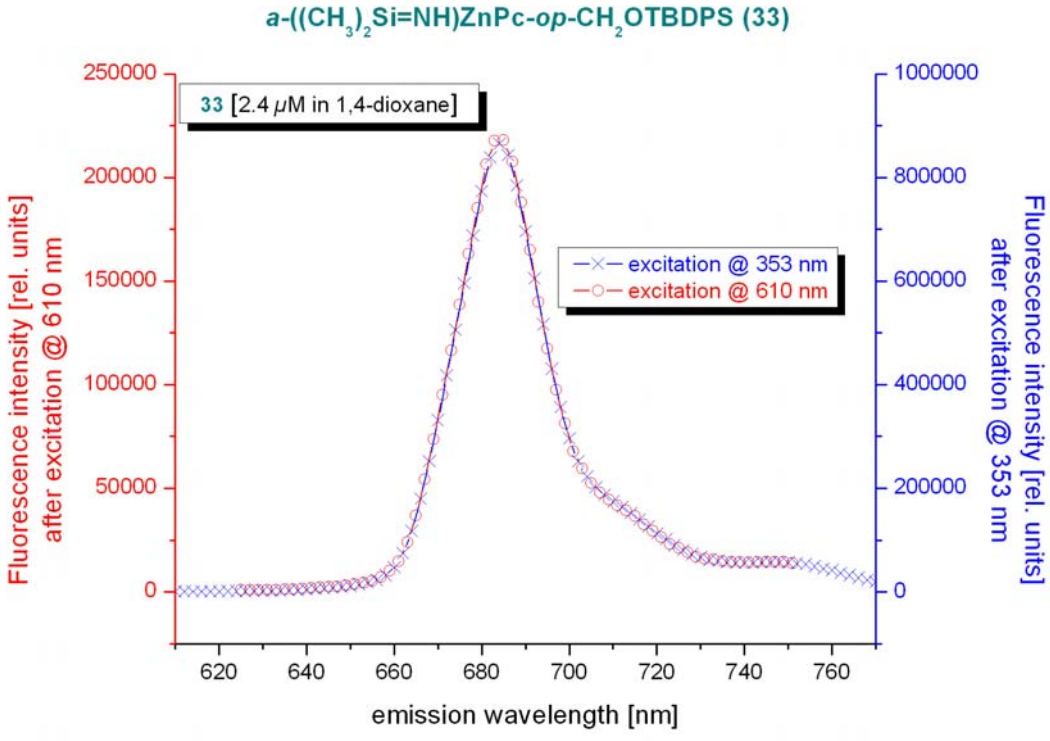

Figure 73 **Superposition of fluorescence spectra of ZnPc-*op*-CH_2OTBDPS (33) after excitation at 353 nm and 610 nm respectively (2.4 μM in 1,4-dioxane).**

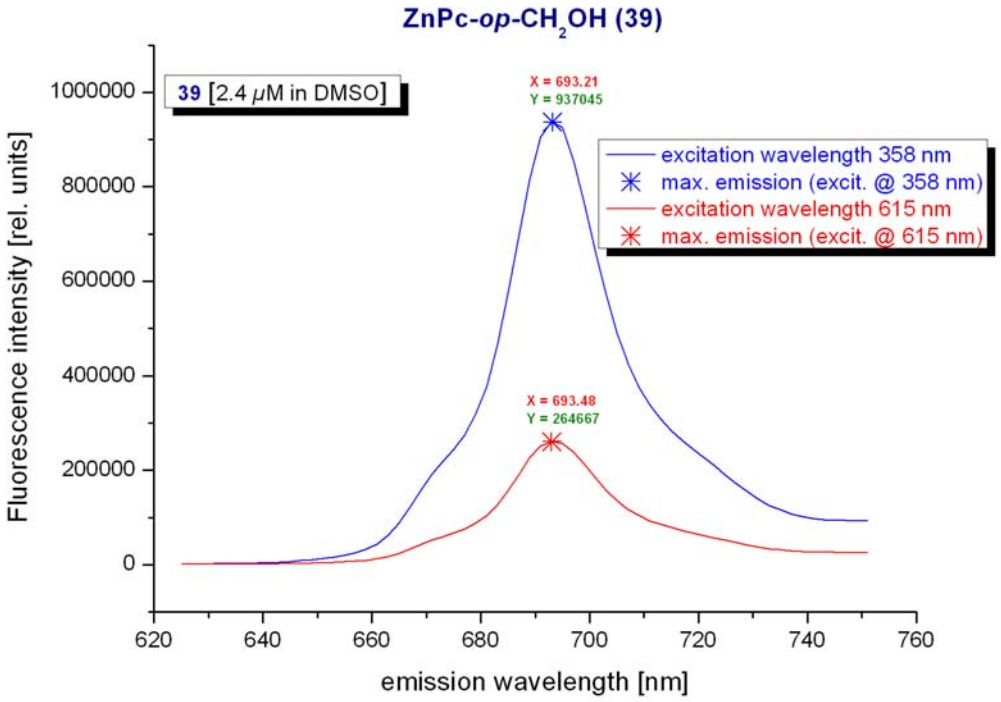

Figure 74 **Fluorescence emission spectra of ZnPc-*op*-CH_2OH (39) in obedience of the excitation wavelength (2.4 μM in DMSO).**

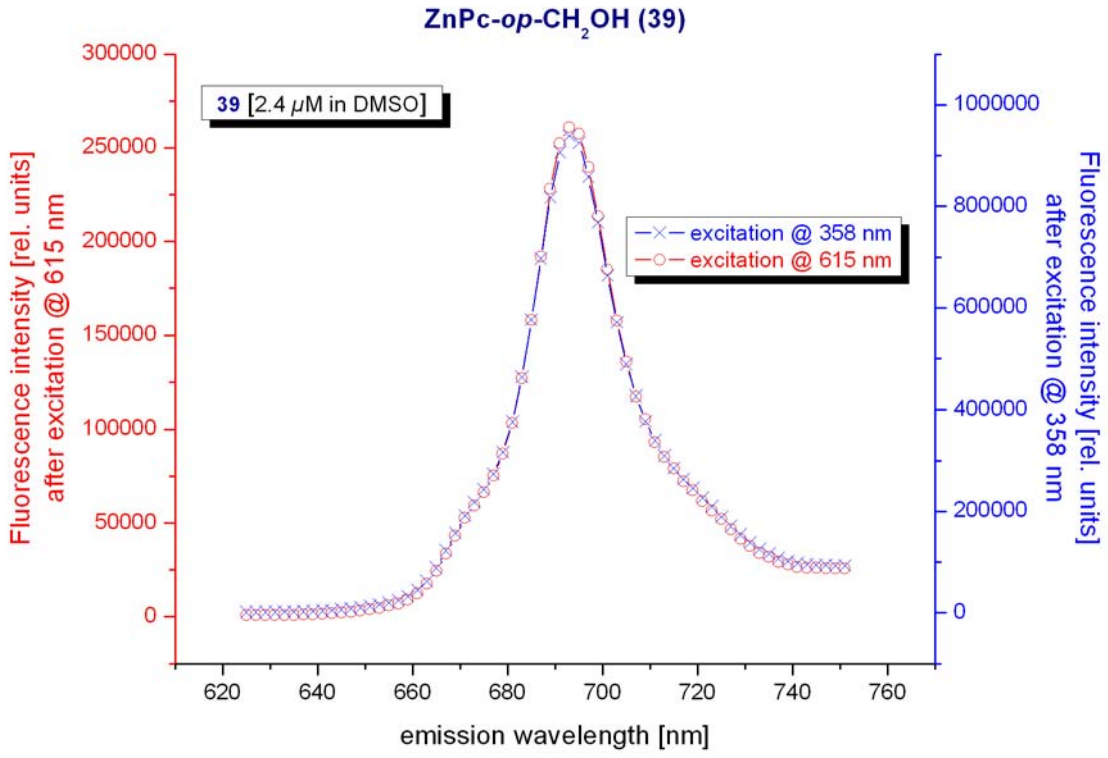

Figure 75 **Superposition of fluorescence emission spectra of ZnPc-*op*-CH_2OH (39) in obedience of excitation wavelength (2.4 μM in DMSO).**

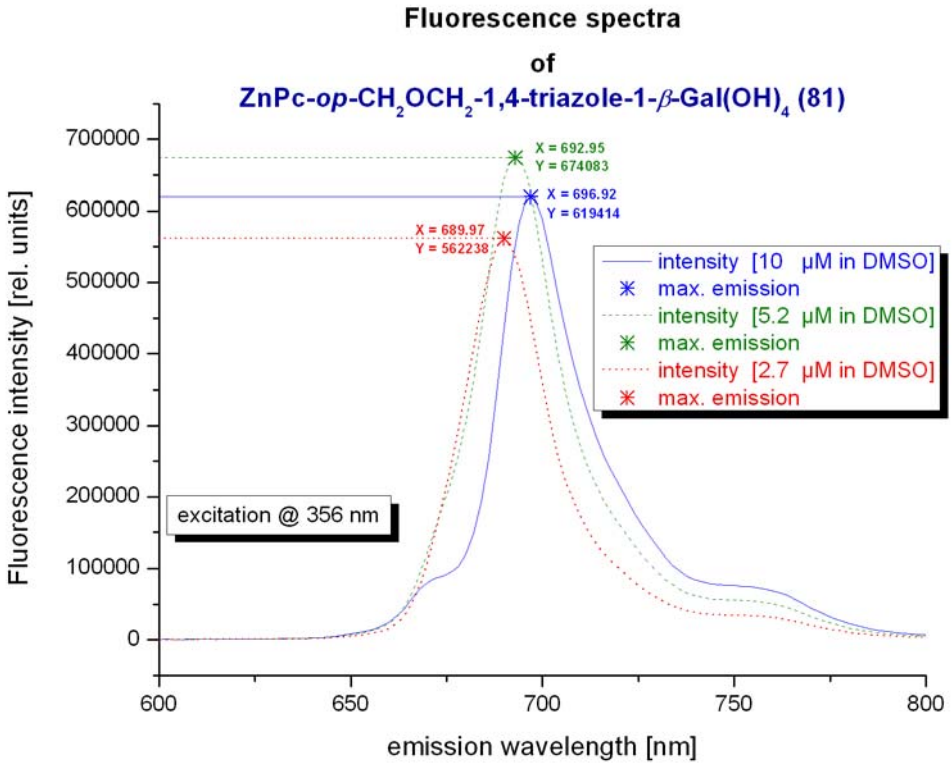

Figure 76 **Fluorescence emission spectra of galactosylated triazole ZnPc 81 in obedience of the molar concentration in DMSO.**

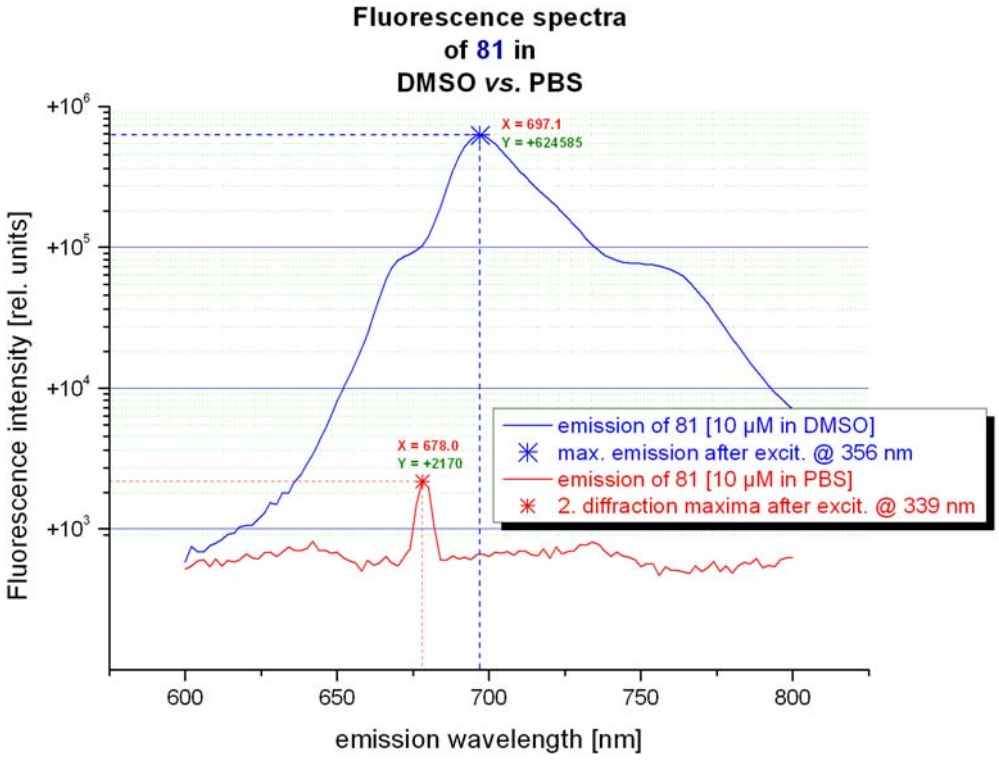

Figure 77 **Fluorescence emission spectra of galactosylated triazole ZnPc 81 in obedience of solvent (DMSO *vs.* PBS).**

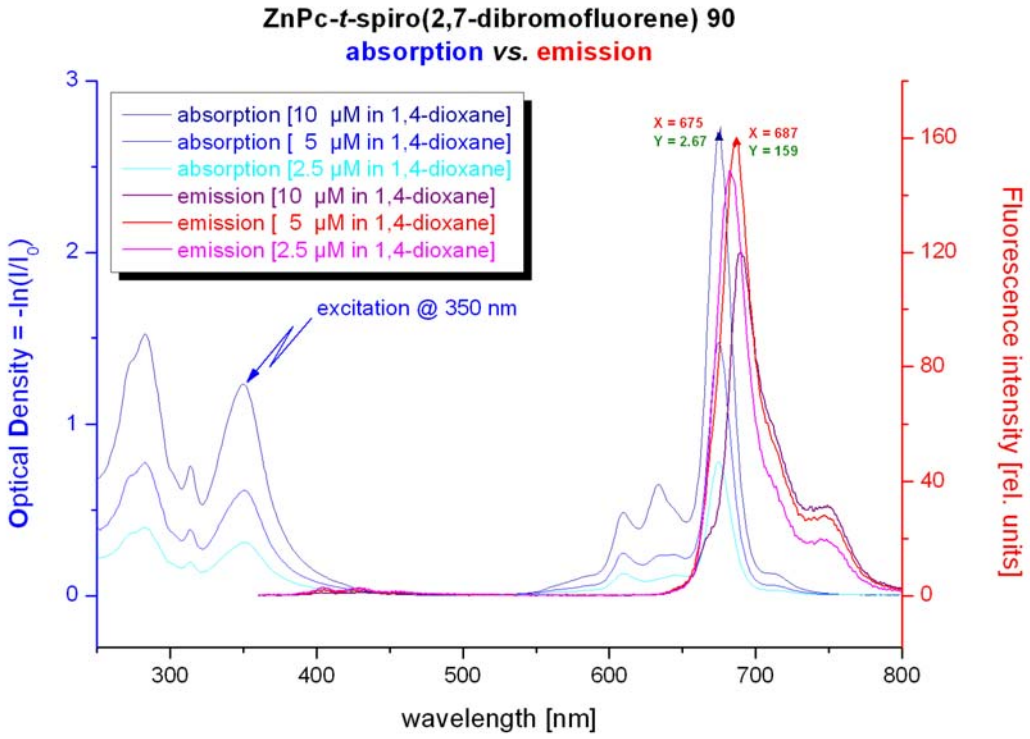

Figure 78 **Superposition of absorption and fluorescence spectra of dibromofluorenyl spiro-annelated ZnPc 90 in 1,4-dioxane of various concentration (2.5, 5.0 and 10 μM).**

Particularly with regard to molecular imaging, the fluorescence characteristics of the herein described, novel Pcs **33**, **39**, **81** and **90** were examined. As expected from UV-vis absorption spectra, the results of the fluorescence spectroscopy were in agreement with the literature. For the Q-band, the Stokes shifts observed were in the range from 7.5 to 13 nm. The intensity of the emitted light displayed the dependency on the energy of the excitation wavelength (Figure 72 and Figure 74) which was in contrast to the shape of the plotted graph as shown by superposition (Figure 73 and Figure 75).

In DMSO as solvent, the maximum of intensity was at 5 μM displaying the influence of the concentration of **81** (Figure 76), whereas in PBS quenching of **81** occurred by aggregation (Figure 77).

MICROSCOPIC STUDIES

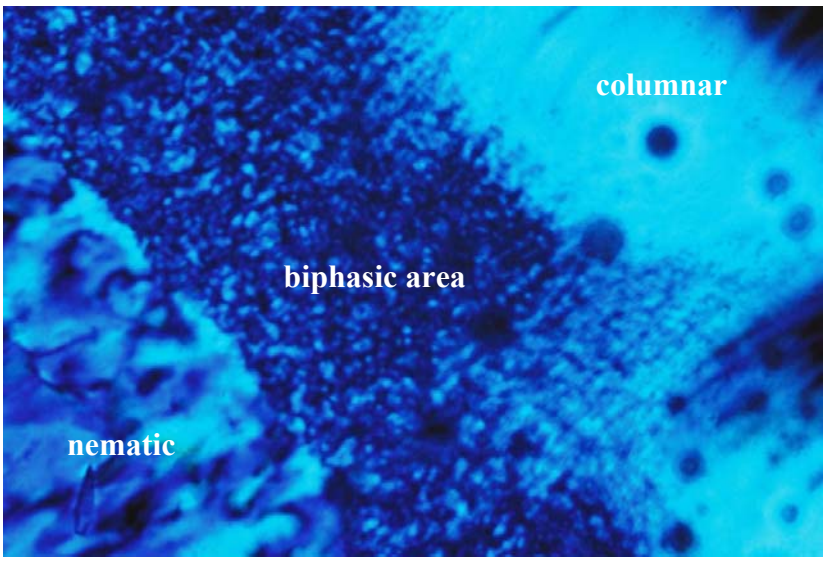

Image 10 **Liquid crystalline behavior of ZnPc 68: formed from a solution in DMSO upon a concentration gradient due to contact with dist. water. bottom left: nematic; middle: biphasic area; top right: columnar.**[3, 151]

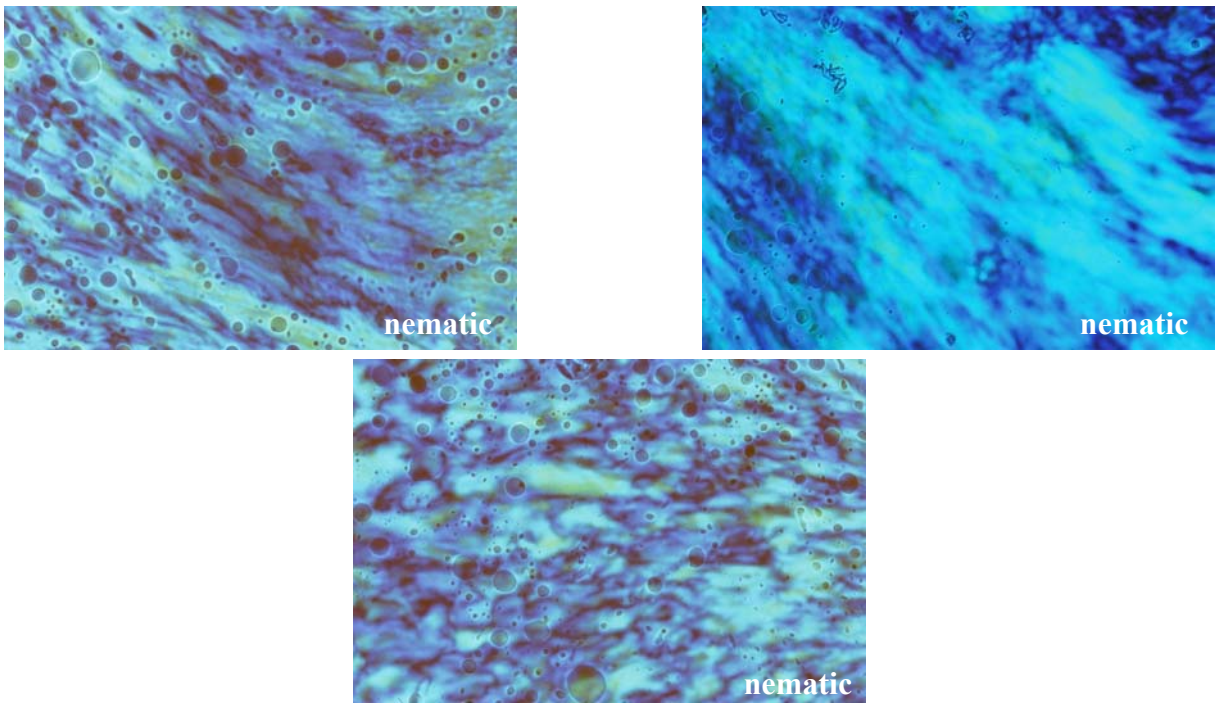

Image 11 **Nematic phases of ZnPc 68: formed from a solution in DMSO upon a concentration gradient due to contact with dist. water.**[3, 151]

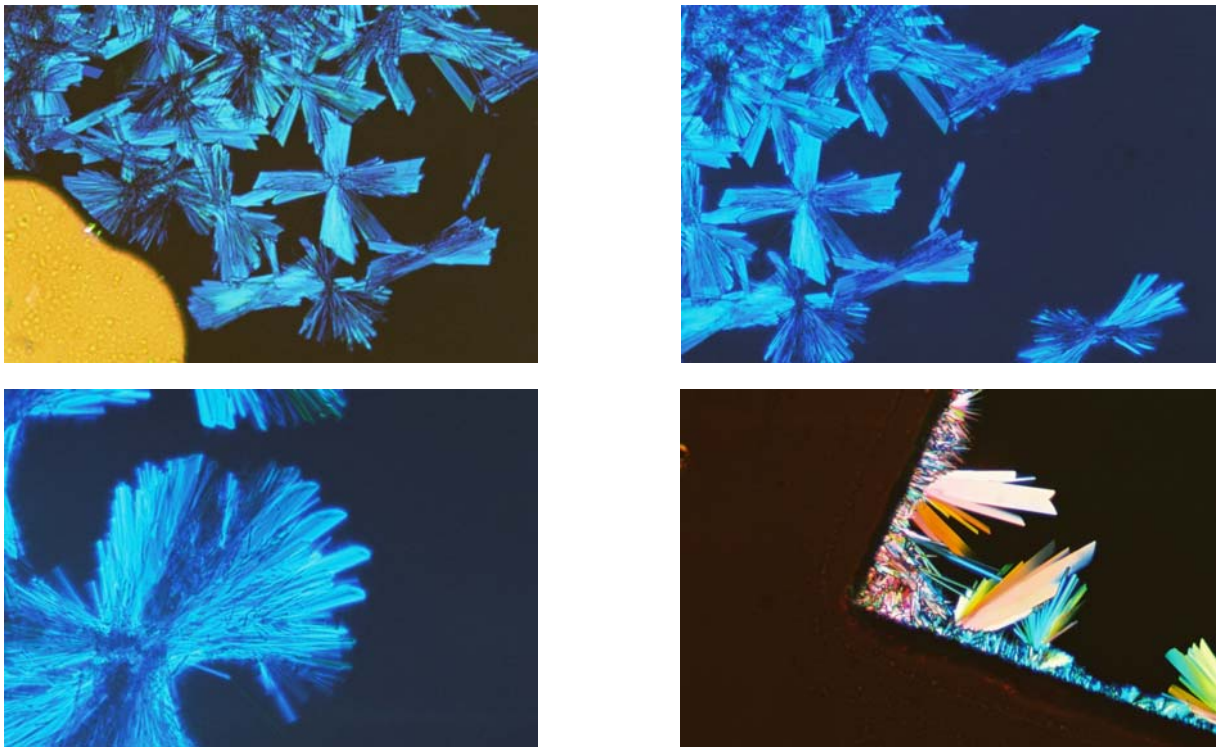

Image 12 **Microscopic images of crystals of ZnPc 70 obtained from a 1,4-dioxane solution upon slow evaporation.**

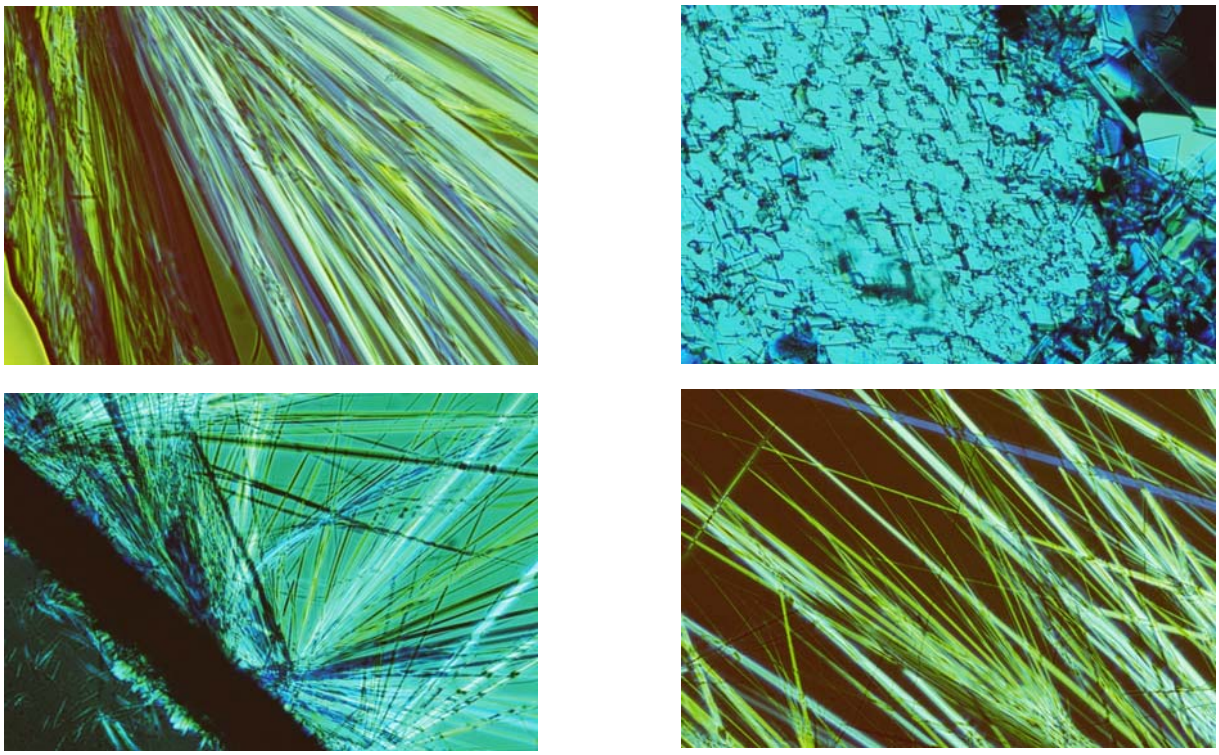

Image 13 **Microscopic images of crystals of ZnPc-*op*-CH_2OTBDPS 34 obtained from a 1,4-dioxane solution upon slow evaporation.**

X-RAY STRUCTURES

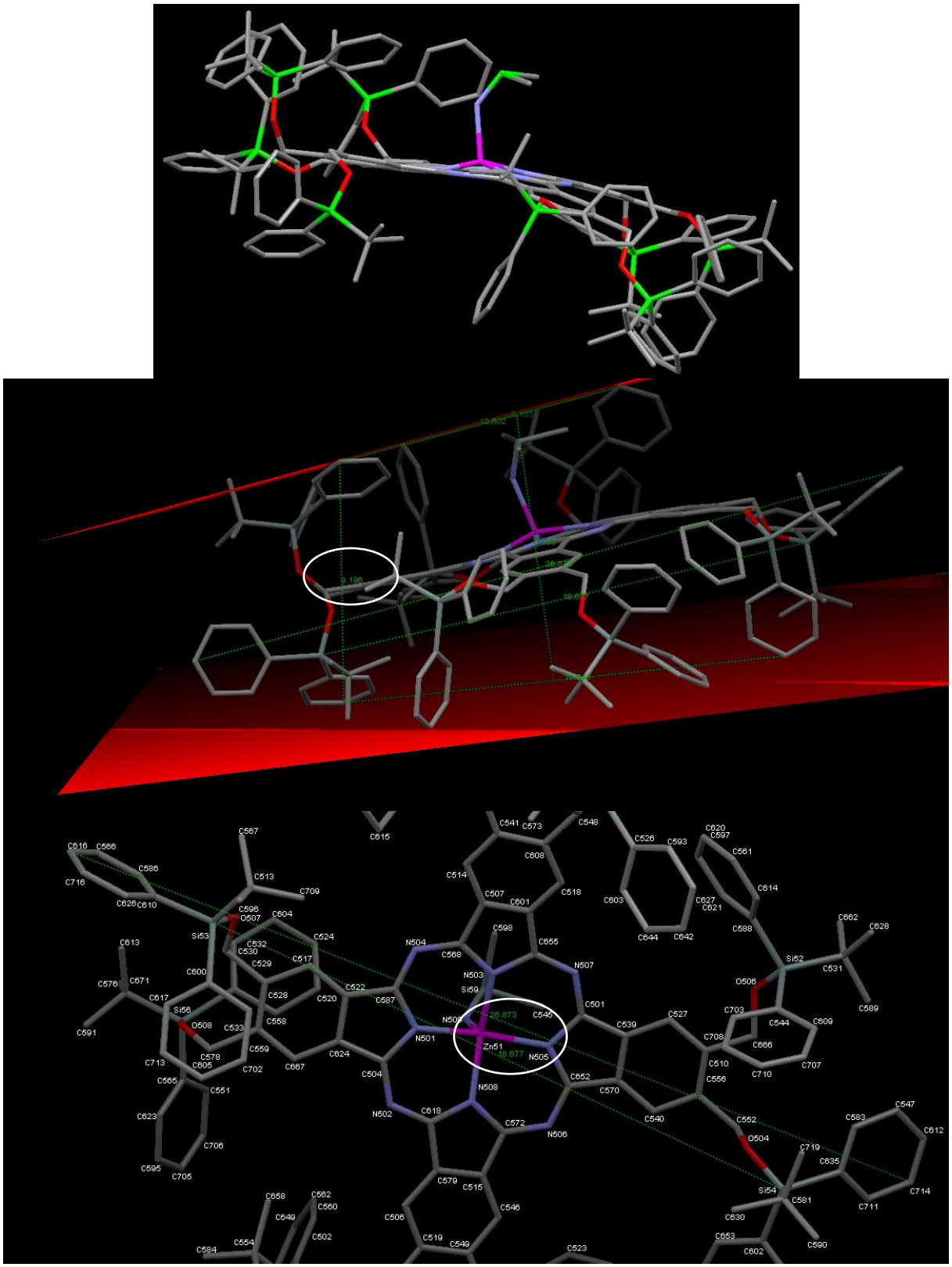

Figure 79 **X-ray structure analysis of *a*-((CH$_3$)$_2$Si=NH)ZnPc-*op*-CH$_2$OTBDPS (33): coordinated Zn (pink) lays above the Pc-core which is slightly distorted. Max. vertical distance 0.92 nm (between red planes). Max. horizontal distance 2.7 nm (C616-C714); 1.9 nm (Si53-Si54).**

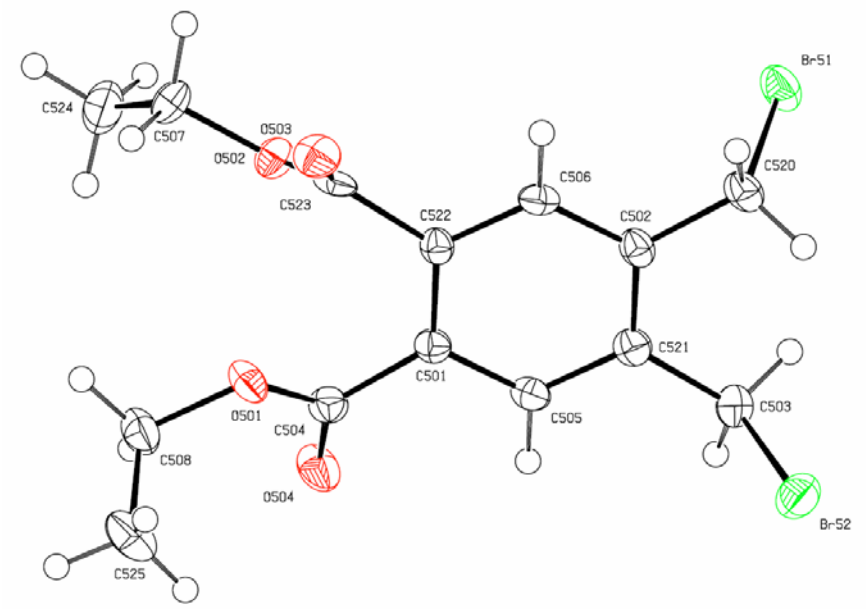

Figure 80 **X-ray structure of 82 shows the electron rich substituents (Br, C=O) alternating above and below the aromatic ring.**

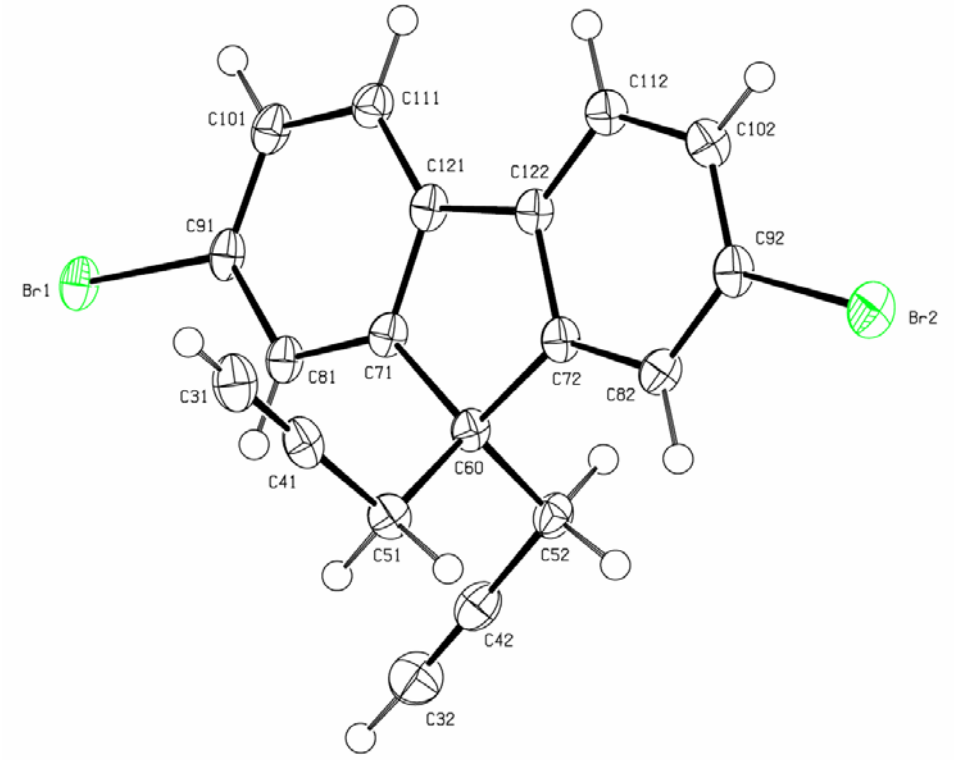

Figure 81 **X-ray structure of 86.**

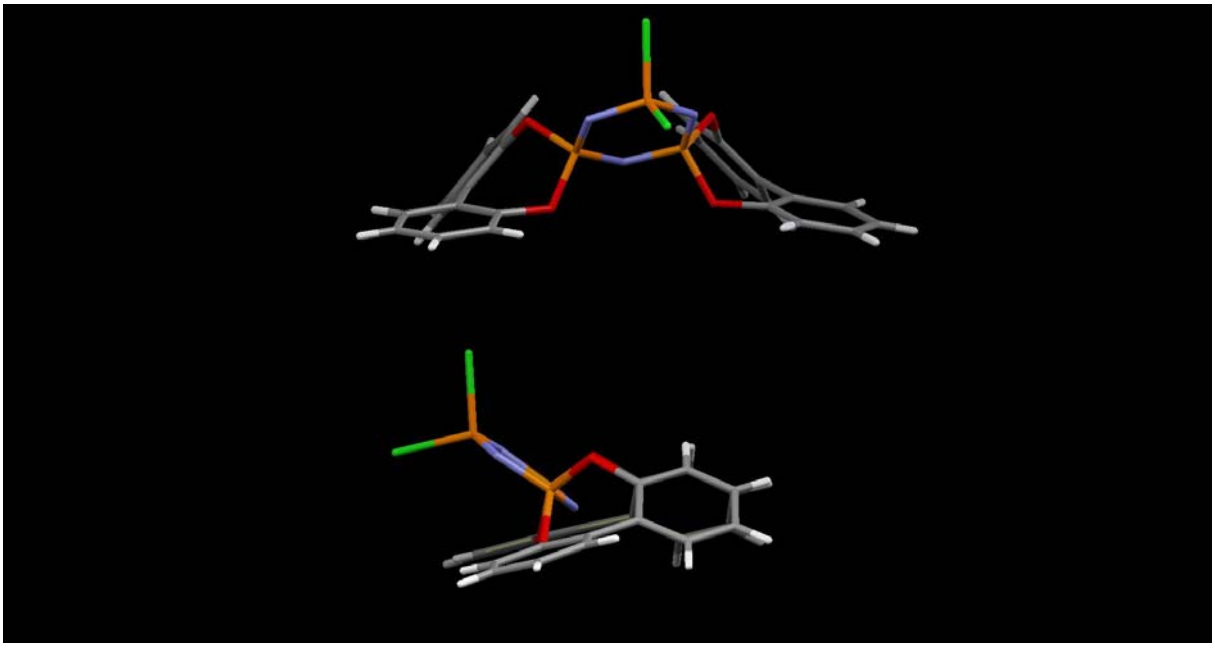

Figure 82 **X-ray structure of 3 showes the twistes biphenol unit and the planar N_3P_3-ring. Atom colors: Cl…green; P…orange; N…violet; O…red; C…grey; H…white.**

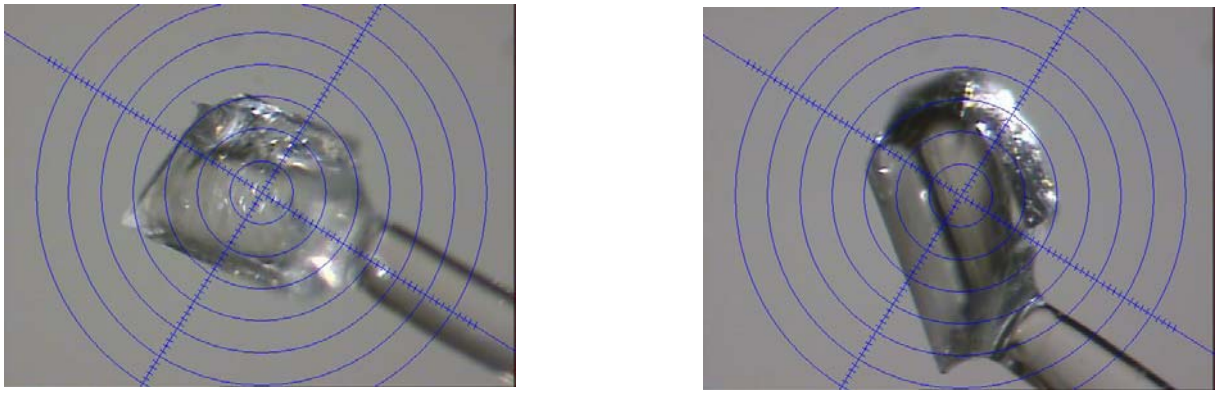

Image 14 **Single crystal for X-ray analysis of dichloro dispiro[6.6]phosphazene 3 (viewing angle 0° and 90°).**

APPENDIX

ABBREVIATIONS

$[\alpha]_{546nm}^{20°C}$	angle of rotation of polarized light (546 nm) at 20 °C
$[M]^{\bullet+}$	cationic radical of molecule
$\tilde{\nu}$	wave number (cm^{-1})
°C	degree **C**elsius
μ	micro- (1×10^{-6})
μg	micro**g**ram (1×10^{-6} gram)
μM	1×10^{-6} mol per liter, 1×10^{-6} millimol per milliliter
^{13}C	**c**arbon isotope
^{1}H	**h**ydrogen isotope
428	lot number; refers to substance **33**
488	lot number; refers to substance **34**
Å	**Å**ngström (1×10^{-10} m)
a.u.	**a**rbitary **u**nits
Ac	**ac**etyl
AcN	**ac**eto**n**itrile
Al	**al**uminum
AM	**a**mmonium **m**olybdate
amu	**a**tom **m**ass **u**nit
aq.	**aq**ueous
b	**b**roadened
Baytron P®	conductive polymer
bp.	**b**oiling **p**oint
BTAF	**b**enzyl **t**rimethyl **a**mmonium **f**luoride
c	**c**oncentration (mg/mL)
C,H-COSY	two dimensional heteronuclear **co**rrelated **s**pectroscop**y**
C_6D_6	deuterated benzene
calc.	**calc**ulated
$CDCl_3$	deuterated chloroform

$CHCl_3$	chloroform
conc.	**conc**entrated
COSY	**co**rrelated **s**pectroscop**y**
$CuSO_4 \bullet 5H_2O$	copper sulfate penta hydrate
CV	**c**yclic **v**oltammogram
d	**d**ay(s)
D	**d**euterium
d	**d**oublet
D	**d**extrorotatory
DCM	**di**chloro**m**ethane
dd(d)	**d**oublet of **d**oublet (of **d**oublet)
dec.	**dec**omposition
DMF	*N*,*N*-**d**i**m**ethyl**f**ormamide
DMF-d_7	**d**euterated *N*,*N*-**d**i**m**ethyl**f**ormamide
DMP	**D**ess-**M**artin **p**eriodinane
DMSO	**di**methyl **s**ulf**o**xide
DMSO-d_6	**d**euterated **di**methyl **s**ulf**o**xide
-d_x	**d**euterated **x**-fold
EA	**e**thyl **a**cetate
EL	**e**lectro **l**uminescence
Et_2O	di**et**hyl ether
EtOH	**et**han**o**l
FAB^+	**f**ast **a**tom **b**ombardment positive ion mode
F_c	**f**actor of **c**learance
Fc	**f**erro**c**ene
Fc^+	ferrocenium cation
GM1	the "prototype" ganglioside, (monosialotetrahexosylganglioside)
h	**h**our(s)
HCl	**h**ydro**ch**l**l**oric acid
HH-COSY	two dimensional homonuclear **co**rrelated **s**pectroscop**y**
HMQC	**h**eteronuclear **m**ulti **q**uantum **c**oherence
HOAc	**ac**etic acid

HOMO	**h**ighest **o**ccupied **m**olecular **o**rbital
HRMS	**h**igh **r**esolution **m**ass **s**pectroscopy
HSQC	**h**eteronuclear **s**ingle **q**uantum **c**oherence
Hz	**H**ert**z**
Ig (-A, B, …M)	**I**mmuno**g**lobulin domains (-A, B, …M)
IR	**i**nfra **r**ed
ITO	**i**ndium **t**in **o**xide
L	liter (dm^3)
LC-MS	**l**iquid **c**hromatography **m**ass **s**pectroscopy
LUMO	**l**owest **u**noccupied **m**olecular **o**rbital
M	**m**olarity [mol/L]
m	**m**ultiplet
m	**m**illi- (1×10^{-3})
m/z	**m**ass-to-charge ratio
MALDI-TOF	**m**atrix **a**ssisted **l**aser **d**esorption **i**onisatio – **t**ime **o**f **f**light
m_c	**c**entered **m**ultiplet
MeOH	**me**than**o**l
mg	**m**illi**g**ram (1×10^{-3} gram)
MHz	**m**ega **h**ert**z**
mL	**m**illi**l**iter (1×10^{-3} liter)
mM	1×10^{-3} mol per liter
mmol	**m**illi**mol** (1×10^{-3} mol)
mol	6.022×10^{23} molecules
mp.	**m**elting **p**oint
MS	**m**ass **s**pectroscopy
MS	**m**olecular **s**ieve
M*t*BE	**m**ethyl ***t**ert*-**b**utyl **e**ther
N	**n**ormal (mol per liter)
n	**n**ano- (1×10^{-9})
n-	linear
Na_2SO_4	sodium sulphate
NaCl	sodium **ch**l**o**ride

NaOH	sodium **h**ydr**o**xide
NaOMe	sodium **me**th**o**xide
NMR	**n**uclear **m**agnetic **r**esonance
o.th.	**o**f **th**eory
-OAc	$-OC(O)CH_3$
OLED	**o**rganic **l**ight **e**mitting **d**evice
op	**o**cta **p**eripheral
PBS	**p**hosphate **b**uffered **s**aline
Pc	**p**hthalo**c**yanine
Pd/C	**p**alla**d**ium on **c**arbon
PDC	**p**yridinium **di**c**h**romate
PE	**p**etrol**e**ther (bp. 40 – 70 °C)
pH	**p**otential of **h**ydrogen
PL	**p**hoto **l**uminescence
PMDA	**p**yro**m**ellitic **di**a**n**hydride
ppm	**p**arts **p**er **m**illion
Pt	**p**la**t**inum
p-TsOH•H_2O	***para*-t**oluene **s**ulfonic acid monohydrate
Py	**py**ridine
q	**q**uadruplet
quint	**quint**et
rel.int.	**rel**ative **int**ensity
R_f	**r**etention **f**actor (cm/cm)
rpm	**r**ounds **p**er **m**inute
R_t	**r**etention **t**ime (minutes)
s	**s**ingulet
s	**s**econd(s)
sat.	**sat**urated
sept	**sept**et
sext	**sext**et
SQRT	**sq**uare **r**oo**t**
t	**t**riplet

t-, *tert*-	**tert**iary
TBAF	*N*,*N*,*N*,*N*-**t**etra**b**utyl **a**mmonium **f**luoride
TBAP	*N*,*N*,*N*,*N*-**t**etra**b**utyl **a**mmonium hexafluoro**p**hosphate
TEA	*N*,*N*,*N*-**t**ri**e**thyl **a**mine
THF	**t**etra**h**ydro**f**urane
TLC	**t**hin **l**ayer **c**hromatography
TsCl	**t**o**s**yl **c**h**l**oride
tt	**t**riplet of **t**riplet
UV-vis	**u**ltra**v**iolet-**vis**ible
V	**V**oltage, electric potential
vol.%	percentage of volume by volume (v/v)
vs.	***vers****us*
wt.%	percentage of **w**eigh**t** by weight (w/w)
^{x}J	coupling constant along **x** numbers of covalent bonds
X-ray	diffraction of roentgen ray
Zn	**z**i**n**c
α	alpha stereoisomere
β	beta stereoisomere
δ	shift in ppm
ε_x	extinction coefficient (L / cm·mol) at a wavelength of x (nm)
λ_{max}	wavelength of maximal absorption (nm)

CHEMICALS

NAME	Risiken	Sicherheitsmaßnahmen
1,1,1,3,3,3-Hexamethyldisilazan [F, Xn]	R 11-20/21/22-36/37/38	S 16-36/37
1,4-Dioxan [F, Xn]	R 11-19-36/37-40-66	S 9-16-36/37-46
4-(Dimethylamino)-pyridin [T]	R 25-36/38	S 37-45
Acetanhydrid [C]	R 10-20/22-34	S (1/2-)26-36/37/39-45
Aceton [F, Xi]	R 11-36-66-67	S 9-16-26
Acetonitril [F, T]	R 11-23/24/25	S 16-27-45
Acetylchlorid [F, C]	R 11-14-34	S 9-16-26-45
Ammoniaklösung 32 % [C, N]	R 34-50	S 26-36/37/39-45-61
Ammoniummolybdat [Xi]	R 36/37/38	S 26-36
Benzol [F, T]	R 45-11-48/23/24/25	S 53-45
Benzyloxyacetylchlorid [C]	R 34-37	S 26-36/37/39-45
Buttersäureanhydrid [C]	R 34	S 26-36/37/39-45
Chloroform [Xn]	R 22-38-40-48/10/22	S 36/37
Dichlormethan [Xn]	R 40	S 23.2-24/25-36/37
Diethylether [F+, Xn]	R 12-19-22-66-67	S 9-16-29-33
Dimethylsulfoxid [Xi]	R 36/38	S 26
Essigsäure [C]	R 10-35	S 23.2-26-45
Essigsäureanhydrid [C]	R 10-34	S 26-45
Ethanol [F]	R 11	S 7-16
Ethanthiol [F, Xn, N]	R 11-20-50/53	S 16-25-60-61
Ethylacetat [F, Xn]	R 11-36-66-67	S 16-26-33
Imidazol [C]	R 22-34	S 22-26-36/37/39-45
Kaliumcarbonat [Xi]	R 36/37/38	S 22-26
Kupfersulfatpentahydrat [Xn,N]	R 22-36/38-50/53	S 22-60-61
Lithiumaluminiumhydrid [F]	R 15	S 24/25-43.12-7/8
Methanol[F, T]	R 11-23/24/25-39	S 7-16-36/37-45
Methansulfonsäure [C]	R 34	S 26-36-45
Natriumazid [T+, N]	R 28-32-50/53	S 28.1-45-60-61
Natriumcyanoborhydrid [F, C]	R 15-32-34	S 26-36/37/39-43-45
Natriumhydroxid [C]	R 45	S 26-37/39-45
Natriummethanolat [F, C]	R 11-14-34	S 8-26-43.6-45
N-Bromsuccinimid [Xn]	R 22-36/37/38	S 26-36
n-Butanol [Xn]	R 10-20	S 16
n-Hexane [F, Xn, N]	R 11-38-48/20-51/53-62-65-67	S 9-16-29-33-36/37-61-62
Ninhydrinlösung [F, Xi]	R 11-36-67	S 7-16-23.3-24-26-51
Petrolether 50-70 [F, Xn]	R 11-52/53-65	S 9-16-23.2-24-33-62
Pivalinsäurechlorid [F, C]	R 11-34-36/37	S 16-26-36/37/39-45
p-Nitrophenol [Xn]	R 20/21/22-33	S 28.1
Propionsäureanhydrid [C]	R 34 S 26-45	
p-Toluolsulfonsäure-Monohydrat [Xi]	R 36-37-38	S 27-37
Pyridin [F, Xn]	R 11-20/21/22	S 26-28.1
Salzsäure [C]	R 34-37	S 26-36/37/39-45

Schwefelsäure [C]	R 35	S-26-30-45
Tetrabutylammoniumbromid [Xi]	R 36/37/38	S 26-36
Tetrahydrofuran [F, X]	R 11-19-36/37	S 16-29-33
Thiophenol [T+]	R 10-24/25-26-36/38	S 26-28.1-36/37-45
Toluol [F, Xn]	R 11-20	S 16-25-29-33
Triethylamin [C, F]	R 11-20/21/22-35	S 3-16-26-29-36/37/39-45
Triflatanhydrid [C]	R 22-35	S 26-30-36/37/39-45
Trifluoressigsäure [C]	R 20-35-52/53	S 9-26-27-28.1-45-61
Trifluoressigsäureanhydrid [C]	R 14-20-35-52/53	S 9-26-36/37/39-45-61
Trimethylorthobutyrat [F, Xi]	R 11-36/38	S 9-16
Trimethylsilyltriflat [C]	R 10-34-37	S 26-36/37/39-45
Triphenylmethylchlorid [C]	R 34	S 26-36/37/39-45
Vinylacetat [F]	R 11	S 16-23.2-29-33
Wasserstoff [F]	R 12	S 9-16-33
Zinkacetat [Xn, N]	R 22-36-50/53	S 26-60-61

DANKSAGUNG

Da so eine Arbeit nicht im luftleeren Raum entstanden ist, möchte ich mich an dieser Stelle an die handelnden Personen dieses, meines Lebensabschnittes der Promotion wenden und ihnen meine Dankbarkeit bekunden!

Mein erster Dank gebührt natürlich Dr. Schotten. Er hat mir überhaupt erst die Möglichkeit geboten dieses interessante Thema zu bearbeiten. Dr. Mark Tebbe möchte ich für die Durchsetzung der Finanzierung meiner Promotion bei der Geschäftsführung von Lilly danken. Prof. J. Thiem gilt mein besonderer Dank dafür, daß er, ohne mich zu kennen, sich bereit erklärte die akademische, „schützende Hand" über mich zu halten und dies auch in besonders schwierigen Zeiten, in „blindem" Vertrauen in mich, getan hat.

Dem Hühnerstall – Angelika, Karin und Kiki – des „Schottenlabors" bei Lilly danke ich für den Einblick in den professionellen Laboralltag in einem amerikanisch geführten, globalen Unternehmen, die persönliche Unterstützung während meiner Zeit bei Lilly und auch noch lange danach.

In dankbarer Erinnerung bin ich den vielen „Lillyputanern" verbunden, von denen ich viel lernen konnte, die auch so entscheidend für meine gute Stimmung bei Lilly gesorgt haben und die sich auch meiner Sache angenommen haben, wenn's mal notwendig war.

Dem Lilly-Betriebsrat darf ich danken, weil er mich tatsächlich davon überzeugen konnte, daß ich es an der Uni besser haben würde!

An meine „neuen Spielkamerad-Innen" des AK-Thiem geht auch ein herzliches Dankeschön, da sie mich so freundschaftlich aufgenommen haben und mich als α-Männchen akzeptierten – allen voran natürlich meine Lieblings-Janna.

Den anderen Arbeitskreisen (OC, AC, PC, BC) danke ich für die gelebte Kollegialität, weil sie mich nie haben spüren lassen, daß ich eigentlich ein Österreicher bin:
→ „Man muß Ihn nicht immer verstehen!"

Dr. Sinnwell und seinen Mitarbeiterinnen möchte ich nicht nur für den, durch mich überdurchschnittlichen genutzen NMR-Service danken, sondern auch, daß sie mir meinen großen Fauxpas letztendlich doch, großmütig und ohne Worte, verziehen haben. Ich bin aber noch immer davon überzeugt, daß etwas mehr zwischenmenschliche Kommunikation nicht schaden würde. Explizit möchte ich Dr. Sinnwell für die unzähligen NMR-Privatissima danken, wodurch mir so manches verständlicher wurde.

Für Expressmessungen und exotische NMRs danke ich Dr. Haupt und seinen Mitarbeiterinnen.

Der MS-Service hat durch das persönliches Engagement von Frau Meiners und die fachkundigen Ausführungen in den persönlichen Gesprächen mit Dr. Franke nachhaltig Eindruck gemacht hat.

Prof. Kopf und Frau Nevoigt verdanke ich meine spektakulären X-rays!

Prof. Francke und Prof. Meier waren mir sehr hilfreiche Ansprechpartner rund ums Thema Uni und haben mir unter anderem die menschliche Seite des Uni-Betriebs vermittelt.

Mein besonderer Dank gilt weiters jenen Wissenschaftlern und Experten, durch die meine Arbeit erst jene intellektuelle Breite bekommen hat, die ich auch anstrebte. Ohne deren Mithilfe und Engagement ich nie so weit gekommen wäre und all das lediglich für Gottes Lohn und meine ewige Dankbarkeit gemacht haben:
Dr. Stephan A. Benning und Prof. Dr. Kitzerow (Univ. Paderborn) danke ich für die physiko-chemischen Untersuchungen der Verbindungen **33** und **34**.
Dr. Nollau (UKE-Hamburg), Dr. Ziegelmüller und Daniel Dauch (Biochemie Univ. Hamburg) möchte ich für die Unterstützung bei den ersten Tests mit Verbindung **81** an HepG2 Zellen danken.
Dr. Jan Niehaus (Univ. Hamburg) danke ich für die Unterstützung bei den ersten UV-vis und Fluoreszenzspektren meiner neuartigen Phthalocyanine.
Herrn Thomas Schuld (Univ. Hamburg) danke ich für die mit viel Geduld ausgeführten CV-Messungen.

Frau Nadine Albrecht, Frau Dr. Astrid Tannert und Prof. Dr. med. Schäfer (Charité / FU-Berlin) danke ich für die Gastfreundschaft, die äußerst unkomplizierte Zusammenarbeit und den unermüdlichen Einsatz bis zur letzten Minute, um innerhalb von fünf Tagen die ersten Erkenntnisse über die Verbindung **81**, bezüglich *in vitro* Aktivität, zu erlangen.
Meinem Kollegen Sven Gerber und Prof. Dr. Volkmar Vill danke ich für die unzähligen Stunden, die sie mit mir am Mikroskop zugebracht haben, um die äußerst eindrucksvollen Mikroskopiebilder zu präparieren und aufzunehmen.

Meinen Praktikanten danke ich dafür, daß sie meine „schwarze Pädagogik“ so geduldig über sich haben ergehen lassen und mir das Gefühl vermittelten, doch nicht umsonst etwas länger studiert zu haben: Annika Frank, Wie-Nien Liao, Katharina Götz, Carsten Schulz, Claudia Schwolow, Tim Raiber, *Bernhard* Bugenhagen & Ariane (*Bianca*) Munk, Adina Jung und Johanna Huchting.

Man mag es kaum glauben, aber es gibt auch für mich so was wie ein Privatleben und an dieser Stelle möchte ich auch meinen Freund-Innen ein paar Zeilen widmen:
Tom der Weltmeister, Stepan Simonyan der russisch-armenische Klavierspieler, Jule die Sportlerin, Catti die Architektin, Michael das Entchen, Heike mein Liebstes, CarO und Julia die Physios, Silvi die Lehrerin, Fritz – DIFriPi – meinem letzten, treuen Gefährten aus der Heimat und Hexe meine kleine, vierbeinige, schwarzhaarige Liebe mit Bikinifigur.

Zu guter Letzt danke ich meiner Mutter und Rudi, die immer an meinen Erfolg glaubten und mich so geduldig unterstützt haben!

LEBENSLAUF

Vornamen	Herwig, Josef
Familienname	Berthold
Geburtsdatum	01. Mai 1972
Geburtsort	Graz
Familienstand	Ledig
Nationalität	Österreichischer Europäer
Berufliche Abschlüsse	Diplomstudium Technische Chemie Ingenieursstudium Maschineningenieurwesen Angestellter der Fa. Metall-Chemie Hamburg (seit 03.2008)
Positionen	Wissenschaftlicher Mitarbeiter an der Universität Hamburg, Department Chemie
Ausbildung	
03.2006 - 06.2008	**Universität Hamburg** Promotion
03.2003 - 02.2006	**Lilly Forschung GmbH Hamburg** Promotion Aufbau des ***S**ample-**M**anagement-**C**enter*
02.2003	**Technische Universität Graz** Diplom für Technische Chemie
03.-09.2002	**Lilly Forschung GmbH Hamburg** Diplomarbeit *„Microwaves in Organic Synthesis“*
01.-07.2000	**Lunds Universitet** (Schweden) Forschungspraktikum (Erasmus) *Porphyrinsynthese*
10.1992	**Technische Universität Graz** Studium der Technischen Chemie
09.1991 - 10.1992	**Diverse Arbeitsverhältnisse** Schaffung eines Startkapitals zur Finanzierung meines Studiums
06.1991	**Höhere technische Bundeslehranstalt** für Maschineningenieurwesen Salzburg Ingenieursstudium und Abitur

EIDESSTATTLICHE ERKLÄRUNG

Hiermit erkläre ich an Eides statt, daß ich die vorliegende Dissertation *„Synthesis of a Phthalocyanine Scaffold as a Core of Highly Glycosylated Dendritic Structures and a Novel Fluorenyl Spiro-Annelated Phthalocyanine"* selbständig angefertigt und nur die von mir angegebenen Quellen und Hilfsmittel verwendet habe.

Ich erkläre außerdem, daß diese Dissertation weder in gleicher noch in anderer Form bereits in einem anderen Prüfungsverfahren vorgelegen hat.

Hamburg, im Juni 2008

Herwig BERTHOLD

LITERATURE

[1] Emmelius, M.; Pawlowski, G.; Vollmann, H. W. *Angew. Chem. Int. Ed.* **1989**, *28*, 1445.
[2] Roth, K. *Chem. Unserer Zeit* **2007**, *41*, 334.
[3] McKeown, Neil B., *Phthalocyanine materials: Synthesis, Structure and Function, Vol. 6*, Cambridge University Press, **1998**.
[4] Leznoff, C. C.; Lever, A. B. P. *Phthalocyanines: Properties and Applications Vol. 1-4* VCH, New York, **1989**, **1993**, **1993**, **1996**.
[5] Saini, S. K.; Jena, A.; Dey, J.; Sharma, A. K.; Singh, R. *Magn. Reson. Imaging* **1995**, *13*, 985.
[6] Bonnett, R. *J. Heterocyclic Chem.* **2002**, *39*, 455.
[7] Bonnett, R. *Chem. Soc. Rev.* **1995**, *24*, 19.
[8] Lee, P. P. S.; Ngai, T.; Huang, J.-D.; Wu, C.; Fong, W.-P.; Ng, D. K. P *Macromolecules* **2003,** *36*, 7527.
[9] Lo, P.-C.; Chan, C. M. H.; Liu, J.-Y.; Fong, W.-P.; Ng, D. K. P. *J. Med. Chem.* **2007**, *50*, 2100.
[10] Dandridge, A. G.; Drescher, H. A. E.; Thomas, J. *GB 322169* **1928**; *Chem. Abstr.* 24:27384.
[11] Barton, D. H. R.; Raydon, H. N.; Elvidge, J. A. *Biographical Memoirs of Fellows of the Royal Society* **1968**, *14*, 309.
[12] Linstead, R. P. *J. Chem. Soc.* **1934**, 1016.
[13] Byrne, G. T.; Linstead, R. P.; Lowe, A. R. *J. Chem. Soc.* **1934**, 1017.
[14] Linstead, R. P.; Lowe, A. R. *J. Chem. Soc.* **1934**, 1022.
[15] Dent, C. E.; Linstead, R. P. *J. Chem. Soc.* **1934**, 1027.
[16] Hueckel, E. *Zeitschrift f. Physik* **1931**, *70*, 204.
[17] Pawlowski, G.; Hanack, M. *Synthesis* **1980**, 287.
[18] Yildiz, S. Z.; Gök, Y. *New. J. Chem.* **1998**, *22*, 1365.
[19] Lowery, M. K.; Starshak, A. J.; Esposito, J. N.; Krueger, P. C.; Kenny, M. E. *Inorg. Chem.* **1965**, *4*, 128.
[20] Cabezón, B.; Quesada, E.; Esperanza, S.; Torres, T. *Eur. J. Org. Chem.* **2000**, 2767.
[21] Cong, F.-D.; Ning, B.; Du, X.-G.; Ma, C.-Y.; Yu, H.-F.; Chen, B. *Dyes and Pigments* **2005**, *66*, 149.
[22] Venugopala Reddy, K. R.; Keshavayya, J. *Dyes and Pigments* **2002**, *53*, 187.
[23] Metz, J.; Schneider, O.; Hanack, M. *Inorg. Chem.* **1984**, *23*, 1065.
[24] Uchida, H.; Yoshiyama, H.; Reddy, P. Y.; Nakamura, S.; Toru, T. *Synlett* **2003**, *13*, 2083.
[25] Joyner, R. D.; Kenney, M. E. *J. Am. Chem. Soc.* **1960**, *82*, 5790.
[26] Cariati, F.; Galizzioli, D.; Morazzoni, F.; Busetto, C. *J. Chem. Soc. Dalton Trans.: Inorg. Chem.* **1975**, *7*, 556.
[27] Robertson, M. J. *J. Chem. Soc.* **1935**, 615.
[28] Huang, J.-D.; Wang, S.; Lo, P.-C.; Fong, W.-P.; Kod, W.-H.; Ng, D. K. P. *New. J. Chem.* **2004**, *28*, 348.
[29] de la Torre, G.; Vázquez, P.; Agulló-López, F.; Torres, T. *J. Mater. Chem.* **1998**, *8*, 1671.
[30] Cole, A.; McIlroy, R. J.; Thorpe, S. C.; Cook, M. J.; McMurdo, J.; Ray, A. K. *Sensors and Actuators, B* **1993**, *13*, 416.
[31] Loutfy, Rafik O.; Sharp, James H. *J. Phys. Chem.* **1978**, *82*, 2787.
[32] Morenzin, J. *Berichte d. Forschungszentrum Juelich* **1999**, *Juel-3730*, 1.
[33] Iwase, T.; Haga, Y. *J. Mater. Sci.: Materials in Electronics* **2004**, *15*, 617.
[34] Chen, Y.; Zhuang, X.; Zhang, W.; Liu, Y.; Lin, Y.; Yan, A.; Araki, Y.; Ito, O. *Chem. Mater.* **2007**, *19*, 5256.
[35] Riess, W.; Beierlein, T. A.; Riel, H. *Physica Status Solidi A: Applied Research* **2004**, *201*, 1360.
[36] Toshima, N.; Kawamura, S.; Tominaga, T. *Chem. Lett.* **1993**, *8*, 1299.
[37] Ohkubo, K.; Takano, K. *J. Coord. Chem.* **1985**, *14*, 169.
[38] Baffou, G.; Mayne, A. J.; Comtet, G.; Dujardin, G.; Sonnet, Ph.; Stauffer, L. *Appl. Phys. Lett*. **2007**, *91*, 073101-1.
[39] Kolotovska, V.; Friedrich, M.; Zahn, D. R. T.; Salvan, G. *J. Cryst. Growth* **2006**, *291*, 166.
[40] Wan, S.; Parrish, J. A.; Anderson, R. R.; Madden, M. *Photochem. Photobio.* **1981**, *34*, 679.
[41] Fabris, C.; Ometto, C.; Milanesi, C.; Jori, G.; Cook, M. J.; Russell, D. A. *J. Photochem. Photobiol., B: Biol.* **1997**, *39*, 279.
[42] Ambroz, M.; Beeby, A.; MacRobert, A. J.; Simpson, M. S. C.; Svensen, R. K.; Phillips, D. *J. Photochem. Photobiol., B: Biol*. **1991**, *9*, 87.
[43] Stranadko, E. P.; Skobelkin, O. K.; Litvin, G. D.; Astrakhankina, T. A. *Proceedings of SPIE-The Int. Soc. for Optical Engineering* **1996**, *2625*, 440.
[44] Leznoff, C. C.; D'Ascanio, A. M.; Yildiz, S. Z. *J. Porphyrins Phthalocyanines* **2000**, *4*, 103.
[45] Leznoff, C. C.; Hu, M.; Nolan, K. J. M. *Chem. Commun.* **1996**, *10*, 1245.

[46] Moor, A. C. E.; Wagenaars van Gompel, A. E.; Hermanns, R. C. A.; van der Meulen, J.; Smit, J.; Wilschut, J.; Brand, A.; Dubbelman, T. M. A. R.; Van Steveninck, J. *Photochem. Photobiol.* **1999**, *69*, 353.
[47] Schmidt, I.; Jiao, J.; Thamyongkit, P.; Sharada, D. S.; Bocian, D. F.; Lindsey, J. S. *J. Org. Chem.* **2006**, *71*, 3033.
[48] Torres, T. *J. Porphyrins Phthalocyanines* **2000**, *4*, 325.
[49] Bonnett, R.; Okolo, K. *J. Porphyrins Phthalocyanines* **1999**, *3*, 530.
[50] Dabak, S.; Bekaroglu, O. *J. Chem. Res.* **1997**, 8.
[51] Bonnett, R.; McManus, K. A. *J. Chem. Soc., Perkin Trans. 1* **1996**, *20*, 2461.
[52] The rights were aquired by Axcan Pharma Inc. (Mont-Saint-Hilaire, Quebec)
[53] Lipinski, Christopher A.; Lombardo, Franco; Dominy, Beryl W.; Feeney, Paul J. *Adv. Drug Deliv. Rev.* **1997**, *23*, 3. reprinted: *Adv. Drug Deliv. Rev.* **2001**, *46*, 3.
[54] Breunig, M.; Bauer, S.; Goepferich, A. *Eur. J. Pharm. Biopharm.* **2008**, *68*, 112.
[55] Sears, P.; Wong, C.-H. *Angew. Chem. Int. Ed.* **1999**, *38*, 2300.
[56] Sears, P.; Wong, C.-H. *Cell. Mol. Life Sci.* **1998**, *54*, 223.
[57] Lis, H.; Sharon, N. *Eur. J. Biochem.* **1993**, *218*, 1.
[58] Varki, A. *Glycobiology* **1993**, *3*, 97.
[59] Mammen, M.; Choi, S.-K.; Whitesides, G. M. *Angew. Chem. Int. Ed.* **1998**, *37*, 2754.
[60] Fukuda, M. *New Comprehensive Biochemistry* **1996**, *30*, 311.
[61] Weber, G. *Adv. Protein Chem.* **1975**, *29*, 1.
[62] Green, N. M. *Adv. Protein Chem.* **1975**, *29*, 85.
[63] Dimmock, N. J. *Trends Biochem. Sci.* **1987**, *12*, 70.
[64] Boyce, N. W.; Holdsworth, S. R. *Kidney Int.* **1989**, *36*, 537.
[65] Dower, S. K.; DeLisi, C.; Titus, J. A.; Segal, D. M. *Biochemistry* **1981**, *20*, 6326.
[66] Engelhardt, W.; Gorczytza, H.; Butterweck, A.; Moenkemann, H.; Frey, J. *Eur. J. Immunol.* **1991**, *21*, 2227.
[67] Indik, Z. K.; Park, J. G.; Hunter, S.; Schreiber, A. D. *Blood* **1995**, *86*, 4389.
[68] Lee, Y.; Lee, R.; *Acc. Chem. Res.* **1995**, *28*, 321.
[69] Firpo, P. P.; Axberg, I.; Scheibel, M.; Clark, E. A. *AIDS Res. Hum. Retroviruses* **1992**, *8*, 357.
[70] Glick, G.; Knowles, J. R. *J. Am. Chem. Soc.* **1991**, *113*, 4701.
[71] Glick, G. D.; Toogood, P. L.; Wiley, D. C.; Skehel, J. J.; Knowles, J. R. *J. Biol. Chem.* **1991**, *266*, 23660.
[72] Lee, R. T.; Lee, Y. C. *Neoglycoconjugates: Preparation and Applications* **1994**, 23.
[73] Park, J.-H.; Kim, K. L.; Cho, E.-W. *Biotechnology Lett.* **2006**, *28*, 1061.
[74] Baenzigesr, J. U.; Maynard, Y. *J. Biol. Chem.* **1980**, *255***,** 4607.
[75] Pricer, W. E. Jr.; Hudgin, R. L.; Ashwell, G.; Stockert, R. J.; Morell, A. G. *Methods Enzymol.* **1974**, *34*, 688.
[76] Treichel, U.; Meyer zum Buschenfelde, K.-H.; Stockert, R. J.; Poralla, T.; Gerken, G. *J. Gen. Virol.* **1994**, *75***,** 3021.
[77] Becker, S.; Spiess, M.; Klenk, H.-D. *J. Gen. Virol.* **1995**, *76*, 393.
[78] Stockert, R. J.; Morell, A. G.; Scheinberg, I. *Science* **1974**, *186*, 365.
[79] Seow, Y.-y. T.; Tan, M. G. K.; Woo, K. T. *Nephron* **2002**, *91*, 431.
[80] Yamamoto, M.; Hayashi, N.; Miyamoto, Y.; Takehara, T.; Mita, E.; Seki, M.; Fusamoto, H.; Kamada, T. *Hepatology* **1995**, *22*, 847.
[81] Wu, G. Y.; Wu, C. H. *Biochemistry* **1988,** *27***,** 887.
[82] Park, J.-H.; Cho, E.-W.; Shin, S. Y.; Lee, Y.-J.; Kim, K. L. *Biochem. Biophys. Res. Commun.* **1998**, *244*, 304.
[83] Lee, P. P. S.; Lo, P.-C.; Chan, E. Y. M.; Fong, W.-P.; Ko, W.-H.; Ng, D. K. P. *Tetrahedron Lett.* **2005**, *46*, 1551.
[84] Singh, M.; Rogers, C. B.; Ariatti, M. *South African J. Sci.* **2007**, *103*, 204.
[85] Hohokabe, M.; Higuchi, Y.; Mukai, H.; Kawakami, S.; Hashida, M. *J. Biomed. Nanotech.* **2007**, *3*, 277.
[86] Satoh, T.; Kakimoto, S.; Kano, H.; Nakatani, M.; Shinkai, S.; Nagasaki, T. *Carbohydr. Res.* **2007**, *342*, 1427.
[87] Marroquin, L. D.; Hynes, J.; Dykens, J. A.; Jamieson, J. D.; Will, Y. *Tox. Sci.* **2007**, *97*, 539.
[88] Plank, C.; Zatloukal, K.; Cotton, M.; Mechtler, K.; Wagner, E. *Bioconjugate Chem.* **1992**, *3*, 533.
[89] Choi, C.-F.; Tsang, P.-T.; Huang, J.-D.; Chan, E. Y. M.; Ko, W.-H.; Fong, W.-P.; Ng, D. K. P. *Chem. Comm.* **2004**, *19*, 2236.
[90] Huang, J.-D.; Fong, W.-P.; Chan, E. Y. M.; Choi, M. T. M.; Chan, W.-K.; Chan, M.-C.; Ng, D. K. P. *Tetrahedron Lett.* **2003**, *44*, 8029.
[91] Lo, P.-C.; Chan, Huang, J.-D.; Cheng, D. Y. Y.; Chan, E. Y. M.; Fong, W.-P.; Ko, W.-H.; Ng, D. K. P *Chem. Eur. J.* **2004**, *10*, 4831.
[92] Law, K.-Y. *Chem. Rev.* **1993**, *93*, 449.

[93]Iino, H.; Hanna, J.; Bushby, R. J.; Movaghar, B.; Whitaker, B. J.; Cook, M. J. *Appl. Phys. Lett.* **2005**, *87*, 132102.
[94] Groothues, H.; Kremer, F.; Schouten, P. G.; Warman, J. M. *Adv. Mater.* **1995**, *7*, 283.
[95] Markovitsi, D., Lecuyer, I., Simon, J. *J. Phys. Chem.* **1991**, *95*, 3620.
[96] Rosenthal, I. *Photochem. Photobiol.* **1991**, *53*, 859.
[97] Nazeeruddin, M. K.; Humphry-Baker, R.; Grätzel, M.; Murrer, B. A. *Chem. Comm.* **1998**, *6*, 719.
[98] Reddy, P. Y.; Giribabu, L.; Lyness, C.; Snaith, H. J.; Vijaykumar, C.; Chandrasekharam, M.; Lakshmikantam, M.; Yum, J.-H.; Kalyanasundaram, K.; Graetzel, M.; Nazeeruddin, M. K. *Angew. Chem. Int. Ed.* **2007**, *46*, 373.
[99] Meunier, B.; Sorokin, A. *Acc. Chem. Res.* **1997**, *30*, 470.
[100] Guillaud, G.; Simon, J.; Germain, J. P. *Coord. Chem. Rev.* **1998**, *178-180*, 1433.
[101] Saini, S. K.; Jena, A.; Dey, J.; Sharma, A. K.; Singh, R. *Magn. Res. Imag.* **1995**, *13*, 985.
[102] Leznoff, C. C.; D'Ascanio, A. M.; Yildiz, S. Z. *J. Porphyrins & Phthalocyanines* **2000**, *4*, 103.
[103] Tomalia, D. A.; Naylor, A. M.; Goddard III, W. A. *Angew. Chem. Int. Ed.* **1990**, *29*, 138.
[104] Hombrecher, H. K.; Schell, C.; Thiem, J. *Bioorg. Med. Chem. Lett.* **1996**, *6*, 1199.
[105] Tomalia, D. A. *Aldrichimica Acta* **1993**, *26*, 91.
[106] Newkome, G. R.; Moorefield, C. N.; Baker, G. R. *Aldrichimica Acta* **1992**, *25*, 31.
[107] Reed, N. N.; Janda, K. D. *Org. Lett.* **2000**, *2*, 1311.
[108] McKeown, N. B.; Helliwell, M.; Hassan, B. M.; Hayhurst, D.; Li, H.; Thompson, N.; Teat, S. J. *Chem. Eur. J.* **2007**, *13*, 228.
[109] Allcock, H. R. *J. Am. Chem. Soc.* **1963**, *85*, 4050.
[110] Allcock, H. R. *J. Am. Chem. Soc.* **1964**, *86*, 2591.
[111] Allcock, H. R.; Stein, M. T.; Stanko, J. A. *J. Am. Chem. Soc.* **1971**, *93*, 3173.
[112] Kajiwara, M.; Saito, H. *J. Inorg. Nucl. Chem.* **1975**, *37*, 29.
[113] Carriedo, G. A.; Fernandez-Catuxo, L.; Alonso, F. J. G.; Gomez-Elipe, P.; Gonzalez, P. A. *Macromolecules* **1996**, *29*, 5320.
[114] Allcock, H. R.; Neenan, T. X. *Macromolecules* **1986**, *19*, 1495.
[115] Ruf, M.; Lawrence, A. M.; Noll, B. C.; Pierpont, C. G. *Inorg. Chem.* **1998**, *37*, 1992.
[116] Vij, A.; Geib, S. J.; Kirchmeier, R. L.; Shreeve, J. M. *Inorg. Chem.* **1996**, *35*, 2915.
[117] Paquette, L. A.; Blankenship, C.; Wells, G. J. *J. Am. Chem. Soc.* **1984**, *106*, 6442.
[118] Kuwajima, I.; Nakamura, E.; Shimizu, M. *J. Am. Chem. Soc.* **1982**, *104*, 1025.
[119] Rivera, J. M.; Martin, T.; Rebek Jr., J. *J. Am. Chem. Soc.* **2001**, *123*, 5213.
[120] Kimura, M.; Narikawa, H.; Ohta, K.; Hanabusa, K.; Shirai, H.; Kobayashi, N. *Chem. Mater.* **2002**, *14*, 2711.
[121] Kaiser, F.; Schwink, L.; Velder, J.; Schmalz, H.-G. *Tetrahedron* **2003**, *59*, 3201.
[122] Wang, C.; Bryce, M. R.; Batsanov, A. S.; Stanley, C. F.; Beeby, A.; Howard, J. A. K. *J. Chem. Soc., Perkin Trans. 2* **1997**, *9*, 1671.
[123] Allevi, P.; Ciuffreda, P.; Longo, A.; Anastasia, M. *Tetrahedron: Asym.* **1998**, *9*, 2915.
[124] Corey, E. J.; Venkateswarlu, A. *J. Am. Chem. Soc.* **1972**, *94*, 6190.
[125] Savage, P. B.; Gellman, S. H. *J. Am. Chem. Soc.* **1993**, *115*, 10448.
[126] Overman, L. E.; Okazaki, M. E.; Mishra, P. *Tetrahedron Lett.* **1986**, *27*, 4391.
[127] Albright, J. D.; Goldman, L. *J. Am. Chem. Soc.* **1967**, *89*, 2416.
[128] Firouzabadi, H.; Ghaderi, E. *Tetrahedron. Lett.* **1978**, *19*, 839.
[129] Bhattacharjee, D.; Popp, F. D. *J. Heterocyclic Chem.* **1980**, *17*, 315.
[130] Farooq, O. *Synthesis* **1994**, 1035.
[131] McKillop, A.; Kemp, D. *Tetrahedron* **1989**, *45*, 3299.
[132] Leonard, N. J.; Kazmierczak, F. *J. Org. Chem.* **1987**, *52*, 2933.
[133] Woehrle, D.; Eskes, M.; Shigehara, K.; Yamada, A. *Synthesis* **1993**, 194.
[134] Liu, W.; Jensen, T. J.; Fronczek, F. R.; Hammer, R. P.; Smith, K. M.; Vicente, M. G. H. *J. Med. Chem.* **2005**, *48*, 1033.
[135] Ricci, A.; Degl'Innocenti, A.; Fiorenza, M.; Taddei, M.; Spartera, M. A.; Walton, D. R. M. *Tetrahedron Lett.* **1982**, *23*, 577.
[136] Corey, E. J.; Schmidt, G. *Tetrahedron Lett.* **1979**, *20*, 399.
[137] Collins, J. C.; Hess, W. W.; Frank, F. J. *Tetrahedron Lett.* **1968**, *9*, 3363.
[138] Czernecki, S.; Georgoulis, C.; Stevens, C. L.; Vijayakumaran, K. *Tetrahedron. Lett.* **1985**, *26*, 1699.
[139] Neumann, J.; Weingarten, S.; Thiem, J. *Eur. J. Org. Chem.* **2007**, 1130.
[140] Nicolaou, K. C.; Montagnon, T.; Baran, P. S.; Zhong, Y.-L. *J. Am. Chem. Soc.* **2002**, *124*, 2245.
[141] De Munari, S.; Frigerio, M.; Santagostino, M. *J. Org. Chem.* **1996**, *61*, 9272.
[142] Le Stang, S.; Meier, R.; Rocaboy, C.; Gladysz, J. A. *J. Fluorine Chem.* **2003**, *119*, 141.

[143] Plusquellec, D.; Lefeuvre, M. *Tetrahedron Lett.* **1987**, *28*, 4165.
[144] Lin, T. S.; Antonini, I.; Cosby, L. A.; Sartorelli, A. C. *J. Med. Chem.* **1984**, *27*, 813.
[145] Wang, H.; Sun, L.; Glazebnik, S.; Zhao, K. *Tetrahedron Lett.* **1995**, *36*, 2953.
[146] Ryu, E.-H.; Zhao, Y. *Org. Lett.* **2005**, *7*, 1035.
[147] Tamura, M.; Kochi, J. *Synthesis* **1971**, 303.
[148] Fouquet, G.; Schlosser, M. *Angew. Chem. Int. Ed.* **1974**, *13*, 82.
[149] Schlosser, M. *Angew. Chem. Int. Ed.* **1974**, *13*, 701.
[150] Juers, S.; Thiem, J. *Tetrahedron: Asym.* **2005**, *16*, 1631.
[151] After personal communication with Sven Gerber and Prof. Dr. Volkmar Vill.
[152] Tosin, M.; Murphy, P. V. *Org. Lett.* **2002**, *4*, 3675.
[153] Malkinson, J. P.; Falconer, R. A.; Toth, I. *J. Org. Chem.* **2000**, *65*, 5249.
[154] Temelkoff, D. P.; Zeller, M.; Norris, P. *Carbohydr. Res.* **2006**, *34*, 1081.
[155] Vagin S.; Hanack, M.; Kammerer, B.; Frickenschmidt, A. *Eur. J. Org. Chem.* **2004**, 4245.
[156] Duggan, M. E.; Imagire, J. S. *Synthesis* **1989**, 131.
[157] Avalos, M.; Babiano, R.; Cintas, P.; Hursthouse, M. B.; Jimenez, J. L.; Light, M. E.; Palacios, J. C.; Perez, E. M. S. *Eur. J. Org. Chem.* **2006**, 657.
[158] Leenders, R. G. G.; Ruytenbeek, R.; Damen, E. W. P.; Scheeren, H. W. *Synthesis* **1996**, 1309.
[159] Ichikawa, Y.; Nishiyama, T.; Isobe, M. *J. Org. Chem.* **2001**, *66*, 4200.
[160] Ichikawa, Y.; Matsukawa, Y.; Nishiyama, T.; Isobe, M. *Eur. J. Org. Chem.* **2004**, 586.
[161] Amore, A.; van Heerbeek, R.; Zeep, N.; van Esch, J.; Reek, J. N.; Hiemstra, H.; van Maarseveen, J. H. *J. Org. Chem.* **2006**, *71*, 1851.
[162] Kolb, H. C.; Finn, M. G.; Sharpless, K. B. *Angew. Chem. Int. Ed.* **2001**, *40*, 2004.
[163] Bock, V. D.; Hiemstra, H.; Maarseveen, J. H. *Eur. J. Org. Chem.* **2006**, 51.
[164] Wu, P.; Feldmann, A. K.; Nugent, A. K.; Hawker, C. J.; Scheel, A.; Voit, B.; Pyun, J.; Fréchet, J. M. J.; Sharpless, K. B.; Fokin, V. V. *Angew. Chem. Int. Ed.* **2004**, *43*, 3928.
[165] Prata, M. I. M.; Santos, A. C.; Torres, S.; André, J. P.; Martins, J. A.; Neves, M. García-Martín, M. L.; Rodrigues, T. B.; López-Larrubia, P.; Cerdán S.; Geraldes, C. F. G. C. *Contrast Med. Mol. Imaging 1:* **2006**, 246.
[166] Esteves, A. P.; Rodrigues, L. M.; Silva, M. E.; Gupta, S.; Oliveira-Campos, A. M. F.; Machalicky, O.; Mendonca, A. J. *Tetrahedron* **2005**, *61*, 8625.
[167] Deng, S.; Gangadharmath, U.; Chang, C.-W., T. *J. Org. Chem.* **2006**, *71*, 5179.
[168] Tietze, L.-F.; Eicher, T. *Reaktionen und Synthesen im organisch-chemischen Praktikum und Forschungslaboratorium*, Georg Thieme Verlag Stuttgart • New York, **1991**, 540.
[169] Jeanes, A. R.; Wilham, C. A.; Hilbert, G. E. *J. Am. Chem. Soc.* **1953**, *75*, 3667.
[170] D'Onofrio, J.; De Champdoré, M.; De Napoli, L.; Montesarchio, D.; Di Fabio, G. *Bioconjugate Chem.* **2005**, *16*, 1299.
[171] Temelkoff, D. P.; Norris, P.; Zeller, M. *Acta Cryst.* **2004**, *E60*, 1975.
[172] Hesse, M.; Meier, H.; Zeeh, B. *Spektroskopische Methoden in der organischen Chemie,* 7., überarbeitete Auflage, Georg Thieme Verlag, Stuttgart • New York, **2005**.
[173] Gao, Y.; Eguchi, A.; Kakehi, K.; Lee, Y. C. *Bioorg. Med. Chem.* **2005**, *13*, 6151.
[174] Augeri, D. J.; O'Connor, S. J.; Janowick, D.; Szczepankiewicz, B.; Sullivan, G.; Larsen, J.; Kalvin, D.; Cohen, J.; Devine, E.; Zhang, H.; Cherian, S.; Saeed, B.; Ng, S.-C.; Rosenberg, S. *J. Med. Chem.* **1998**, *41*, 4288.
[175] Chen, S. H.; Geng, Y. *PCT Int. Appl.* **2003**, WO 03/008475; *Chem. Abstr.* 138:137724.
[176] De Frutos, O.; Granier, T.; Gomez-Lor, B.; Jimenez-Barbero, J.; Monge, A.; Gutierrez-Puebla, E.; Echavarren, A. M. *Chem. Eur. J.* **2002**, *8*, 2879.
[177] Belfield, K. D.; Schafer, K. J.; Mourad, W.; Reinhardt, B. A. *J. Org. Chem.* **2000**, *65*, 4475.
[178] Tregre, G. J.; Mathias, L. J. *J. Polym. Sci., Part A: Polym. Chem.* **1997**, *35*, 587.
[179] Pawlowski, G.; Hanack, M. *Synthetic Comm.* **1981**, *11*, 351.
[180] Kotha, S.; Brahmachary, E. *Bioorg. Med. Chem.* **2002**, *10*, 2291.
[181] Vollhardt, K. P. C. *Angew. Chem. Int. Ed.* **1984**, *23*, 539.
[182] Kotha, S.; Mohanraja, K.; Durani, S. *Chem. Comm.* **2000**, *19*, 1909.
[183] Witulski, B.; Zimmermann, A. *Synlett* **2002**, *11*, 1855.
[184] Uchida, H.; Reddy, P. Y.; Nakamura, S.; Toru, T. *J. Org. Chem.* **2003**, *68*, 8736.
[185] Uchida, H.; Tanaka, H.; Yoshiyama, H.; Reddy, P. Y.; Nakamura, S.; Toru, T. *Synlett* **2002**, *10*, 1649.
[186] Uchida, H.; Mitsui, M.; Reddy, P. Y.; Nakamura, S.; Toru, T. *ARKIVOC* **2005**, *11*, 17.
[187] Vagin, S.; Hanack, M. *Eur. J. Org. Chem.* **2004**, 600.

[188] Benning, S. A. *Lumineszenz mesogener Halbleiter* PhD-thesis Univ. Paderborn **2004**.
[189] Tauc, J.; Grigorovici, R.; Vancu, A. *Physica Status Solidi* **1966**, *15*, 627.
[190] Fukuda, T.; Homma, S.; Kobayashi, N. *Chem. Eur. J.* **2005**, *11*, 5205.
[191] Hong, Y.; Kanicki, J. *IEEE Transaction on Electron. Devices* **2004**, *51*, 1562.
[192] Kobayashi, N.; Fukuda, T. *J. Am. Chem. Soc.* **2002**, *124*, 8021.
[193] Kobayashi, N.; Miwa, H.; Nemykin, V. N. *J. Am. Chem. Soc.* **2002**, *124*, 8007.
[194] Fukuda, T.; Makarova, E. A.; Luk'yanets, E. A.; Kobayashi, N. *Chem. Eur. J.* **2004**, *10*, 117.
[195] Mack, J.; Stillman, M. J. *Inorg. Chem.* **1997**, *36*, 413.
[196] Mack, J.; Stillman, M. J. *J. Am. Chem. Soc.* **1994**, *116*, 1292.
[197] Nyokong, T.; Gasyna, Z.; Stillman, M. J. *Inorg. Chem.* **1987**, *26*, 1087.
[198] Zheng, G.; Chen, J.; Li, H.; Glickson, J. D. *Proc. Nat. Acad. Sci.* **2005**, *102*, 17757.
[199] Hassan, B. M.; Li, H.; McKeown, N. B. *J. Mater. Chem.* **2000**, *10*, 39.
[200] Blower, M. A.; Bryce, M. R.; Devonport, W. *Adv. Mater.* **1996**, *8*, 63.
[201] Leclaire, J.; Dagiral, R.; Fery-Forgues, S.; Coppel, Y.; Donnadieu, B.; Caminade, A.-M.; Majoral, J.-P. *J. Am. Chem. Soc.* **2005**, *127*, 15762.
[202] Ng, D. K. P. *C. R. Chimie* **2003**, *6*, 903.
[203] Biessen, E. A. L.; Beuting, D. M.; Roelen, H. C. P. F.; van de Marel, G. A.; van Boom, J. H.; van Berkel, T. J. C. *J. Med. Chem.* **1995**, *38*, 1538.
[204] Sengupta, S.; Sadhukhan, S. K. *Carbohydr. Res.* **2001**, *332*, 215.
[205] Whitesides, G. M.; Laibinis, P.E. *Langmuir* **1990**, *6*, 87.
[206] Ulman, A. *An Introduction to Ultrathin Organic Films*; Academic Press: San Diego, **1991**.
[207] Bain, C. D.; Troughton, E. B.; Tao, Y. T.; Evall, J.; Whitesides, G. M.; Nuzzo, R. G. *J. Am. Chem. Soc.* **1989**, *111*, 321.
[208] Schaller, T.; Buechele, U. P.; Klaerner, F.-G.; Blaeser, D.; Boese, R.; Brown, S. P.; Spiess, H. W.; Koziol, F.; Kussmann, J.; Ochsenfeld, C. *J. Am. Chem. Soc.* **2007**, *129*, 1293.
[209] Weiss, S. T.; McIntyre, N. R.; McLaughlin, M. L.; Merkler, D. J. *Drug discovery today* **2006**, *11*, 819.
[210] Kondratenko, R. M.; Baltina, L. A.; Mustafina, S. R.; Vasil'eva, E. V.; Pompei, R.; Deidda, D.; Plyasunova, O. A.; Pokrovskii, A. G.; Tolstikov, G. A. *Russ. J. Bioorg. Chem.* **2004**, *30*, 275.
[211] Grayson, E. J.; Ward, S. J.; Hall, A. L.; Rendle, P. M.; Gamblin, D. P.; Batsanov, A. S.; Davis, B. G. *J. Org. Chem.* **2005**, *70*, 9740.
[212] Tackley, D. R.; Geoffrey, D.; Smith, W. E. *Phys. Chem. Chem. Phys.* **2001**, *3*, 1419.
[213] Claessens, C. G.; Hahn, U.; Torres, T. *The Chemical Record* **2008**, *8*, 75.